

AD-A065 388

KAMAN AVIDYNE BURLINGTON MASS
WIND-TUNNEL SHOCK-TUBE SIMULATION AND EVALUATION OF BLAST EFFEC--ETC(U)
MAR 78 J R RUETENIK, R F SMILEY

F/G 21/5

DNA001-76-C-0107

UNCLASSIFIED

KA-TR-147

DNA-4590F

NL

1 of 3
ADA
065388



①2 LEVEL II

AD-E300 451

✓ DNA 4590F

AD AO 65388

WIND-TUNNEL SHOCK-TUBE SIMULATION AND EVALUATION OF BLAST EFFECTS ON AN ENGINE INLET

Kaman AviDyne
83 Second Avenue
Burlington, Massachusetts 01803

15 March 1978

Final Report for Period October 1975—December 1977

CONTRACT No. DNA 001-76-C-0107

APPROVED FOR PUBLIC RELEASE;
DISTRIBUTION UNLIMITED.

THIS WORK SPONSORED BY THE DEFENSE NUCLEAR AGENCY
UNDER RDT&E RMSS CODE B342076464 N99QAXAE51014 H2590D.

Prepared for
Director
DEFENSE NUCLEAR AGENCY
Washington, D. C. 20305

DDC
RECEIVED
MAR 7 1978
B

79 01 22 090

DDC FILE COPY

Destroy this report when it is no longer
needed. Do not return to sender.

[PLEASE NOTIFY THE DEFENSE NUCLEAR AGENCY,
ATTN: TISI, WASHINGTON, D.C. 20305, IF
YOUR ADDRESS IS INCORRECT, IF YOU WISH TO
BE DELETED FROM THE DISTRIBUTION LIST, OR
IF THE ADDRESSEE IS NO LONGER EMPLOYED BY
YOUR ORGANIZATION.



UNCLASSIFIED

18 DNA, SBIE

SECURITY CLASSIFICATION OF THIS PAGE (When Data Entered)

19 REPORT DOCUMENTATION PAGE		READ INSTRUCTIONS BEFORE COMPLETING FORM	
1. REPORT NUMBER DNA 4590F, AD-E300 454	2. GOVT ACCESSION NO.	3. RECIPIENT'S CATALOG NUMBER 9	
4. TITLE (and Subtitle) WIND-TUNNEL SHOCK-TUBE SIMULATION AND EVALUATION OF BLAST EFFECTS ON AN ENGINE INLET.		5. TYPE OF REPORT & PERIOD COVERED Final Report, for Period Oct 75-Dec 77	
7. AUTHOR(s) J. Ray Ruetenik Robert F. Smiley		6. PERFORMING ORG. REPORT NUMBER KA-TR-147	
9. PERFORMING ORGANIZATION NAME AND ADDRESS Kaman Avidyne 83 Second Avenue Burlington, Massachusetts 01803		8. CONTRACT OR GRANT NUMBER(s) DNA 001-76-C-0107	
11. CONTROLLING OFFICE NAME AND ADDRESS Director Defense Nuclear Agency Washington, D.C. 20305		10. PROGRAM ELEMENT, PROJECT, TASK AREA & WORK UNIT NUMBERS NWED Subtask N99QAXAE510-14	
14. MONITORING AGENCY NAME & ADDRESS (if different from Controlling Office) 12 240 p.		12. REPORT DATE 15 Mar 78	17 E510
		13. NUMBER OF PAGES 236	
		15. SECURITY CLASS (of this report) UNCLASSIFIED	
		15a. DECLASSIFICATION/DOWNGRADING SCHEDULE	
16. DISTRIBUTION STATEMENT (of this Report) Approved for public release; distribution unlimited.			
17. DISTRIBUTION STATEMENT (of the abstract entered in Block 20, if different from Report)			
18. SUPPLEMENTARY NOTES This work sponsored by the Defense Nuclear Agency under RDT&E RMSS Code B342076464 N99QAXAE51014 H2590D.			
19. KEY WORDS (Continue on reverse side if necessary and identify by block number) Aircraft Computer Studies Inlet Shock Tube Blast Engine Pressure Subsonic B-1 Experimental Test Shock Wind Tunnel			
20. ABSTRACT (Continue on reverse side if necessary and identify by block number) A development and test program is described for simulation of blast wave intercepts with a scaled aircraft engine in subsonic flight, using the shock tube technique for firing the blast-type waves. The program initially consisted of preliminary theoretical calculations and tests with two-inch-diameter shock tubes fired into the AEDC 17 transonic tunnel, followed by the design, construction and testing of three large 22.6 inch-diameter shock tubes. These shock tubes were installed in the AEDC 16T (16 foot square)			

62764H

This report describes a program for simulating

194 970 9

01

[Handwritten signature]

UNCLASSIFIED

SECURITY CLASSIFICATION OF THIS PAGE(When Data Entered)

ϕ deg and 5 deg

20. ABSTRACT (Continued)

transonic wind tunnel and were used to project blast waves at a 0.1-scale B-1 aircraft model. Forty-five firings were made, covering tunnel speeds of Mach 0, 0.55, 0.70, 0.85 and 0.90, blast overpressures (scaled to 1 atm. ambient pressure) from 2 to 6 psi, ~~0°~~ and 5° yaw, and inlet flow rates representative of cruise and maximum power conditions. The model inlets were instrumented with 40 combination steady-state and dynamic total-pressure probes at each engine face section and other dynamic transducers to measure incident blast wave properties and inlet internal ramp and cowl pressures. The test data were digitized and used to determine time histories of inlet distortion during the blast encounter.

Calculations of blast pressures in the inlets made with the KA BID code satisfactorily reproduced the principal features of the observed inlet duct and engine face pressures.

Blast-induced distortions during the time of definite blast-type flow in the inlet were generally smaller than but did sometimes exceed normal inlet allocation levels for the B-1 aircraft. Distortions at later times greatly exceeded this allocation.

Four potentially adverse effects to engine operation from blast interaction were identified: blast-induced distortion, fan choking, afterburner blow-out and shock-boundary layer induced distortion.

A

UNCLASSIFIED

SECURITY CLASSIFICATION OF THIS PAGE(When Data Entered)

PREFACE

This work was performed by the Avidyne Division of the Kaman Sciences Corporation for the Defense Nuclear Agency under Contract DNA-001-76-C-0107. MAJ David W. Garrison of the DNA Shock Physics Directorate served as technical monitor to July 31, 1977, and CAPT Michael Rafferty from August 1, 1977, through the remainder of the program.

Dr. J. Ray Ruetenik of Kaman Avidyne was the project leader under Dr. Norman P. Hobbs, Technical Director of KA. Mr. Robert F. Smiley performed engineering functions. Professor Jack L. Kerrebrock, Professor and Director of the Gas Turbine and Space Propulsion Laboratories, MIT, served as technical consultant on propulsion.

Appreciation is expressed to MAJ Garrison and CAPT Rafferty for their continuing interest and significant support of this program. Appreciation is also expressed to CAPT William Tuck, AEDC, for test coordination, and the ARO personnel for their dedicated work, in particular Mr. H. Eldon McDill and Mr. Richard J. Christenson, Test directors of the 1T and 16T tests, respectively, and Mr. Karl F. Thormaehlen, mechanical engineer. Appreciation is also extended to Rockwell International personnel, particularly Mr. Ray L. Noonan, Mr. W. Robert Haagenson and Mr. Clarence E. Mitchell, for their contributions to the test program.

ACCESSION for		
NTIS	White Section	<input checked="" type="checkbox"/>
DDC	B.H. Section	<input type="checkbox"/>
UNANNOUNCED		<input type="checkbox"/>
JUSTIFICATION		
BY		
DISTRIBUTION/AVAILABILITY CODES		
Dist.	AVAIL	SPECIAL
A		

**Conversion factors for U.S. customary
to metric (SI) units of measurement.**

To Convert From	To	Multiply By
angstrom	meters (m)	1.000 000 X E -10
atmosphere (normal)	kilo pascal (kPa)	1.013 25 X E +2
bar	kilo pascal (kPa)	1.000 000 X E +2
barn	meter ² (m ²)	1.000 000 X E -28
British thermal unit (thermochemical)	joule (J)	1.054 350 X E +3
calorie (thermochemical)	joule (J)	4.184 000
cal (thermochemical)/cm ²	mega joule/m ² (MJ/m ²)	4.184 000 X E -2
curie	*giga becquerel (GBq)	3.700 000 X E +1
degree (angle)	radian (rad)	1.745 329 X E -2
degree Fahrenheit	degree kelvin (K)	$t_K = (t_F + 459.67)/1.8$
electron volt	joule (J)	1.602 19 X E -19
erg	joule (J)	1.000 000 X E -7
erg/second	watt (W)	1.000 000 X E -7
foot	meter (m)	3.048 000 X E -1
foot-pound-force	joule (J)	1.355 818
gallon (U.S. liquid)	meter ³ (m ³)	3.785 412 X E -3
inch	meter (m)	2.540 000 X E -2
jerk	joule (J)	1.000 000 X E +9
joule/kilogram (J/kg) (radiation dose absorbed)	Gray (Gy)	1.000 000
kilotons	terajoules	4.183
kip (1000 lbf)	newton (N)	4.448 222 X E +3
kip/inch ² (ksi)	kilo pascal (kPa)	6.894 757 X E +3
ktap	newton-second/m ² (N-s/m ²)	1.000 000 X E +2
micron	meter (m)	1 000 000 X E -6
mil	meter (m)	2.540 000 X E -5
mile (international)	meter (m)	1.609 344 X E +3
ounce	kilogram (kg)	2.834 952 X E -2
pound-force (lbs avoirdupois)	newton (N)	4.448 222
pound-force inch	newton-meter (N·m)	1.129 848 X E -1
pound-force/inch	newton/meter (N/m)	1.751 268 X E +2
pound-force/foot ²	kilo pascal (kPa)	4.788 026 X E -2
pound-force/inch ² (psi)	kilo pascal (kPa)	6.894 757
pound-mass (lbm avoirdupois)	kilogram (kg)	4.535 924 X E -1
pound-mass-foot ² (moment of inertia)	kilogram-meter ² (kg·m ²)	4.214 011 X E -2
pound-mass/foot ³	kilogram/meter ³ (kg/m ³)	1.601 846 X E +1
rad (radiation dose absorbed)	**Gray (Gy)	1.000 000 X E -2
roentgen	coulomb/kilogram (C/kg)	2.579 760 X E -4
shake	second (s)	1.000 000 X E -8
slug	kilogram (kg)	1.459 390 X E +1
torr (mm Hg, 0° C)	kilo pascal (kPa)	1.333 22 X E -1

*The becquerel (Bq) is the SI unit of radioactivity; 1 Bq = 1 event/s.

**The Gray (Gy) is the SI unit of absorbed radiation.

A more complete listing of conversions may be found in "Metric Practice Guide E 380-74," American Society for Testing and Materials.

TABLE OF CONTENTS

	<u>Page</u>
1. INTRODUCTION	11
2. PRELIMINARY INVESTIGATIONS FOR DEVELOPMENT OF TEST TECHNIQUE	13
2.1 THEORETICAL STUDIES - REFLECT/S2D	13
2.2 SHOCK TUBE FIRINGS IN AEDC 1T WIND TUNNEL	13
3. DEVELOPMENT OF 16T BLAST TEST FACILITY	21
3.1 GENERAL DESIGN CRITERIA	21
3.2 SHOCK TUBE DESIGN AND TESTING	22
3.3 BLAST INPUT INSTRUMENTATION	30
3.4 TUNNEL WALL MODIFICATIONS	30
4. 16T WIND TUNNEL BLAST TEST PROGRAM	32
4.1 GENERAL TEST SETUP	32
4.2 MODEL AND INSTRUMENTATION DETAILS	32
4.3 16T WIND TUNNEL TESTS	37
4.3.1 Unyawed steady-state tests	39
4.3.2 Yawed steady-state tests	39
4.3.3 Shock tube firings	39
4.4 DATA REDUCTION	42
4.5 SAMPLE TEST RESULTS	42
4.6 OBSERVATIONS ON BLAST INPUT CONDITIONS	55
4.6.1 Blast Input to the Inlets	55
4.6.2 Shock Tube Location Effects on Blast Input and Inlet Response	61
5. ANALYSIS OF 16T TEST RESULTS	66
5.1 GENERAL PHENOMENA	66
5.1.1 Differences Between Shock Tube and Nuclear Blast Flows	76
5.2 SHOCK PATTERN IN THE INLETS	77
5.3 ANALYSIS OF INLET DISTORTION	81
5.3.1 Data Presentation	91
5.3.2 Effects at low mass flow rates	91
5.3.3 Effects at high mass flow rates	117
5.3.4 Mach number effects	119
5.3.5 Effects of yaw angle	119
5.3.6 Long Duration Distortion Effects	119
5.3.7 Concluding Remarks on Distortion Effects	121

TABLE OF CONTENTS (CONCL'D)

	<u>Page</u>
6. COMPARISON OF THEORY AND EXPERIMENT	123
7. SHOCK ORIENTATION EFFECTS	132
8. INTERACTION OF BLAST SHOCK WITH THE ENGINE FAN	138
8.1 QUASI-STEADY BLAST SHOCK INTERACTION WITH A FAN	138
8.2 BLAST SHOCK AT ENGINE FACE	141
8.3 ENGINE FAN CHARACTERISTICS	141
8.4 BLAST EFFECT ON FAN OPERATION	145
8.5 FAN REFLECTED SHOCK	147
9. REFLECTED SHOCK-BOUNDARY LAYER INTERACTION WITHIN INLET	155
9.1 SHOCK-BOUNDARY LAYER CALCULATION	155
9.2 SHOCK-BOUNDARY LAYER RESULTS	157
10. DISCUSSION	164
10.1 BLAST GENERATORS	164
10.2 16T WIND TUNNEL TESTS AND ANALYSIS	165
11. CONCLUSIONS	170
REFERENCES	172
APPENDIX A - THEORETICAL STUDIES OF THE FLOW FIELD PRODUCED BY FIRING A SHOCK TUBE INTO A STATIONARY FLUID	175
A.1 INTRODUCTION	175
A.2 S2D CODE STUDIES	175
A.3 REFLECT2 CODE STUDIES	177
A.4 CONCLUSIONS	179
APPENDIX B - STEADY-STATE PRE-BLAST TEST CONDITIONS IN THE AEDC 16T TUNNEL	181
APPENDIX C - LIST OF COMMON SYMBOLS AND CONVENTIONS	231

LIST OF ILLUSTRATIONS

<u>Figure</u>		<u>Page</u>
2.1	Test setup for blast tests in the AEDC 1T transonic wind tunnel.	14
2.2	Shadowgrams of blast field produced by firing a shock tube into air at rest, $\phi=90^{\circ}$.	16
2.3	Shadowgrams of blast field produced by firing a shock tube into a wind tunnel at Mach 0.80, $\phi=90^{\circ}$.	17
2.4	Transient blast pressures for a firing of a shock tube into a Mach 0.75 wind tunnel flow, $\phi=90^{\circ}$.	19
3.1	Top view of test installation in AEDC wind tunnel.	23
3.2	Blast test setup in the AEDC 16T transonic wind tunnel.	24
3.3	23-inch-diameter shock tube setup for testing.	28
3.4	Typical diaphragm rupture pattern.	29
3.5	Oblique view of a claw probe mounted above the inlet model.	31
4.1	Details of inlet model and engine simulation.	33
4.2	Closeup view of engine inlet and claw probes in the AEDC 16T wind tunnel.	34
4.3	Engine face transducer locations.	35
4.4	Inlet instrumentation.	36
4.5	Sample test results for Run 8 (Part 573), Mach 0.70, flow rate ≈ 303 lb/sec, tube 2, $\Delta p \approx 5.0$ psi.	
4.6	Typical blast pressure measurements for firings from three shock tubes, Mach 0.85, flow rate ≈ 300 lb/sec.	57
4.7	Comparison of engine face pressures for firings from shock tubes 2 and 3.	62
4.8	Comparison of blastward inlet ramp pressure time histories for Mach 0.85 firings from two shock tubes.	65
5.1	Variation of blast-induced side-slip angle with intercept angle and overpressure.	67

LIST OF ILLUSTRATIONS (Cont'd)

<u>Figure</u>		<u>Page</u>
5.2	Variation of blast-induced total pressure with intercept angle and overpressure.	71
5.3	Inlet time-distance relationships.	78
5.4	Typical shock wave pattern in the inlets.	79
5.5	Distortion time histories for Run 8 (Part 573), Mach 0.70, $\Delta p=5.0$ psi; $\phi=98^\circ$, flow rate ≈ 303 lb/sec, tube 2.	82
5.6	Range of distortion indices for B-1 inlet at subsonic cruise.	92
5.7	Distortion time histories for two overpressures at Mach 0.70, flow rate ≈ 300 lb/sec, tube 2.	93
5.8	Distortion time histories for four overpressures at Mach 0.70 for the blastward inlet, flow rate ≈ 350 lb/sec, tube 2.	94
5.9	Distortion time histories for three overpressures at Mach 0.70 for the leeward inlet, flow rate ≈ 350 lb/sec, tube 2.	97
5.10	Distortion time histories for four overpressures at Mach 0.85 for the blastward inlet, flow rate ≈ 300 lb/sec, tube 1.	100
5.11	Distortion time histories for four overpressures at Mach 0.85 for the leeward inlet, flow rate ≈ 300 lb/sec, tube 1.	103
5.12	Distortion time histories for two overpressures at Mach 0.85, flow rate ≈ 350 lb/sec, tube 2.	104
5.13	Distortion time histories for four Mach numbers for the blastward inlet, flow rate ≈ 350 lb/sec, tube 2.	107
5.14	Distortion time histories for four Mach numbers for the leeward inlet, flow rate ≈ 350 lb/sec, tube 2.	110
5.15	Distortion time histories for four Mach numbers for the blastward inlet, flow rate ≈ 350 lb/sec, tube 1.	113
5.16	Distortion time histories for four Mach numbers for the leeward inlet, flow rate ≈ 350 lb/sec, tube 1.	114
5.17	Distortion time histories for three yawed runs at Mach 0.70, yaw = 5° , flow rate ≈ 350 lb/sec.	115

LIST OF ILLUSTRATIONS (CONT'D)

<u>Figure</u>		<u>Page</u>
5.18	Outboard inlet total pressure contours for a large blast-induced distortion condition.	118
5.19	Comparison of ramp pressure time histories for four Mach numbers, tube 2, flow rate ≈ 350 lb/sec.	120
6.1	Comparison of theoretical and experimental time histories of ramp and cowl pressures at Mach 0.70, flow rate ≈ 350 lb/sec.	125
6.2	Comparison of theoretical and experimental time histories of ramp pressures in the blastware inlet at Mach 0.85, tube 1 data, flow rate ≈ 350 lb/sec.	126
6.3	Comparison of theoretical and experimental time histories of ramp pressures in the blastward inlet at Mach 0.85, tube 2 data, flow rate ≈ 350 lb/sec.	127
6.4	Comparison of theoretical and experimental time histories of cowl pressures at Mach 0.85, flow rate ≈ 350 lb/sec.	128
6.5	Comparison of theoretical and experimental total pressure time histories at the engine face for the blastward inlet.	129
7.1	Comparison of engine face total pressure time histories for three blast intercept angles.	133
7.2	Comparison of engine face total pressure ratio time histories for three blast intercept angles.	135
8.1	Shock interaction with fan.	139
8.2	Configuration of NASA two-stage axial-flow fan.	143
8.3	Performance maps for NASA two-stage axial-flow fan.	144
8.4	Two-stage-fan overall performance map.	146
8.5	Variation of fan reflected shock properties with incident shock pressure ratio.	148
8.6	Variation of fan transmitted shock properties with incident shock pressure ratio.	153
9.1	Boundary layer separation and distortion from fan reflected shock wave.	156
9.2	Effect of fan reflected shock on boundary layers of inlets.	158

LIST OF ILLUSTRATIONS (CONCL'D)

<u>Figure</u>		<u>Page</u>
9.3	Inlet time-distance relationships for a flight Mach number of 0.85 and a mass flow rate of 350 lb/sec.	162
A.1	Problem of a shock tube firing into a stationary fluid.	176
A.2	Theoretical blast pressures outside of a shock tube.	178
A.3	Variation of overpressure with distance from shock tube.	180

LIST OF TABLES

<u>Table</u>		<u>Page</u>
4.1	Locations of dynamic pressure transducers	38
4.2	Nominal test conditions	40
4.3	Steady-state yaw conditions	41
4.4	16T wind tunnel test conditions	43
5.1	Equations for calculating distortion parameters IDC, IDR, IDL, IDA and IDT.	89
8.1	Inlet data of Run 40 (Part 619) pertinent to blast shock-fan interaction.	142

SECTION I
INTRODUCTION

This study is concerned with the simulation of the situation where an aircraft inlet is subjected to a blast wave of sufficient strength and long enough duration to produce significant distortion of the flow field at the engine face. For critically designed engine-inlet systems, such blasts, produced by nuclear explosions, might cause severe engine stall or flameout problems.

The objective of the test program reported here was to develop a test technique for measuring blast interaction with an aircraft inlet and to conduct a series of tests for the development of prediction methods.

Wind tunnels provide a well-developed means for the simulation of flight flow conditions for an engine inlet. A technique for the simulation of blast waves in a supersonic wind tunnel by employing a shock tube mounted in the wind tunnel wall has been demonstrated by Pierce (Ref. 1.1).

A development and test program, conducted at the Arnold Engineering Development Center (Ref. 1.2), is reported here for the simulation of blast wave intercepts with a scaled aircraft inlet in subsonic flight using the shock-tube technique for firing the blast-type waves. Pilot tests of the technique were performed in a 1-ft wind tunnel during August 1975, followed by "bench" tests of a prototype shock tube during August 1976. A wind tunnel test program then was conducted in the AEDC 16T wind tunnel with a 0.1-scale B-1 inlet during September 24-28, 1976.

This report is concerned primarily with documentation of the development of the facility to test the response of engine-inlet systems to blast waves in high speed wind tunnels, with the presentation of test results from the facility for a 0.1-scale aircraft inlet, and with the discussion and application of associated analytical techniques to predict inlet behavior in a blast environment.

Section 2 of the report describes preliminary analytical studies and small model wind tunnel tests performed to assess the feasibility of performing well controlled inlet blast tests in a high speed wind tunnel with blast waves produced by shock tubes fired into the tunnel. Section

3 describes the subsequent development of a large shock tube facility for use in the AEDC 16T (16 foot square) transonic wind tunnel (Ref. 1.2). Section 4 describes and presents sample results of a blast test program performed in this facility, using three 23 in.-diameter shock tubes and a 0.1-scale B-1 inlet model. Section 5 presents a general analysis of the test results, pointing out some basic characteristics of the inlet blast interaction process and presenting an analysis of the inlet distortion measurements obtained during the tests.

Section 6 presents a comparison of experimental blast pressure time histories with theoretical calculations made with the BID computer code. Section 7 supplements the test results by presenting some blast calculations made with the BID code to illustrate some blast-inlet interaction effects over a greater range of blast intercept angles than were covered by the tests.

Section 8 discusses the interaction of a blast-induced inlet shock with an engine fan and Section 9 discusses blast-induced boundary layer interactions in an inlet.

The overall study results are discussed in Section 10 and conclusions are given in Section 11.

Appendix A discusses some theoretical studies of the firing of a shock tube into a stationary fluid. Appendix B presents the steady-state pre-blast measurements made during the 16T tests.

SECTION II
PRELIMINARY INVESTIGATION FOR DEVELOPMENT OF TEST TECHNIQUE

As the first stage of the development of a wind-tunnel shock-tube blast test facility, a program of preliminary theoretical calculations and model tests was undertaken to establish the feasibility of the test concept and to provide design information for construction of a full-scale installation.

2.1 THEORETICAL STUDIES-REFLECT/S2D

The first development step consisted of theoretical calculations for the problem of a circular shock tube fired into stationary air. These calculations, made with the Kaman Avidyne REFLECT-2 and S2D computer codes (see Appendix A) indicated that useful shock wave patterns simulating nuclear blast wave patterns in the 2 to 5 psi overpressure range could be obtained at distances 3 to 10 diameters downstream of the end of a shock tube. In particular, these calculation results, summarized in Appendix A, indicated that, at a distance of about 4.5 diameters downstream of the end of a shock tube, a blast duration of nearly constant overpressure could be obtained for about 2.5 milliseconds per foot of tube diameter.

2.2 SHOCK TUBE FIRINGS IN AEDC 1T WIND TUNNEL

Using the results of the above theoretical calculations as a guideline, a small 2 in.-dia shock tube was constructed and was fired into the AEDC 1T (one-foot-square) transonic wind tunnel for a wide range of flow and shock tube conditions, during which pressure measurements were made for a large number of locations inside the wind tunnel.

The geometric setup used in the AEDC 1T tunnel is indicated in Figure 2.1. Three shock tube configurations were tested, about 14 inches long, with ratios of the driven-tube lengths to driver-tube lengths of about 0.5, 2 and 8. The end of each shock tube protuded into the tunnel by about one inch (perpendicular to the floor) where it was terminated by a 8 in-dia. circular flange (Fig. 2.1). Firings were made with the angle of the shock tube axis to the tunnel axis, ϕ , (see Figure 2.1), being 90° , 60° and 45° . Tunnel ambient pressures were in

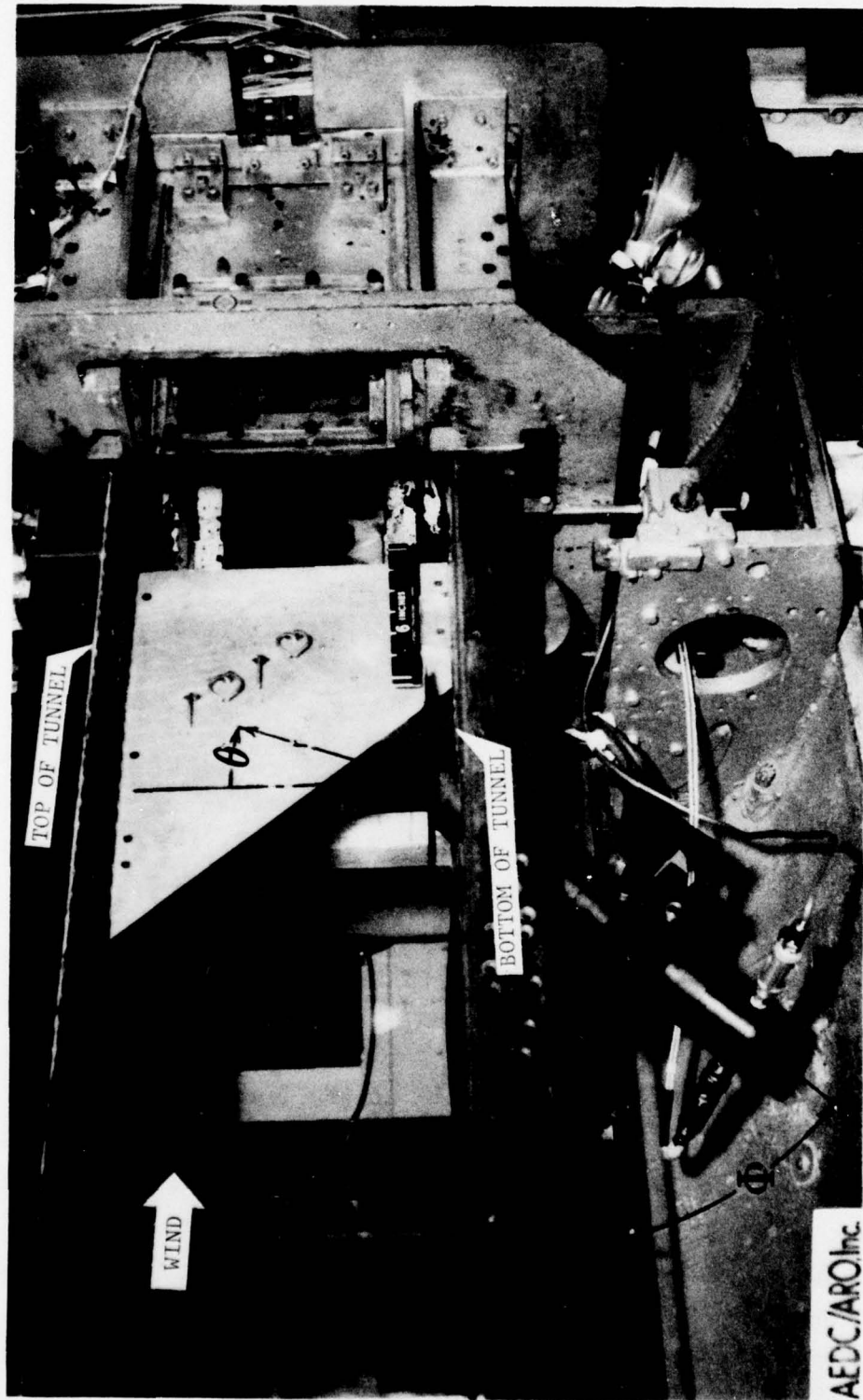


Figure 2.1. Test setup for blast tests in the AEDC IT transonic wind tunnel (tunnel side walls removed).

the range 11 to 16 psia and shock tube driver pressures ranged from about 60 to 380 psia.

Transient blast pressure measurements were made inside the wind tunnel by means of pressure transducers imbedded in the surface of a thin plate placed in the plane of symmetry, as shown in Figure 2.1. Measurements were made of local blast pressure time histories for radial distances from the shock tube exit of 2.5, 3.5 and 4.5 tube diameters (r/d) and for polar angle locations (θ in Fig. 2.1) of -15° , 0° , 15° , 30° , 45° , 60° and 75° . Also, for several locations, measurements of transient total pressure and flow velocities were made with two total-pressure and two claw probes mounted about a half inch from the face of the thin plate, as shown in the figure. Kulite XCQL-093-025 pressure transducers were used in the plate and probes.

Sample shadowgrams showing the blast field produced by firing the 2-in shock tube into the wind tunnel are presented in Figures 2.2 and 2.3. Figure 2.2 shows three shadowgrams of one firing into still air and Figure 2.3 shows two shadowgrams for a firing into a Mach 0.8 tunnel flow. The shadowgrams are taken looking into the side of the tunnel, with the tunnel flow proceeding from left to right, and with the shock tube being fired into the tunnel vertically up ($\phi=90^\circ$) through the bottom wall of the tunnel.

In Figure 2.2, the lowest shadowgram was taken first (before blast exit from the tubes) and the upper one last. The blast front can be clearly seen in these shadowgrams and becomes essentially a circular arc after the front of the blast wave has moved several tube diameters away from the tube exit. In the upper shadowgram of Figure 2.2, between the top of the blast front and the shock-tube exit is seen a nearly horizontal dark line which roughly delineates the contact surface between the "hot" tunnel air (above) and the "cold" expanded air (below) from the driver section of the shock tube. This cold gas can also be more clearly seen as the dark jet core in Figure 2.3. From the viewpoint of simulating a nuclear blast or other long-duration blast wave, it should be noted that only that portion of the blast wave lying between the blast front and the hot-cold gas contact surface is of interest.

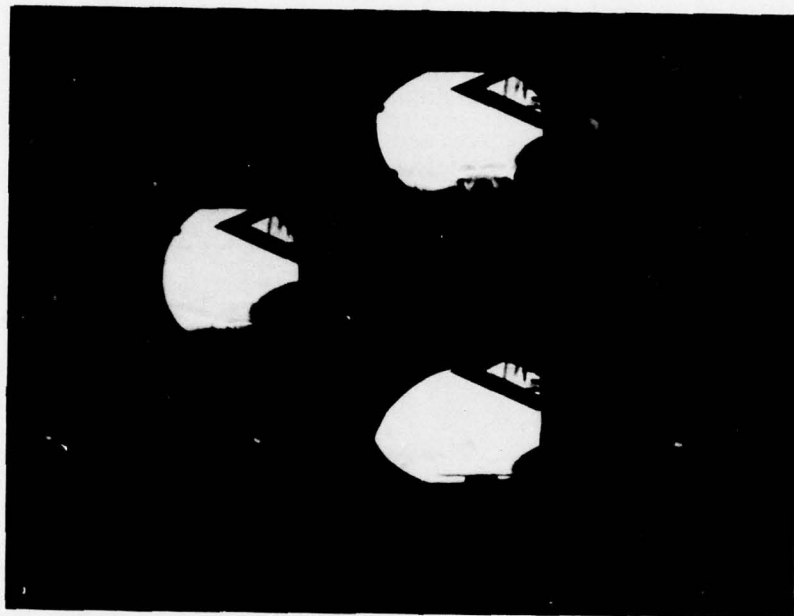


Figure 2.2. Shadowgrams of blast field produced by firing a shock tube into air at rest, $\phi = 90^\circ$.

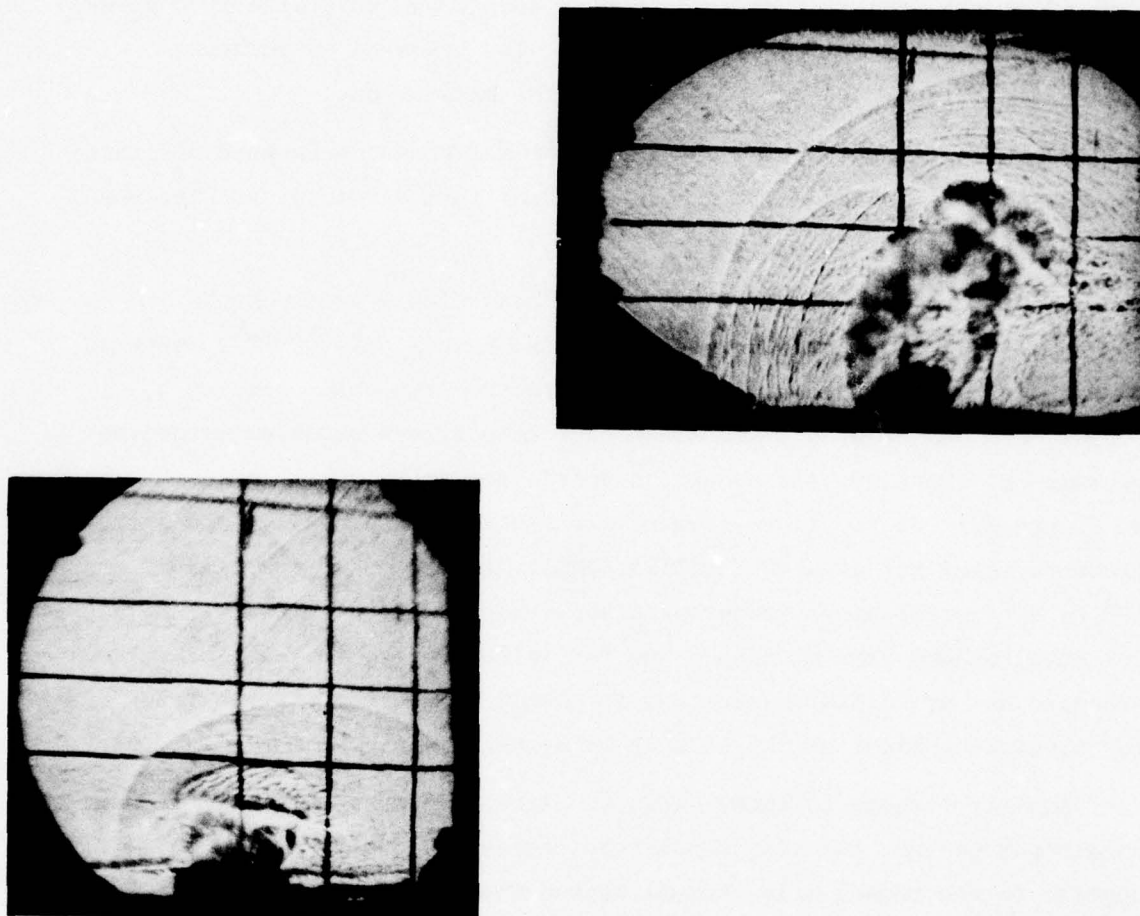


Figure 2.3. Shadowgrams of blast field produced by firing a shock tube into a wind tunnel at Mach 0.80, $\phi = 90^\circ$.

The effect of the tunnel flow on the shape of the blast shock front was found to be relatively small in the sense that the blast front shape remained essentially circular for all Mach numbers tested (up to 0.9), but, of course, the pattern is convected downstream more with increasing tunnel speed. The central cold-gas core also tends to be convected downstream (Fig. 2.3), but less so than the blast front.

Pressure time histories obtained from all transducers were digitized by ARO and were subsequently provided in the form of plots, tabulations and magnetic tapes (Ref. 2.1).

Sample pressure measurements in the blast field are shown in Figure 2.4 for the shock tube normal to the tunnel axis, $\phi=90^\circ$, measured at a radial distance of 4.5 tube diameters from the tube exit, at a tunnel Mach number of 0.8 and a ratio of tube driver pressure to driven pressure of about 10. It should be noted that for a polar angle (θ in Figure 2.1) of 15° a blast wave is produced with a nearly constant pressure level for about 0.2 milliseconds. In the polar angle range -15° to 30° useful nearly-constant blast durations of at least 0.1 millisecond are seen to have been produced; but for larger angles ($\theta \geq 45^\circ$) the pressure has an initial spike-behavior which makes it of little value for simulating blast shocks of long duration.

Similar results to those shown in Figure 2.4 were obtained for most conditions tested, covering shock-tube angles (ϕ) of 45, 60 and 90 degrees to the tunnel axis, tunnel Mach numbers of 0, 0.6, 0.75 and 0.9 and driver/driven-tube pressure ratios between about 4 and 30. Useful nearly-constant pressure blast durations up to a maximum of about 0.3 millisecond were obtained for some conditions.

In order to provide a more quantitative index of the obtained duration of nearly constant pressure, estimates were made for the 90° tube angle ($\phi = 90^\circ$) from curves like Figure 2.4 of the time, t_{30} , required for the blast overpressure to decay (or increase) 30 percent from the initial shock value. For blast overpressures between 2 and 5 psi at a radial distance of 4.5 diameters ($r/d = 4.5$), the 30-percent-

PART 120.3

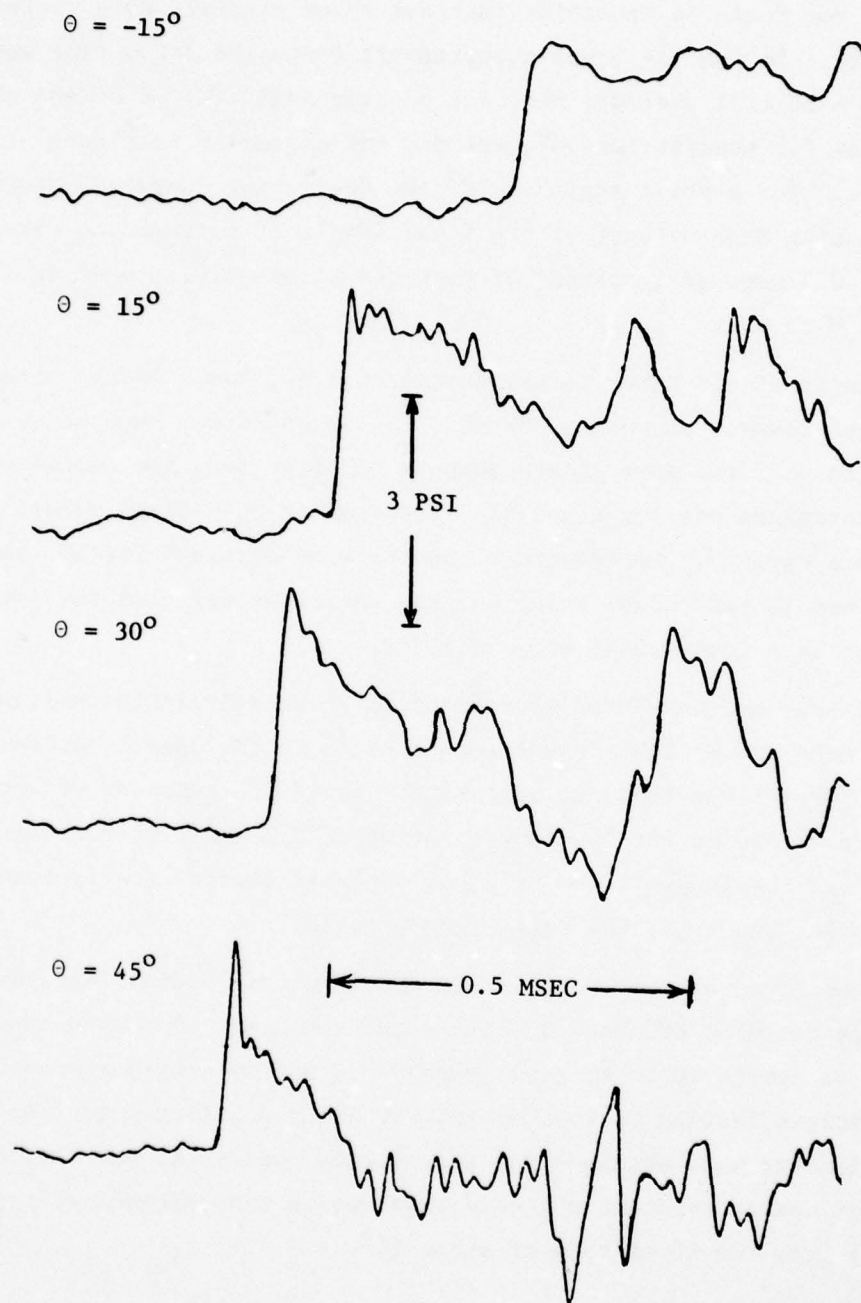


Figure 2.4. Transient blast pressures for a firing of a shock tube into a Mach 0.75 wind tunnel flow, $\phi = 90^\circ$.

decay time was found to generally increase about linearly with increasing overpressure. In the 4 - 5 psi overpressure range the decay time was about 0.16 msec or 1 msec/ft. dia. for a polar angle (θ) of 0° and about 0.09 msec or 0.5 msec/ft for 30° , and did not appear to vary much with Mach number. For a polar angle of 15° the decay time decreased considerably with increasing Mach number; at the 5 psi level, it appeared to vary from about 0.3 msec or 2 msec/ft at Mach 0.6 to about 0.18 msec or 1.1 msec/ft at Mach 0.9.

The angle of the tubes to the tunnel axis (ϕ) had a marked effect on the blast waves that were produced. As the angle was reduced, causing the blast to be fired more in the downstream direction, the resulting shock overpressure was lower and the overpressure at a fixed point decayed more rapidly. Satisfactory results were obtained for the tube at 90 degrees to the tunnel axis, so this angle was selected for later development of a large shock tube facility.

Blast pressure waveforms were found to be relatively insensitive to the shock-tube driven-tube/driver length ratio in the useful early-time (hot-gas) part of the flow period. Hardly any difference was observed between the waveforms for the length ratios of 0.5 and 2.0, but some waveforms for the length ratio of 8 had somewhat shorter nearly-constant durations than those for the other length ratios.

To summarize the test results, it appeared that useful long duration blast waves could be obtained by firing shock tubes into a wind tunnel operating at speeds up to at least Mach 0.9. Nearly constant pressure blast durations lasting up to a maximum of about 2 milliseconds per foot of tube diameter were obtained for some firing conditions and the longest duration of nearly constant pressure blast waves was obtained at polar angles (θ) from the shock tube of about 15° .

SECTION III
DEVELOPMENT OF 16T BLAST TEST FACILITY

Having established the feasibility of shock tube-wind tunnel blast tests by small model tests in the 1T tunnel, a program was undertaken to develop and apply a similar large shock tube facility for engine inlet testing in the AEDC 16T (sixteen foot square) transonic wind tunnel (Ref. 2.1). Development of this facility consisted of selection and modification of a inlet model, shock tube design, construction and testing, selection of dynamic instrumentation for measuring the blast field, and tunnel modifications.

The test installation was designed to take as much advantage as possible of existing hardware and fixtures.

3.1 GENERAL DESIGN CRITERIA

The inlet model selected for blast testing in the AEDC 16T tunnel is designated as the 0.1-scale B-1 Inlet Development Model II. This model was selected as having a representative transonic inlet of modern design which was already well instrumented with dynamic pressure engine face transducers of high enough frequencies to respond to blast induced transients. The model required only small modifications to strengthen it for blast testing and it was compatible with existing mounting fixtures for the 16T tunnel.

The important features of the model with respect to shock tube design are the size of the inlet opening, which is about 5.5" long by 4.4" wide by 3.3" high for each inlet, and the length of the inlet, about 25". Other model characteristics are discussed in Section 4.2.

The shock tubes had to be designed to produce a sufficiently small variation of incident shock pressure across the above inlet opening. Also the duration of the blast wave produced had to be at least long enough so that the blast wave does not decay significantly before its front has had time enough to pass down the inlet into the engine and to be reflected back past the engine face.

It appeared that the most cost-effective facility design satisfying the above requirements was to position the test model near the center of the tunnel, permitting use of existing fixtures, and to mount shock tubes in both tunnel walls, two in one wall and one in the other, as indicated in Figures 3.1 and 3.2. This design concept, using three shock tubes, permitted the firing of three blast waves at the model before the tunnel had to be shut down to change shock tube diaphragms, thus saving considerable time and expense. Dimensions and orientations of the three shock tubes were chosen to conform as close as practical to the optimum conditions obtained from the 1T model tests, namely, ratio of tube-to-inlet distance to tube diameter of about 4.5, polar angles from shock tube to inlet (θ) between -15° and $+30^\circ$, with about 15° being optimum, and shock tube axis perpendicular to tunnel wall ($\phi=90^\circ$). A common inside diameter of 22.6 inches appeared to be the best choice, which gave distance/diameter ratios of 4.3, 3.8 and 4.3 for shock tubes 1, 2, and 3, respectively. The resulting geometrical arrangement of tunnel, shock-tubes and model is shown schematically in Figure 3.1 and photographs of the setup are presented in Figure 3.2.

With respect to the question as to how uniform the blast pressure would be across the inlet opening, the results of the 1T tests indicated that for the above-selected model and shock tube geometry, the intensity of the blast wave would generally vary across one inlet not more than ± 2 percent from the mean value and at worst not exceeding ± 4 percent.

3.2 SHOCK TUBE DESIGN AND TESTING

Using the guidelines discussed in Section 3.1, ARO designed and constructed three similar 22.6 in-dia* shock-tube blast generators for

* A necked down shock tube driven section having a 13.1-inch exit diameter was also designed as an insert for any of the three shock tubes. This smaller diameter insert was constructed and several static firings were made with it to explore the possibility of obtaining a better blast waveform at low blast pressures than could be obtained with the large diameter tubes. This insert was also intended to provide more flexibility in the range of blast overpressures which could be obtained with a particular pair of diaphragms. However, the few firings made with this insert produced no obviously improved waveforms and the time required to install and remove the insert from a shock tube when installed in the 16T wind tunnel proved to be too long to be tolerated for the limited test time available. Consequently, no wind tunnel firings were made with the small diameter driven section insert.

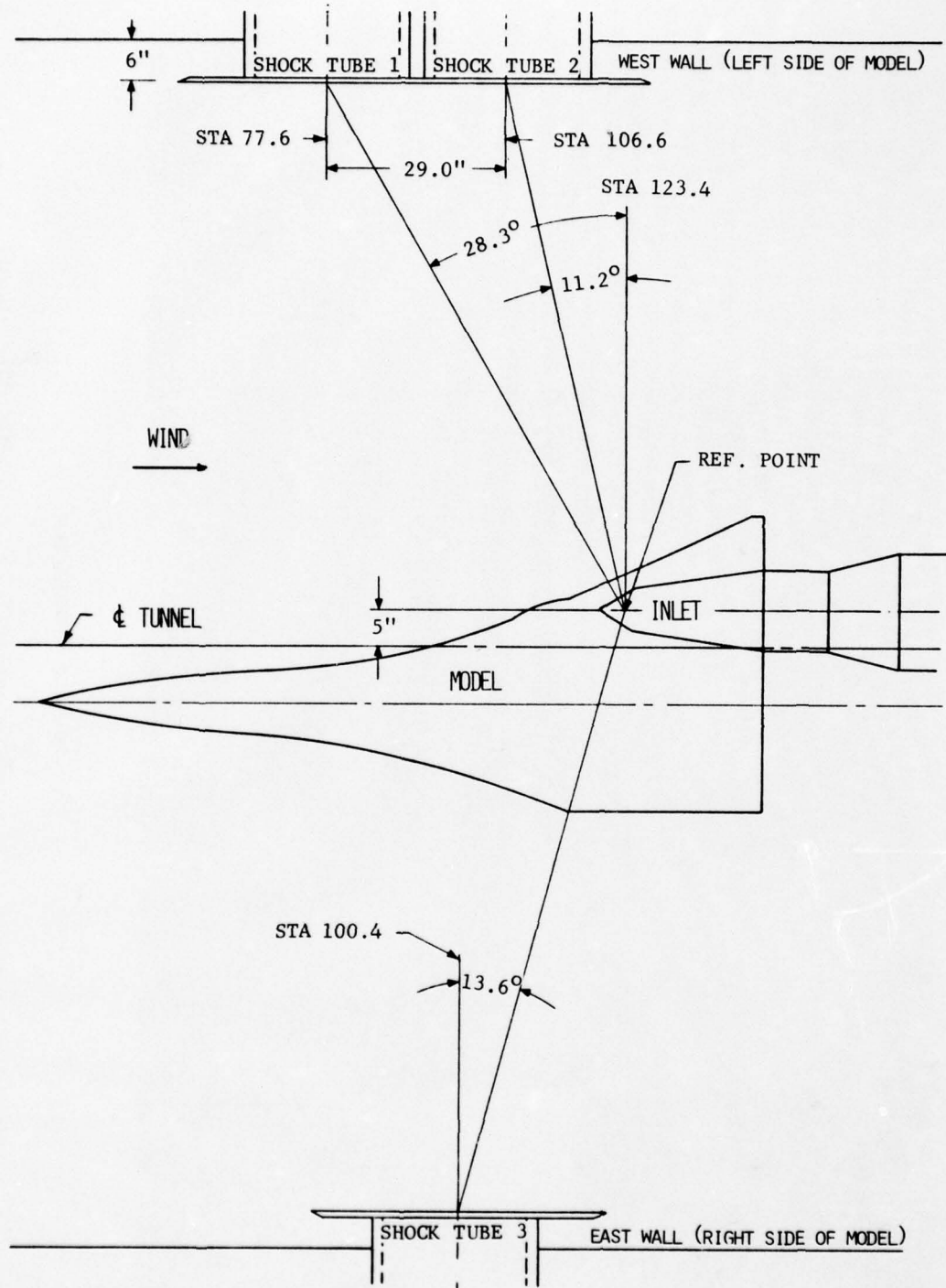
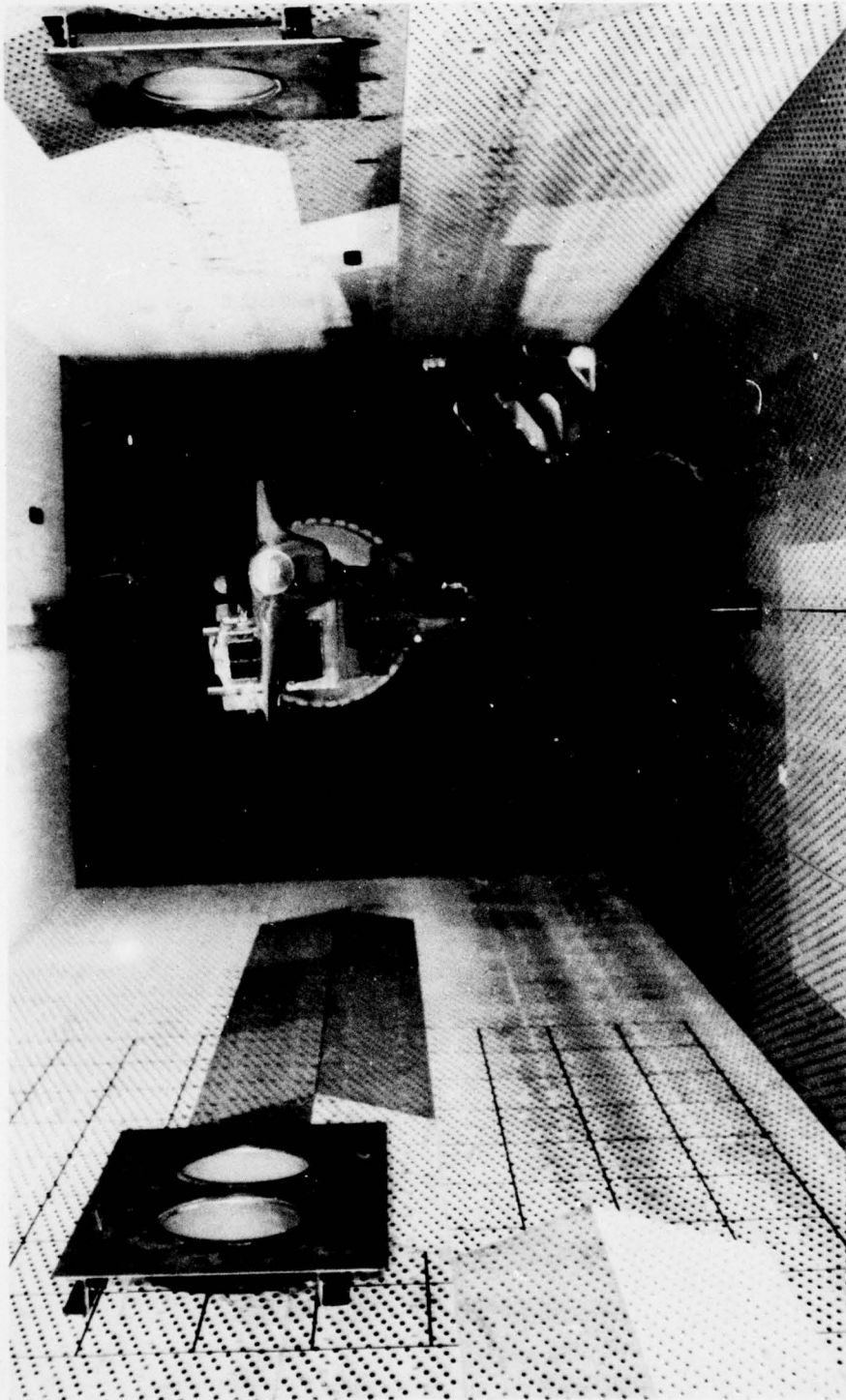
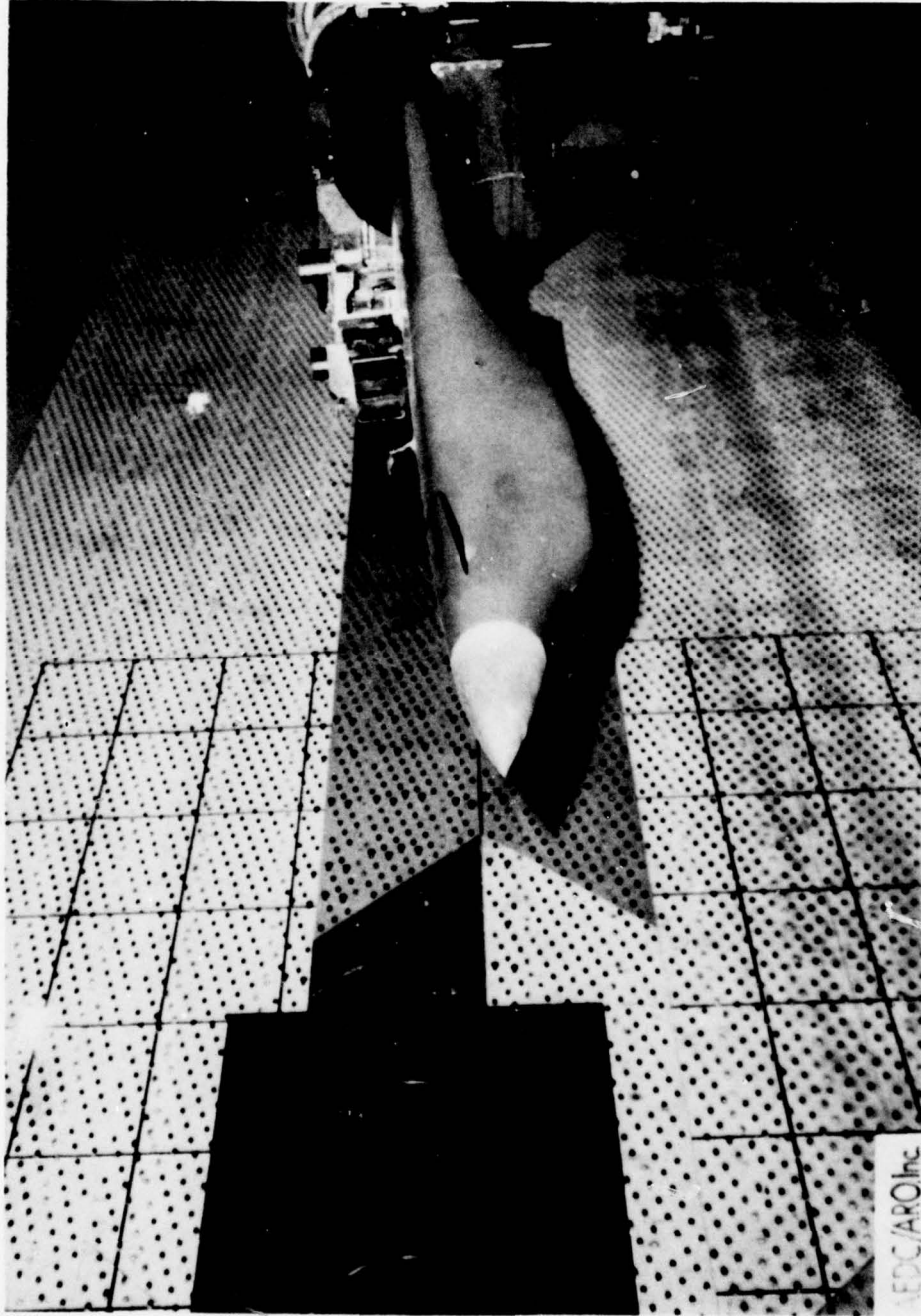


Figure 3.1. Top view of test installation in AEDC wind tunnel.



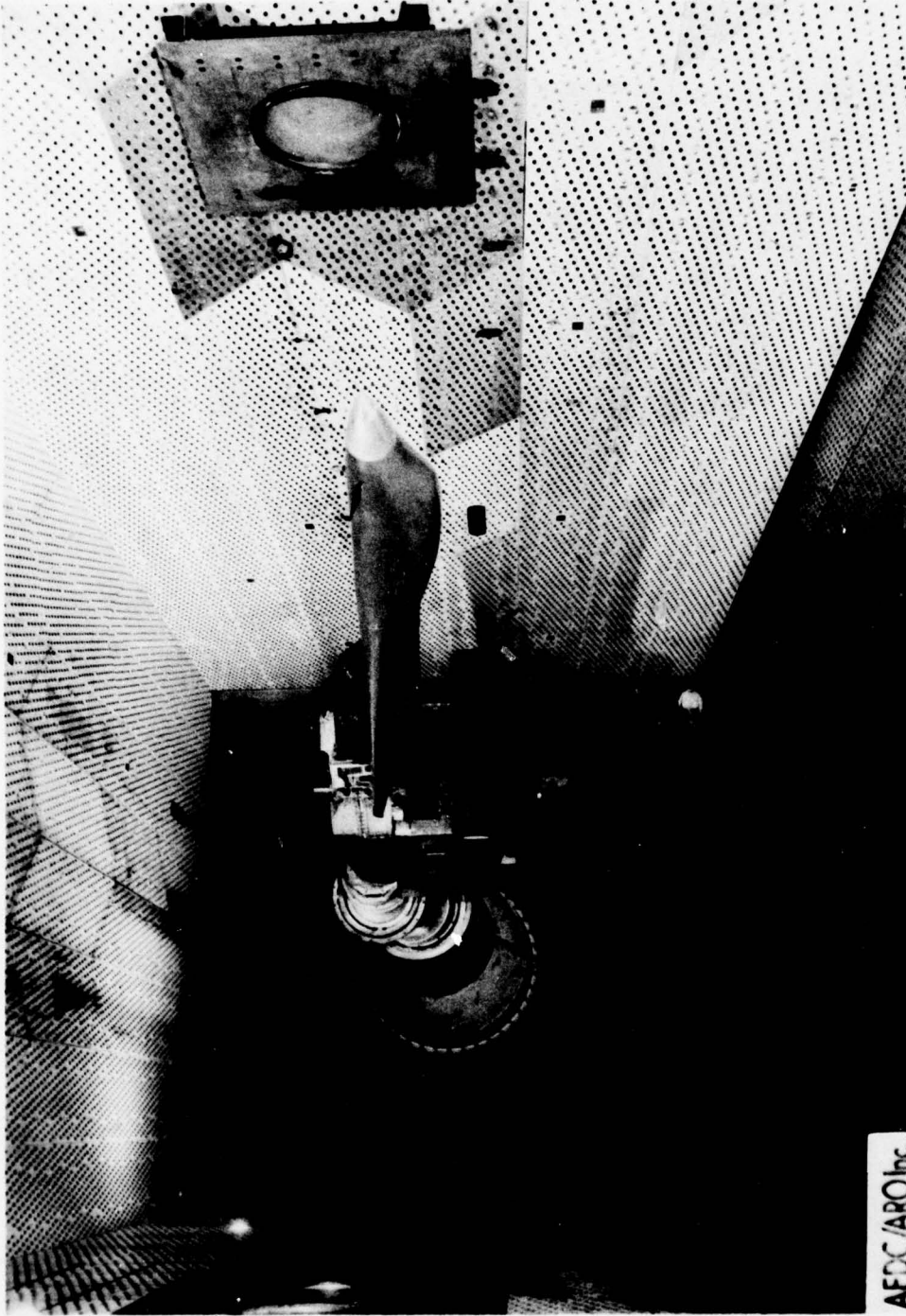
(a) View looking downstream.

Figure 3.2. Blast test setup in the AEDC 16T transonic wind tunnel.



(b) View showing model forebody and west wall.

Figure 3.2. Continued.



(c) View showing model, supports and east wall.

Figure 3.2. Concluded.

firing shock waves into the AEDC 16T tunnel. Some details of one of these tubes can be seen in Figure 3.3. The shock tube is about 17 feet long. The driven-tube length is about twice the driver tube length. The tube has a double diaphragm construction, and uses pre-scored prestressed 24 in-dia diaphragms. Diaphragms are constructed either of aluminum, nickel steel or 316 stainless steel, depending on the firing pressure level.

All three shock tubes had essentially the same design dimensions except that the ratio of the length of the driven section to that of the driver section had to be varied somewhat to permit close mounting of two of the tubes side by side in the 16T tunnel without interference. Judging from the results of the 1T tests (Sec. 2.2), these differences in lengths would not be expected to produce any significant differences between the blast waves generated by the three tubes.

Considerable effort was devoted to the design and operational use of the diaphragms. A series of 17 static firings was run to establish the range of loading pressures and other requirements for achievement of satisfactory diaphragm bursts in respect to the blast wave produced and avoidance of ejecta. A typical diaphragm break pattern is shown in Figure 3.4. The diaphragms generally broke cleanly on the pre-scored lines, forming four petals, and never produced any observable flying metallic debris.

Shock-tube operations were automated as much as possible in order to obtain a maximum number of firings in the few test days available for wind tunnel testing. Semi-automated diaphragm removal and replacement required less than 15 minutes per diaphragm pair and nearly fully automated pressurization and firing of a shock tube generally took less than 5 minutes.

The above-mentioned 17 static firings, made in the AEDC 16S wind tunnel facility at an ambient pressure of 0.5 atmosphere at driver pressures from 62 to 233 psia, were also utilized to obtain measurements of blast overpressures and impact pressures produced by the shock tube flow, both for protective design of wind tunnel equipment to be in the path of the jet from the shock tube and for providing a guide for diaphragm

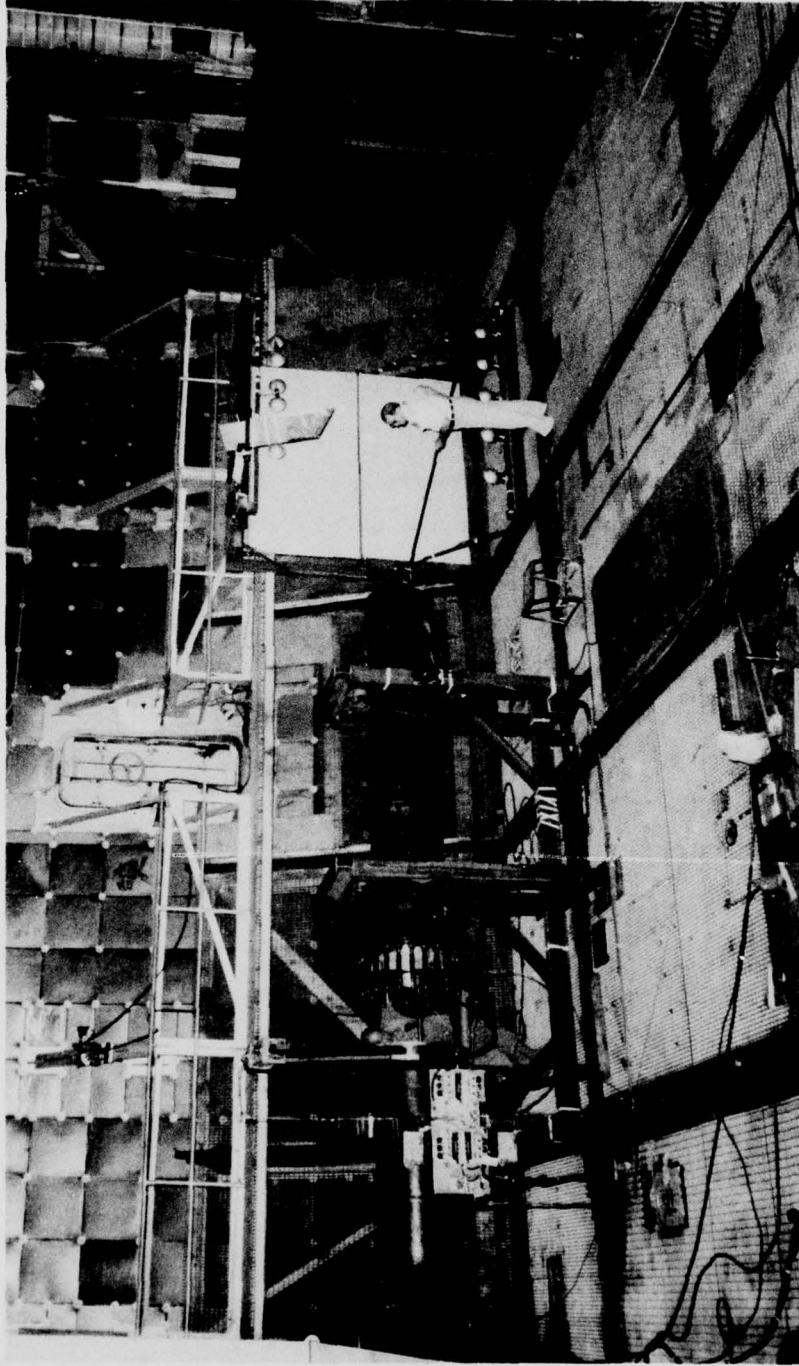
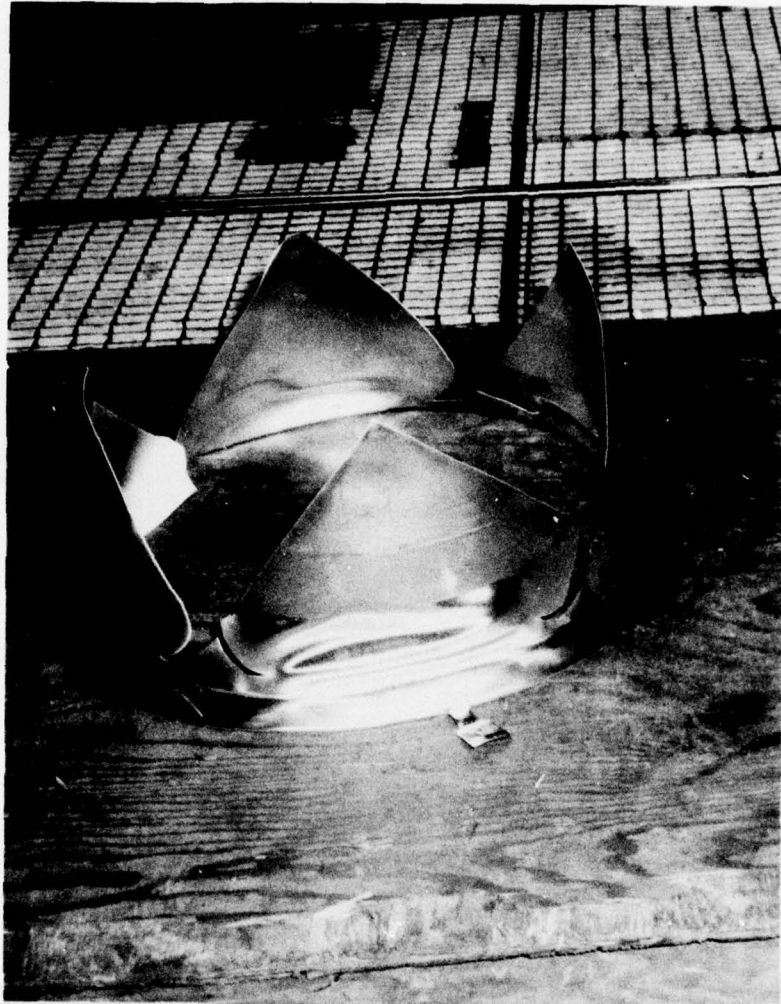


Figure 3.3. 23-inch-diameter shock tube setup for testing.



AEDC/ARO, Inc.

Figure 3.4. Typical diaphragm rupture pattern.

selection to achieve desired levels of blast overpressure at the test model during wind tunnel firings.

3.3 BLAST INPUT INSTRUMENTATION

In order to provide measurements of blast wave intensity and direction as the blast wave strikes the inlet, three similar claw probes were designed to be mounted on or near the test model. Figure 3.5 shows a photograph of one of these probes mounted above the tested inlet. Each probe consists basically of two 45°-swept claw arms (90° apart) with Kulite series XCQL-093-025 type dynamic pressure transducers at the tips, to measure total pressure and flow direction, and of a flat plate surface toward the rear of the probe with one static pressure orifice and one imbedded Kulite LQ series wafer pressure transducer to measure the pre-blast and transient "static" blast pressures, respectively. The three claw probes were calibrated in the AEDC 16T tunnel for sideslip angles from about -50 to + 50 degrees at Mach numbers of 0.6, 0.7, 0.85 and 0.95. The calibration data indicated that the probes could provide reasonable estimates of flow characteristics for sideslip angles between about -30 and +30 degrees.

3.4 TUNNEL WALL MODIFICATIONS

Preliminary KA estimates of the forces which would be imposed on the 16T wind tunnel wall opposite a firing shock tube indicated that the local wall pressures could greatly exceed the tunnel wall design criterion of 3 psi differential pressure. To obtain design information on such wall loads, during the shock tube calibration test (Sec. 3.2), ARO fired one of the 22.6 in-dia shock tube at a large plate instrumented with an array of pressure transducers. Using these test results as a guideline, the tunnel walls were strengthened in critical areas. In the subsequent test program in the wind tunnel, no damage was experienced to the tunnel walls during any shock tube firing.

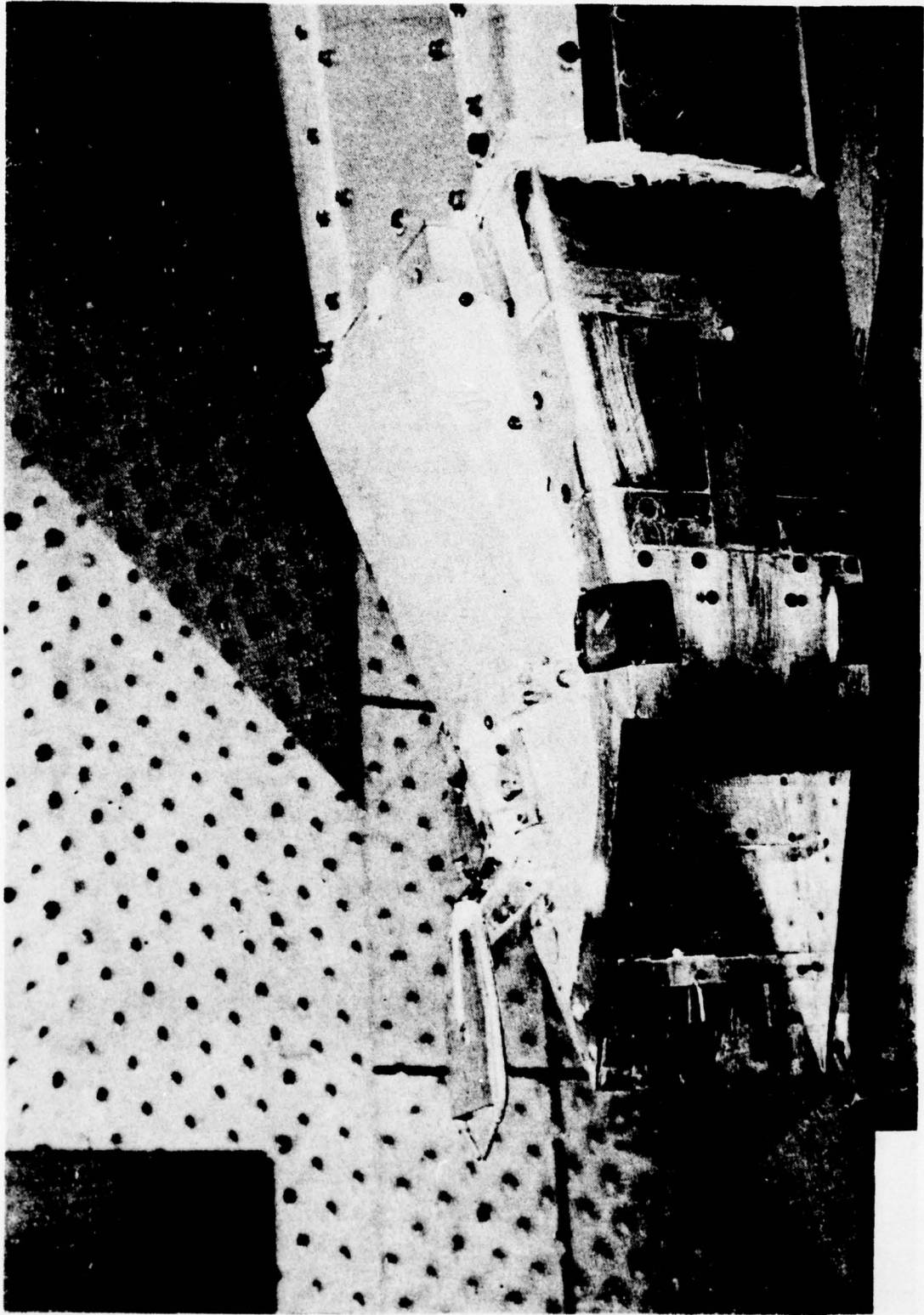


Figure 3.5. Oblique view of a claw probe mounted above the inlet model.

SECTION IV

16T WIND TUNNEL BLAST TEST PROGRAM

Following development of the 16T wind tunnel blast test facility, a series of 45 wind tunnel shock tube firings were performed with the 0.1-scale B-1 inlet model. This section presents a discussion of the details of the test setup, instrumentation, and firing conditions and presents and discusses some aspects of sample data obtained from the tests.

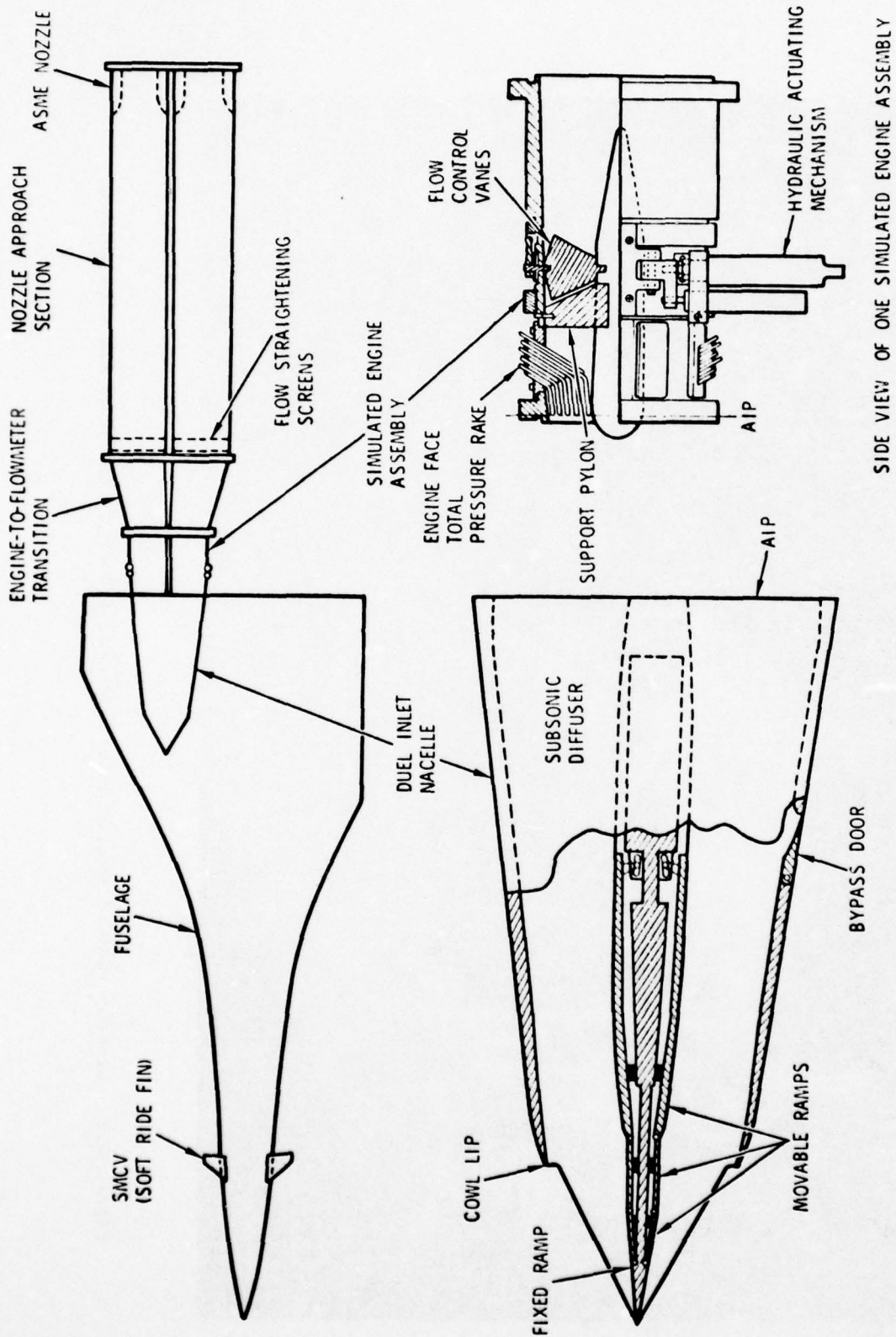
4.1 GENERAL TEST SETUP

As was mentioned in Section 3, the test setup consisted of a 0.1-scale B-1 model installed in an inverted position near the center of the AEDC 16T transonic tunnel, with three shock tubes projecting through the tunnel side walls (Fig. 3.1). Figure 3.2 presents photographs of the model and shock tube setup inside the tunnel. Various details of model construction are shown in Figures 3.5, 4.1 and 4.2. During all tests the model was maintained at an angle of attack of +3 degrees.

Blast waves can be fired at the model inlet from any of the three 22.6 in-dia shock tubes seen projecting into the tunnel about 6 inches from the side walls in Figure 3.2. The shock-tube axes are perpendicular to the side walls ($\phi=90^\circ$) and the axis of each tube is located at a fixed location between 1 and 4 feet upstream of the inlet opening, so that, for all three shock tubes, the inlet is located within the polar angle range (θ) 12 to 29 degrees from the shock-tube exit (Figure 3.1), the angles being 28.3° , 11.2° and 13.6° for tubes 1, 2 and 3, respectively. These locations were chosen to give blast waves of as long duration as practical, whose fronts would generally strike the inlet roughly side-on or slightly from the rearward.

4.2 MODEL AND INSTRUMENTATION DETAILS

The most important features of the inlet model used for the blast test are illustrated in Figures 4.1 through 4.4 (see also Ref. 4.1). The model is a 0.1-scale representation of the forward part of the B-1 aircraft fuselage with a left-hand stub wing set at the 67.5° - sweep position and a left-hand dual inlet. The normally variable geometry



SIDE VIEW OF ONE SIMULATED ENGINE ASSEMBLY

Figure 4.1. Details of inlet model and engine simulation. (Rockwell drawing)

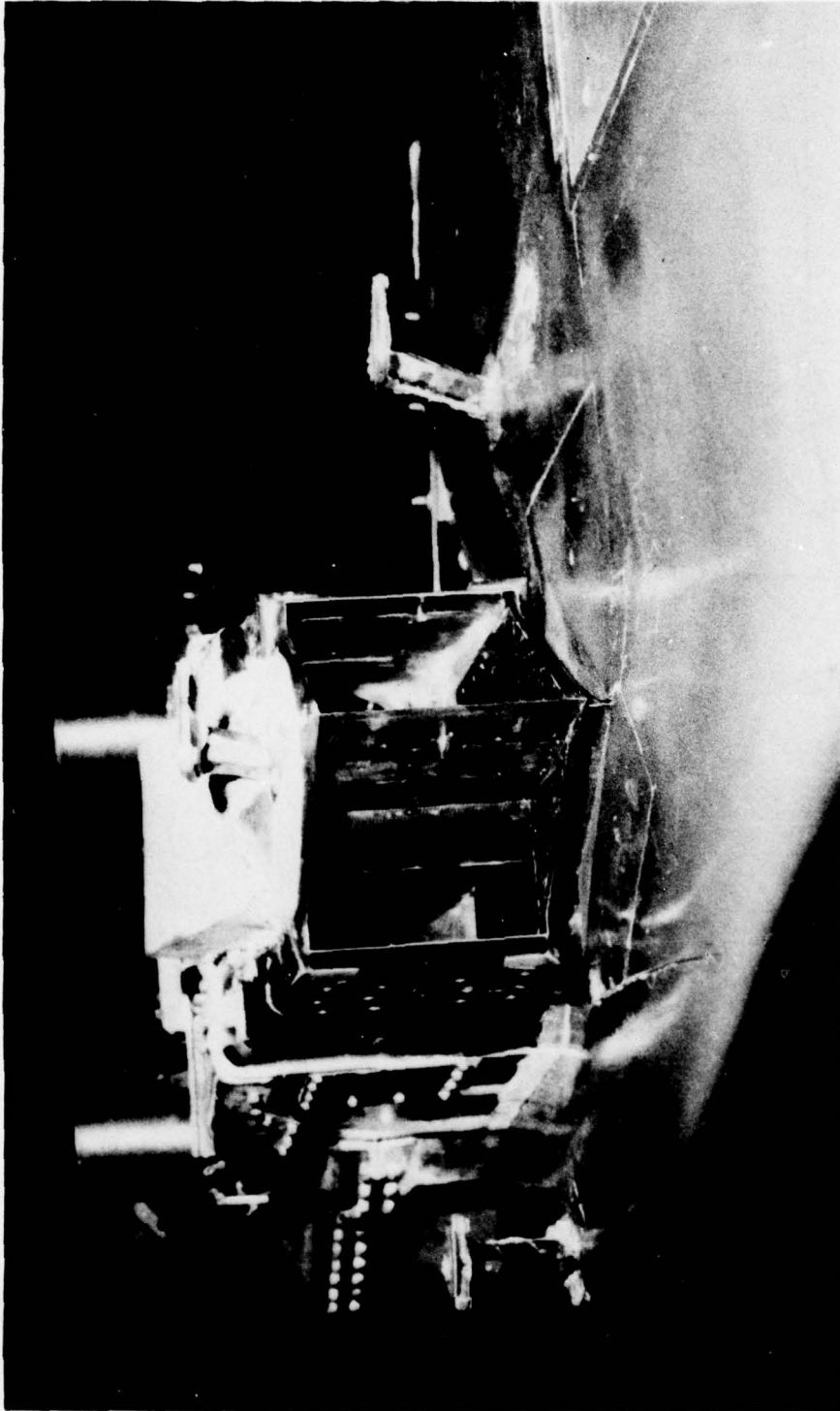


Figure 4.2. Closeup view of engine inlet and claw probes in the AEDC 16T wind tunnel.

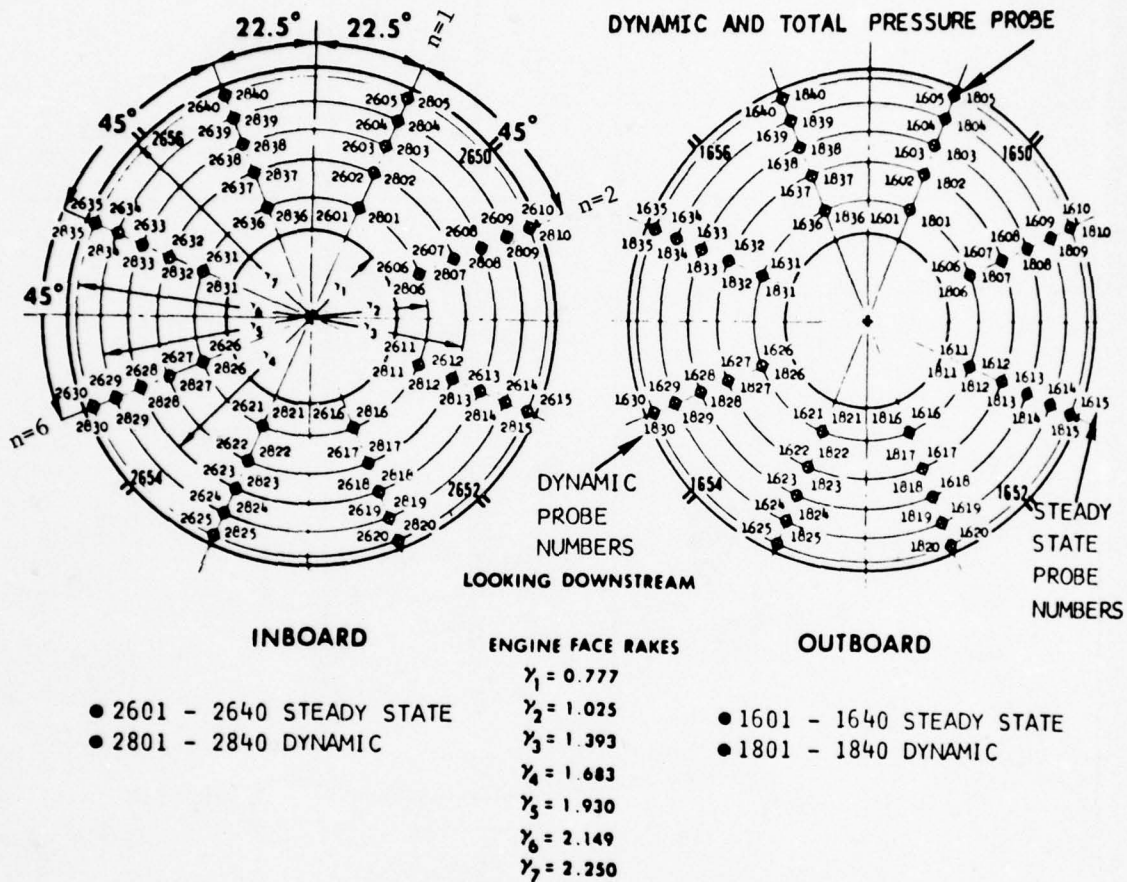


Figure 4.3. Engine face transducer locations. (Rockwell drawing)

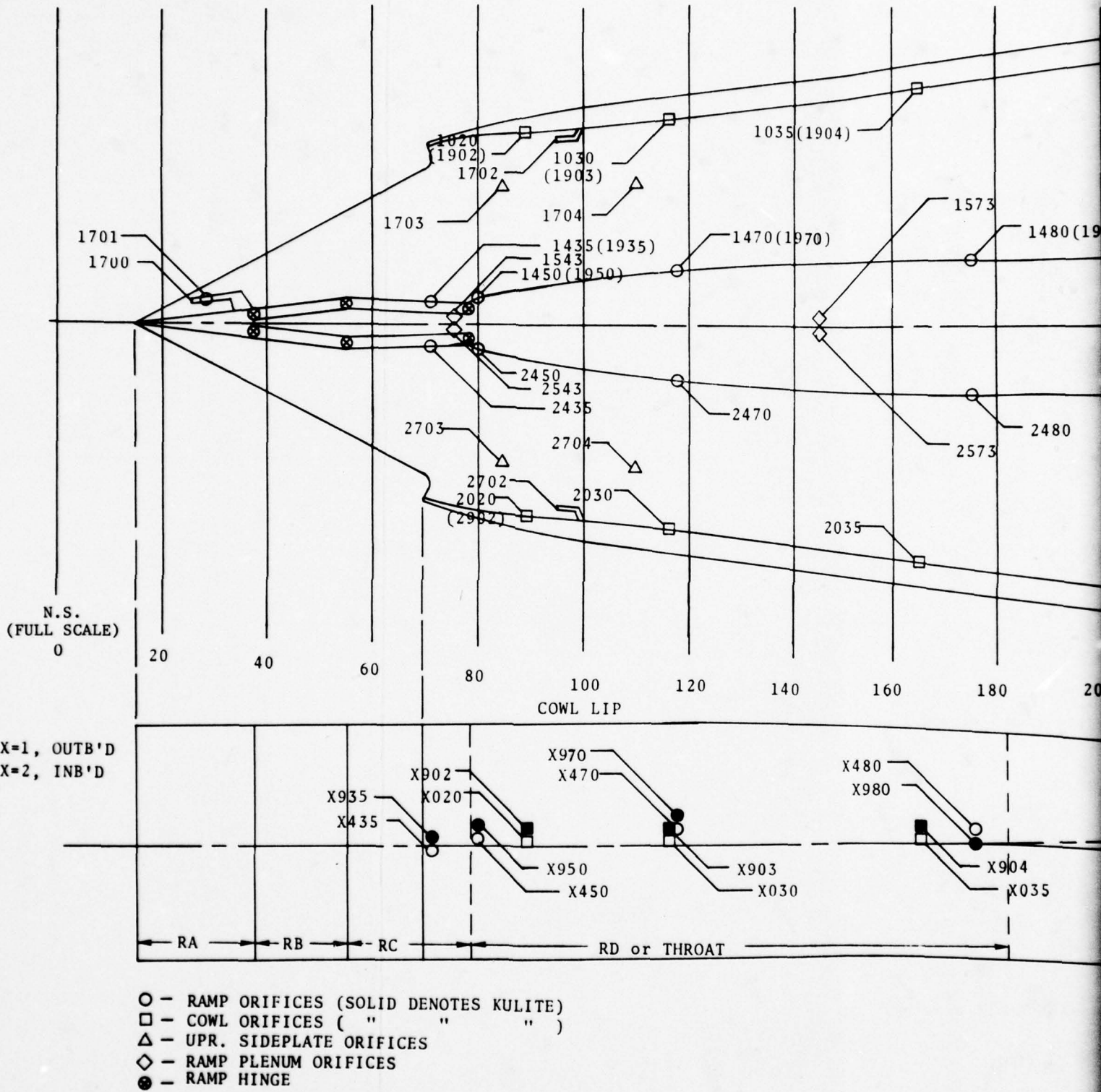


Figure 4.4.

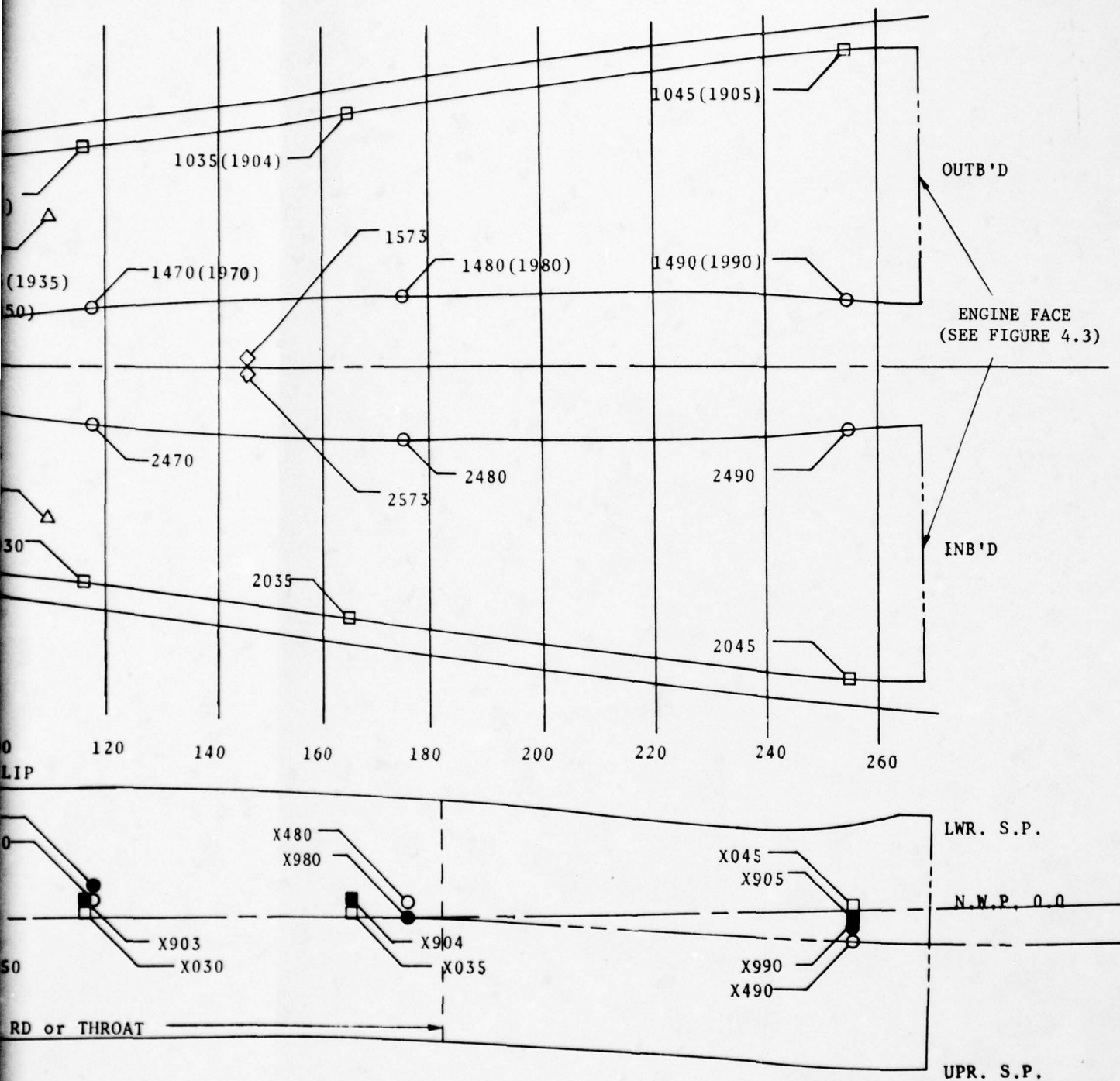


Figure 4.4. Inlet instrumentation. (Rockwell drawing)

inlet ramp system for the model was fixed for these tests in the normal subsonic cruise position. The engine face is located at Nacelle Station 269.5. The aircraft engine is simulated by an engine hub structure and by remotely actuated hydraulically operated flow control vanes which produce prescribed choked flow rates in the simulated engine at a position about 4.5 inches downstream of the engine face.

Forty combination steady-state and dynamic total-pressure probes are located in each inlet at the engine face section, located as indicated in Figures 4.3 and 4.4 and in Table 4.1. The dynamic probes used Kulite type CQL-080-25 transducers, which were found, from pre-test shock tube calibrations, to generally have response times to transient pulses of about 25 microseconds or less. These Kulite transducers had a 25-psi range, 0.080-in diameter and about 125 kHz natural frequency.

Other model instrumentation consisted of 54 static-pressure orifices and 10 dynamic Kulite transducers whose locations are described in Reference 4.1 (some indicated in Fig. 4.4). The 10 Kulite transducers, each accompanied by a static-pressure orifice, were mounted inside and flush with the inlet wall in the locations indicated in Figure 4.4 (also Fig. 5.4) and Table 4.1. These transducers were used to monitor inlet ramp and cowl pressures. All but one of these transducers were mounted in the outboard inlet.

Also mounted on the model were three claw probes, described in Section 3.3, to measure the characteristics of the blast wave at the model. Figures 3.5 and 4.2 indicate the locations of these three probes. Probe 2 was located just above the forward tip of the inlet; Probes 1 and 3 were located just above the wing surface, about 9.3 inches outboard and inboard of the inlet centerline, respectively, with their tips located at the same longitudinal station as the inlet cowl tips.

4.3 16T WIND TUNNEL TESTS

The 16T wind-tunnel blast test program was designed to obtain data on the blast response of the test model for a range of overpressures from 2 to 5 psi (scaled to 1 atmosphere ambient pressure) for tunnel

TABLE 4.1
LOCATIONS OF DYNAMIC PRESSURE TRANSDUCERS⁺

Engine face pressures (see Figure 4.3)

TYPE	RADIUS (Inches)	ORIFICE NUMBER							
		$\emptyset=22.5$	67.5°	112.5°	157.5°	202.5°	247.5°	292.5°	337.5°
Total ↓	1.025	801	806	811	816	821	826	831	836
	1.393	802	807	812	817	822	827	832	837
	1.683	803	808	813	818	823	828	833	838
	1.930	804	809	814	819	824	829	834	839
	2.149	805	810	815	820	825	830	835	840

Add 1000 to tube number for outboard inlet; add 2000 to tube number for inboard inlet.

Cowl unsteady-state pressures (see Figure 4.4 or 5.4)

Transducer Number		Type	Location	
Outboard	Inboard		N.S.*	Remarks
1902	2902	Static	8.90	Buzz indicator
1903	-	"	11.60	Cowl static
1904	-	"	16.50	Cowl static
1905	-	"	25.45	Cowl static

Ramp unsteady-state pressures outboard inlet (see Figure 4.4 or 5.4)

1935		Static	6.90	Third ramp
1950		"	7.91	Aft ramp
1970		"	11.70	Aft ramp
1980		"	17.42	Aft ramp
1990		"	25.45	Aft ramp

*Nacelle station in inches (model scale).

⁺This page modified from Reference 4.1.

Mach numbers from 0.55 to 0.90 and for inlet flow rates representative of cruise and maximum power conditions. Table 4.2 outlines the test matrix which was followed to cover these conditions.

Tunnel testing was performed over a three night period, on 24 September and 27-28 September 1976. Testing consisted of calibrations, steady-state runs and a series of blast firings as described below. All tests were performed at below one atmosphere ambient pressures (usually 0.5 atmosphere) to minimize blast loads on the model and equipment, subject to the limit of a minimum Reynolds number per foot of 2.5×10^6 .

4.3.1 Unyawed Steady-State Tests

Prior to the blast tests, a series of unyawed steady-state runs were made covering all Mach number and inlet mass flow rate ranges of interest. These runs were made partly as a calibration of the inlet model vanes to control mass flow rate and partly to verify that the inlet steady-state distortion properties were the same as were found in previous tests of the model.

Steady state runs were also made immediately before each shock tube firing to provide reference (pre-blast) pressures at all dynamic pressure transducer locations. (The dynamic pressure transducers measure only changes of pressure; absolute pressures are obtained by adding pre-blast (steady-state) pressures to the dynamic pressures). Results of these pre-blast steady-state tests are presented in Appendix B.

4.3.2 Yawed Steady-State Tests

A few steady-state runs were made with the model at various yawed positions in the range -10 to +10 degrees, according to the schedule given in Table 4.3. These runs were made partly to calibrate the inlet flow controls under yawed conditions and partly to aid in assessing the quasi-steady late-time response of the inlet to the side-slip effects of blast waves of very long duration.

4.3.3 Shock Tube Firings

Forty-five shock tube firings were performed in the AEDC 16T tunnel at tunnel Mach numbers of 0, 0.55, 0.70, 0.85 and 0.90. Tests were

TABLE 4.2

NOMINAL TEST CONDITIONS

Mach No.	Flight conditions	Mass flow (lb/sec [†])	Overpressure* (psi)	Yaw (deg)
0	Parked	0	4	0
0.55	Cruise	235	4	0
0.55	Max. power	350	4	0
0.70	Cruise	300	2,3,4	0
0.70	Max. power	350	2,3,4,5	0,5
0.85	Cruise	300	2,3,4,5	0
0.85	Max. power	350	4,5	0
0.90	Max. power	350	4	0

[†] Full scale values (divide by 100 to obtain model values)

* Scaled to ambient pressure of one atmosphere

TABLE 4.3

STEADY-STATE YAW CONDITIONS

Mach no.	Flow rate (lb/sec)	Yaw angle range (deg)
0.55	352	-10 to +10
0.70	303	-10 to +10
0.70	352	-10 to +10
0.85	350	-10 to +7.5

generally performed with the tunnel static pressure set at about 1/2 atmosphere, except for the Mach 0.55 runs, for which about 2/3 atmosphere was used. The inlet mass flow rate was generally set to simulate both cruise and maximum power flight conditions for each Mach number condition according to the schedule in Table 4.2. This schedule required testing at mass flow rates of about 235, 300, and 350 lb/sec (full scale)*.

Tunnel steady-state pre-blast conditions are tabulated in Table 4.4 and Appendix B. Tunnel total temperature was 569° ($\pm 1^{\circ}$) for all firings with the tunnel turned on and was 534° R for the one static firing. Firings were made over a range of overpressures from about 2 to 6 psi, scaled to a tunnel ambient pressure of one atmosphere.**

Also presented in Table 4.4 are estimated values of the blast overpressure (Δp) and the blast intercept angle (ϕ) as the blast wave strikes the inlet. The source and accuracy of these values is discussed subsequently in Section 4.6.

4.4 DATA REDUCTION

The test data obtained from each shock tube firing were digitized by ARO at time intervals of 10.45 microseconds for a total of 2048 samples per firing. The resulting digital data were provided to KA in the form of magnetic tapes and time history plots of most of the basic data and derived quantities (Ref. 4.2). Tabular time history printouts of a few variables were also provided by ARO.

4.5 SAMPLE TEST RESULTS

Pressure time histories for typical pressure transducers are presented in Figure 4.5 for a typical shock tube firing (Run 8/Part 573) to illustrate the major features of the test data. In general, in this figure, the ordinate label designates the variable measured and the vertical scale is always either pressure/ p_{t_0} or pressure/ p_0 (the latter

* All mass flow rates in this report are scaled to full scale conditions. Model values are 1/100 of these values.

** It should be noted that all blast pressure values designated as Δp in this report are all scaled to a tunnel ambient pressure of one atmosphere. Pressures not specifically designated as Δp , such as shock tube driver pressures in Table 4.4 and all pressure values in Appendix B are actual test pressures.

TABLE 4.4
16T WIND TUNNEL TEST CONDITIONS

Run	Part Point No.	Mach No.	Flow Rate (lb/sec)		Tube No.	Tube Pressure (psia)	Nominal Shock Overpressure (psi)	Intercept Angle (deg)	Yaw Ang. (deg)			
			OB Inlet	IB Inlet								
1	501.01	0	0	0	2	69	2.7	79	0			
2	615.03	.552	235	235	3	186	4.7	91	↓			
3	591.03	.550	351	348	1	157	3.7	76				
4	589.03	.551	351	348	2	115	3.8	97				
5	590.02	.549	351	349	3	124	4.0	94				
6	602.02	.700	302	300	1	72	2.6	86				
7	600.04	.701	302	302	2	58	2.6	106				
8	573.04	.700	304	302	↓	112	5.0	98				
9	601.03	.701	302	300	3	69	3.0	104				
10	574.03	.701	303	300	↓	132	4.4	97				
11	621.03	.700	351	351	1	73	3.0	84				
12	519.02	.699	348	344	↓	103	3.8	88				
13	527.02	.700	349	344	↓	135	4.8	78				
14	626.02	.701	352	352	↓	142	4.8	79				
15	512.03	.700	351	344	2	59	2.8	103				
16	517.02	.700	349	344	↓	85	3.8	103				
17	525.02	.701	348	344	↓	113	5.0	100				
18	624.02	.700	350	350	↓	139	5.2	99				
19	513.03	.700	351	344	3	70	3.0	102				
20	518.02	.700	348	343	↓	102	4.2	99				
21	526.02	.700	349	344	↓	133	4.8	98				
22	625.02	.701	350	350	↓	155	5.6	92				
23	570.03	.699	351	350	1	144	3.6	87		+5.0		
24	568.04	.700	350	349	2	132	5.8	103		+5.0		
25	569.03	.703	350	349	3	143	4.2	105		-5.0		
26	559.02	.850	300	298	1	61	2.2	89		0		
27	598.03	.848	299	299	↓	90	3.0	85	↓			
28	584.03	.847	294	293	↓	122	5.0	82				
29	608.04	.850	299	299	↓	142	4.4	82				
30	557.04	.850	300	298	2	55	-	-		↓		
31	596.05	.848	300	300	↓	73	3.8	108				
32	582.03	.847	300	297	↓	94	4.4	105				
33	606.03	.849	300	299	↓	120	-	-				
34	558.03	.850	303	301	3	60	>2	-				
35	597.03	.848	300	300	↓	85	4.0	104				
36	583.03	.847	298	296	↓	114	4.4	102				
37	607.03	.850	299	298	↓	140	4.8	108				
38	546.02	.847	348	347	1	121	3.6	84			↓	
39	544.04	.847	348	347	2	94	4.0	107				
40	619.02	.850	352	351	↓	120	5.8	110				
41	545.03	.847	348	347	3	113	4.4	105				
42	620.02	.850	351	350	↓	139	5.6	100				
43	553.03	.900	327	329	1	117	3.0	86				↓
44	550.02	.899	349	354	2	86	4.0	107				
45	551.01	.900	349	354	3	104	4.2	105				

FIGURE 4.5.
SAMPLE TEST RESULTS
FOR RUN 8 (PART 573), MACH 0.70,
FLOW RATE \approx 303 LB/SEC, TUBE 2, $\Delta p = 5.0$ PSI

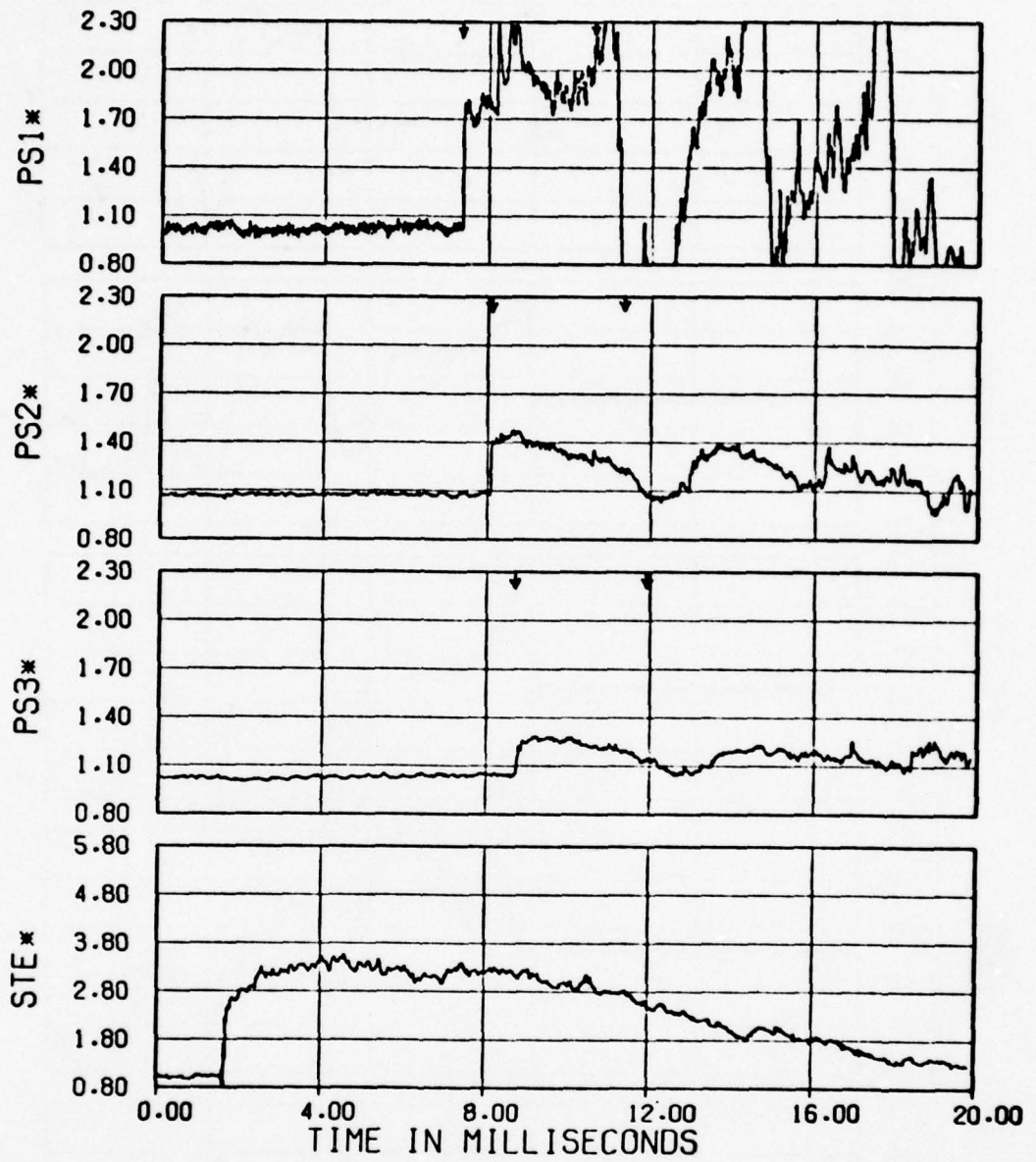


Figure 4.5a. Blast and shock tube pressures.

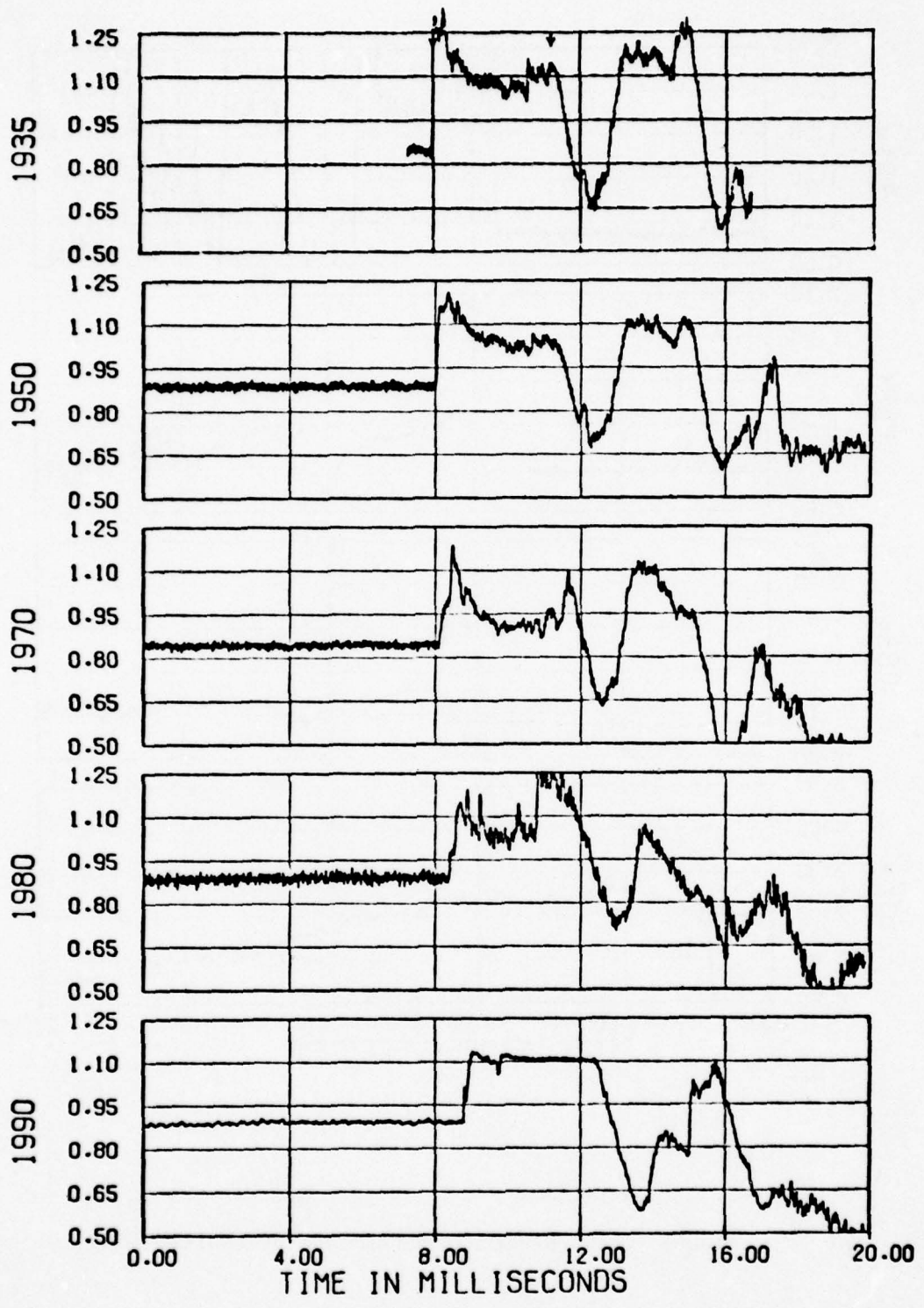


Figure 4.5b. Ramp pressures.

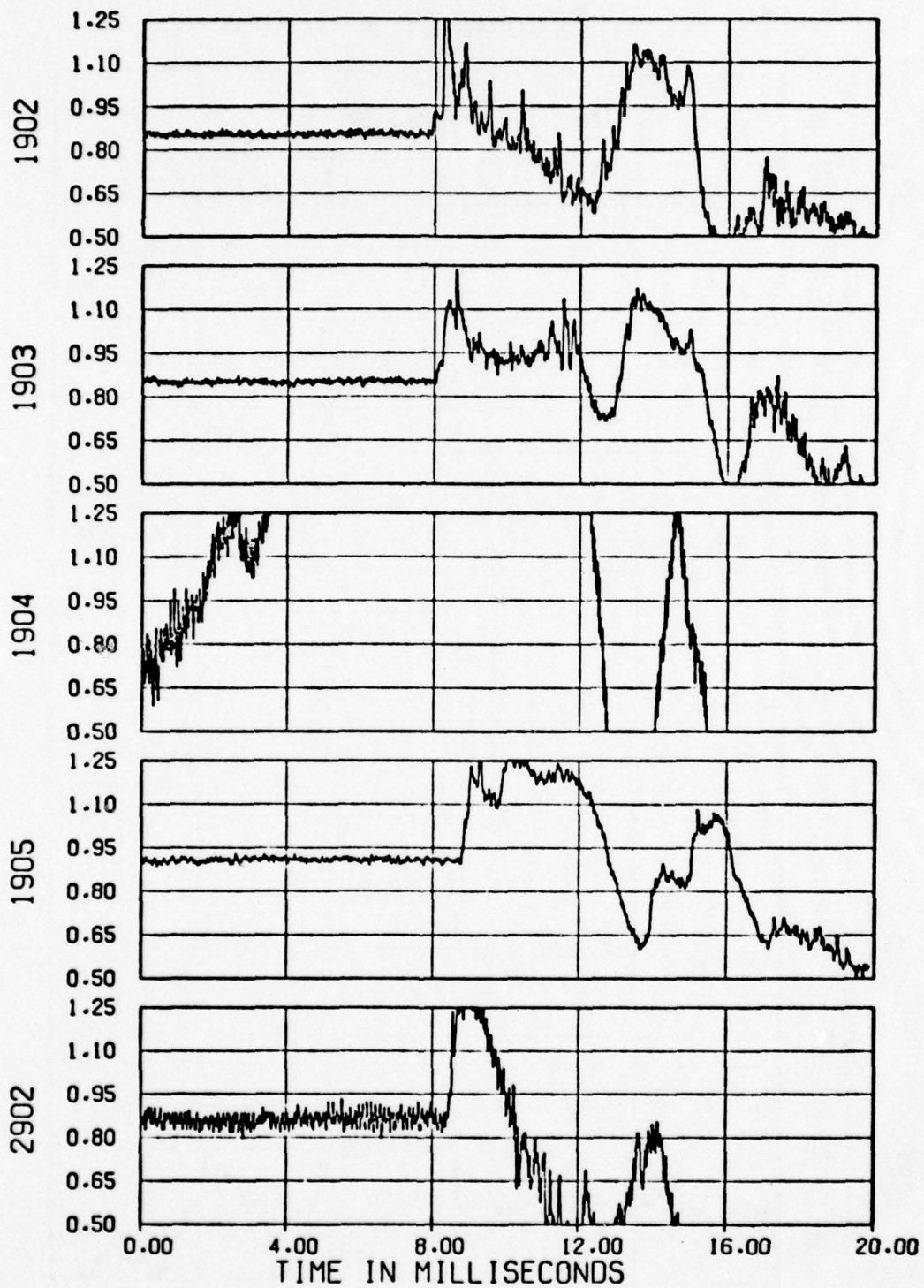


Figure 4.5c. Cowl pressures.

OUTBOARD INLET

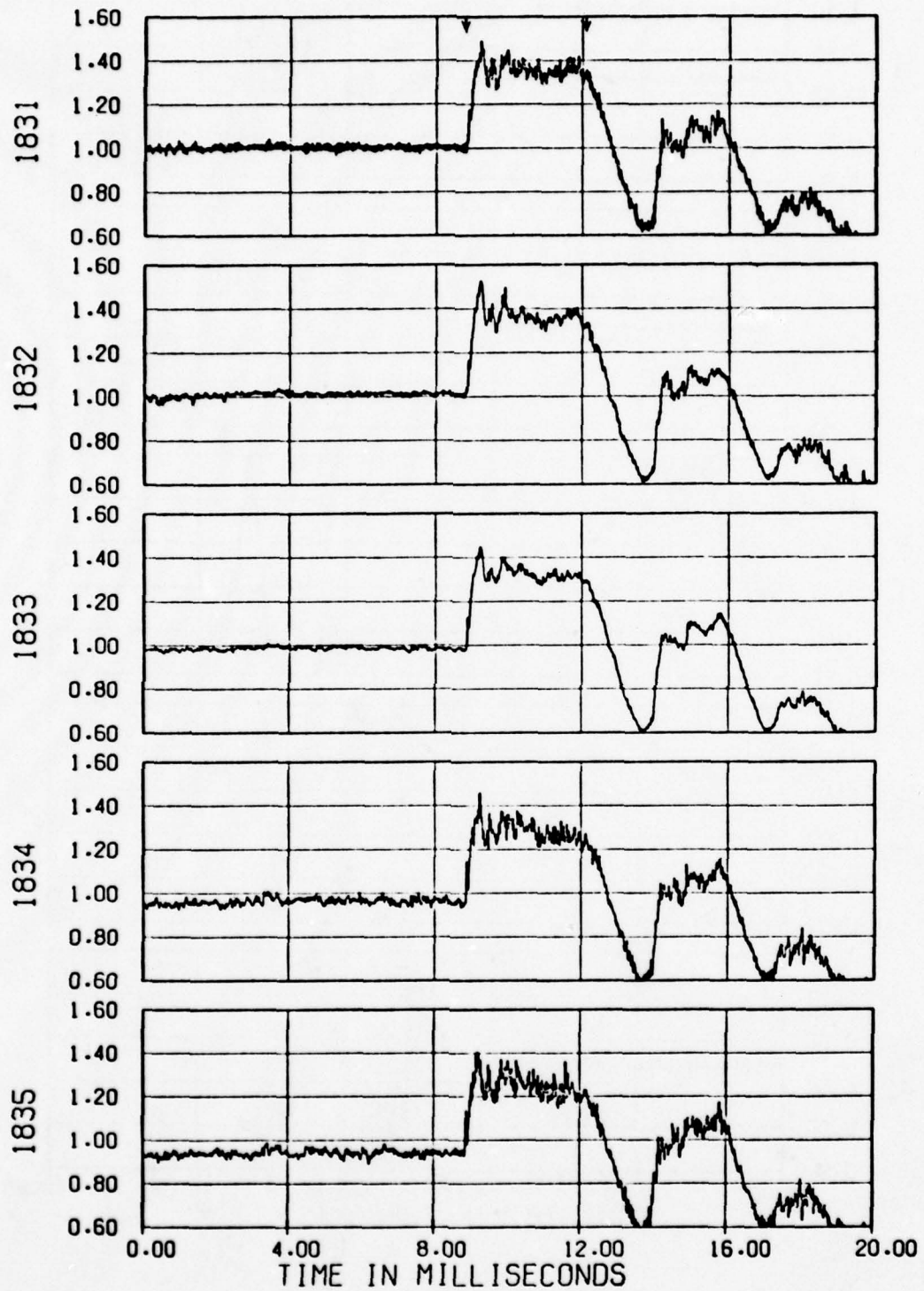


Figure 4.5d. Blastward inlet engine face total pressures.

INBOARD INLET

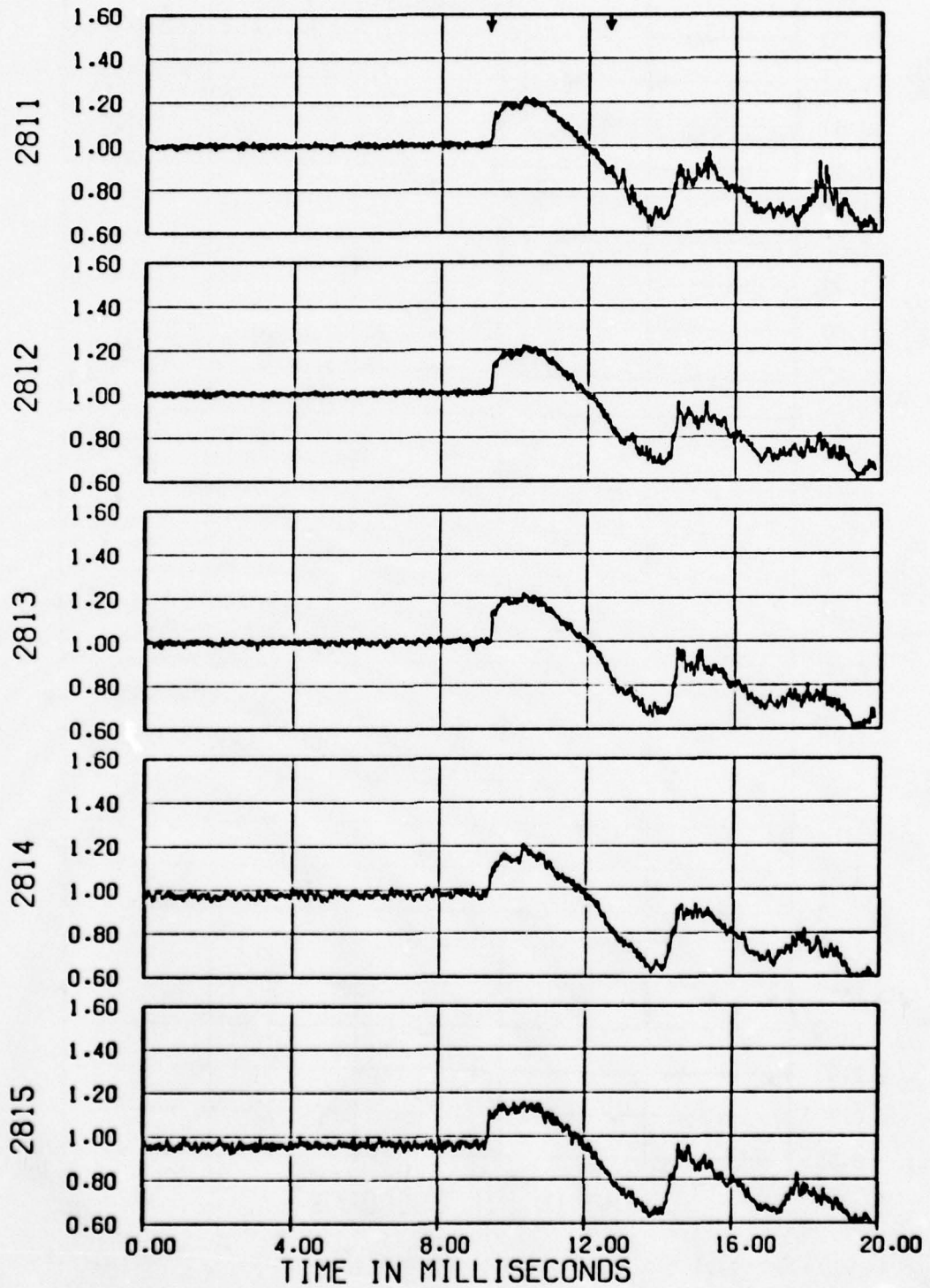


Figure 4.5e. Leeward inlet engine face total pressures.

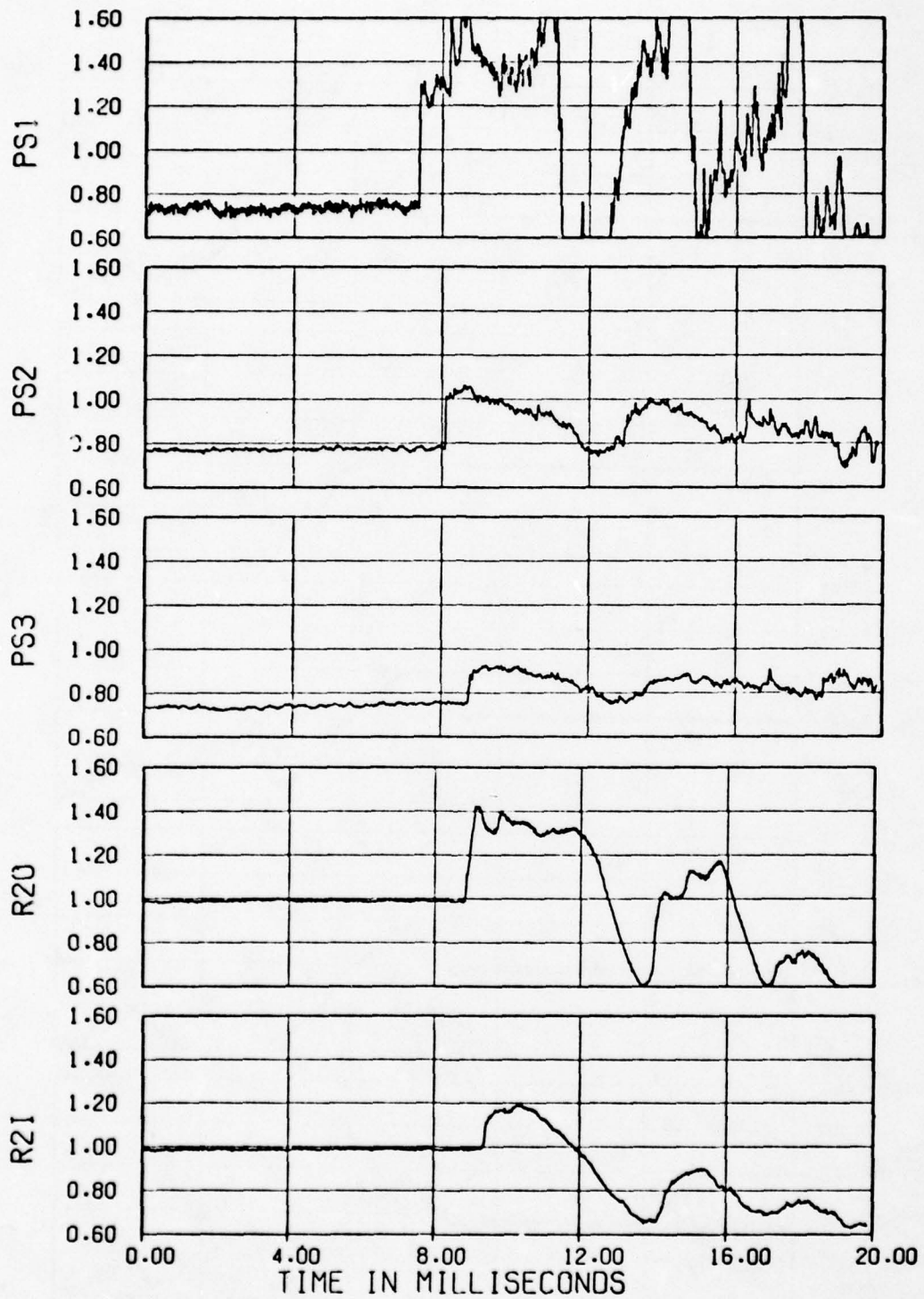


Figure 4.5f. External blast pressures and average engine face total pressures.

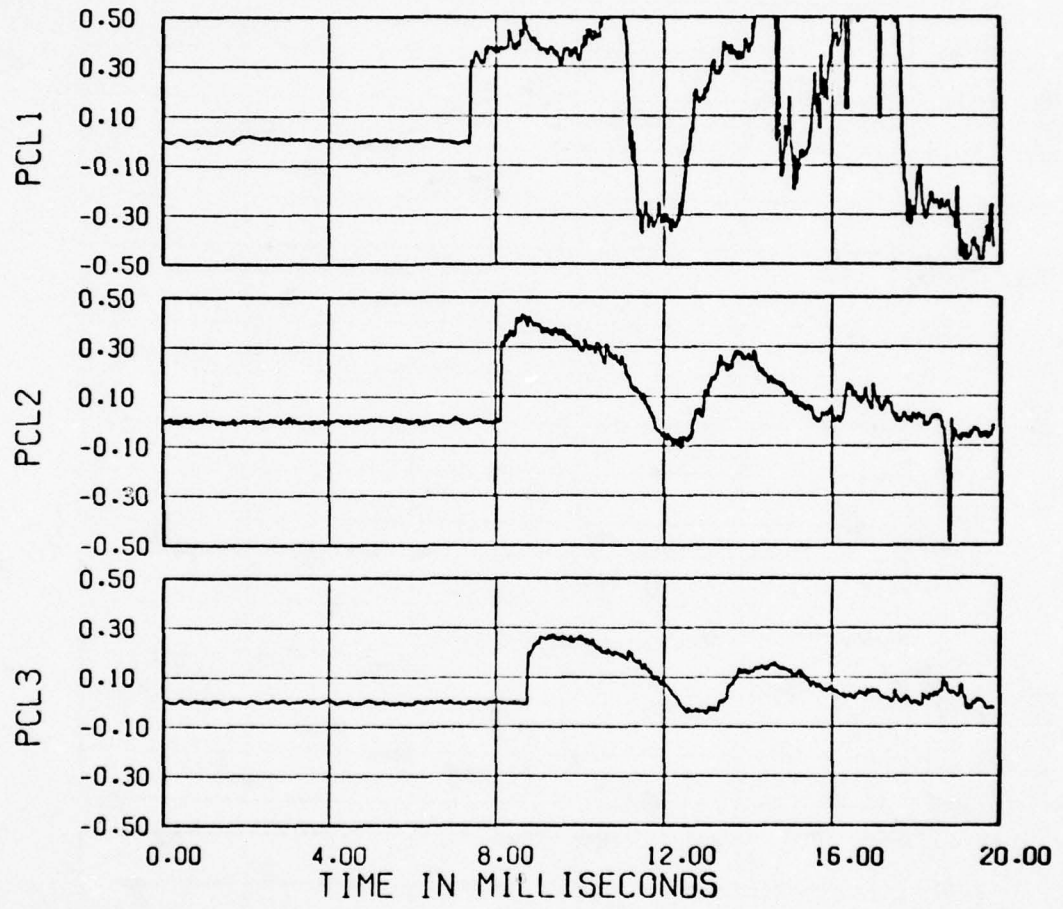


Figure 4.5g. Left claw arm pressures.

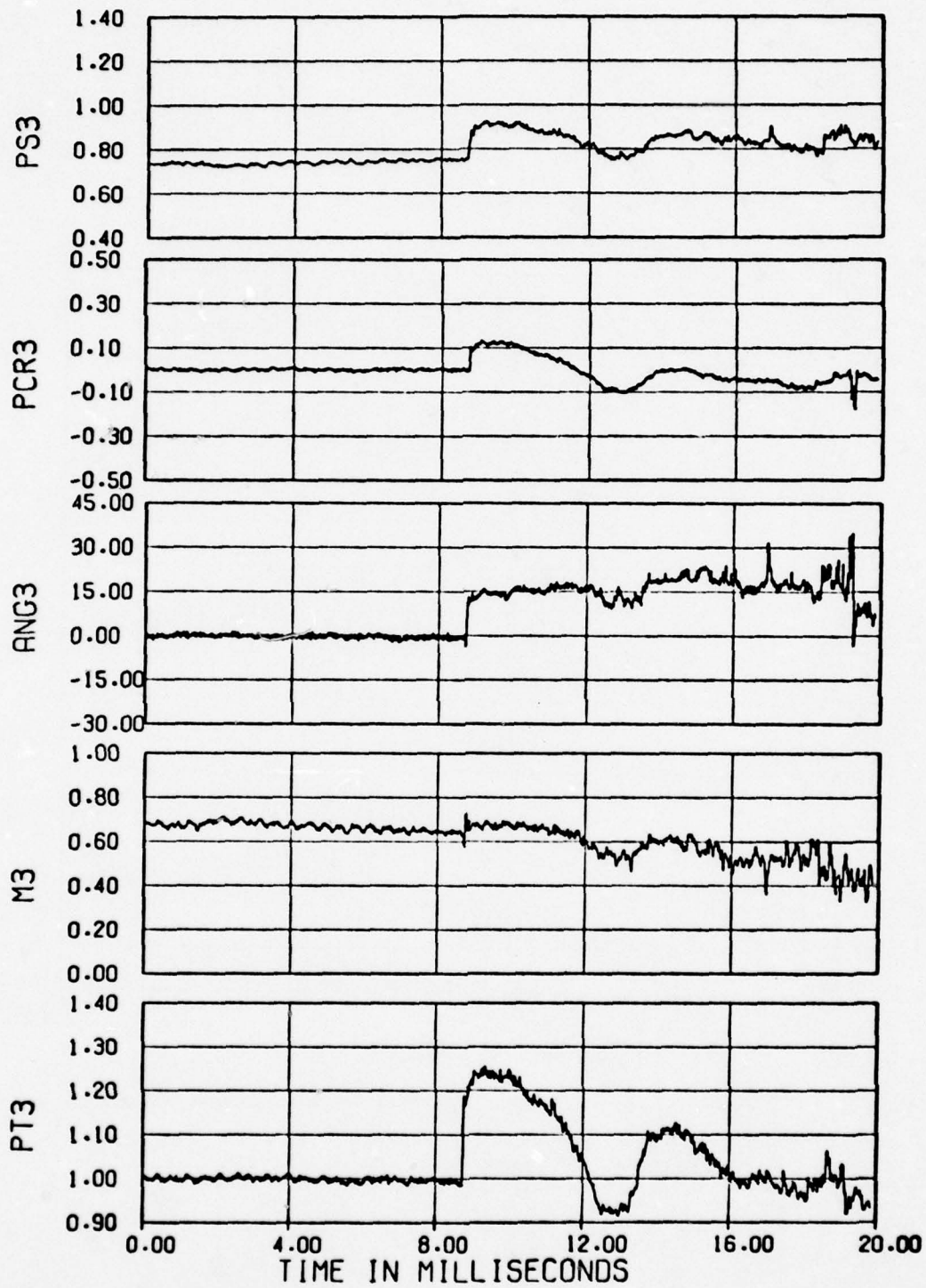


Figure 4.5h. Claw 3 parameters.

being designated by an asterisk after the label), where p_t is the steady-state (pre-blast) tunnel total pressure and p_o is the steady-state tunnel ambient static pressure.

The lowest part of Figure 4.5a shows the blast pressure inside the firing shock tube 14 inches from the muzzle end (STE). The pressure variation consists of a initial shock, followed by a slight rise and a nearly constant level for about 8 milliseconds, after which a slow decay follows.

The upper parts of Figure 4.5a give the (static) local blast pressures (PS) measured on the three claw probes, which provide an indication of the strength of the blast wave as it strikes the inlets. Looking first at PS2, which is near to the forward tip of the inlet, it may be noted that the pressure rises immediately on blast arrival to a large shock value, appears to increase slightly more over a period of about one millisecond, decays slowly until a time typically of about 3.3 milliseconds after initial blast arrival and then decays more rapidly. Similar variations are seen for the other two probes (PS1 and PS3), except that the signal for PS1, on the blastward side of the inlet, is complicated by the appearance of the reflection of the shock wave from the blastward blunt side of the inlet at about one millisecond after blast arrival.

It should be noted that for nuclear blast wave simulation purposes only the part of the signal from shock arrival to the rapid pressure change, starting at about 3.3 msec after blast arrival for PS2 in Figure 4.5a, is directly of interest. This rapid change can appear either as a rapid pressure drop usually at about 3.3 msec., as for PS2, or it may take the form of a rapid increase in pressure at about the same time followed by an abrupt pressure drop at a slightly later time, as for PS1 (Fig. 4.5a). At later times (after about the 3.3 msec) the flow pattern is more like a quasi-steady flow where the shock tube exit flow can be considered similar to a nozzle or jet flow. More specifically, from our two-dimensional REFLECT2 theoretical calculations (Appendix A), it appears that the rapid change in the blast pressure (at about 3.3 msec) corresponds generally to the arrival of the contact surface between the

"hot" tunnel gas and the "cold" gas jet from the shock tube. In most figures hereafter, the time of blast arrival at the transducer and a time 3.3 msec^{*} later are indicated as a pair of vertical arrows in order to permit the reader to focus his attention more easily on the range of primary significance for nuclear blast simulations (between the arrows). While the test results for larger times may also be of some significance for blast simulations, this remains to be demonstrated.

Time histories of ramp and cowl pressures are presented in Figures 4.5b and 4.5c. (See Fig. 4.4 and Table 4.1 for transducer locations). It may be noted that there is considerable variation of waveform for the different locations for reasons to be discussed later. (It should be noted that transducer 1990 generally appears to be truncated, 1904 is generally unreliable and the calibration constant used for 2902 appears generally unreliable).

Typical time histories of blast-induced total pressure at the blastward engine face location are shown in Figure 4.5d. Roughly, the same variations are seen to be experienced for all locations and the general trends are similar to those of the input blast pressure (e.g., PS2 in Figure 4.5a).

Typical time histories of blast total pressure at the leeward engine face location are shown in Figure 4.5e. The leeward pressures are somewhat similar to those for the blastward side (Fig. 4.5d) but are clearly different from those for the blastward side in two significant respects. First the initial pressure rise is more rapid for the leeward side (essentially a single shock) whereas for the blastward side the rise time is relatively large (say about 0.3 msec), and generally appears to involve a sequence of several small shocks. Secondly, the blast pressure appears to decay more rapidly for the leeward side at late times.

* For a few firings the onset of this cold gas effect appeared to occur somewhat later, but for most cases where a definite onset could be estimated, it appeared to occur at between about 3.2 and 3.5 milliseconds after blast intercept.

Figure 4.5f presents time histories of the already presented three blast pressure measurements PS1, PS2 and PS3 as a fraction of pre-blast free stream total pressure (p_t) and also presents the average engine face total pressures R20 and R21, for the outboard (blastward) and inboard (leeward) inlets, respectively. As would be expected, these last two variables correspond closely to the corresponding variations for the individual transducers in Figures 4.5d and 4.5e, respectively.

Typical claw probe results are shown in Figure 4.5g and 4.5h. Directly measured parameters are the "static" pressure PS_i and the left and right claw arm pressures, PCL_i and PCR_i , where i designates the probe number. Derived quantities are the resultant flow (sideslip) angle, ANG , the local Mach number, M_i , and the total pressure, PT_i .

4.6 OBSERVATION ON BLAST INPUT CONDITIONS

Before proceeding to an analysis of the significance of the test results in Section 5 it is important to first indicate briefly the source and reliability of the blast input overpressure (Δp) and intercept angle (ϕ) data presented in Table 4.4 and to indicate what differences in blast input and inlet response behavior may be attributed to the different locations of the three firing shock tubes.

4.6.1 Blast Input to the Inlets

The strength and orientation of the initial blast wave incident on the inlets and its subsequent time history variations must be known in order to evaluate the significance of any test firing. However, insomuch as the blast waves for these tests were not simple constant strength plane waves it is not a simple task to deduce the blast strength from the test data. More specifically, the orientation of the blast wave at the inlet depends on the tunnel flow conditions (Mach number), on the location of the shock tube, and on the shock tube firing conditions (tube driver pressure/tunnel pressure) and may be time dependent. The intensity of the blast depends on the radial distance and polar angle of the inlet from the shock tube axis and on the tunnel flow conditions and the shock tube firing conditions. Furthermore the strength of the blast wave striking the inlet and the blast measurement probes can be significantly modified by interferences between the blast wave, the

model wing and fuselage and the inlet, particularly at late times after arrival of the blast at the inlet.

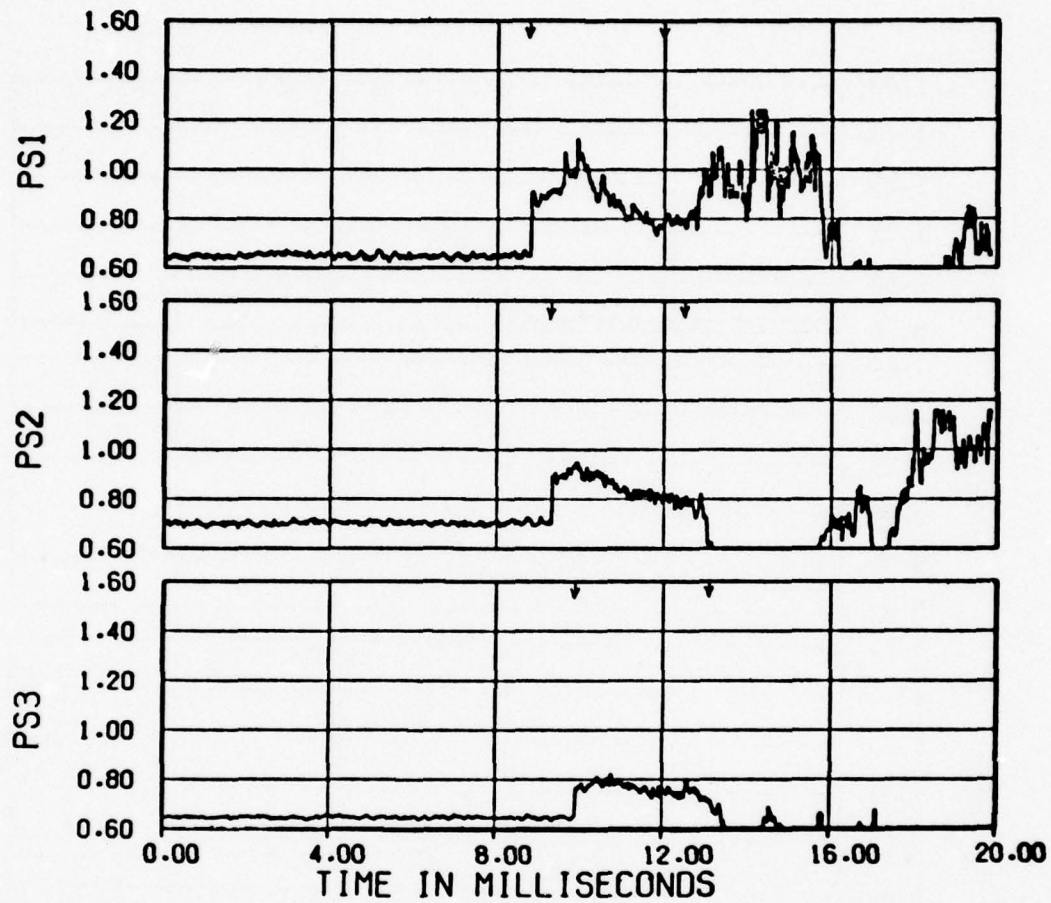
4.6.1.1 Blast Strength

A first approximation for the blast input to the inlet is given by the static pressure transducers mounted on the claw probes as indicated in Figure 4.2. Typical time histories of the blast signal seen by these static transducers are shown in Figure 4.6 for firings from the three shock tubes.

Referring first to the firing from tube No. 1 (Fig. 4.6a), probe 1 (PS1) is struck first by the blast wave, probe 2 second, and probe 3 last. Probe 1 defines the blast wave as it is seen from a position slightly downstream of the inlet cowl lip and about 6 inches outboard of the cowl lip. This record should provide a reasonable estimate of the incident blast strength at the probe location for a time duration of about one millisecond, at the end of which time the blast wave has reflected from the blunt side of the inlet model and returned to the probe, thereby providing the second shock pressure increase observed on that probe at that time. In view of this reflection effect it is difficult to determine the late time history of the incident blast wave for tube 1 firings from probe 1 measurements. (The same argument applies to probe 3 measurements for firings from tube 3, as can be seen from Figure 4.6c).

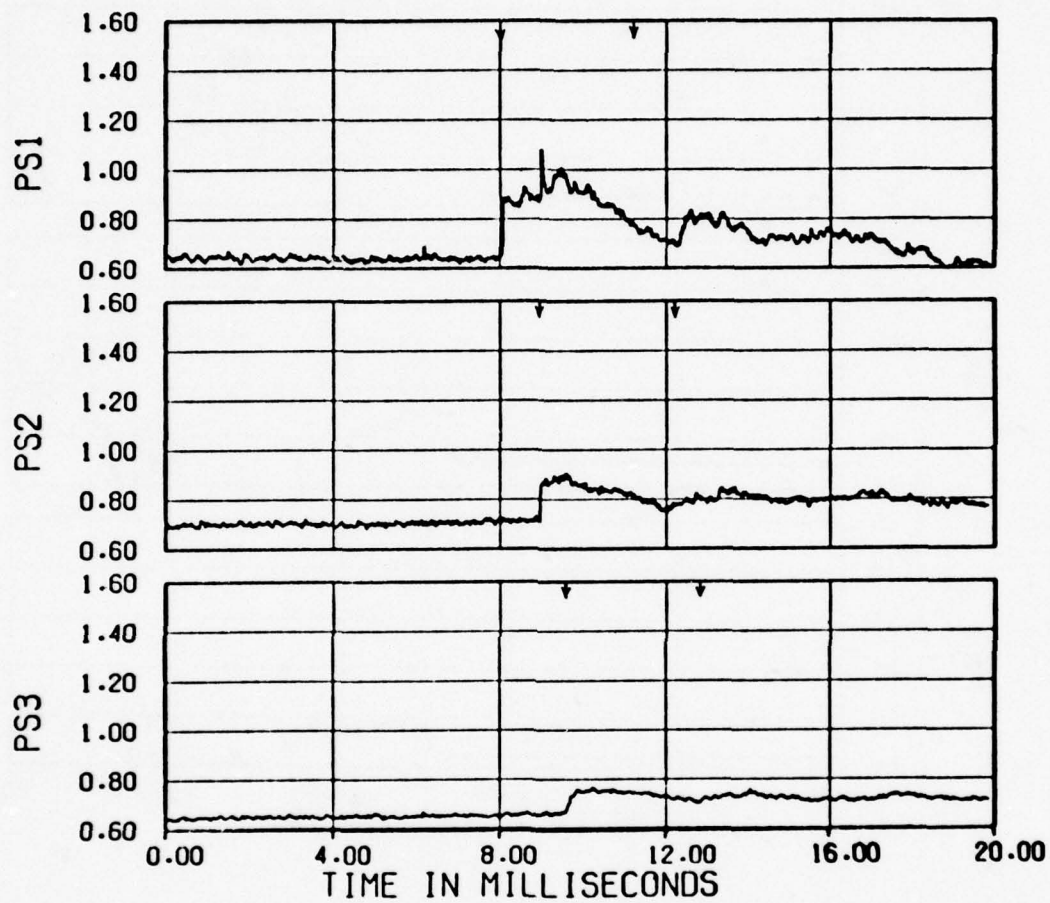
The blast strength time history obtained from probe 2, located above and near the forward end of the inlet appears to generally give the best representation of the blast wave input that can be obtained without a detailed analysis of the claw probe data. There are no obvious strong interference reflections in the probe 2 data (at least up to about 3.3 milliseconds after blast arrival), although there certainly must be some interferences due to diffraction of the blast wave about the inlet structure.

The blast strength record obtained from probe 3 for firings from tube 1 or 2 (or from probe 1 for tube 3 firings) is considered only qualitatively representative of the true blast input to the inlet because the blast wave experiences substantial diffraction about the inlet structure before reaching this probe.



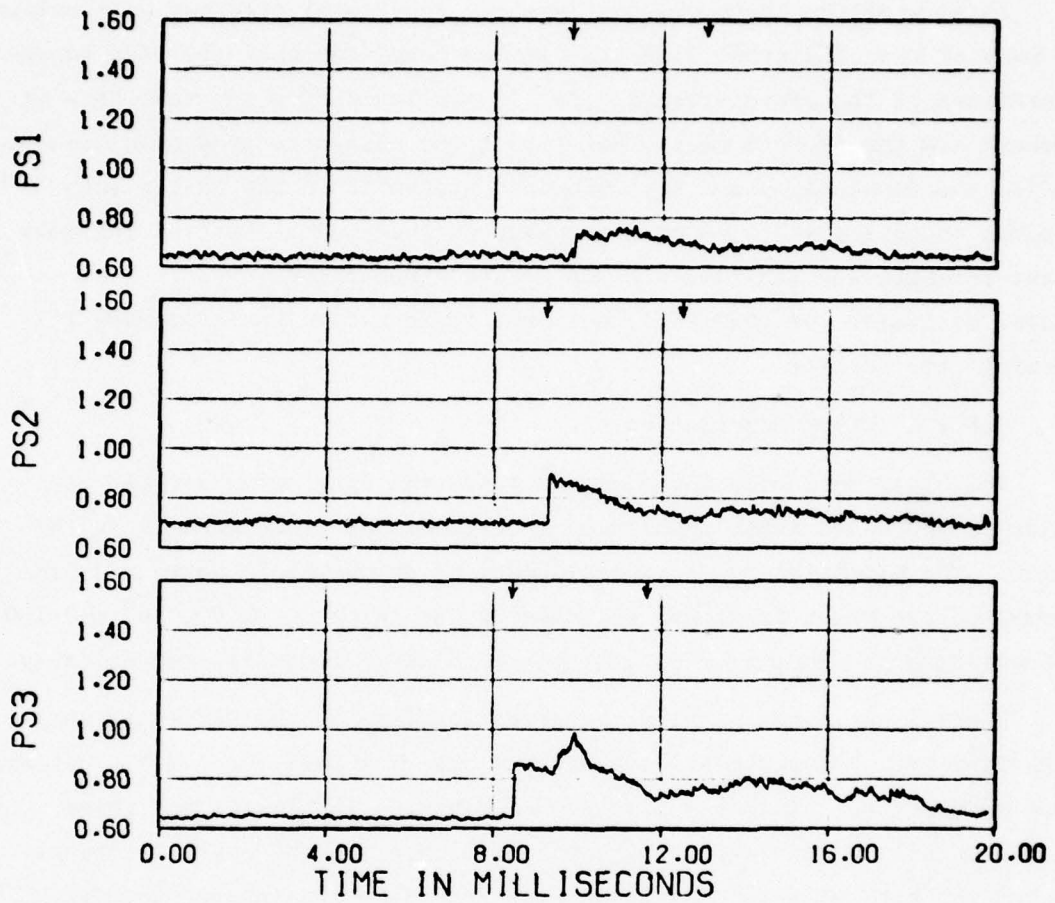
(a) Shock tube 1 firing, Run 29 (Part 608)

Figure 4.6. Typical blast pressure measurements for firings from three shock tubes, Mach 0.85, flow rate \approx 300 lb/sec.



(b) Shock tube 2 firing, Run 31 (Part 596)

Figure 4.6. Continued.



(c) Shock tube 3 firing, Run 35 (Part 597)

Figure 4.6. Concluded.

In view of the above observations and in view of frequent malfunctions of many of the claw probe elements, it was concluded that the best representations of the blast strength that is available from the test data at present are the probe 2 static data and these data were generally used to define the (nominal) blast strength data presented in the tables and figures of this report. A more accurate evaluation of the true incident blast strength and its time history derived from the claw probe data would, of course, be desirable, but insufficient time was available to develop this subject.

4.6.1.2 Blast Orientation

The blast incidence angle, ϕ , at which the blast wave strikes the inlet is of considerable importance in determining blast effects on the inlet. The blast intercept angle is defined as the angle between a line normal to the blast front and the axis of the inlet, with 0° , 90° and 180° representing head-on, side-on and tail-on blast intercepts, respectively.

Initial estimates of blast intercept angles for the 16T tests were made from the shadowgram studies made in the 1T tunnel (Sec. 2.2). Attempts were made to take similar shadowgrams during the 16T tests, but these were generally unsuccessful. Instead, estimates of the blast intercept angles for the 16T test conditions were generally obtained by observing the differences in arrival times of the blast wave at claw probe 2 and at the transducers 1935, 1902 and 2902* located near the inlet mouth, under the assumption that the blast wave could be considered to be locally a plane shock wave, travelling with respect to the local pre-blast fluid at a shock speed corresponding to the shock overpressure in Table 4.4. The resulting intercept angle estimates are presented in Table 4.4. Generally these angles are in reasonable agreement with estimates from the 1T test shadowgrams, for cases of comparable test conditions.

* See Figure 4.4.

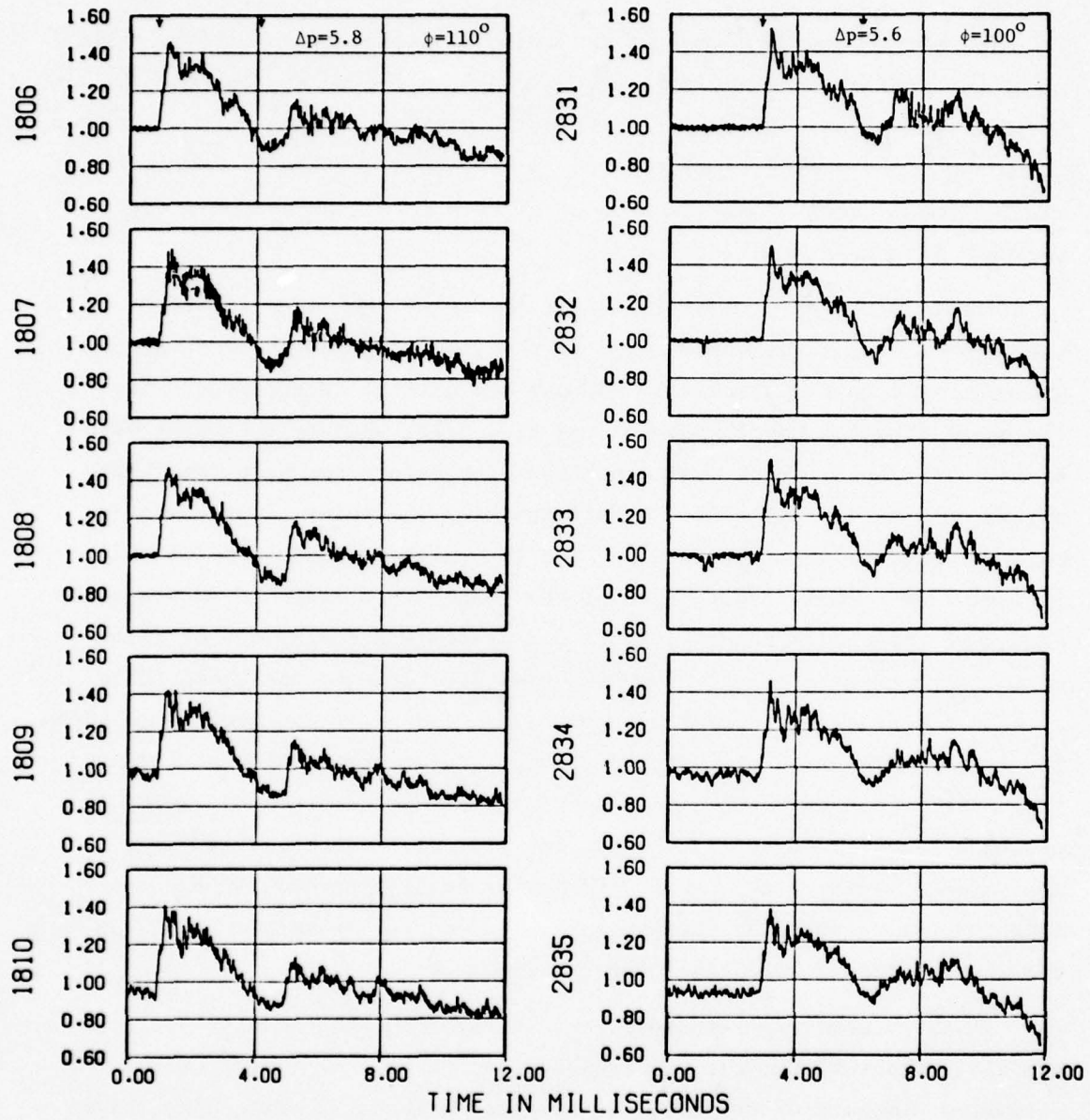
4.6.2 Shock Tube Location Effects on Blast Input and Inlet Response

The blast waves produced at the inlet by firings from different shock tubes can produce somewhat different effects on the inlet response due to factors other than obvious differences in intercept angles and overpressures. It is the purpose of this section to clarify this question somewhat by examination of some of the test data before proceeding to a more extensive analysis of the data in Section 5.

Consider the effects of firing at the inlet from opposite sides of the tunnel. The blast waves fired at the model from shock tubes 1 and 2 encounter the inlet essentially without any initial interferences from the model wing and fuselage body (see Fig. 3.1), whereas the blast wave from shock tube 3, which must cross the wing before reaching the inlet, may be substantially modified before striking the inlet. Consequently, some differences might be expected for the inlet response conditions to firings from the different sides of the tunnel. In order to indicate the extent of these differences, Figure 4.7 presents a comparison of inlet engine face total pressure time histories for firings from shock tubes 2 and 3 for roughly comparable overpressure and blast intercept conditions. The left-hand side of this figure presents inlet pressure for a firing from tube 2 and the right hand side presents the corresponding inlet pressure for a firing from tube 3. For example, transducer 1806 (in the outboard inlet) for a tube 2 firing would be expected to have the same type of response as the symmetrically located transducer 2831 (in the inboard inlet) would have for a firing from tube 3.

It is evident from Figure 4.7a that the inlet response pressures are about the same for firings from the two tubes, certainly for the estimated duration of the blast event, say to about 3.3 msec after blast arrival. For much later times, there are appreciable differences, but this is not of great importance for the present study.

For the leeward inlet, Figure 4.7b indicates the same general shape of pressure histories for the two firings but does indicate an appreciably more rapid decay of pressure for the firing from tube 3. This more rapid

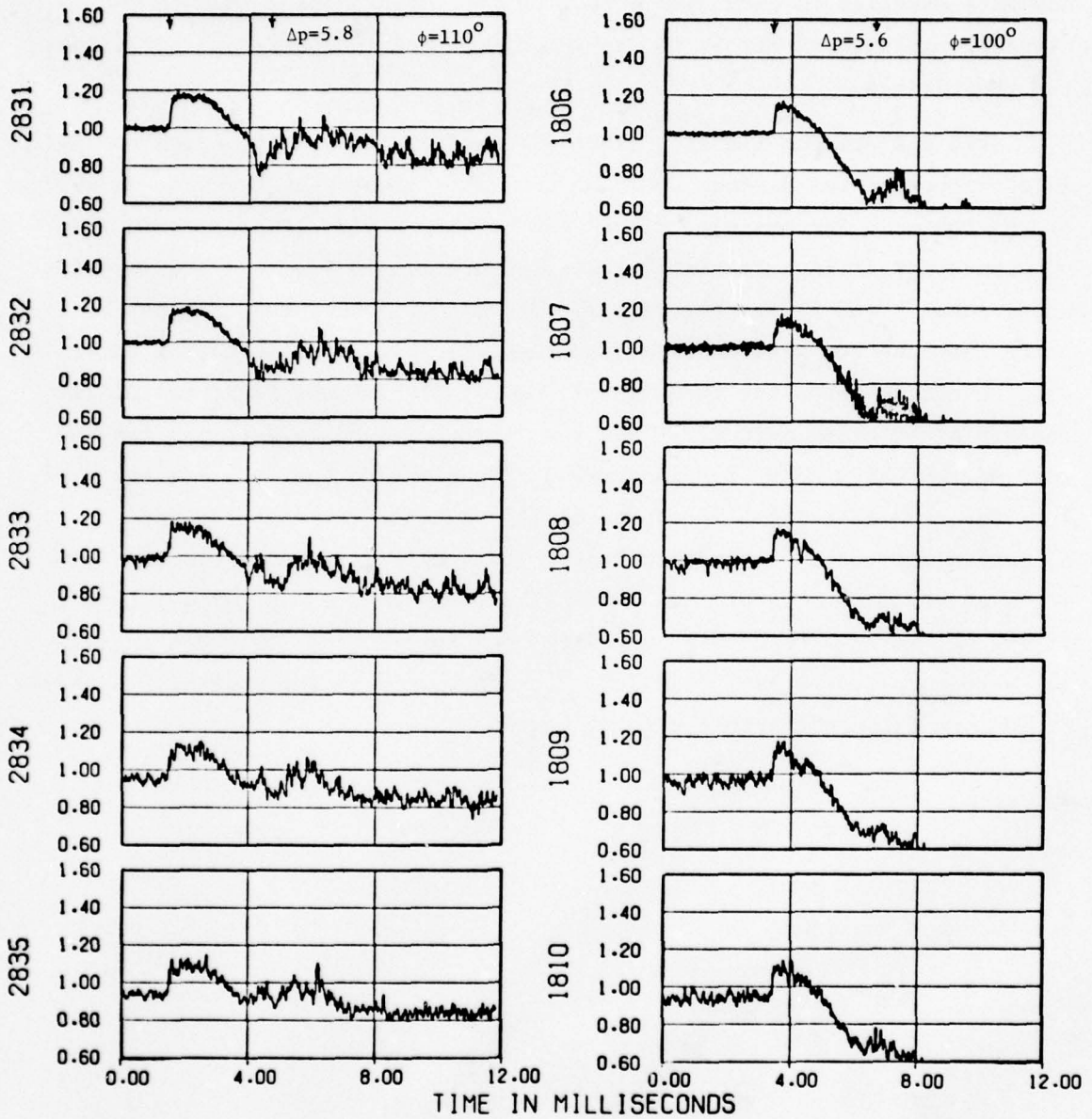


Tube 2 - Run 40 (Part 619)

Tube 3 - Run 42 (Part 620)

(a) Blastward inlet

Figure 4.7. Comparison of engine face pressures for firings from shock tubes 2 and 3.



Tube 2 - Run 40 (Part 619)

Tube 3 - Run 42 (Part 620)

(b) Leeward inlet

Figure 4.7. Concluded.

decay can be attributed partly to wing-fuselage-inlet interference, which would be expected to have more effect on the leeward inlet than on the blastward inlet, and partly to the 10° difference in intercept angles for the two firings.

Some differences are also observable between the blast inputs and inlet responses for firings from the two tubes located on the same side of the tunnel. For example, Figure 4.8 compares inlet ramp pressure time histories for firings at similar overpressure levels from the side-by-side shock tubes 1 and 2 (see Fig. 4.4 for transducer locations). It may be noted that the two sets of time histories are quite similar during the blast event (between the two arrows), especially for the first two milliseconds after blast arrival. Then the pressures tend to decrease for the rest of the blast event for the tube 2 firing and to increase for the tube 1 firing, and after the end of the blast event the two sets of time histories are considerably different. The greater pressures and fluctuations observed toward the end of and after the blast event for the tube 1 firing may be attributed partly to its much lower blast incidence angle, 84° here compared to 110° (see Sec. 7), and partly to the greater closeness of the jet from tube 1 to the inlet mouth.

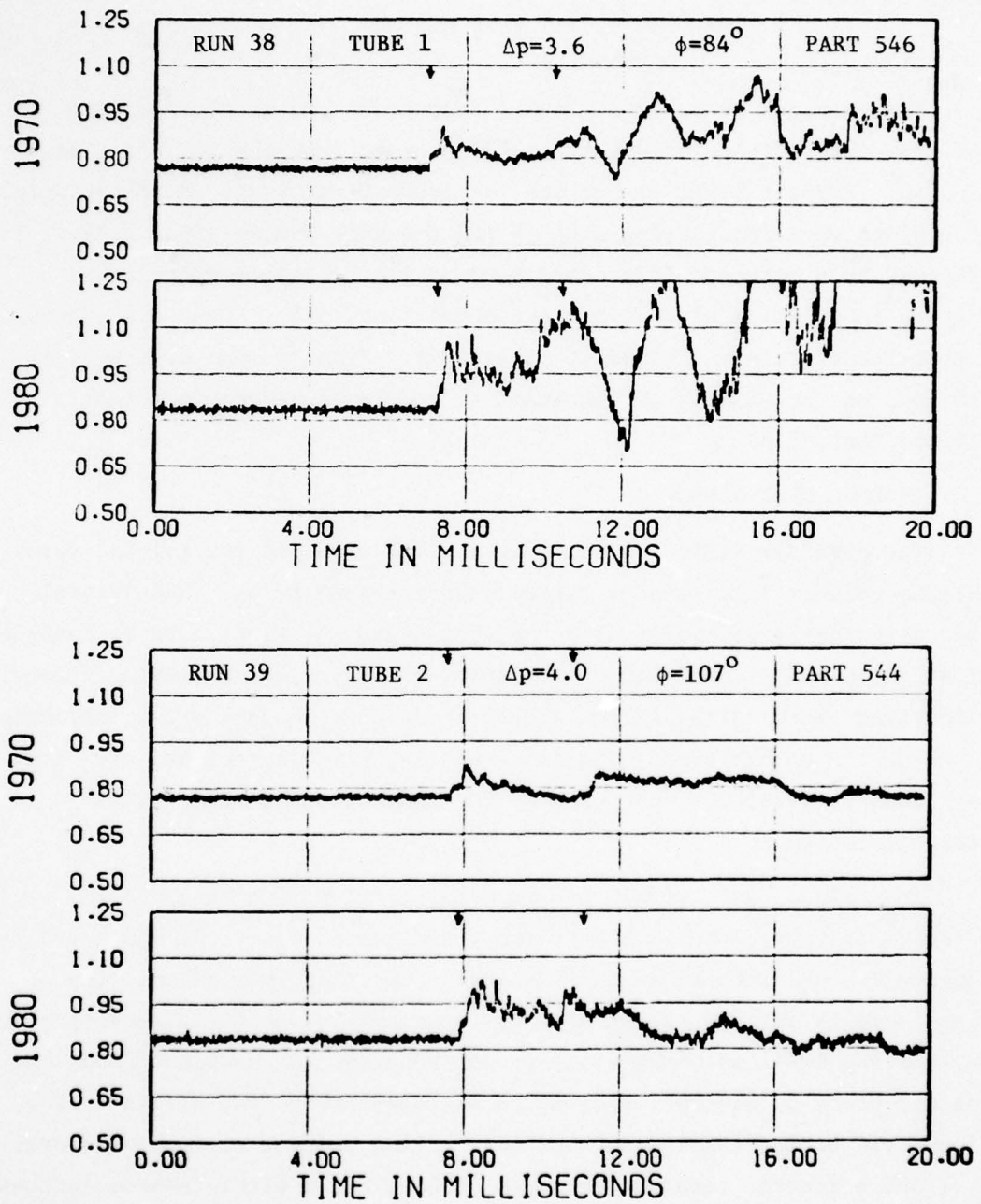


Figure 4.8. Comparison of blastward inlet ramp pressure time histories for Mach 0.85 firings from two shock tubes.

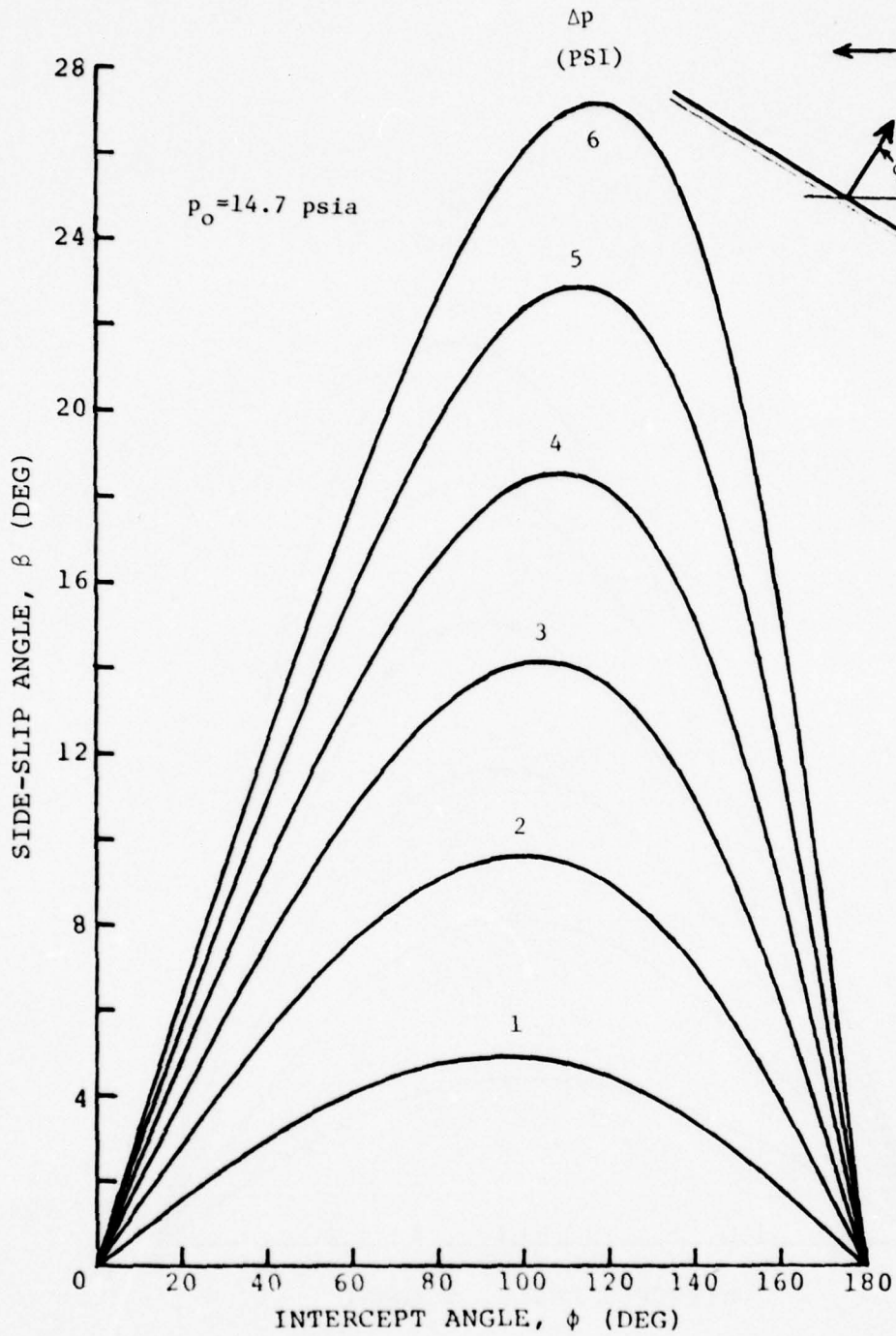
SECTION V
ANALYSIS OF 16T TEST RESULTS

This section presents a general discussion and analysis of some of the principal effects relevant to and observed from the 16T blast test results. First a brief discussion is given of the basic characteristics of a blast wave interacting with an inlet-engine system (Sec. 5.1), followed by a more specific discussion of the transient shock wave pattern in an inlet after blast encounter (Sec. 5.2). Next are discussed distortion effects in the inlet (Sec. 5.3). Finally some observations are made on the ability of the inlet to endure long-duration blast effects (Sec. 5.4).

5.1 GENERAL PHENOMENA

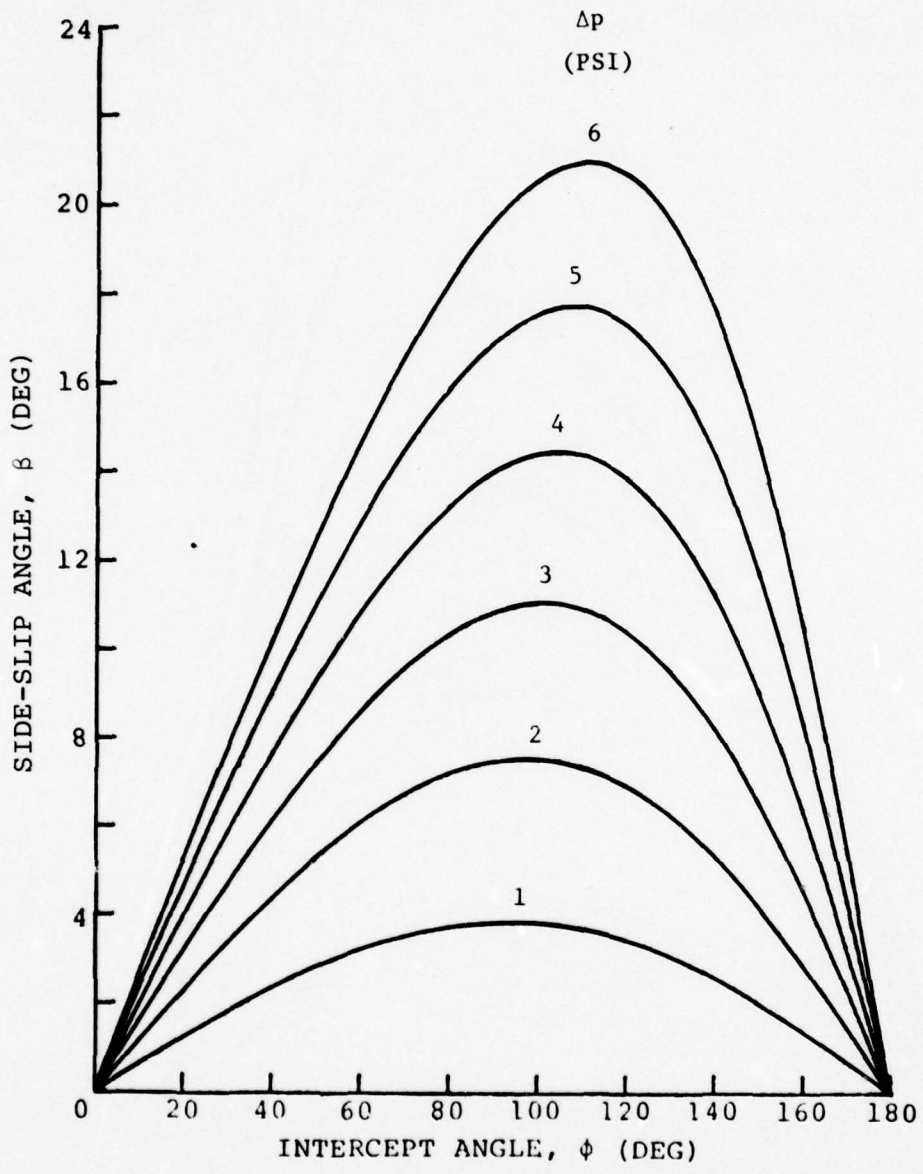
The physical characteristics of a blast wave and its initial interactions with an inlet-engine system are discussed below. The initial discussion deals primarily with the case where the blast wave is considered as a simple plane shock wave of constant or very slowly decaying strength, resembling the blast wave from a nuclear weapon. Subsequently, attention is given to the differences in phenomena which are associated with the more complex blast wave produced by the shock tubes as used in the present studies.

As a blast wave travels toward an aircraft moving in space it produces changes in the ambient atmosphere behind its front which are imposed on the aircraft as it is enveloped by the blast field. The blast wave is defined essentially by two characteristics, the overpressure, Δp , and the intercept angle, ϕ , between a normal to the blast front and the direction of aircraft motion. With reference to the aircraft, the flow field behind the blast front will have a greater ambient pressure, $p_o + \Delta p$, a greater total pressure, $p_t + \Delta p_t$, and a blast-induced increased side-slip angle, $\psi = \psi_o + \Delta\psi$. Figures 5.1 and 5.2 illustrate the magnitude of these blast-induced side-slip angle and total pressure changes for several Mach numbers. For example, it is seen from



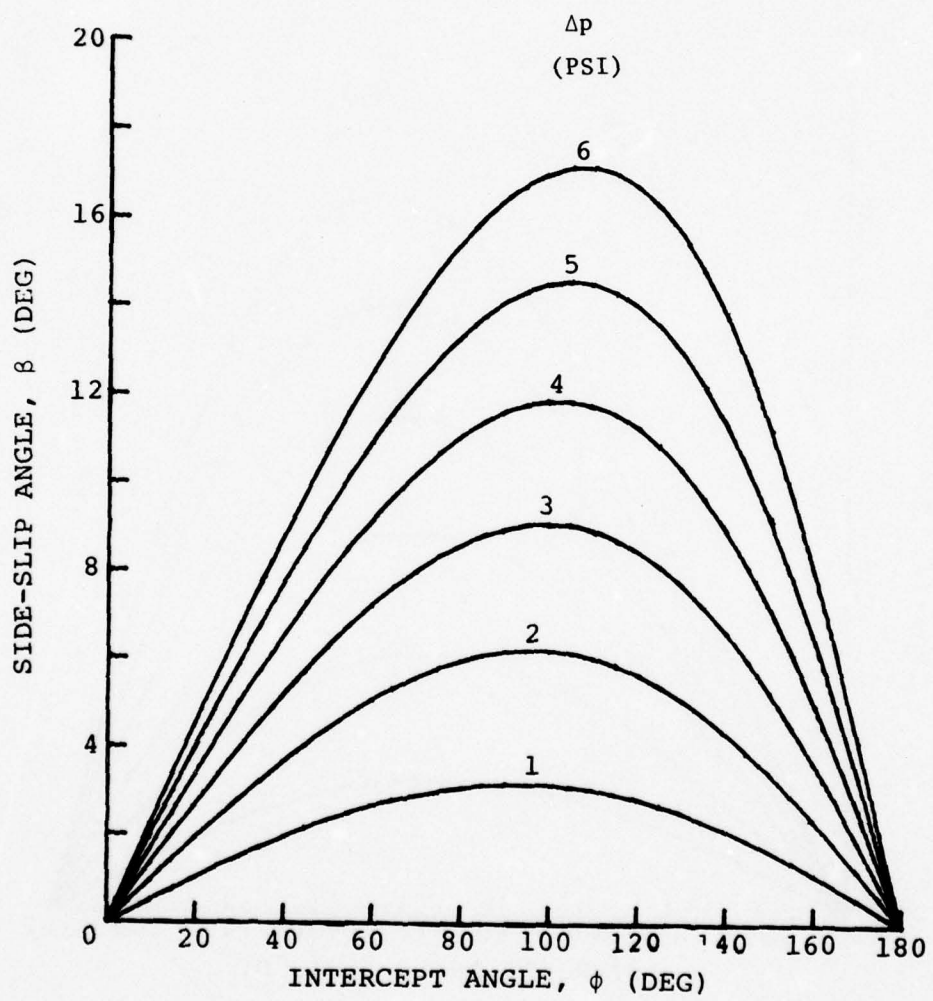
(a) MACH 0.55

Figure 5.1. Variation of blast-induced side-slip angle with intercept angle and overpressure.



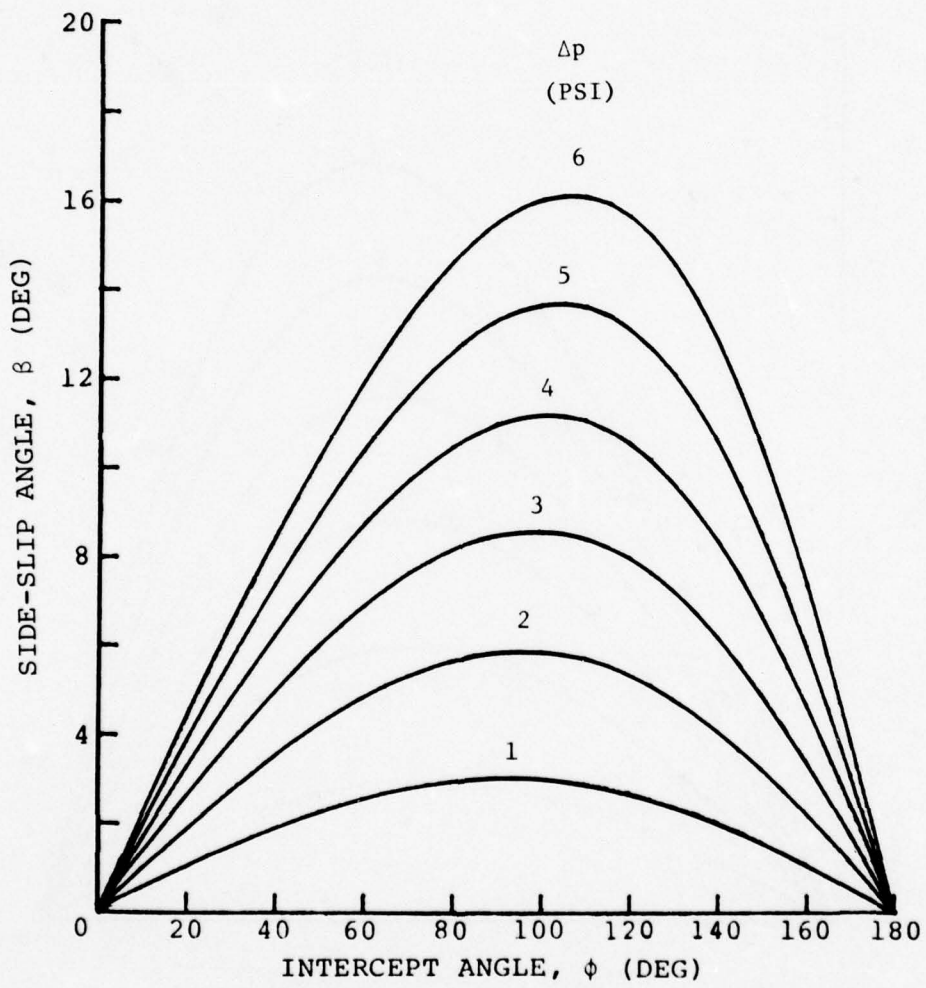
(b) MACH 0.70

Figure 5.1. Continued



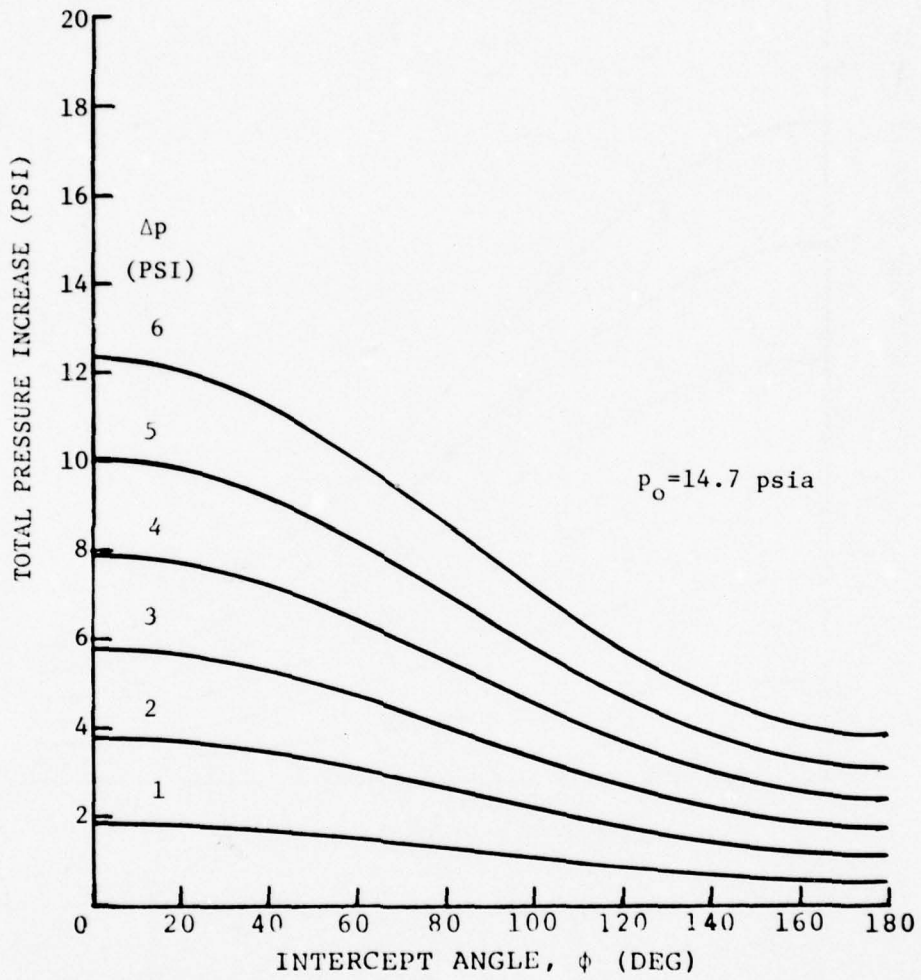
(c) MACH 0.85

Figure 5.1. Continued



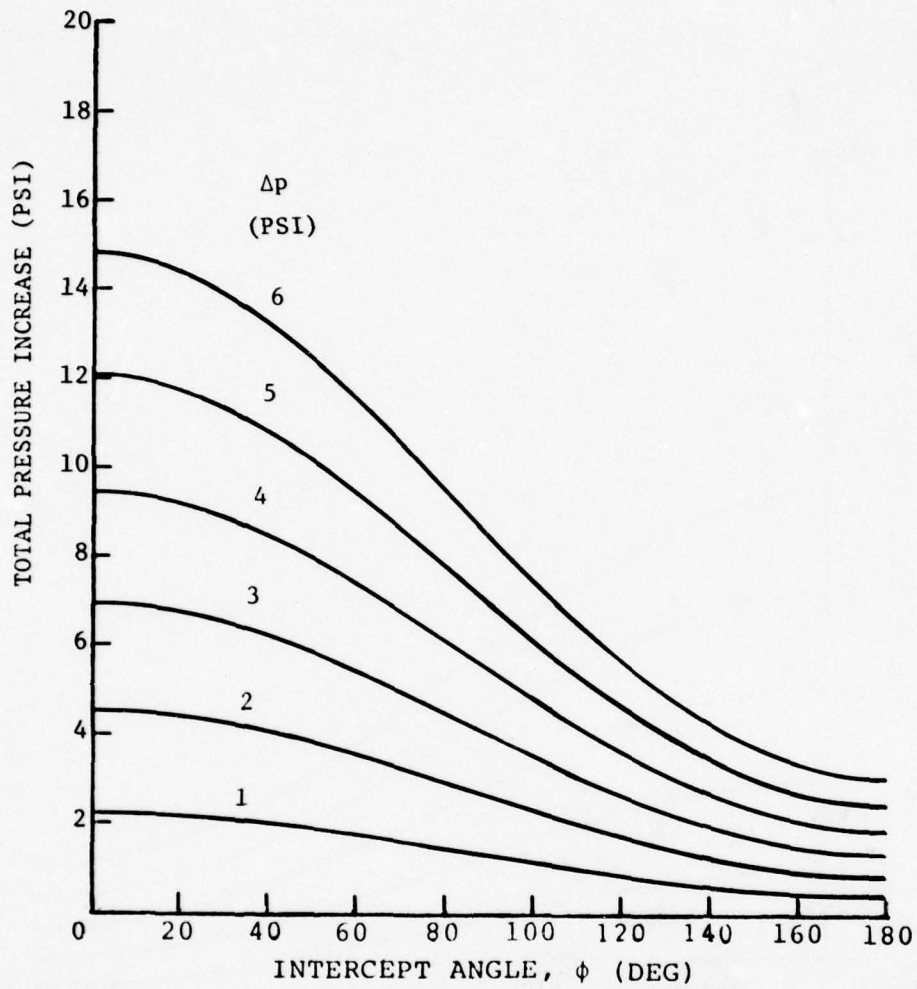
(d) MACH 0.90

Figure 5.1. Concluded.



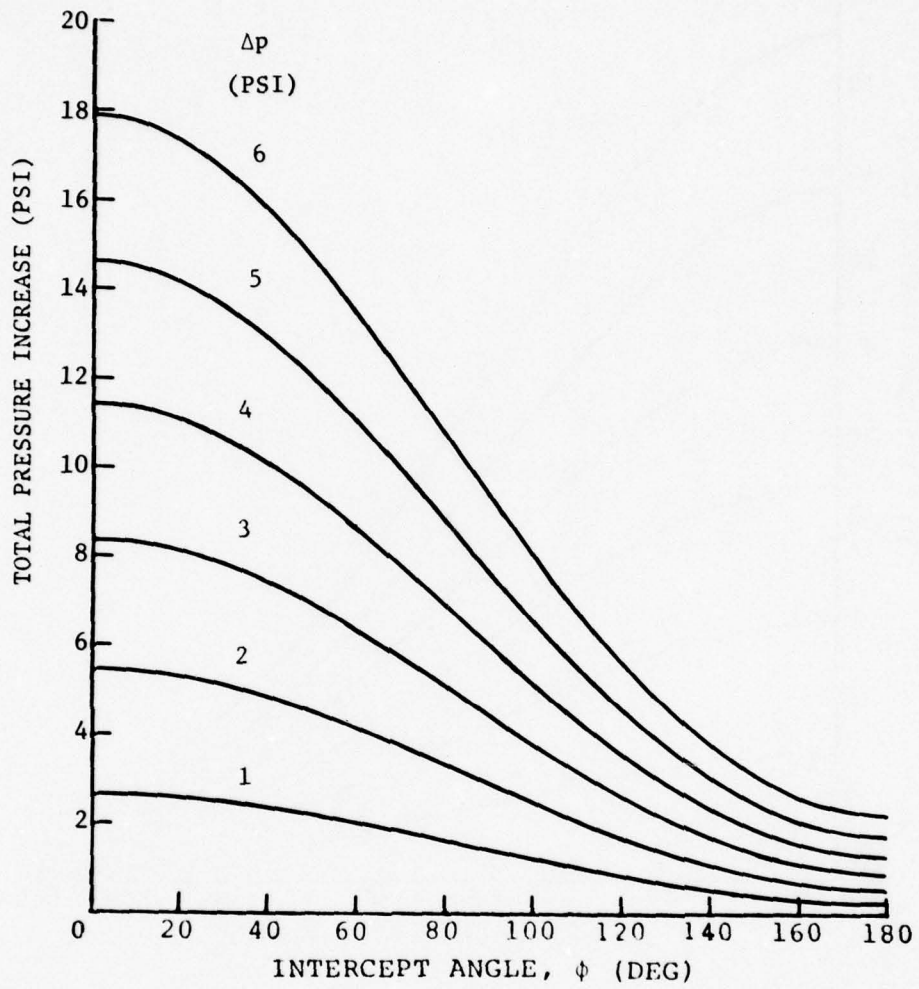
(a) MACH 0.55

Figure 5.2. Variation of blast-induced total pressure with intercept angle and overpressure.



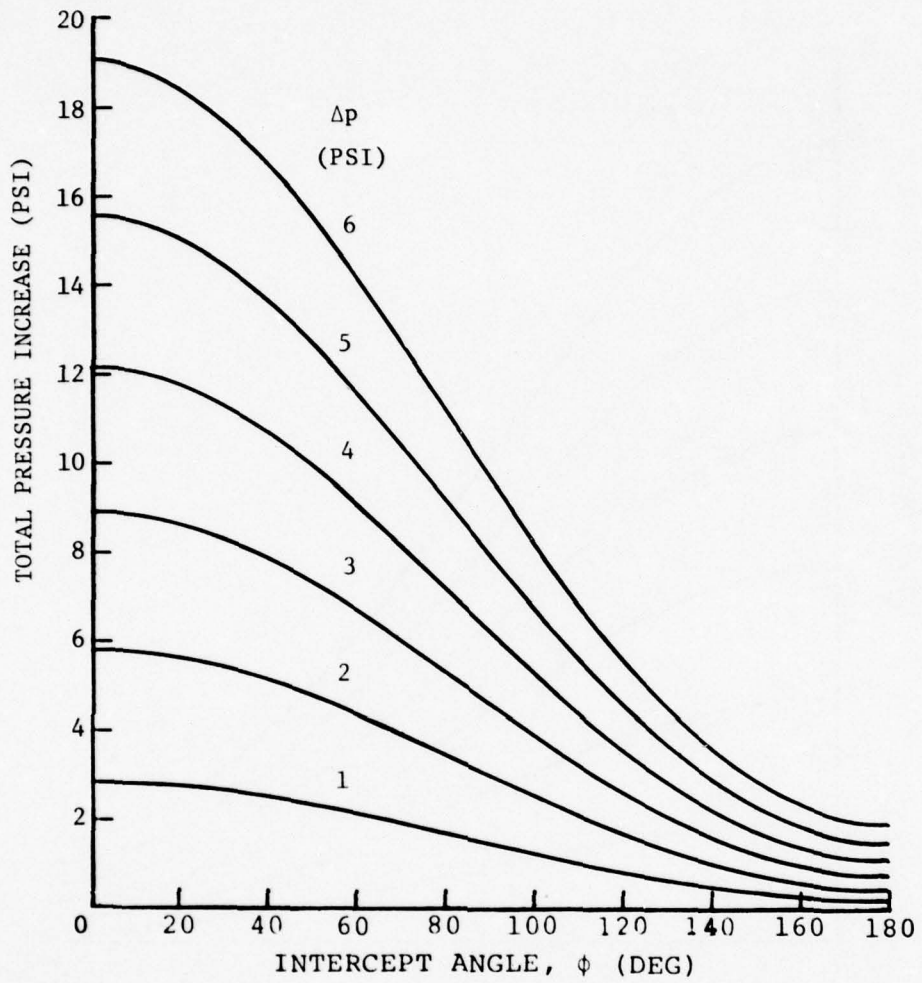
(b) MACH 0.70

Figure 5.2. Continued



(c) MACH 0.85

Figure 5.2 Continued



(d) MACH 0.90

Figure 5.2. Concluded

Figure 5.1 that the greatest blast-induced yaw angles are produced by intercept angles somewhat over 90° (i.e., slightly from the rear). Blast-induced total pressure changes in Figure 5.2 are seen to be largest for zero intercept angle and to decrease subsequently to relatively small values for tail-on ($\phi=180^{\circ}$) intercepts.

As a blast wave envelopes an aircraft these blast properties may be substantially modified by diffraction and reflections from various parts of the structure before and after the wave encounters the engine inlet.

As the wave proceeds into an engine inlet it may experience a sequence of reflections from the walls of the inlet (as discussed in Sec. 5.2) and from engine components, and may penetrate in part completely through the engine system.

Eventually, if the blast wave is of sufficient duration, these blast reflection effects will be resolved and the inlet-engine system will come to a quasi-steady equilibrium condition consistent with the blast-induced overpressure, total pressure and side-slip angle, characterized by an engine mass flow rate which can be different from that for the pre-blast condition.

In discussing the effects of a blast wave on inlet-engine performances it is convenient to think of the phenomena in terms of the following somewhat overlapping three stages of the blast encounter.

The first or initial stage consist of the time during which the blast wave moves down the inlet into the engine, reflects in part from the engine structure or fan of a turbofan engine and subsequently moves upstream and out the mouth of the inlet. In the case of the present 0.1-scale model the time required for these events up to the time when the reflected shock wave has moved upstream of the simulated engine face section is on the order of 2 milliseconds. (Time zero is defined here as the time when the blast wave first strikes the cowl lip of the blastward inlet.)

The second stage of the blast flow encounter is associated with the inception and convection of boundary-layer disturbances down the inlet. In particular, boundary-layer separation and vortex formations may be

produced at the cowl lip by large blast-induced side-slip angles and will be convected downstream at speeds comparable to or lower than the particle velocity in the inlet, which is generally much smaller than the rate at which a blast wave moves down the inlet. In the case of the tested inlet, it would take on the order of 3 milliseconds (after cowl lip blast encounter) for such particle velocity effects to reach the engine face. Other boundary layer effects which might be expected in this same time period would be boundary layer instabilities excited by the reverse flow reflected upstream from the engine throat. For the present inlet, such effects would not be expected to begin at the engine face before times of about 2 milliseconds after blast intercept.

The third stage of the blast flow consists of the late time stage when all significant internal shock wave systems have been dissipated or reflected from the inlet-engine system and boundary layer effects have reached a quasi-steady equilibrium condition. This stage was not reached in the present tests because of the limited duration of the blast waves used.

5.1.1 Differences Between Shock Tube and Nuclear Blast Flows

The initial flow from the shock tubes used in the present tests generally resembles the essential features of a nuclear blast wave at least for part of the blast-type flow period described (in Section 4.5) of about 3.3 milliseconds. However there are some noteworthy features, which should be borne in mind, where the shock tube flow differs from that for a nuclear blast. First the strength of the shock tube blast wave remains relatively constant for only one or two milliseconds, after which its strength generally tends to decrease toward zero at 4 to 6 seconds after initial shock arrival. Also, in the late decay stage, "cold" air blown out of the shock tube produces a high velocity jet with a complex spatial variation of fluid properties which bears little resemblance to a nuclear blast field. As a general rule of thumb for the present tests, it appears that this "cold" jet does not strongly influence the test results for times after blast arrival less than about 3.3 milliseconds (see Sec. 4.5).

A sketch illustrating the above-discussed sequence of events in the blastward inlet is presented as Figure 5.3 in the form of a time distance plot for an inlet mass flow rate of 350 lb/sec. The time origin is the time when the blast wave first arrives at the cowl lip. The initial blast wave moves down the inlet to the simulated engine throat vane system and is reflected back upstream as indicated by the "shock" curve. The "particle velocity" curve indicates the convective speed of material in the inlet; "vortex" motions are indicated here as travelling at speeds between 1/2 and 1 times the particle velocity and are indicated to reach the engine face at times on the order of 3-6 milliseconds, depending on the vortex speed. The cold gas motion is indicated by the two upper curves, starting at time 3.3 msec. This cold gas effect might be expected to travel down the inlet at some speed between the particle velocity and the sound(+ particle) velocity, depending on how close the inlet mouth is to the jet from the shock tube. It is important to note here that large shock-type cold gas effects (see lower cold gas curve) can arrive at the engine face before vortex effects arrive, hence making it difficult to unambiguously evaluate vortex effects at the engine face by simple inspection of test records.

5.2 SHOCK PATTERN IN THE INLETS

As a guide to the discussion in later sections of blast-induced distortion and its effects on engine performance, this section briefly discusses some details of the character of the blast-induced shock flow pattern in the inlet.

Figure 5.4 presents a sketch of the tested inlet configuration and shows the shock wave pattern inside the inlet for a time when the blast shock has penetrated down the blastward (outboard) inlet to slightly beyond the engine face location. In this figure, the blast is assumed to have struck the inlet about perpendicular to the inlet axis ($\phi=90^\circ$) from the outboard side of the inlet. After encountering the lip of the outboard cowl, the blast shock wave begins to diffract about the cowl lip and to penetrate into the inlet at a downstream speed about equal

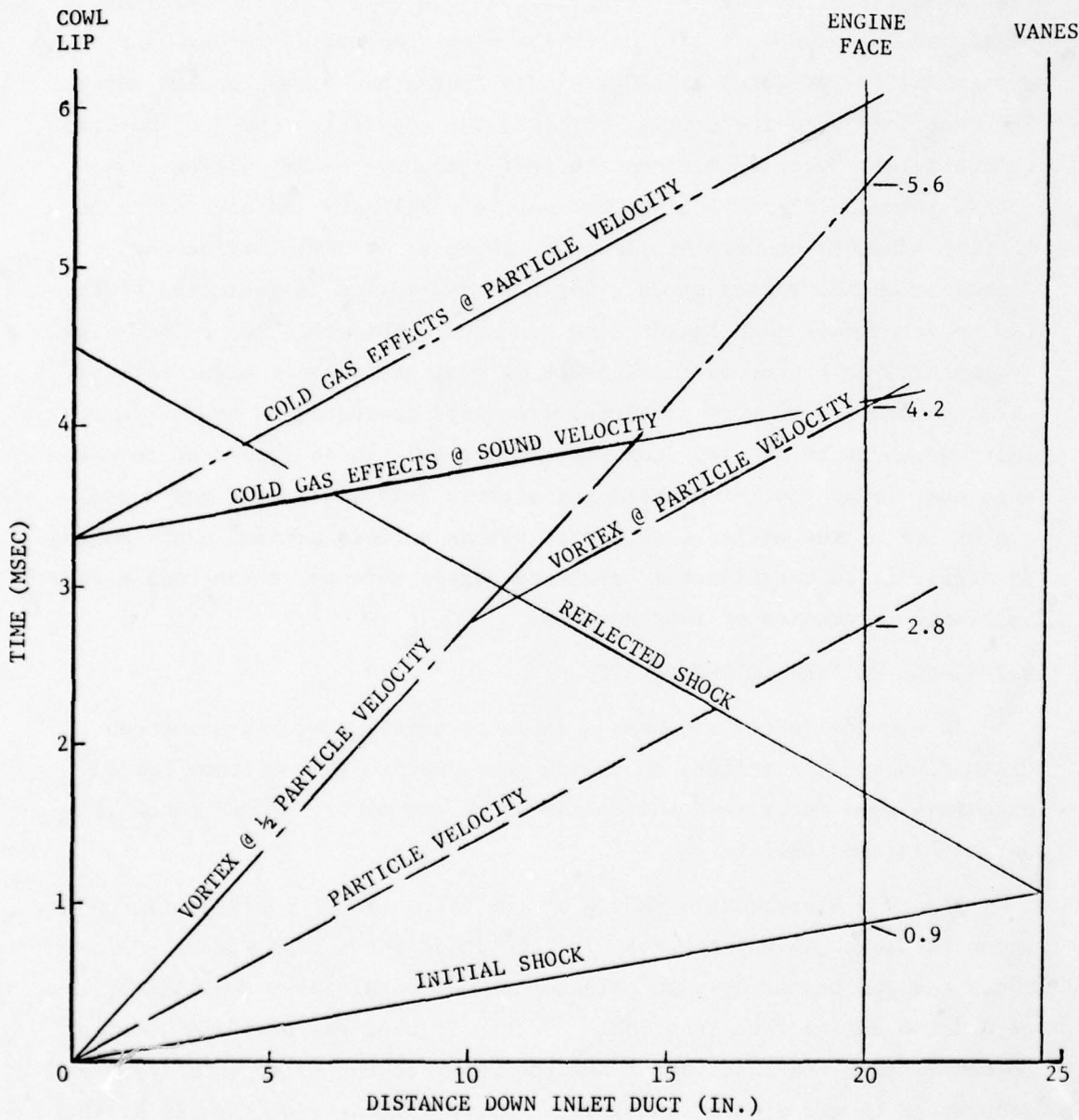


Figure 5.3. Inlet time-distance relationships.

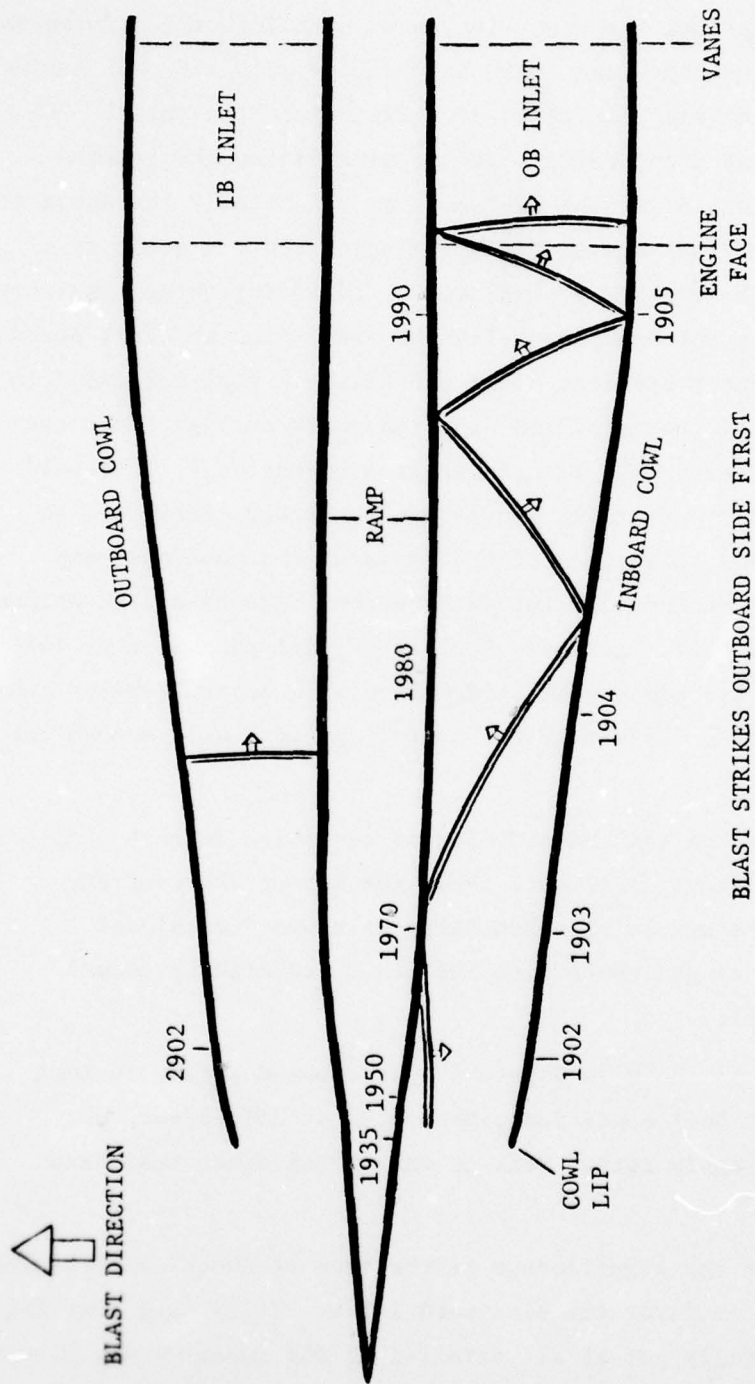


Figure 5.4. Typical shock wave pattern in the inlets.

to the sum of the (pre-blast) flow velocity in the inlet plus the speed of sound in the inlet. At the same time the part of the shock wave upstream of the cowl lip proceeds to the outboard ramp surface, experiences essentially normal reflection there, with about doubling of its intensity, and then tends to bounce back and forth between the ramp and cowl surfaces while being at the same time convected downstream into the inlet. The resulting overall blast front pattern at any time can be constructed graphically by assuming the shocks to travel at essentially the speed of sound relative to the local ambient inlet velocity and the accuracy of the construction can be checked or improved by adjusting these constructions slightly to conform to the experimentally observed times of blast arrivals at the various transducer stations along the ramp and cowl indicated in Figure 5.4. (Generally the first two or three shock arrival times can be clearly distinguished in the transducer time histories.) It should be noted that the shock pattern in Figure 5.4 is rather simplified in that it assumes regular reflection of the waves at the cowl and ramp surfaces and it does not consider the interference effects of the engine hub structure (Figure 4.1). Actually Mach stems will tend to form for some reflected waves and additional reflections will occur from the hub; however, Figure 5.4 does illustrate the overall pattern well enough for the present discussions.

The shock pattern on the leeward side of the inlet is much simpler. Here, the shock wave simply diffracts about the tip of the ramp and tends to enter the leeward inlet essentially as a one-dimensional disturbance having a single shock with its front essentially normal to the inlet side walls.

The shock patterns shown in Figure 5.4 were based partly on test data for Run 39 (Part 544) conditions, Mach 0.85 at 350 lb/sec, but would be expected to apply rather well to any of the other test Mach numbers as well.

Now, to indicate the significance of the type of shock pattern seen in Figure 5.4, consider first the blastward inlet. It is seen that the shock waves are generally not at all parallel to the inlet walls, except

for the initial blast front. Hence, there is generally an appreciable time-varying spatial variation of blast pressure across any section of the inlet, which lasts from the time of first blast arrival until that time when all of the incident blast front and its reflections will have been either convected downstream through the engine or reflected from the engine throat back upstream and out the mouth of the inlet. This spatial pressure variation across any section of the inlet will, of course, produce flow distortion in the section, the intensity of which will be related to the intensity of the shock or shocks passing through or near to that section at the time in question.

Another consequence of the complex shock pattern in the blastward inlet is its effect on the rate at which the shock pressure builds up. Essentially, for the blastward inlet, the pressure buildup consists of a sequence of separated shocks adding to each other, so that the resultant effect is a relatively slow staircase type buildup of pressure, taking on the order of 0.3 millisecond for typical cases. On the leeward inlet, however, where there is essentially a single shock front, the pressure buildup is essentially instantaneous.

5.3 ANALYSIS OF INLET DISTORTION

A primary objective of the test program was to obtain time histories of the inlet distortion parameters resulting during blast wave inlet interactions. In this study, time histories of the following inlet distortion parameters were calculated from the test data for both inlets for all runs and were plotted as illustrated in Figure 5.5 for Run 8 (Part 573): IDC_i , IDR_i , IDC_{12} , IDC_{45} , IDR , IDC , IDL , IDA and IDT , where i designates the i th instrumented engine face ring ($i = 1$ to 5). These particular distortion parameters, defined in Table 5.1, were selected because they are standard for the analysis of the B-1 inlet and engine system. The discussion of distortion in this report is, however, restricted to the parameters IDC , IDR and IDL , and primarily to IDL . IDC is the total circumferential distortion index, IDR is the total radial distortion index and IDL is the fan stall margin ratio. IDL is an overall measure of the inlet distortion, which depends on IDC ,

OUTBOARD INLET

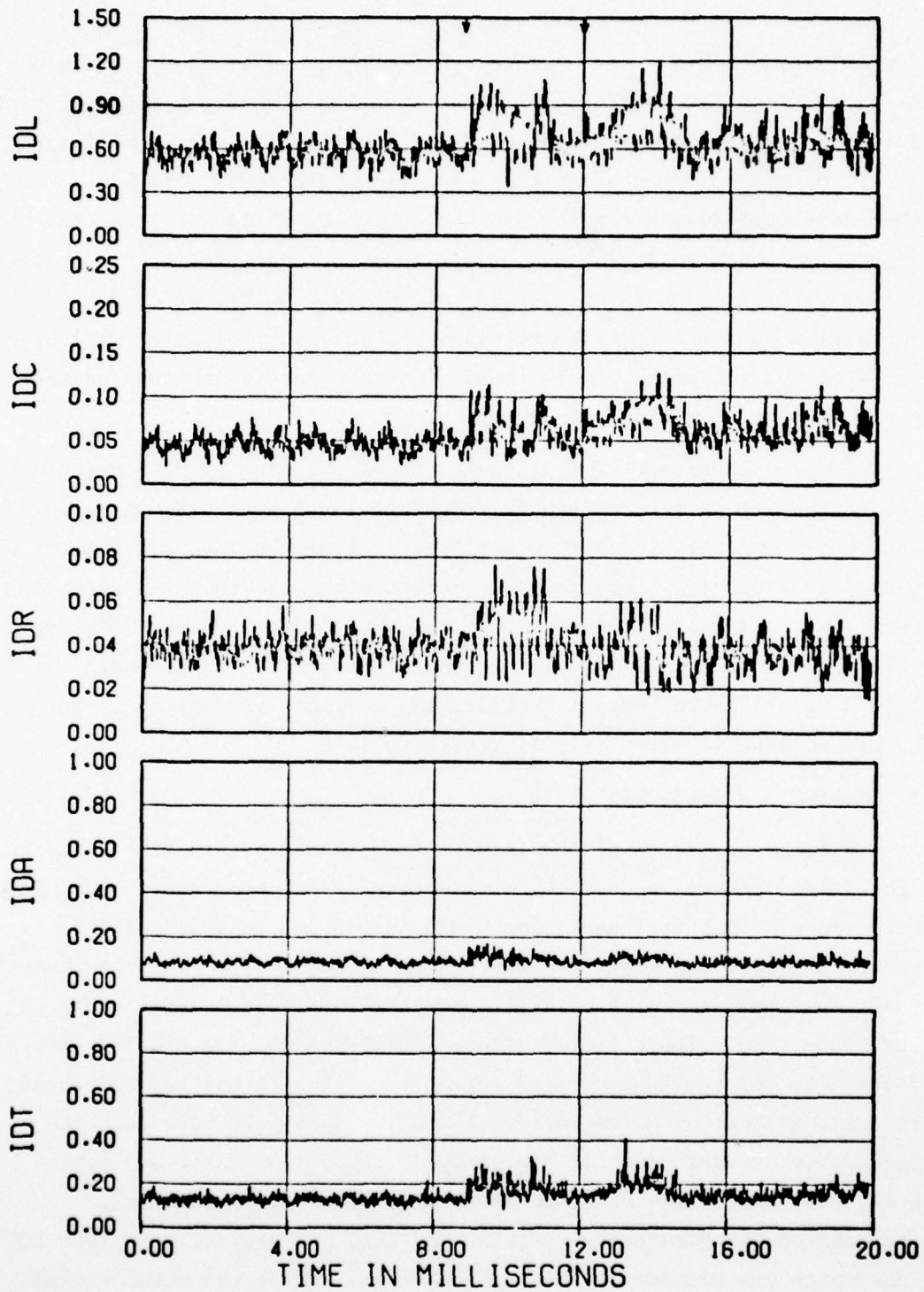


Figure 5.5. Distortion time histories for Run 8 (Part 573), Mach 0.70, $\Delta p = 5.0$ psi, $\phi = 98^\circ$, flow rate ≈ 303 lb/sec, tube 2.

OUTBOARD INLET

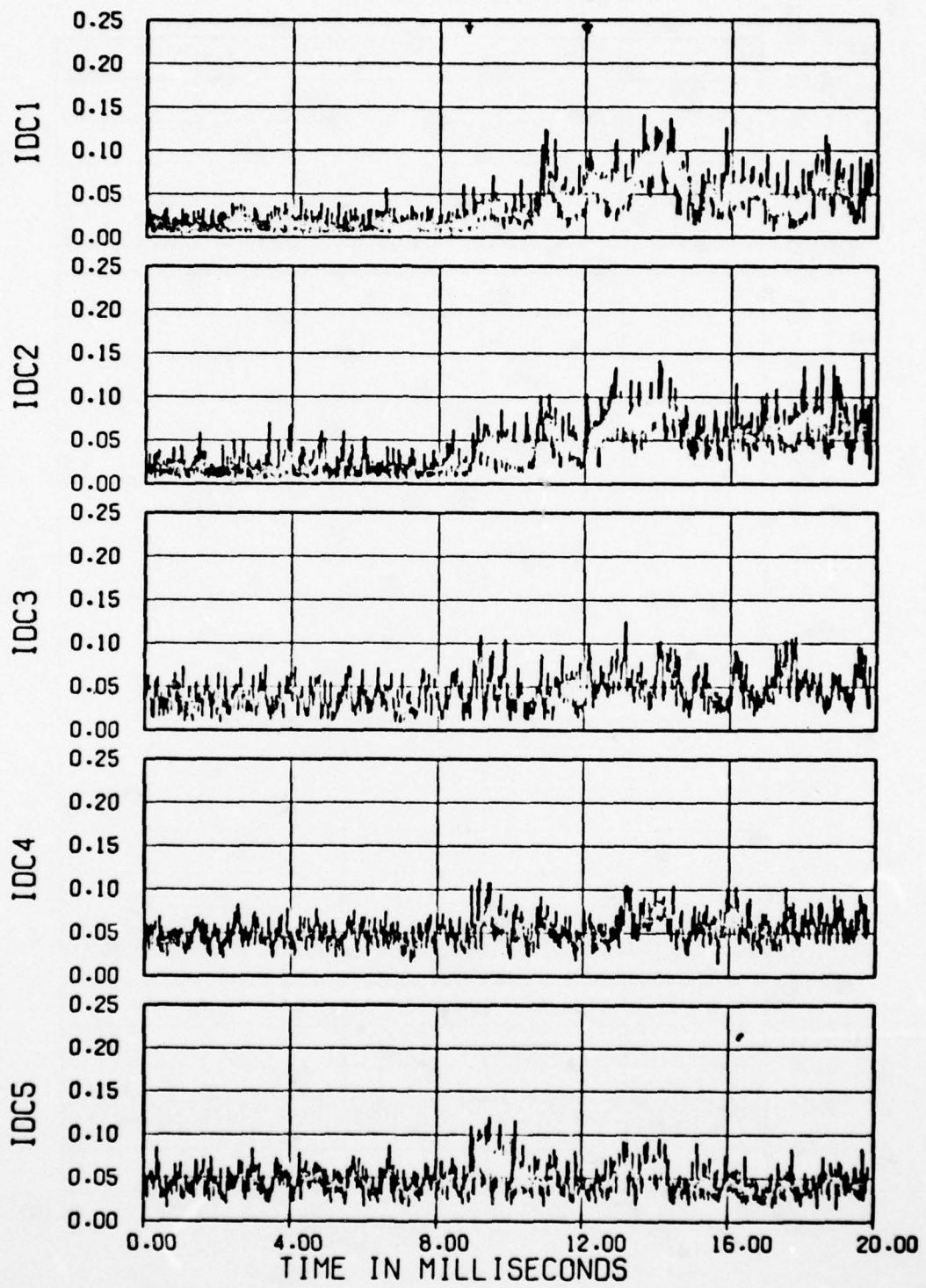


Figure 5.5. Continued.

OUTBOARD INLET

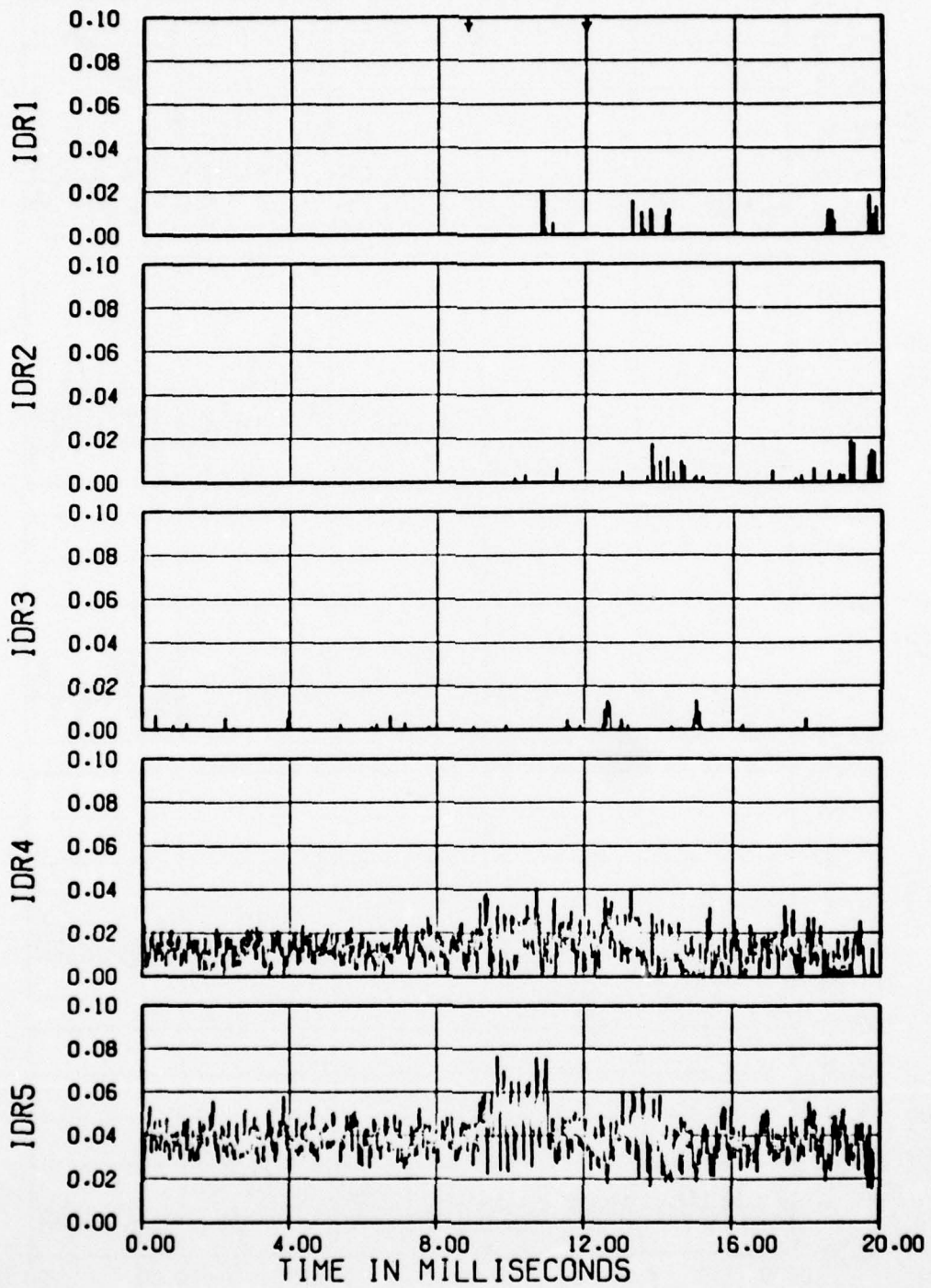


Figure 5.5. Continued.

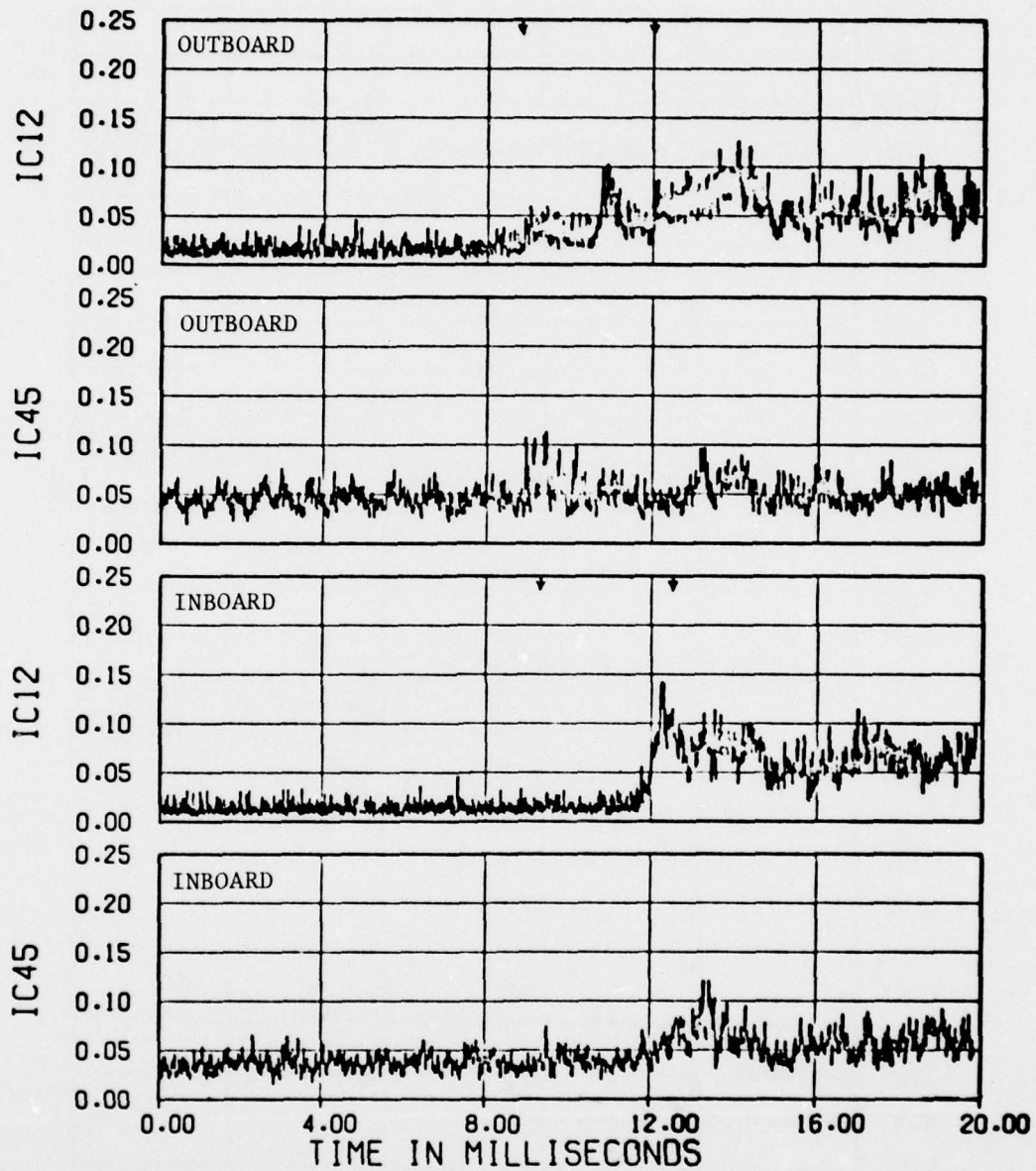


Figure 5.5. Continued.

INBOARD INLET

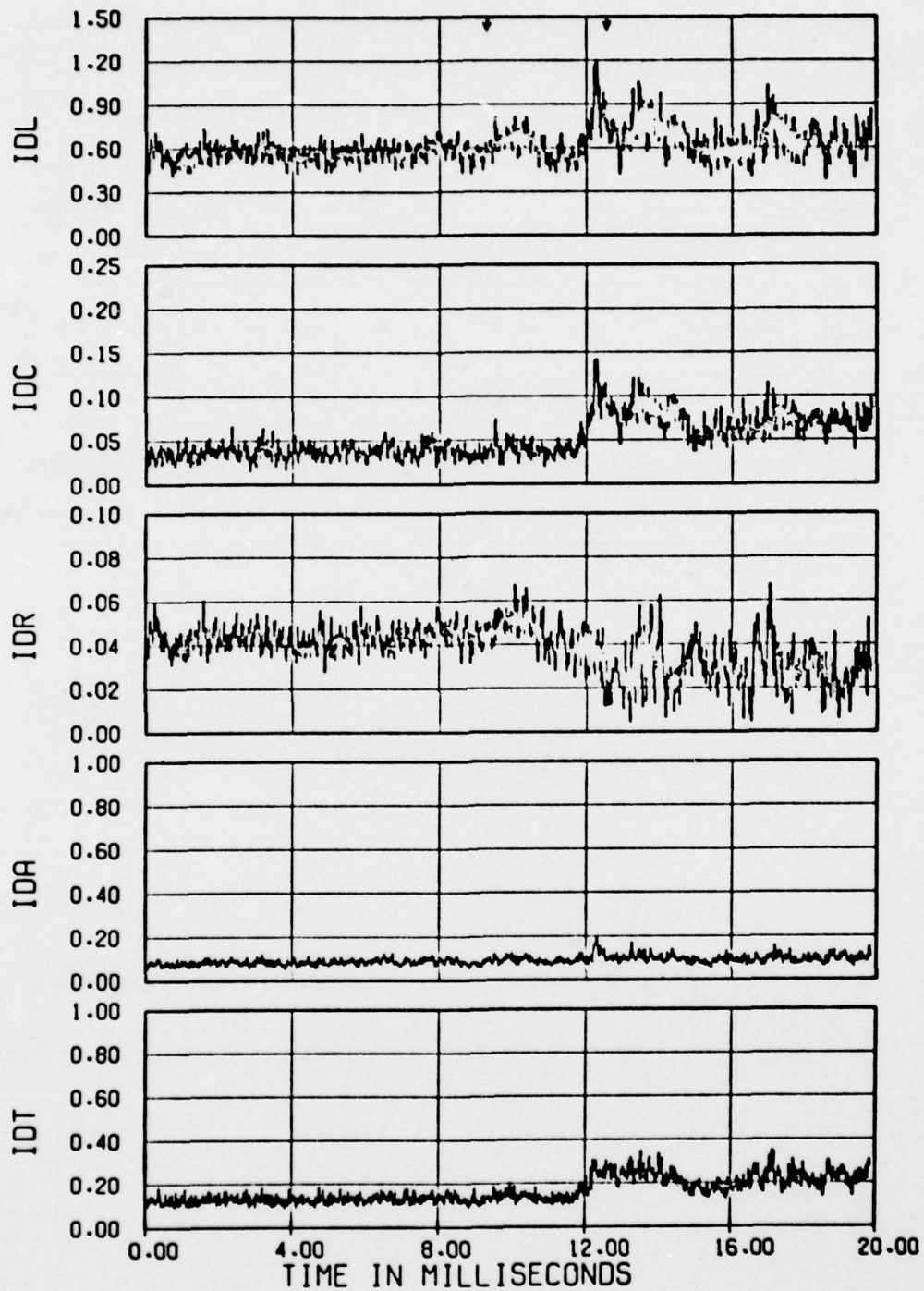


Figure 5.5. Continued.

INBOARD INLET

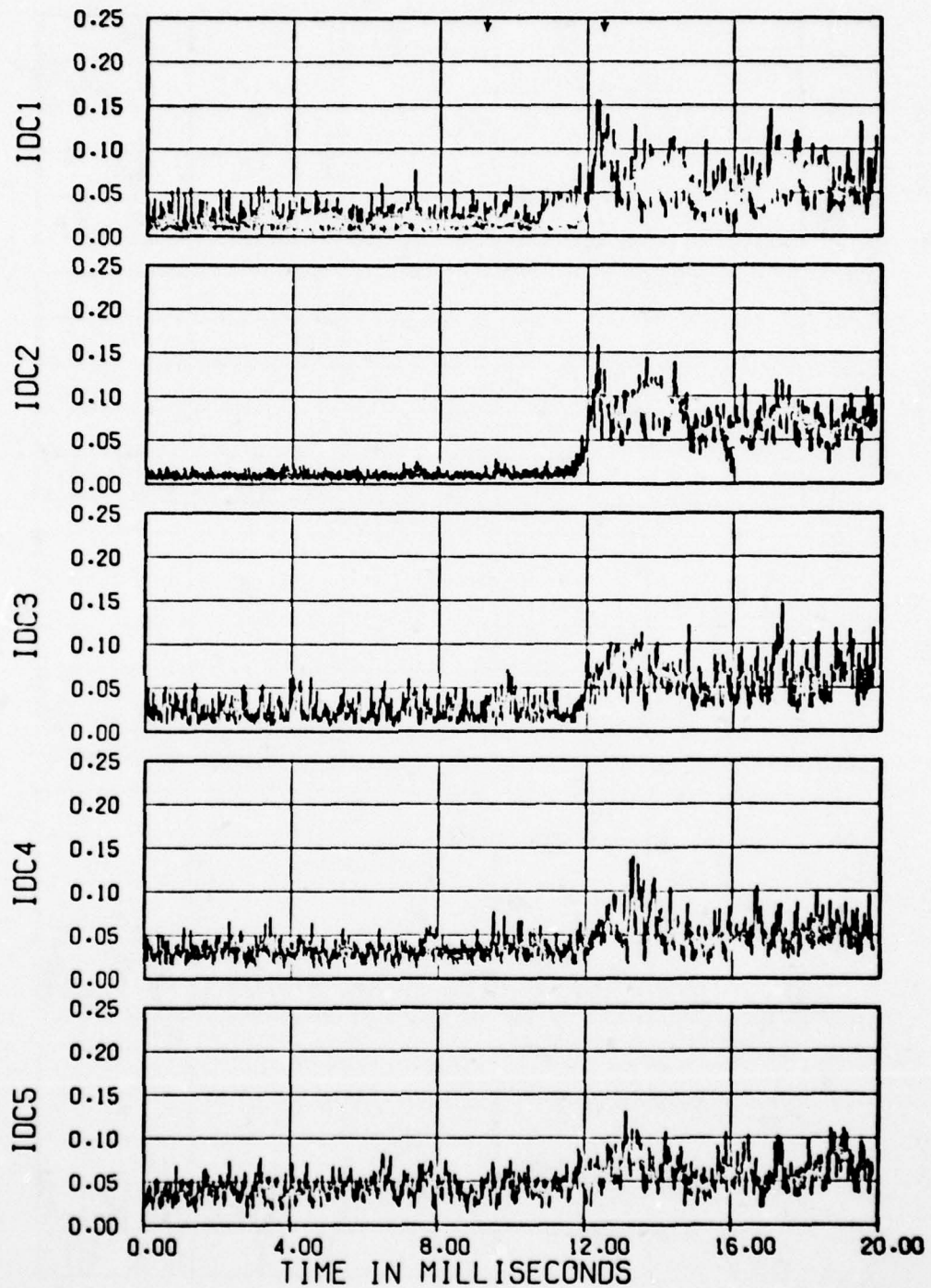


Figure 5.5. Continued.

INBOARD INLET

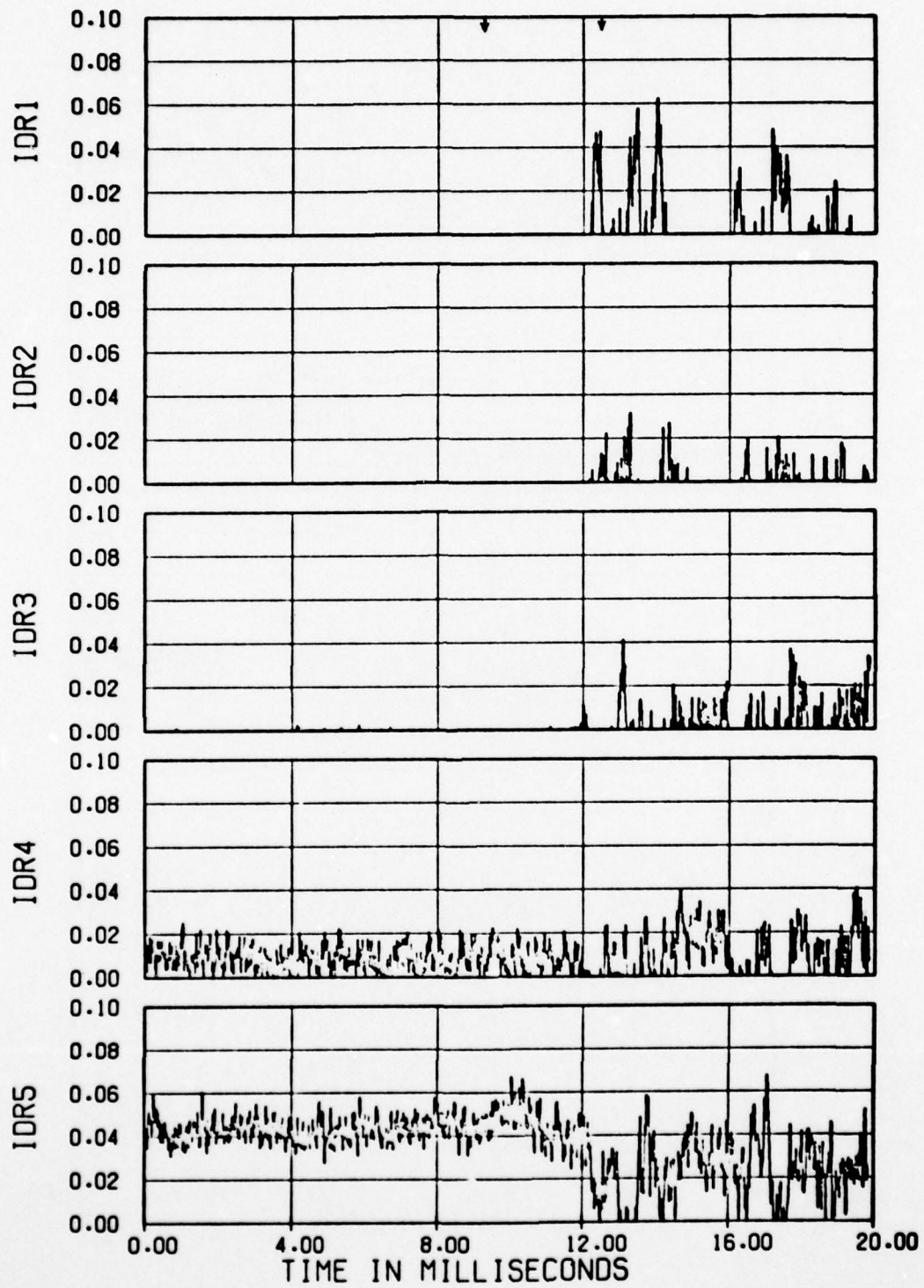


Figure 5.5. Concluded.

TABLE 5.1

EQUATIONS FOR CALCULATING DISTORTION
PARAMETERS IDC, IDR, IDL, IDA AND IDT

Circumferential Distortion on Individual Rings

$$IDC_i = (p_{t2_{avci}} - p_{t2_{min_i}}) / \bar{p}_{t2}$$

where

$$i = 1 \text{ to } 5 \text{ rings}$$

Hub Distortion

$$IDC_{12} = (IDC_1 + IDC_2) / 2$$

Tip Distortion

$$IDC_{45} = (IDC_4 + IDC_5) / 2$$

Total Circumferential Distortion

$$IDC = \text{Largest of } IDC_{12} \text{ or } IDC_{45}$$

Radial Distortion on Individual Rings

$$IDR_i = \text{Largest of } (1.0 - \frac{p_{t2_{ave_i}}}{\bar{p}_{t2}}, 0)$$

Total Radial Distortion

$$IDR = \text{Largest of } IDR_1, IDR_2, IDR_4, \text{ or } IDR_5$$

Fan Stall Margin Ratio

$$IDL = b(KCIRC)IDC + (KRAD)IDR$$

where

$$b = \frac{IDR/IDC}{A+B(IDR/IDC)} + C$$

TABLE 5.1. CONCLUDED

MACH NUMBER	TUNNEL TOTAL TEMPERATURE (°R)	KCIR	KRAD	SUPER POSITION FACTOR b		
				A	B	C
0 ≤ .15	All	7.93	12.41	-0.536	-0.591	1.
.15 ≤ .35	All	7.69	11.76	-0.520	-0.643	1.
.35 ≤ .65	All	7.69	12.28	-0.520	-0.644	1.
.65 ≤ .75	All	7.69	12.42	-0.520	-0.644	1.
.75 ≤ 1.5	Less Than/Equal To 560.	7.69	12.83	-0.520	-0.644	1.
.75 ≤ 1.5	Greater Than 560.	7.93	12.99	-0.553	-0.532	1.
1.5 ≤ 2.3	All	7.69	11.75	-0.560	-0.920	1.

Average Distortion:

$$IDA = (\bar{p}_{t2} - p_{t_{min}}) / \bar{p}_{t2}$$

Total Distortion:

$$IDT = (p_{t_{max}} - p_{t_{min}}) / \bar{p}_{t2}$$

IDR and the speed altitude regime. An indication of the normally allowable range of these distortion parameters for subsonic flight of the B-1 aircraft is given in Figure 5.6 (from Ref. 5.1). Generally, the inlet and engine can be considered to perform satisfactorily at values of IDL up to unity, which corresponds to values of IDC and IDR to the left of and below the solid line curve in Figure 5.6. For larger values of IDC, IDR or IDL the engine can stall, but will not necessarily do so.

5.3.1 Data Presentation

Typical time histories of distortion parameters for various over-pressure levels are presented in Figures 5.7 through 5.17. Figure 5.7 presents IDL for the lower tested mass flow rate (≈ 300 lb/sec) at Mach 0.70 for both inlets and Figures 5.8 and 5.9 present similar data for the higher tested mass flow rate (≈ 350 lb/sec) for the blastward and leeward inlets, respectively. Figure 5.10 presents IDC, IDR and IDL for the lower mass flow rate (≈ 300 lb/sec) at Mach 0.85 for the blastward inlet and Figure 5.11 presents IDL for the leeward inlet; Figure 5.12 presents IDC, IDR and IDL for the higher mass flow rate (≈ 350 lb/sec). Mach number effects on IDC, IDR and IDL are indicated in Figures 5.13 and 5.14 for blastward and leeward inlets for firings from Tube 2 and, for IDL only, in Figures 5.15 and 5.16 for firings from Tube 1. IDL measurements made during the three yawed firings are presented in Figure 5.17.

5.3.2 Effects at Low Mass Flow Rates

Considering now the distortion effects at the lower tested mass flow rate of about 300 lb/sec (full scale), it can be seen from Figure 5.7 for Mach 0.70 and from Figure 5.10c and 5.11 for Mach 0.85 that the stall margin, IDL, is usually well below the normally safe limit of unity, usually being near to or below 0.5, for the time range where the test data are definitely representative of a blast wave (between the two arrows in the figures). Corresponding values of IDC and IDR, shown in Figure 5.10 for Mach 0.85 are similarly rather low, being generally below 0.10 for IDC and below 0.05 for IDR.

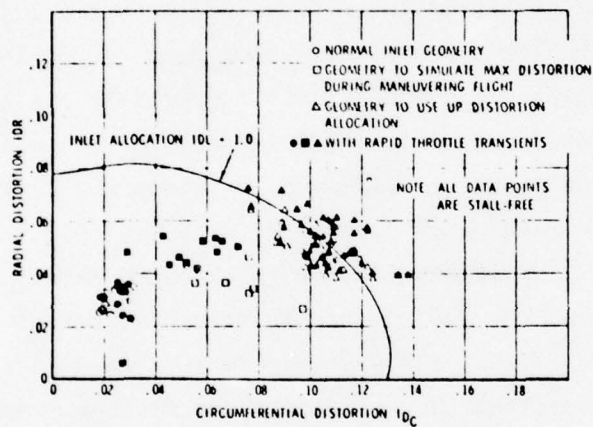


Figure 5.6. Range of distortion indices for B-1 inlet at subsonic cruise.

AD-A065 388

KAMAN AVIDYNE BURLINGTON MASS
WIND-TUNNEL SHOCK-TUBE SIMULATION AND EVALUATION OF BLAST EFFEC--ETC(U)
MAR 78 J R RUETENIK, R F SMILEY

F/G 21/5

DNA001-76-C-0107

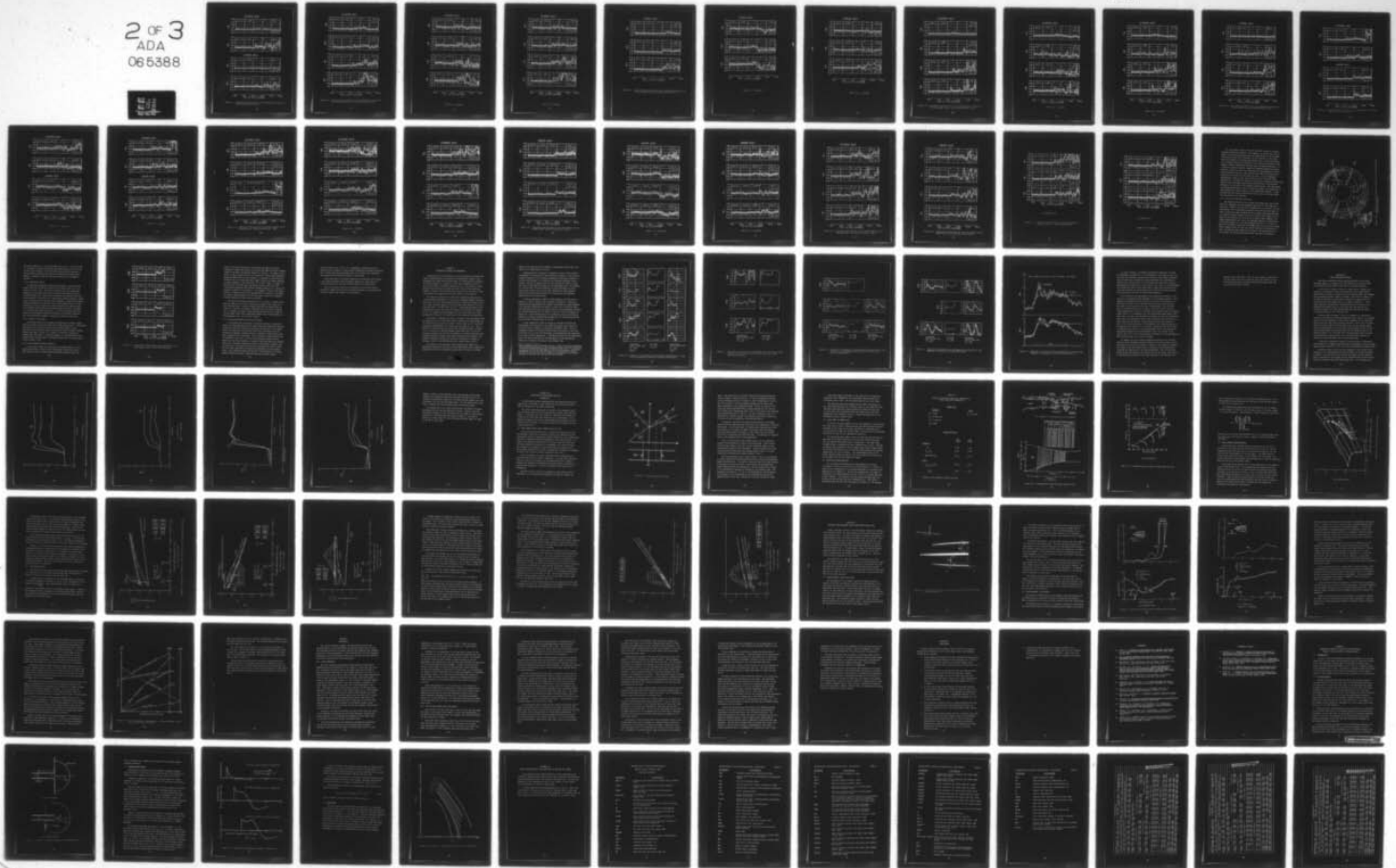
UNCLASSIFIED

KA-TR-147

DNA-4590F

NL

2 of 3
ADA
06 5388



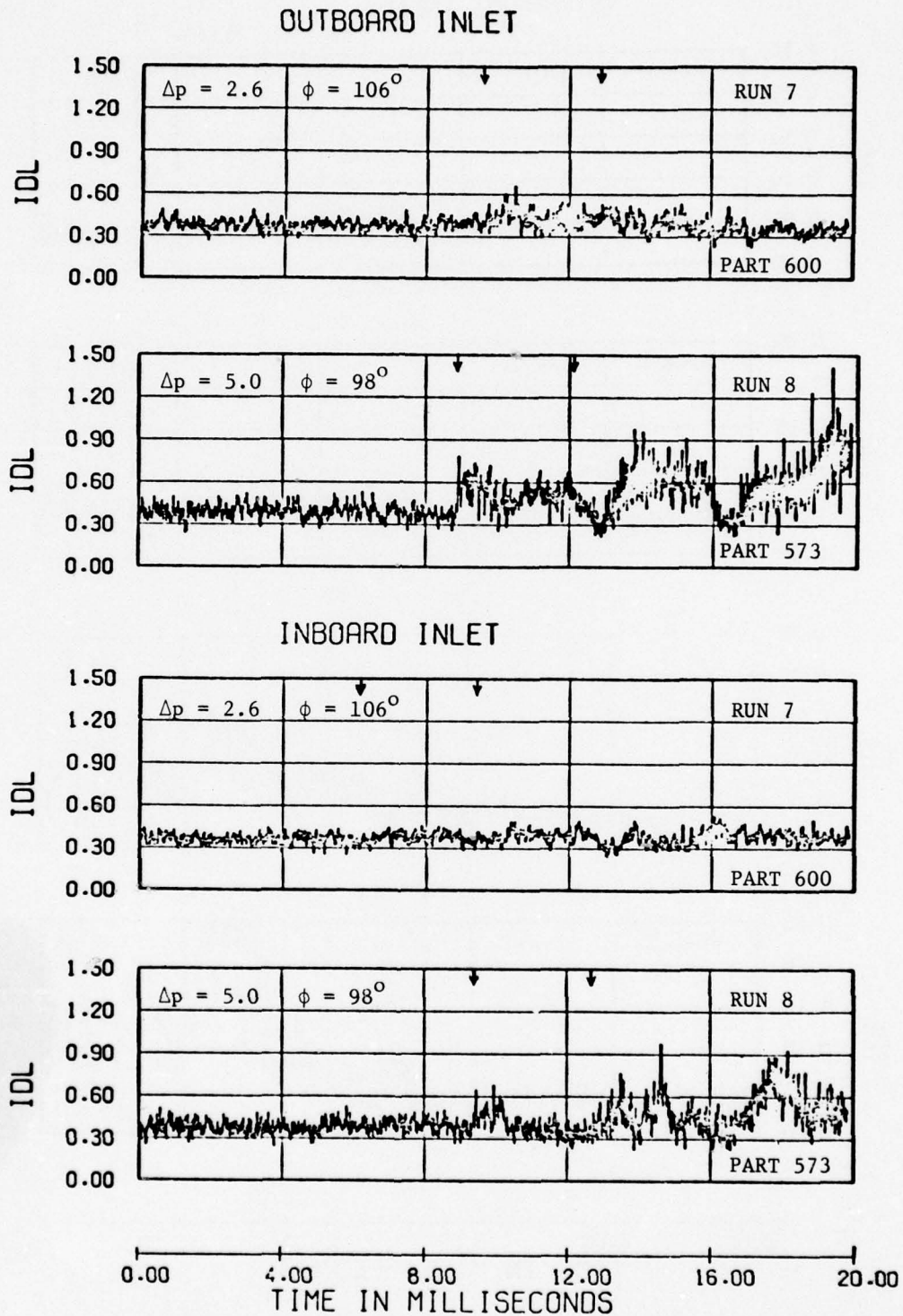


Figure 5.7. Distortion time histories for two overpressures at Mach 0.70, flow rate \approx 300 lb/sec, tube 2.

OUTBOARD INLET

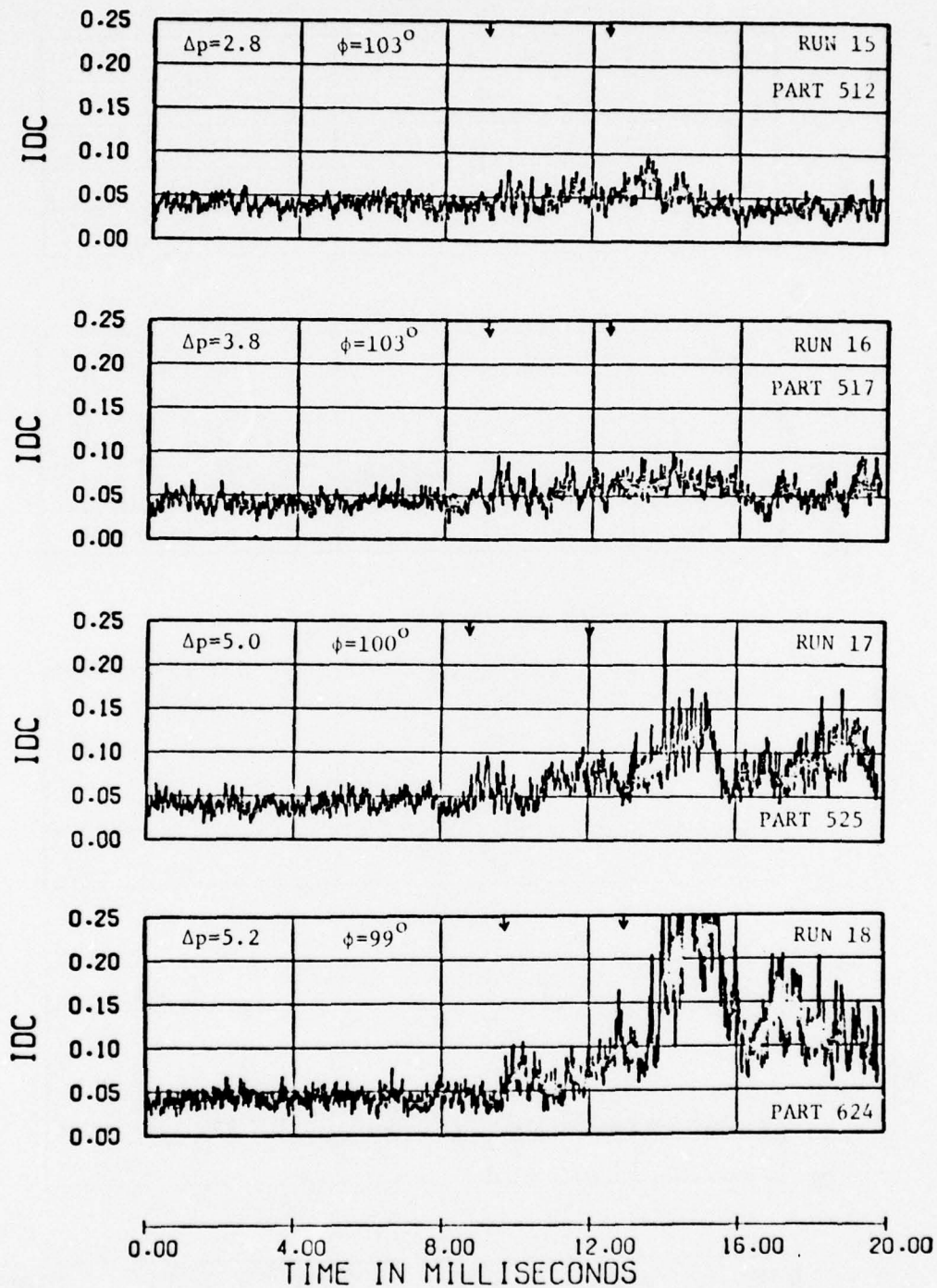


Figure 5.8. Distortion time histories for four overpressures at Mach 0.70 for the blastward inlet, flow rate ≈ 350 lb/sec, tube 2.

OUTBOARD INLET

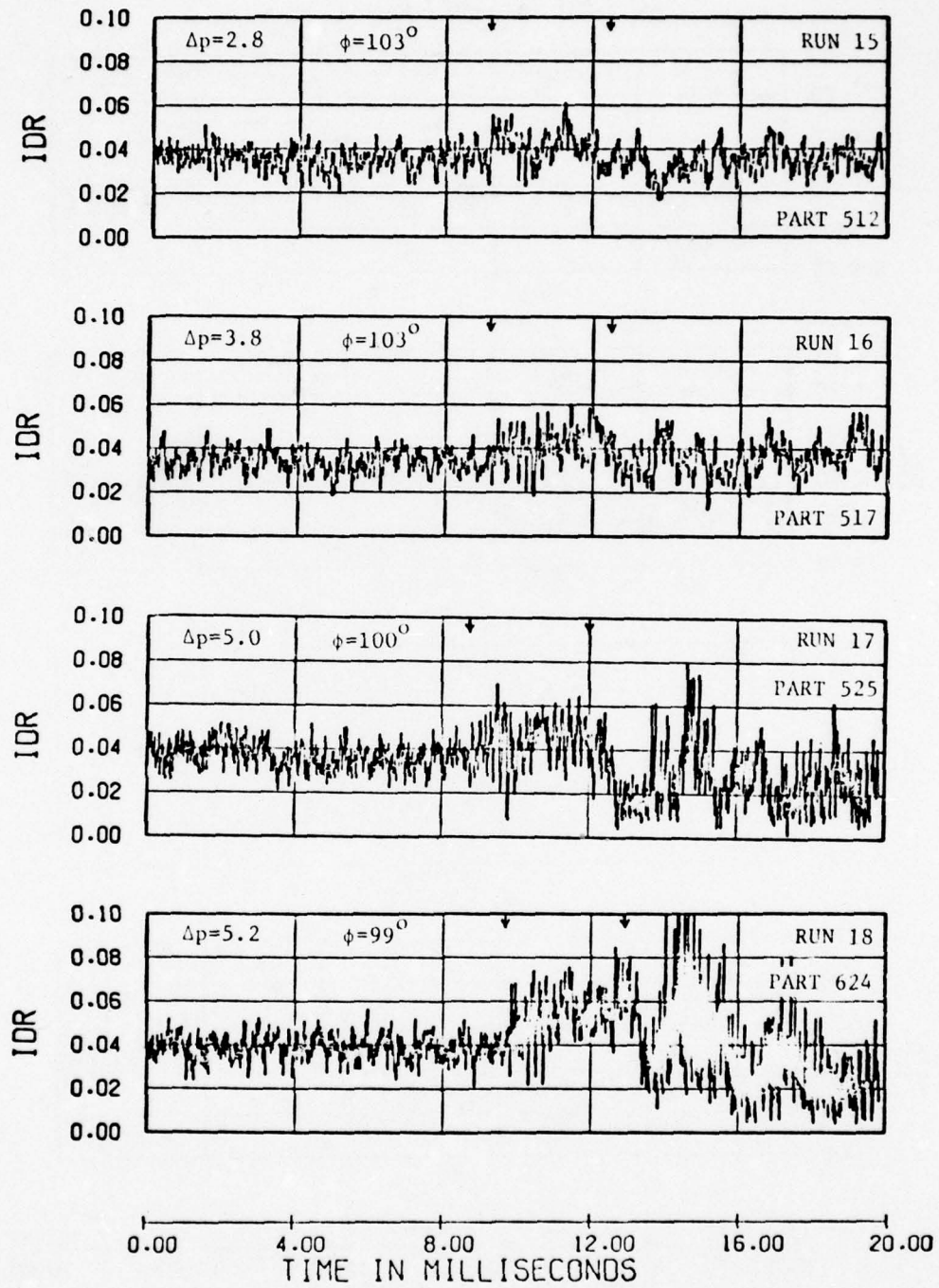


Figure 5.8. Continued.

OUTBOARD INLET

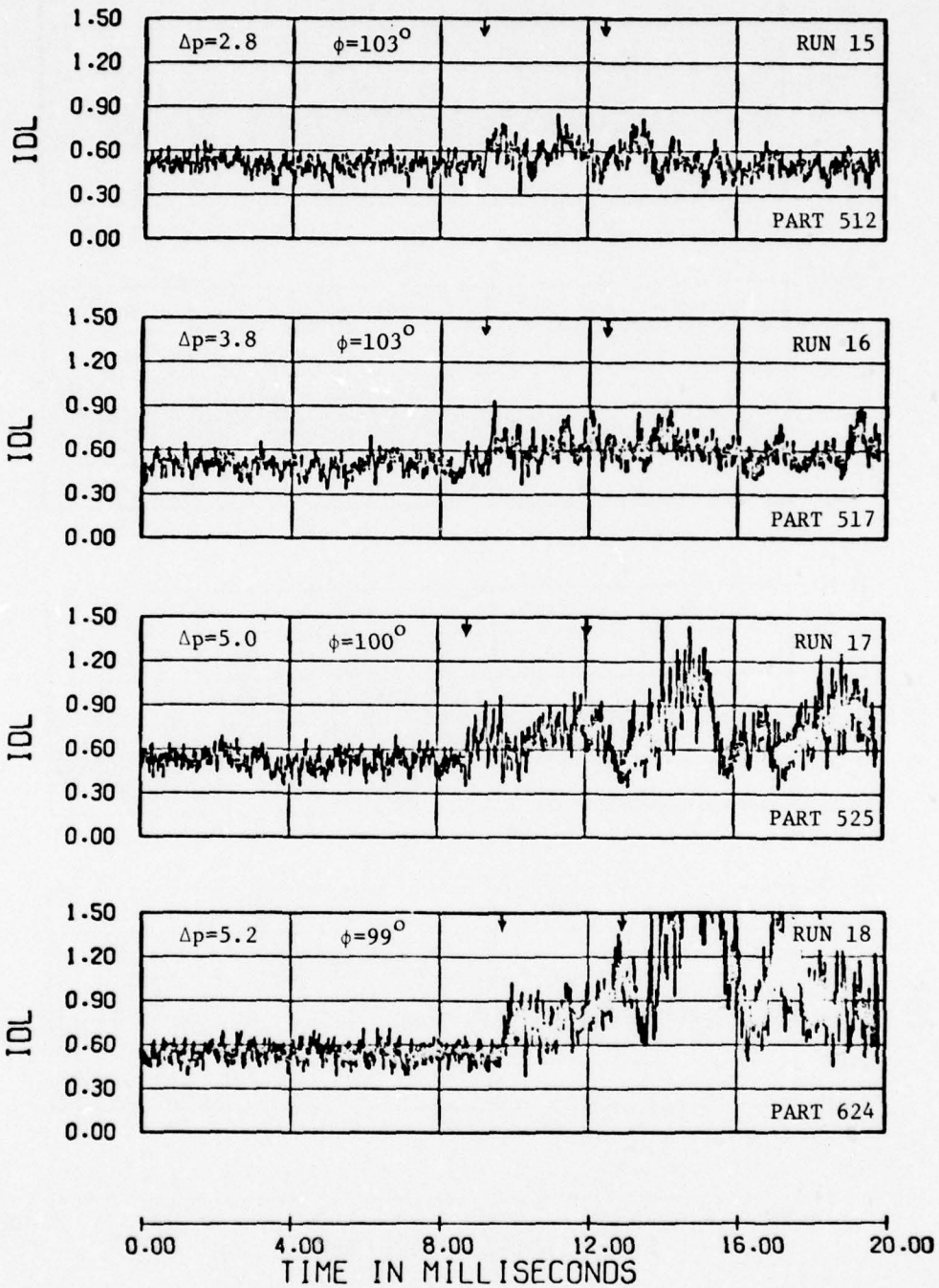


Figure 5.8. Concluded.

INBOARD INLET

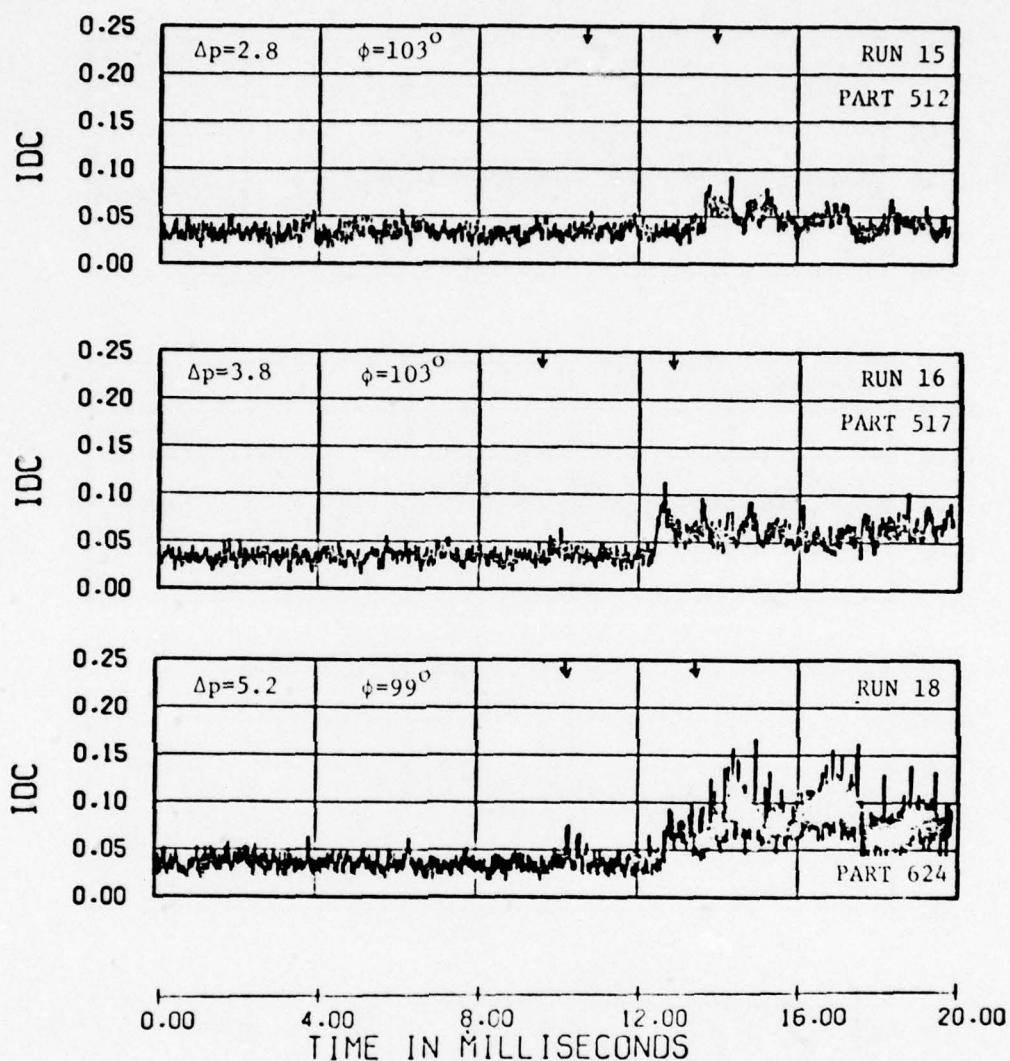


Figure 5.9. Distortion time histories for three overpressures at Mach 0.70 for the leeward inlet, flow rate ≈ 350 lb/sec, tube 2.

INBOARD INLET

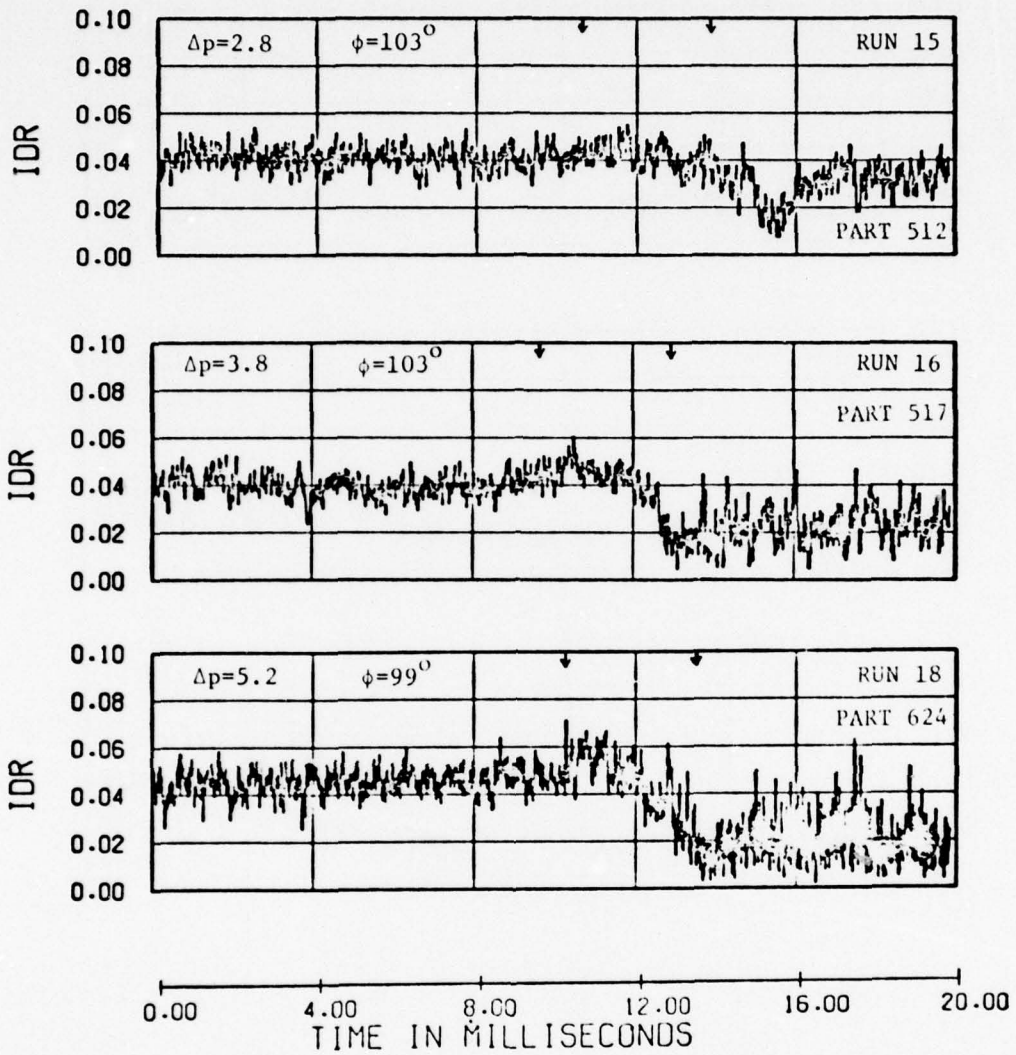


Figure 5.9. Continued.

INBOARD INLET

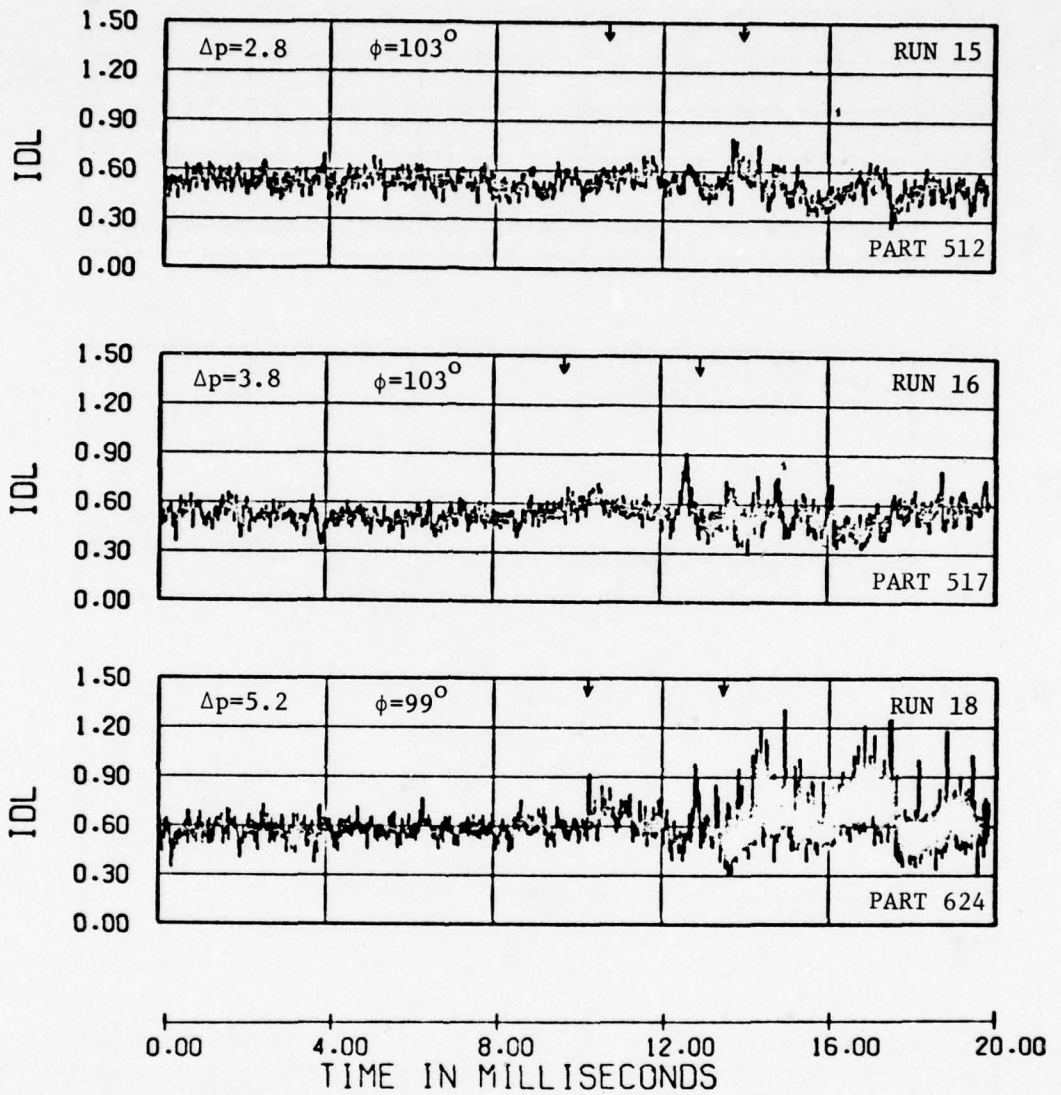


Figure 5.9. Concluded.

OUTBOARD INLET

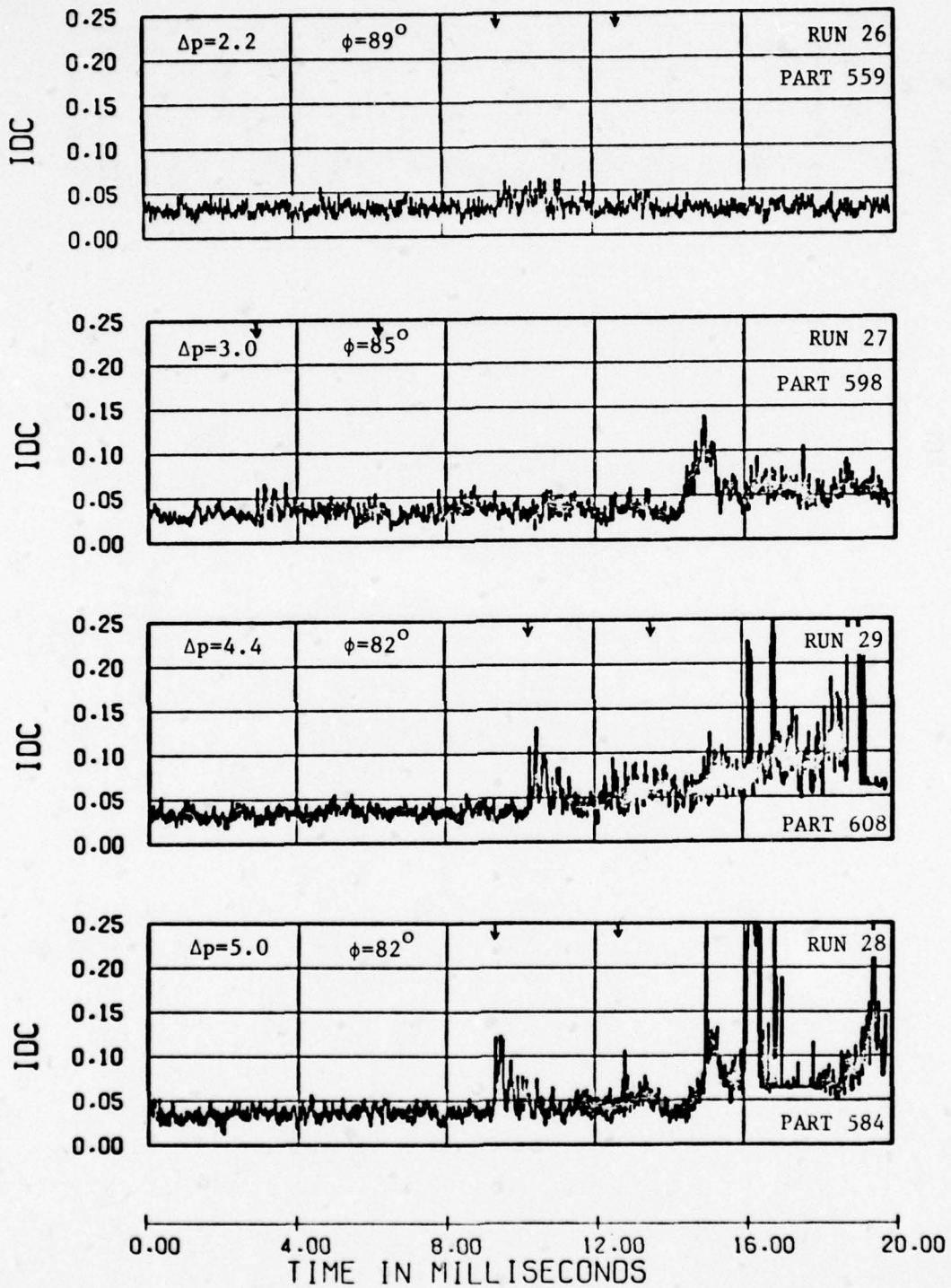


Figure 5.10. Distortion time histories for four overpressures at Mach 0.85 for the blastward inlet, flow rate ≈ 300 lb/sec, tube 1.

OUTBOARD INLET

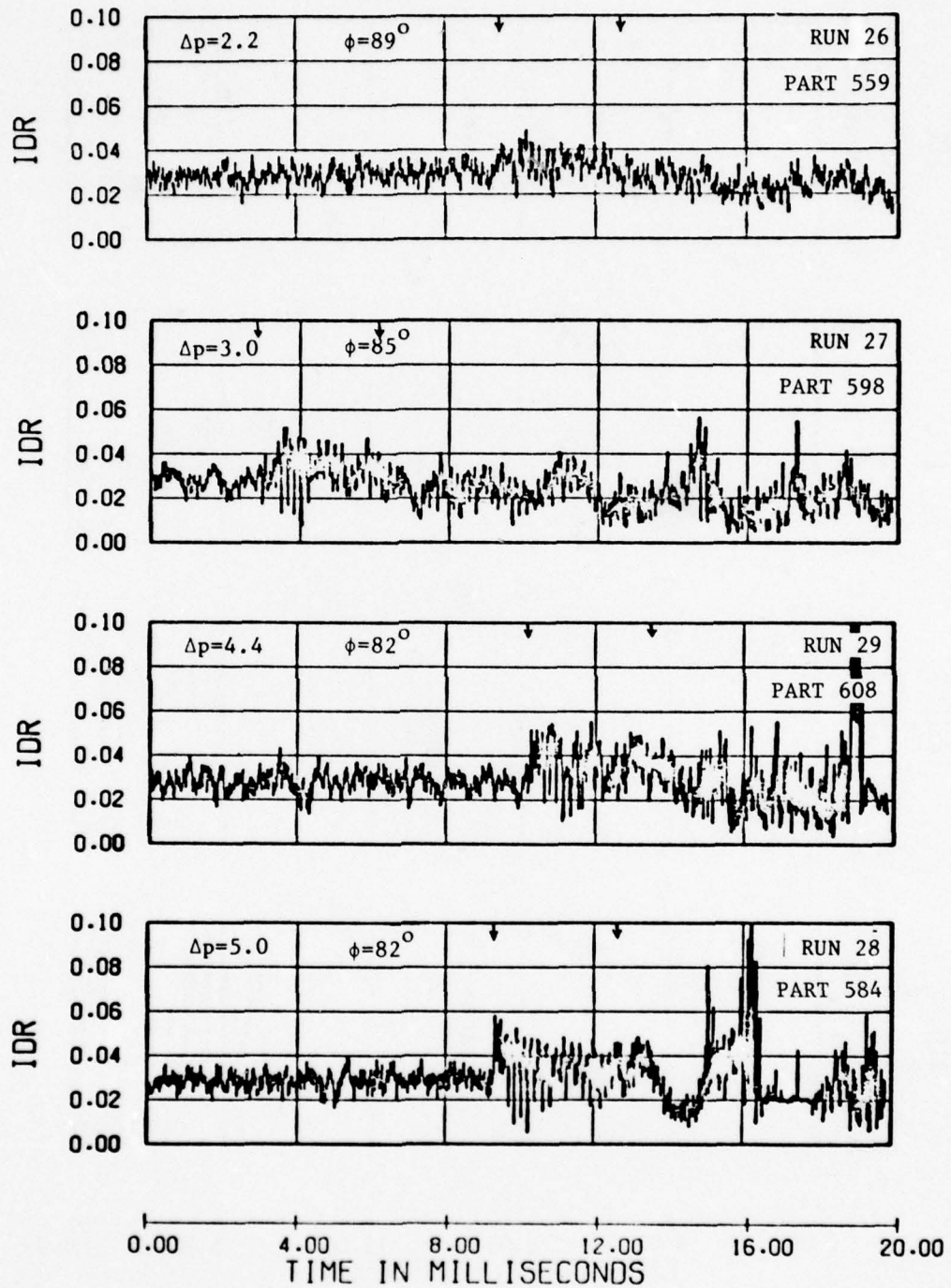


Figure 5.10. Continued.

OUTBOARD INLET

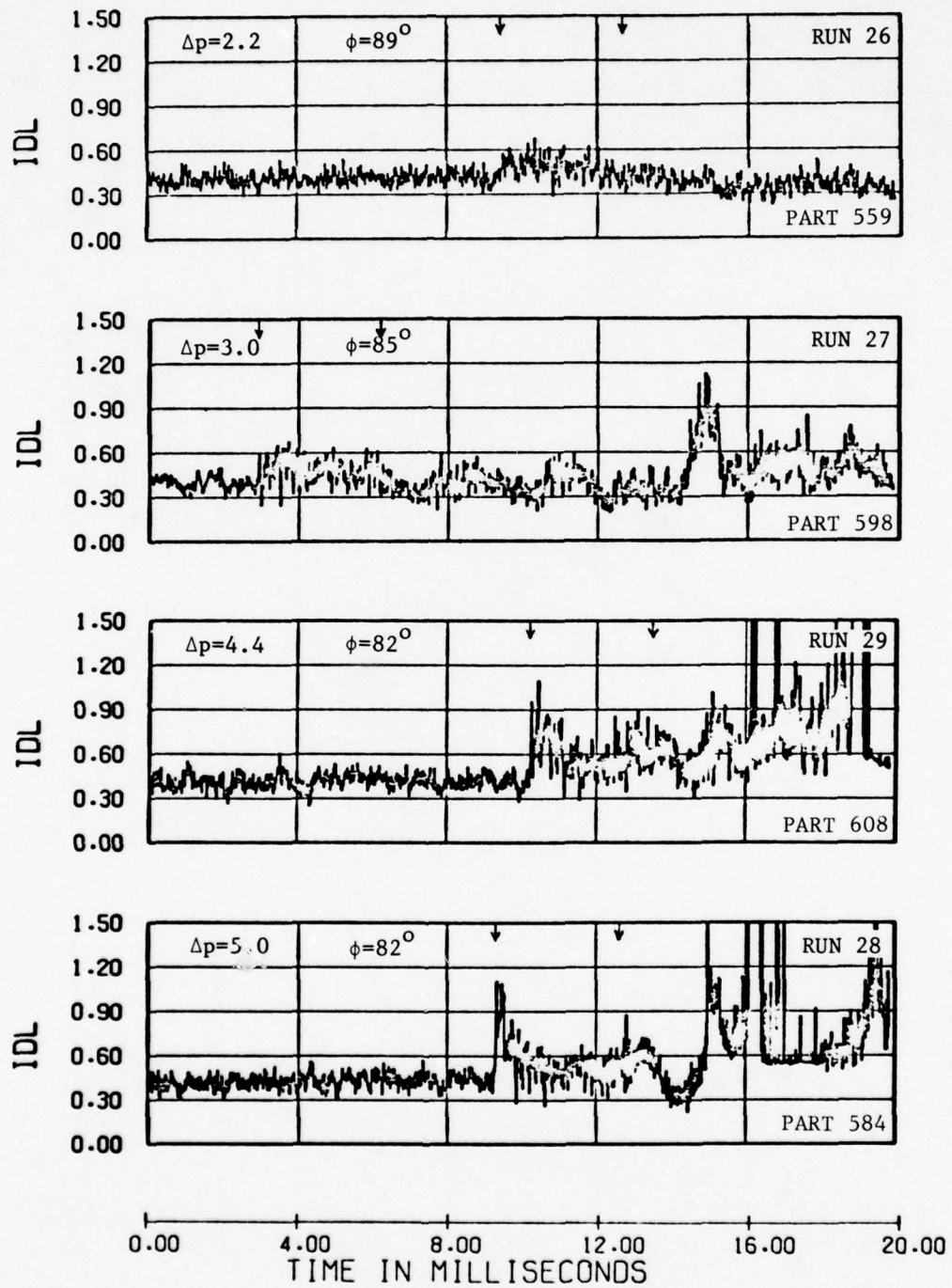


Figure 5.10. Concluded.

INBOARD INLET

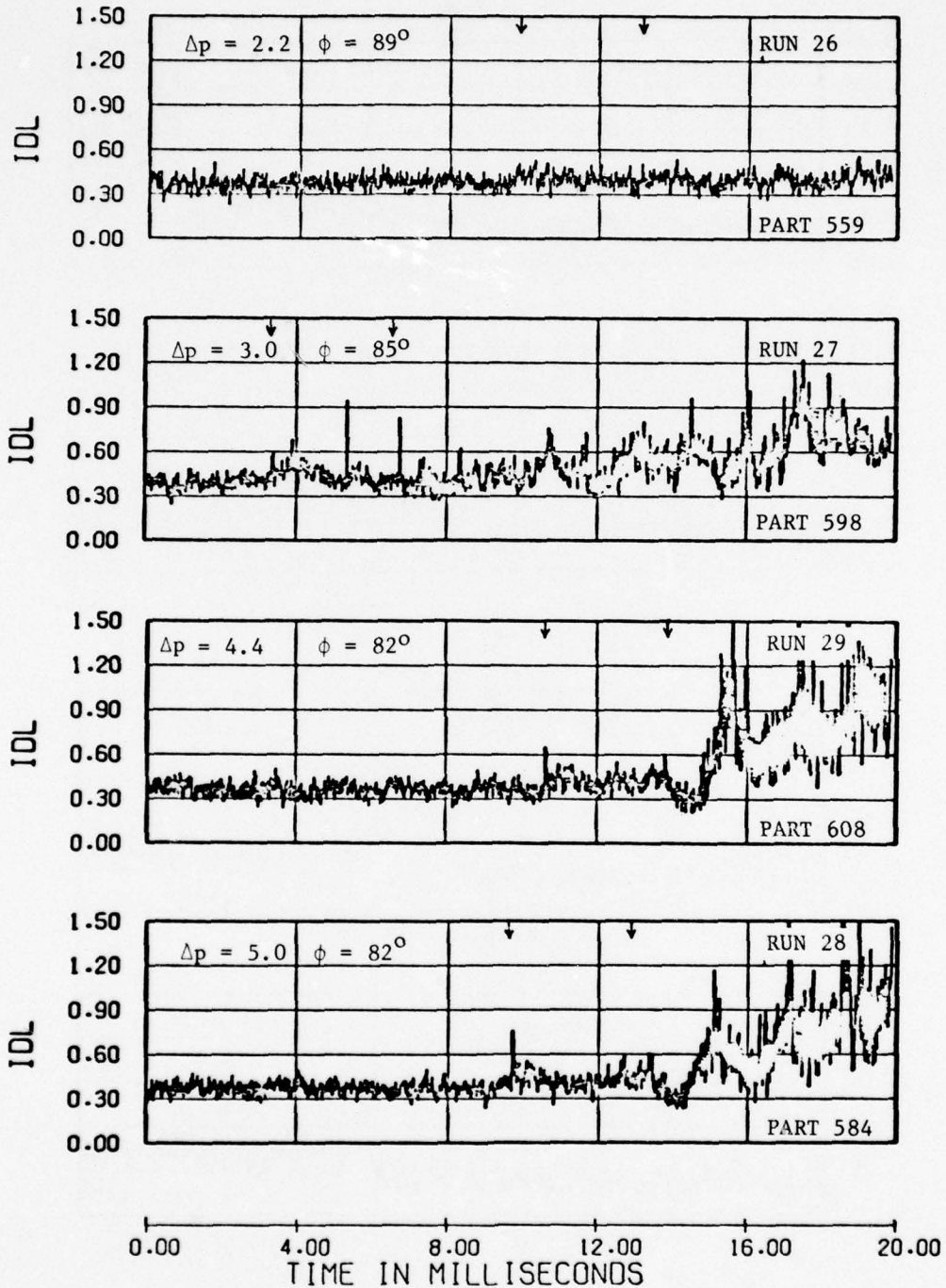


Figure 5.11. Distortion time histories for four overpressures at Mach 0.85 for the leeward inlet, flow rate ≈ 300 lb/sec, tube 1.

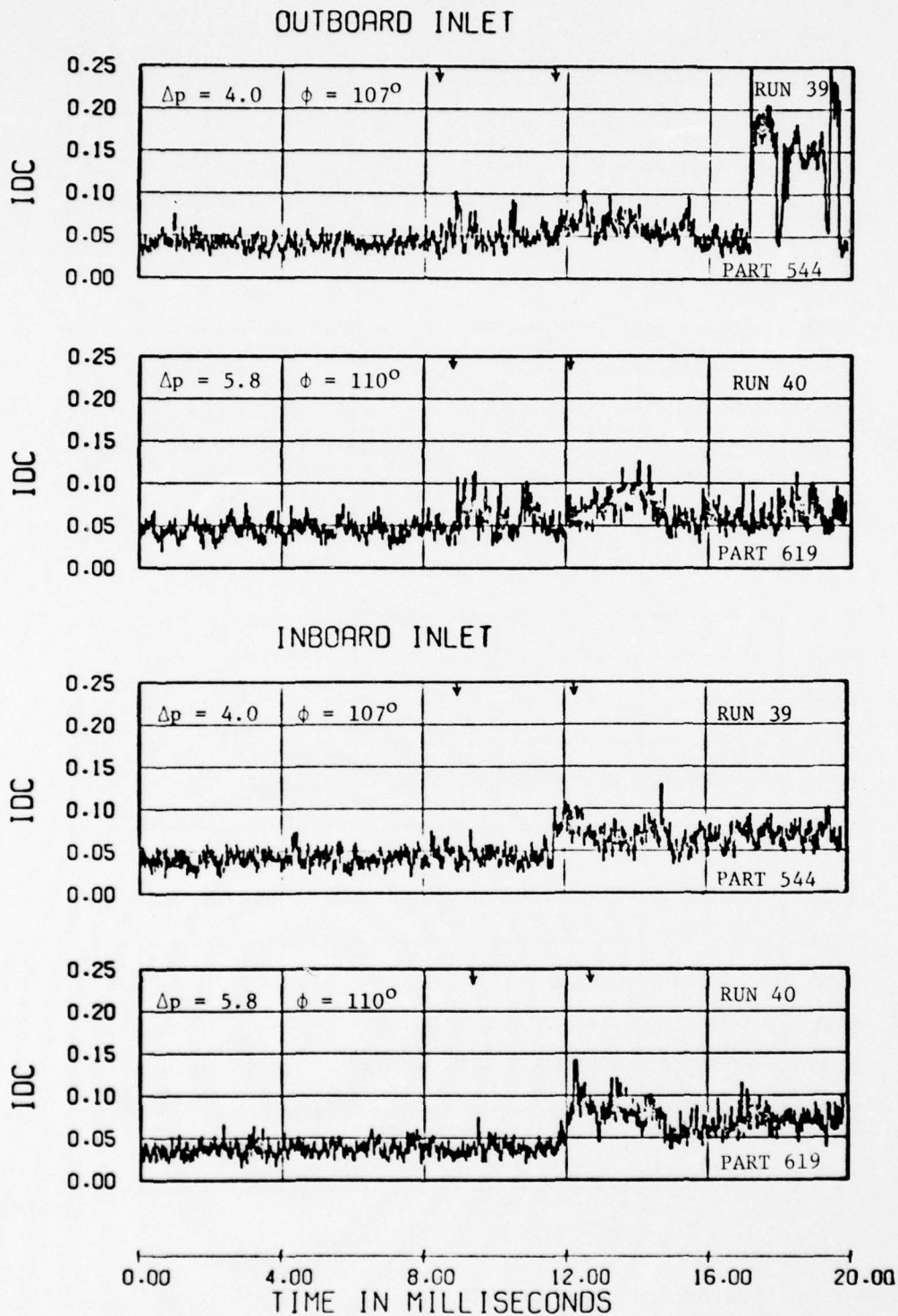
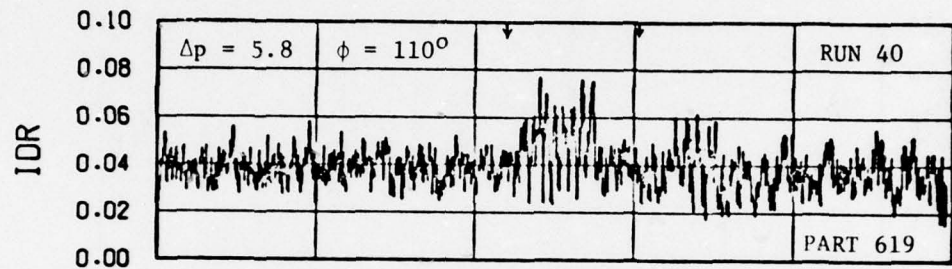
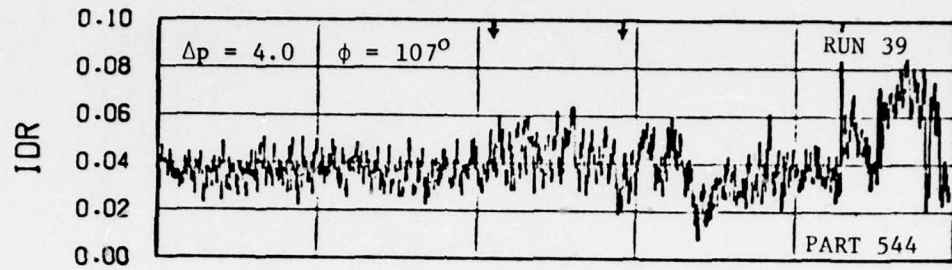
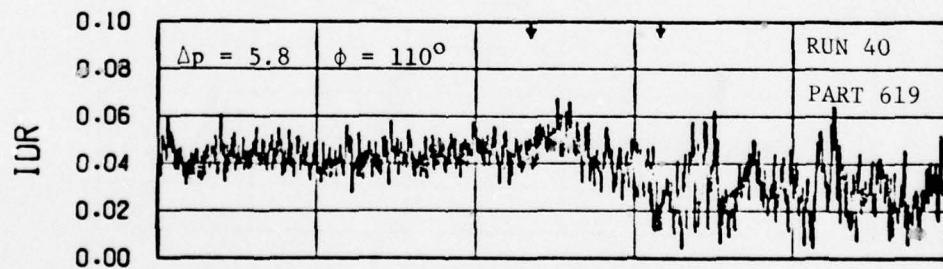
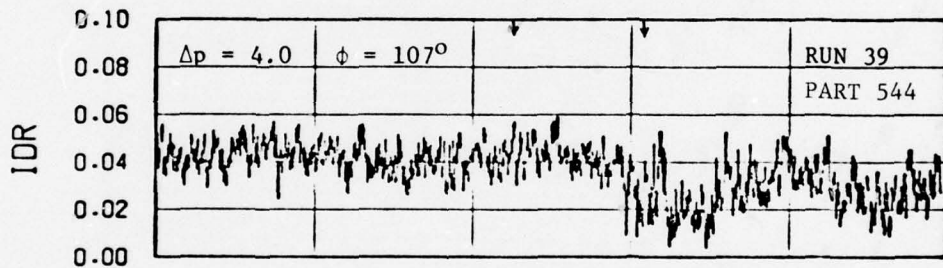


Figure 5.12. Distortion time histories for two overpressures at Mach 0.85, flow rate ≈ 350 lb/sec, tube 2.

OUTBOARD INLET



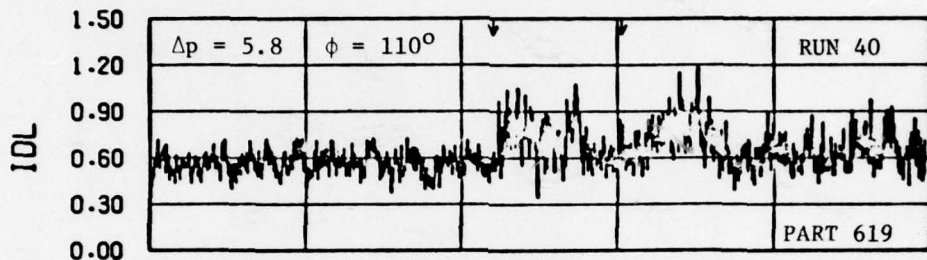
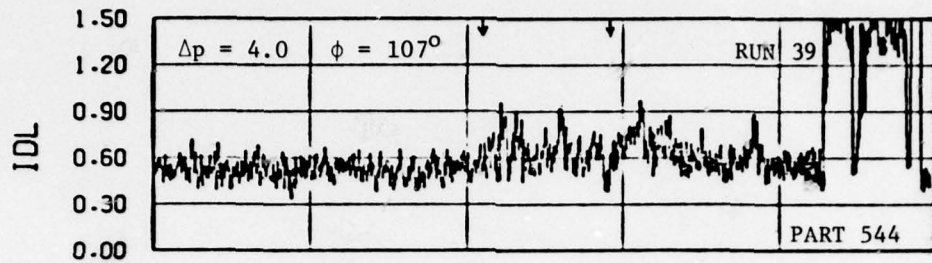
INBOARD INLET



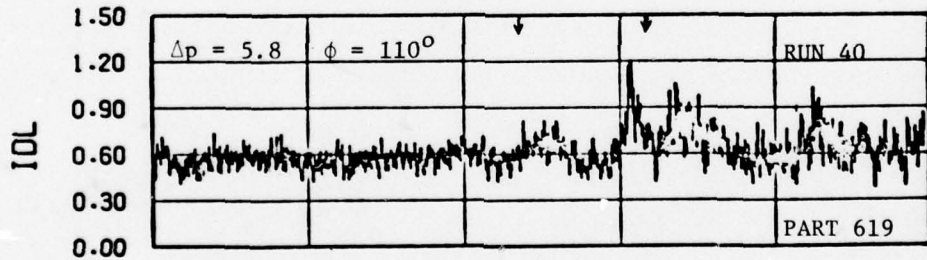
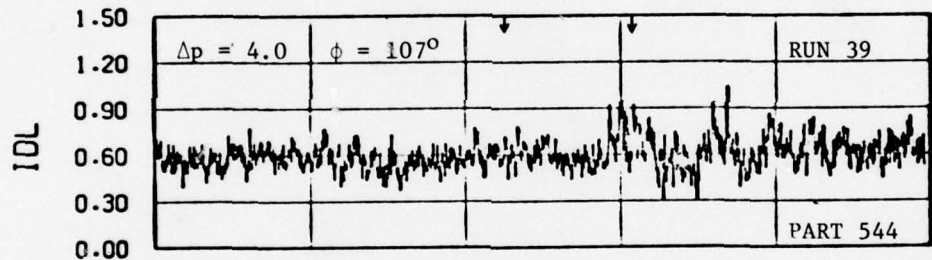
0.00 4.00 8.00 12.00 16.00 20.00
TIME IN MILLISECONDS

Figure 5.12. Continued.

OUTBOARD INLET



INBOARD INLET



0.00 4.00 8.00 12.00 16.00 20.00
 TIME IN MILLISECONDS

Figure 5.12. Concluded.

OUTBOARD INLET

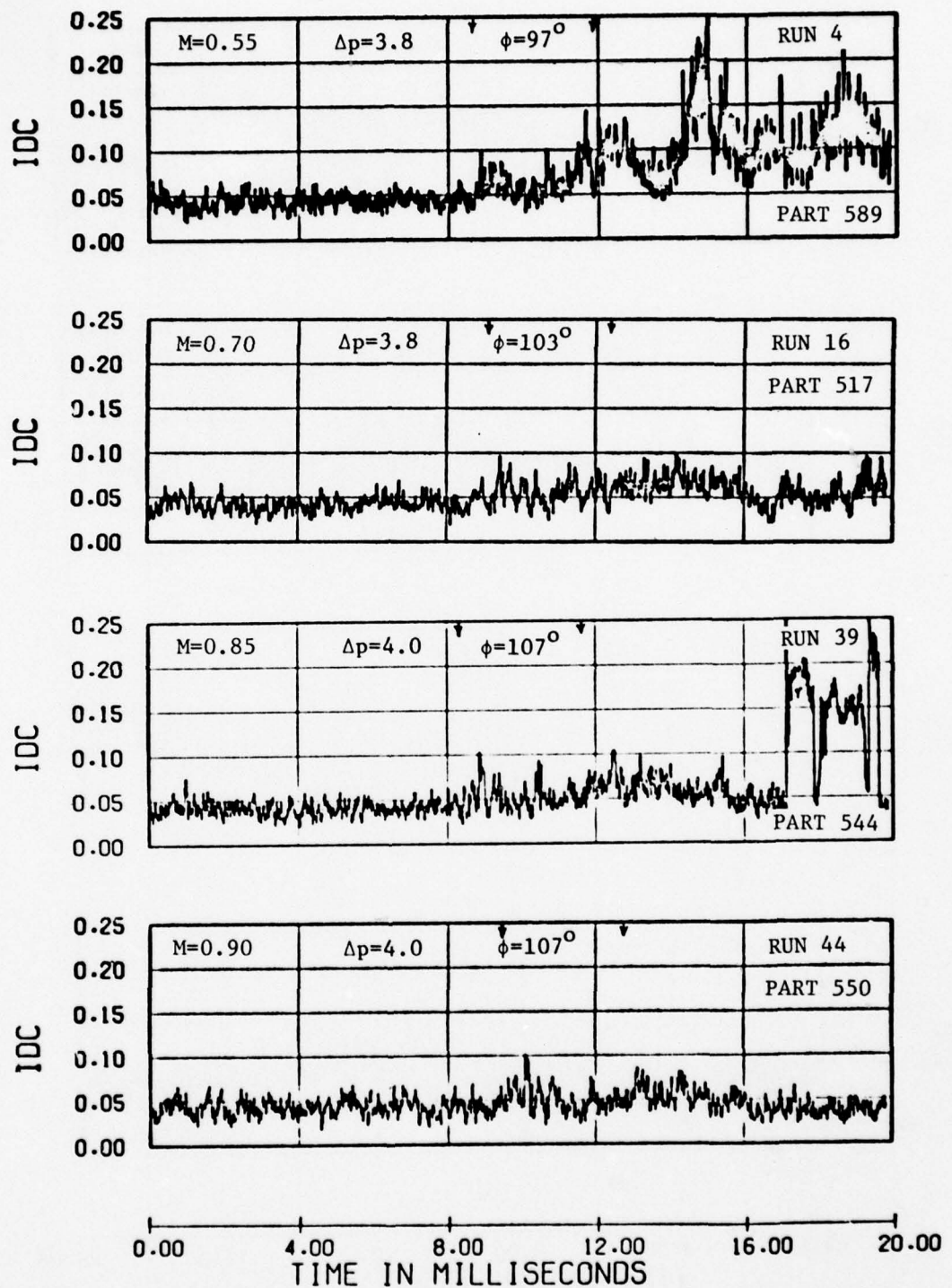


Figure 5.13. Distortion time histories for four Mach numbers for the blastward inlet, flow rate ≈ 350 lb/sec, tube 2.

OUTBOARD INLET

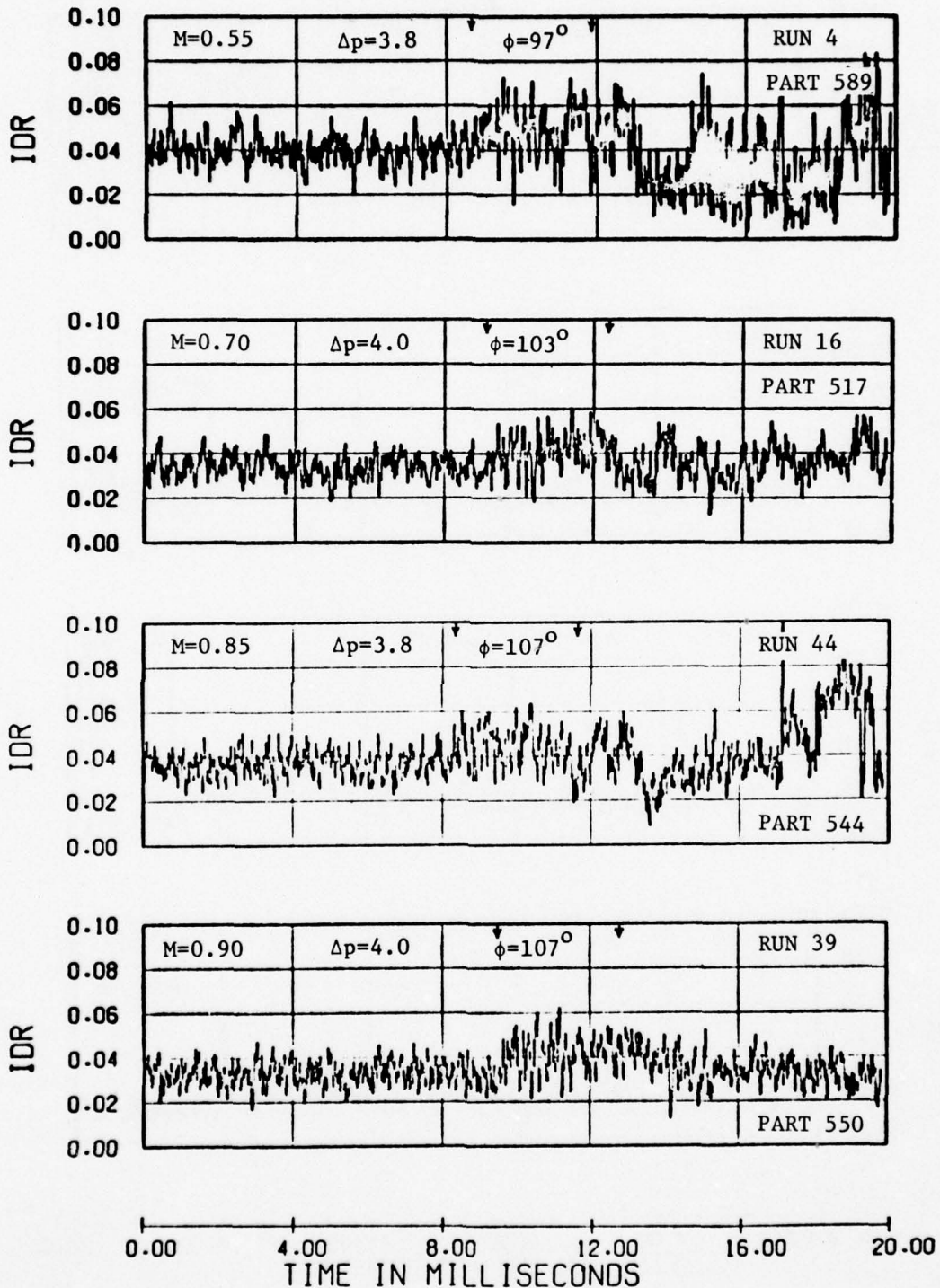


Figure 5.13. Continued.

OUTBOARD INLET

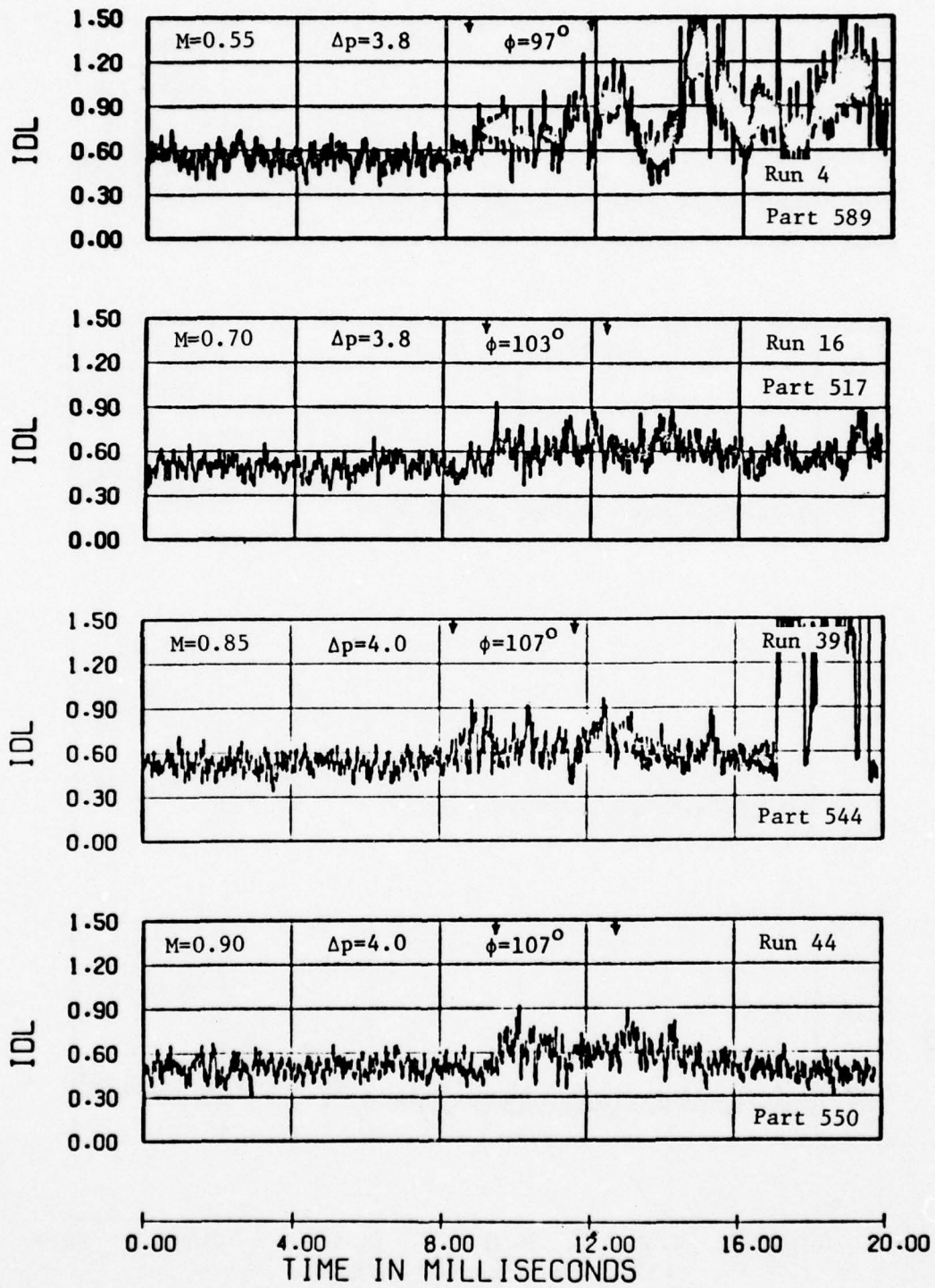


Figure 5.13. Concluded.

INBOARD INLET

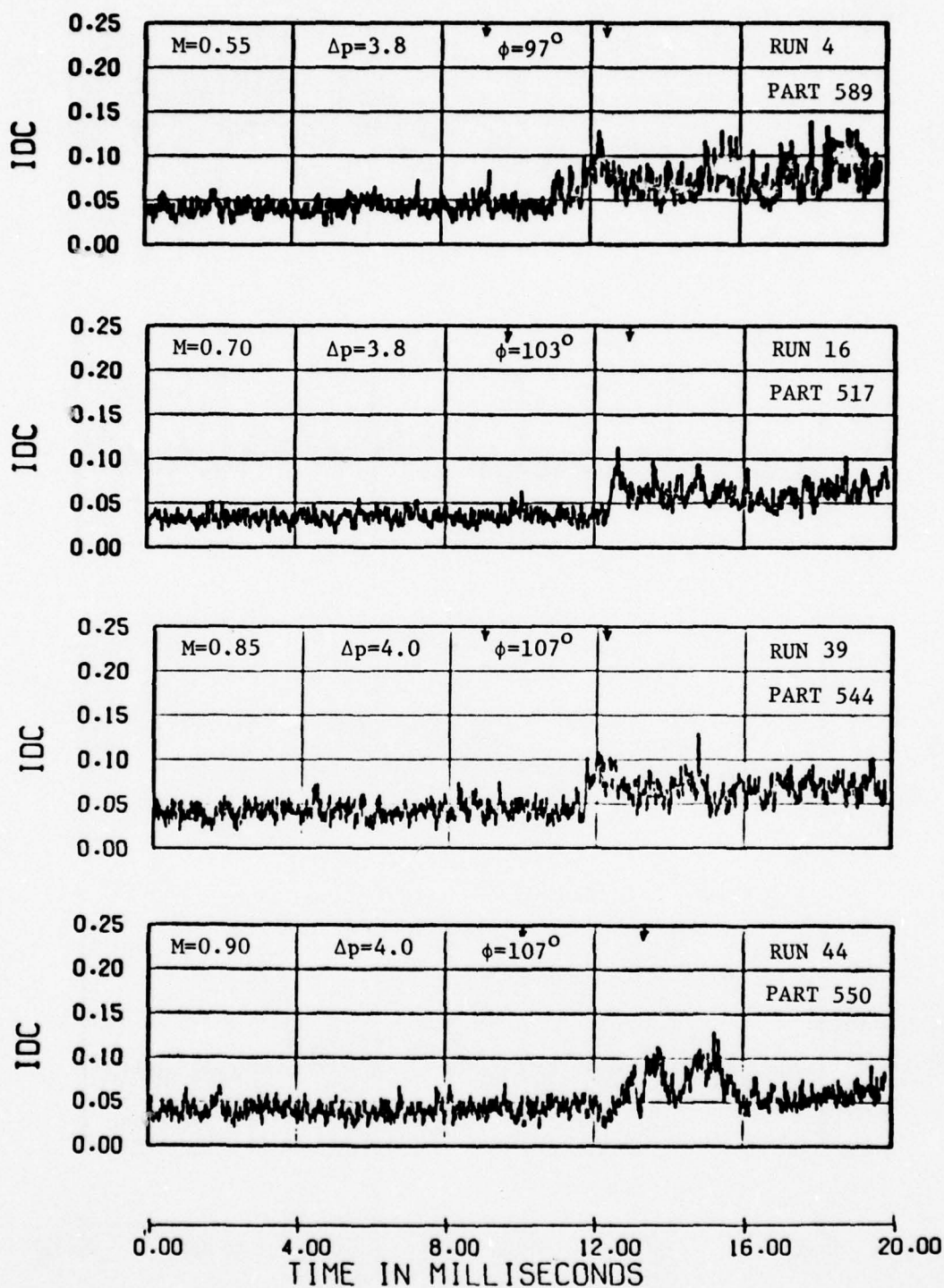


Figure 5.14. Distortion time histories for four Mach numbers for the leeward inlet, flow rate ≈ 350 lb/sec, tube 2.

INBOARD INLET

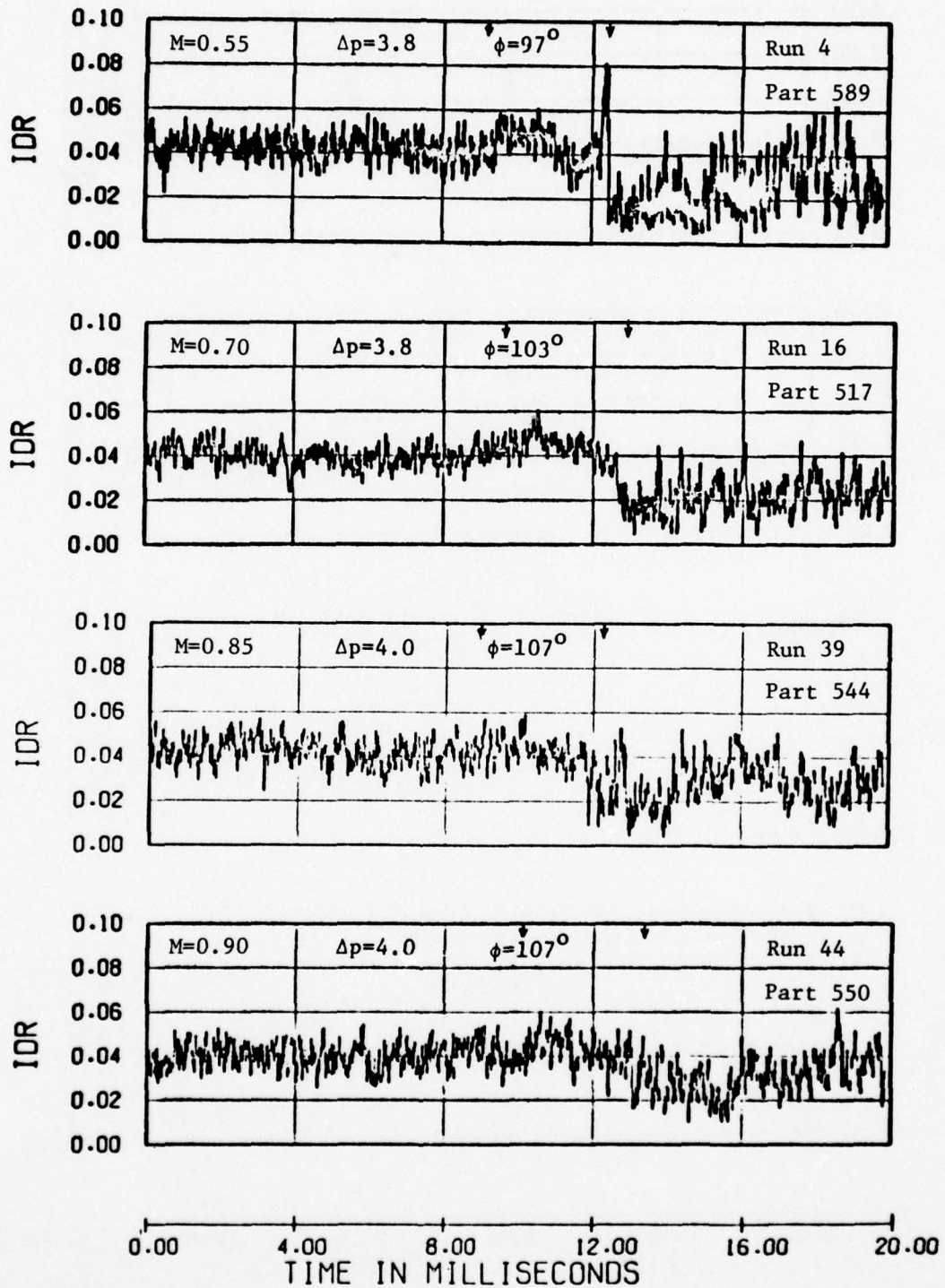


Figure 5.14. Continued.

INBOARD INLET

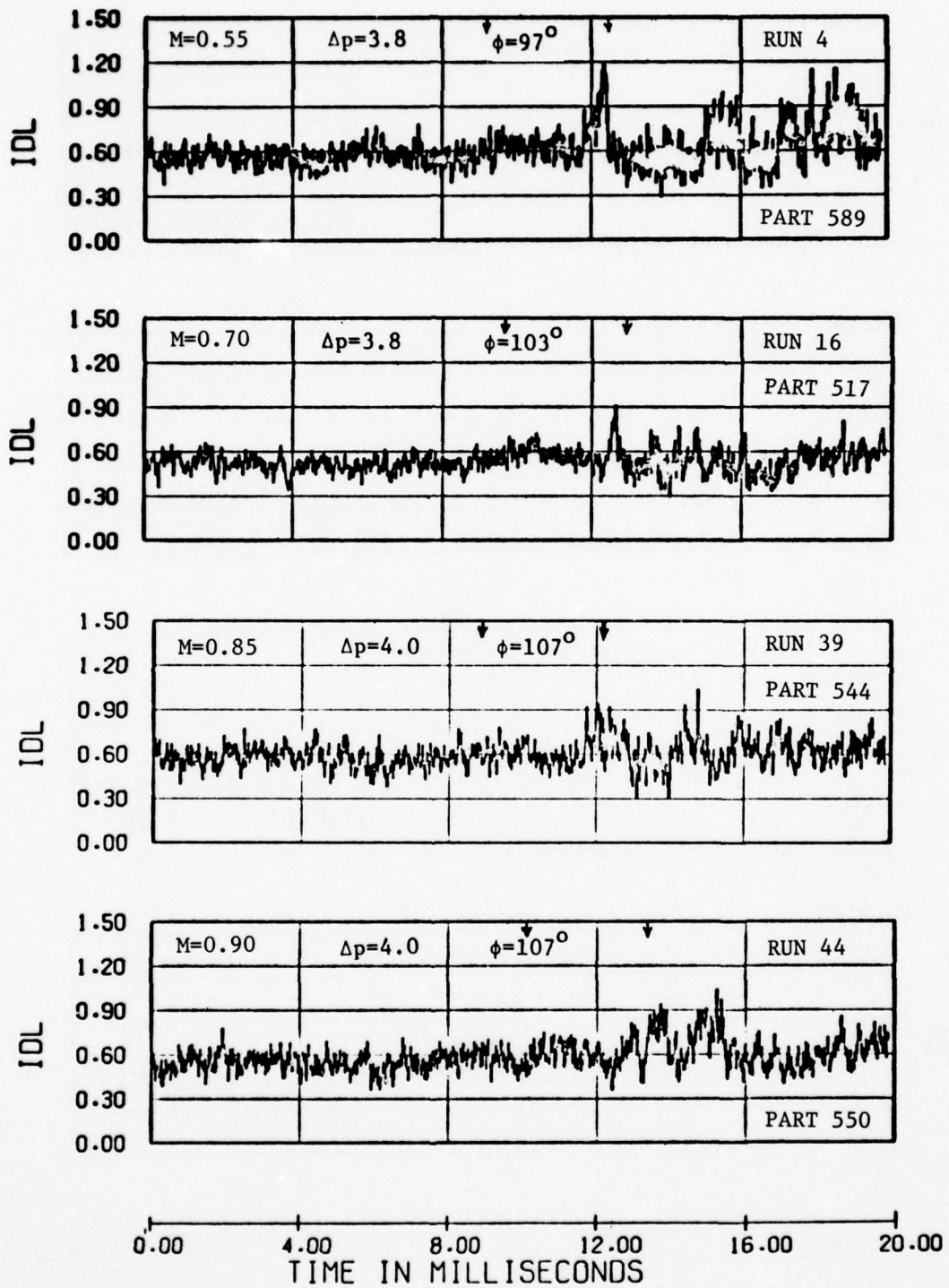


Figure 5.14. Concluded.

OUTBOARD INLET

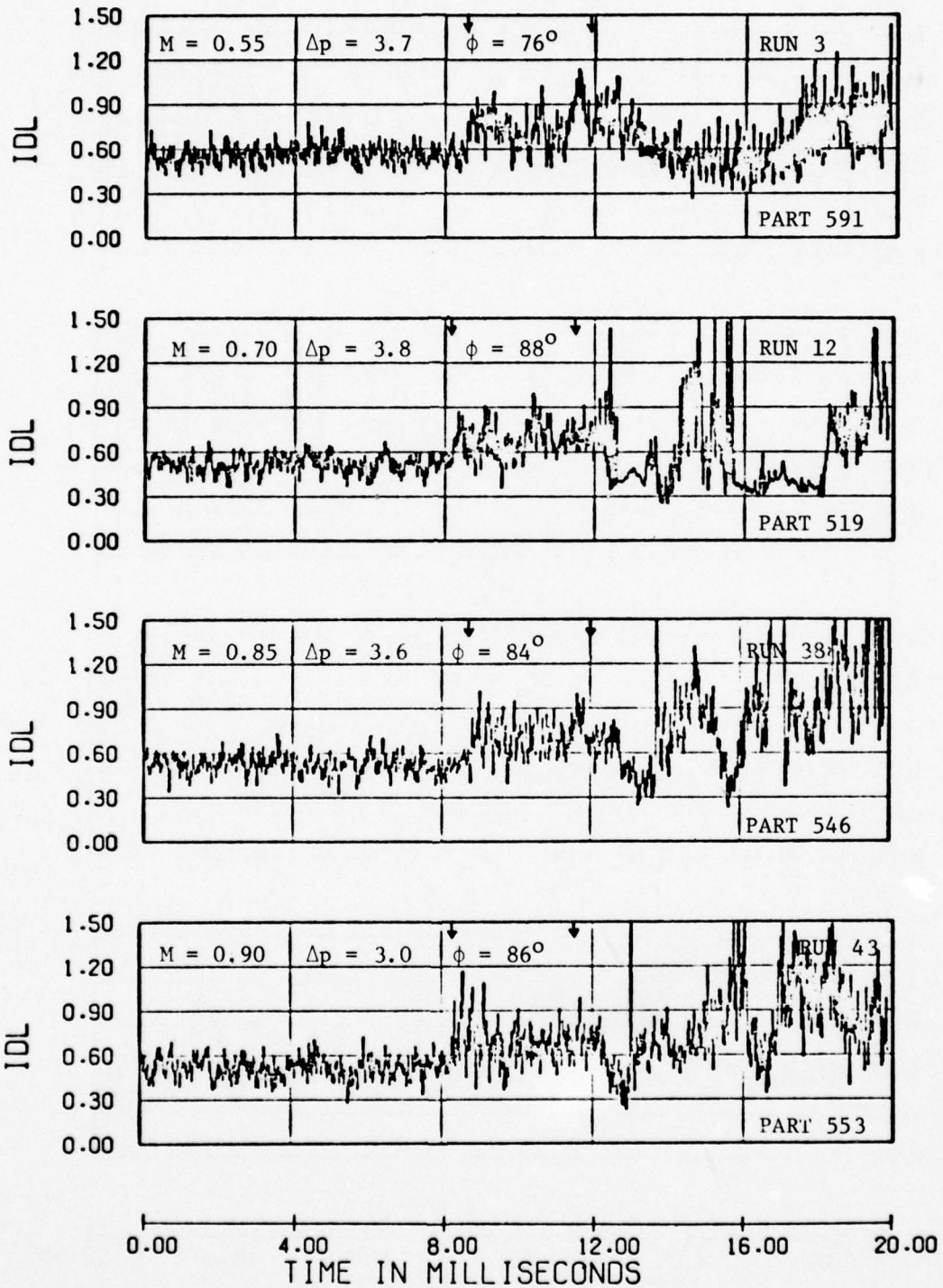


Figure 5.15. Distortion time histories for four Mach numbers for the blastward inlet, flow rate ≈ 350 lb/sec, tube 1.

INBOARD INLET

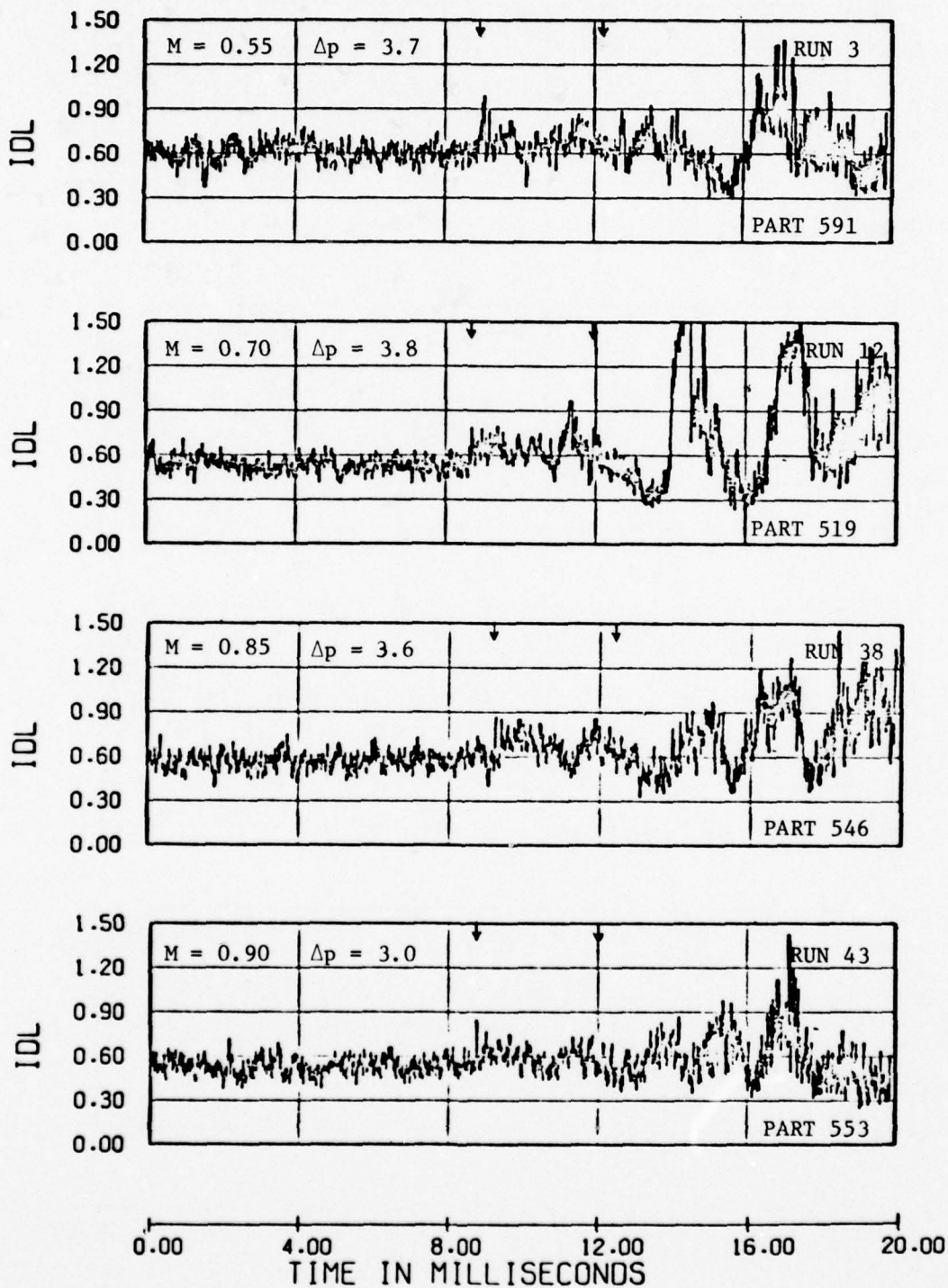
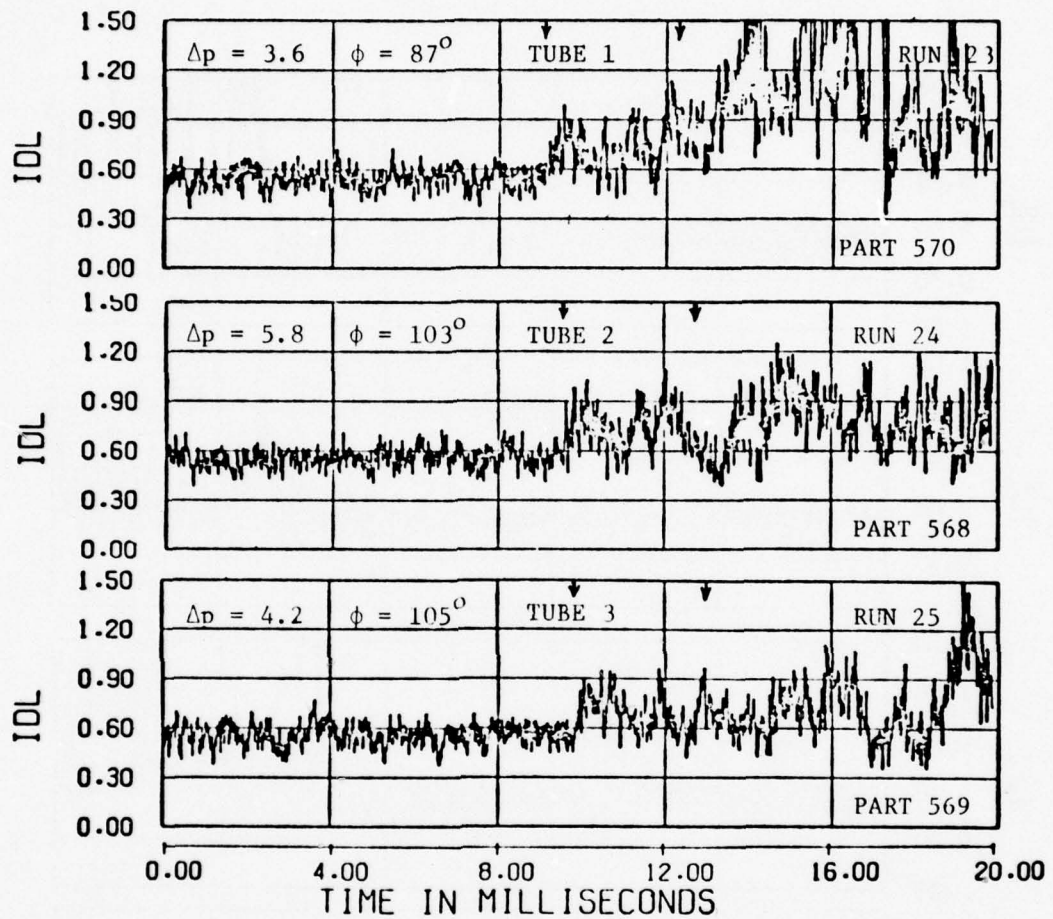
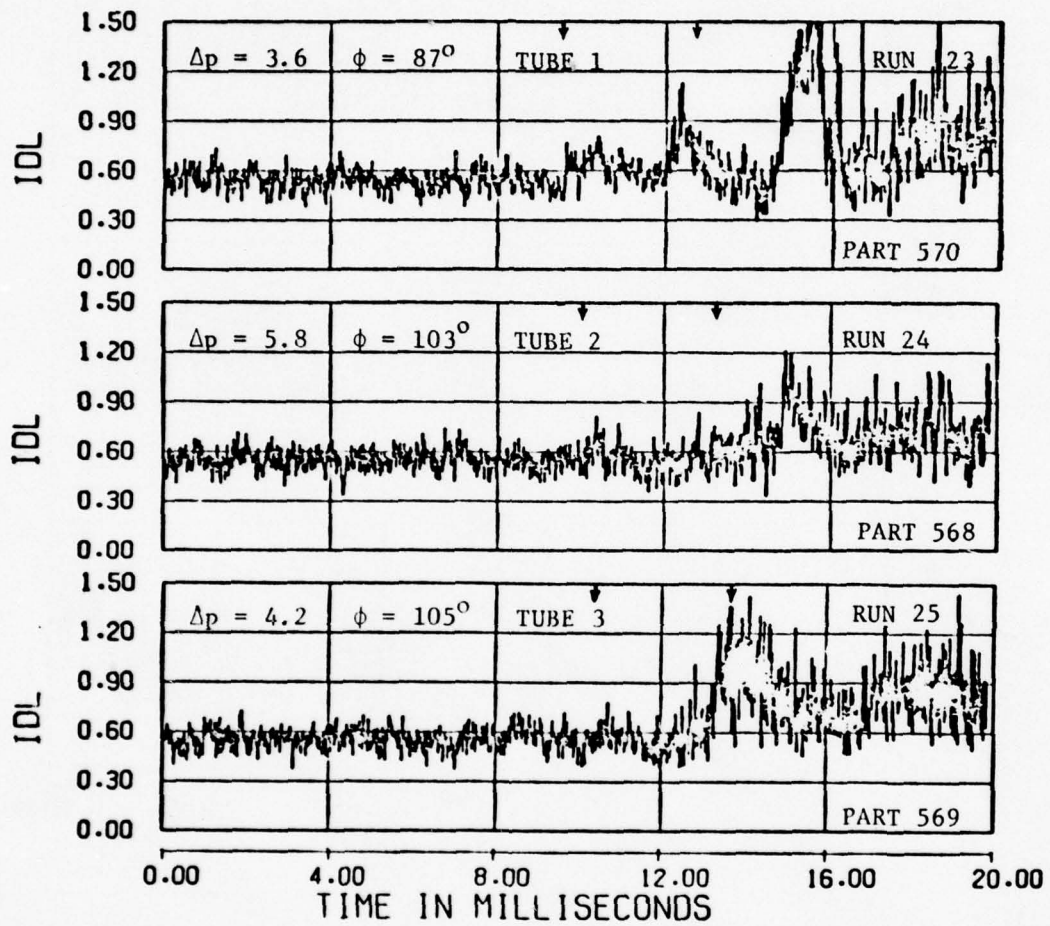


Figure 5.16. Distortion time histories for four Mach numbers for the leeward inlet, flow rate ≈ 350 lb/sec, tube 1.



(a) Blastward Inlet

Figure 5.17. Distortion time histories for three yawed runs at Mach 0.70, yaw = 5°, flow rate \approx 350 lb/sec.



(b) Leeward Inlet

Figure 5.17. Concluded.

In a few cases, values of IDL, IDC and IDR in excess of normally allowable limits were observed. For example, for Run 28 (Part 584) in Figure 5.10, large distortion values were experienced in the blastward inlet shortly after blast intercept, but the duration of this large distortion appears to have been less than 0.1 msec (1 msec full-scale). It is uncertain whether the duration of this distortion pulse was long enough to imply a significant adverse effect on engine performance. As a matter of possible interest, Figure 5.18 presents engine-face total-pressure contours for this run, indicating the total-pressure variation across the engine face at a time close to the time of peak distortion (indicated by the arrow in the inset IDL plot). The corresponding instantaneous values of IDL, IDC and IDR are 1.05, 0.103 and 0.061, respectively. The numerical values in this figure represent the difference between the face-average total-pressure and the local total-pressure, expressed as a fraction of face-average total-pressure. Test data points (or interpolations thereof for a few bad data points) are represented as large numbers and contour levels by small handwritten numbers. It may be noted that the lowest total-pressure drop is about 17 percent below the face-average total-pressure.

5.3.3 Effects at High Mass Flow Rates

The distortion effects at the higher tested mass flow rate of 350 lb/sec are generally at least somewhat larger than for the lower mass flow rate. However, for the lower overpressures, up to about 4 psi, the stall margin, IDL, is generally observed to be well below the limit of unity in the blast range (between the two arrows), being generally near to or below 0.9 (see Figures 5.8 and 5.9 for Mach 0.70, Figure 5.12 for Mach 0.85 and Figures 5.13 and 5.14 for a range of Mach numbers). For higher overpressures than 4 psi, IDL sometimes appears to exceed unity in the blast range (e.g., for the blastward inlet at $\Delta p = 5.2$ psi at Mach 0.70 in Figure 5.8 and for the leeward inlet for $\Delta p = 5.8$ psi at Mach 0.85 in Figure 5.12), but only for a small fraction of a millisecond at most. Outside the blast range (to the right of the second arrows in the figures) IDL values appreciably larger than unity are observed

RUN 28
 PART 584
 TUBE 2
 MACH 0.85
 294 LB/SEC FS

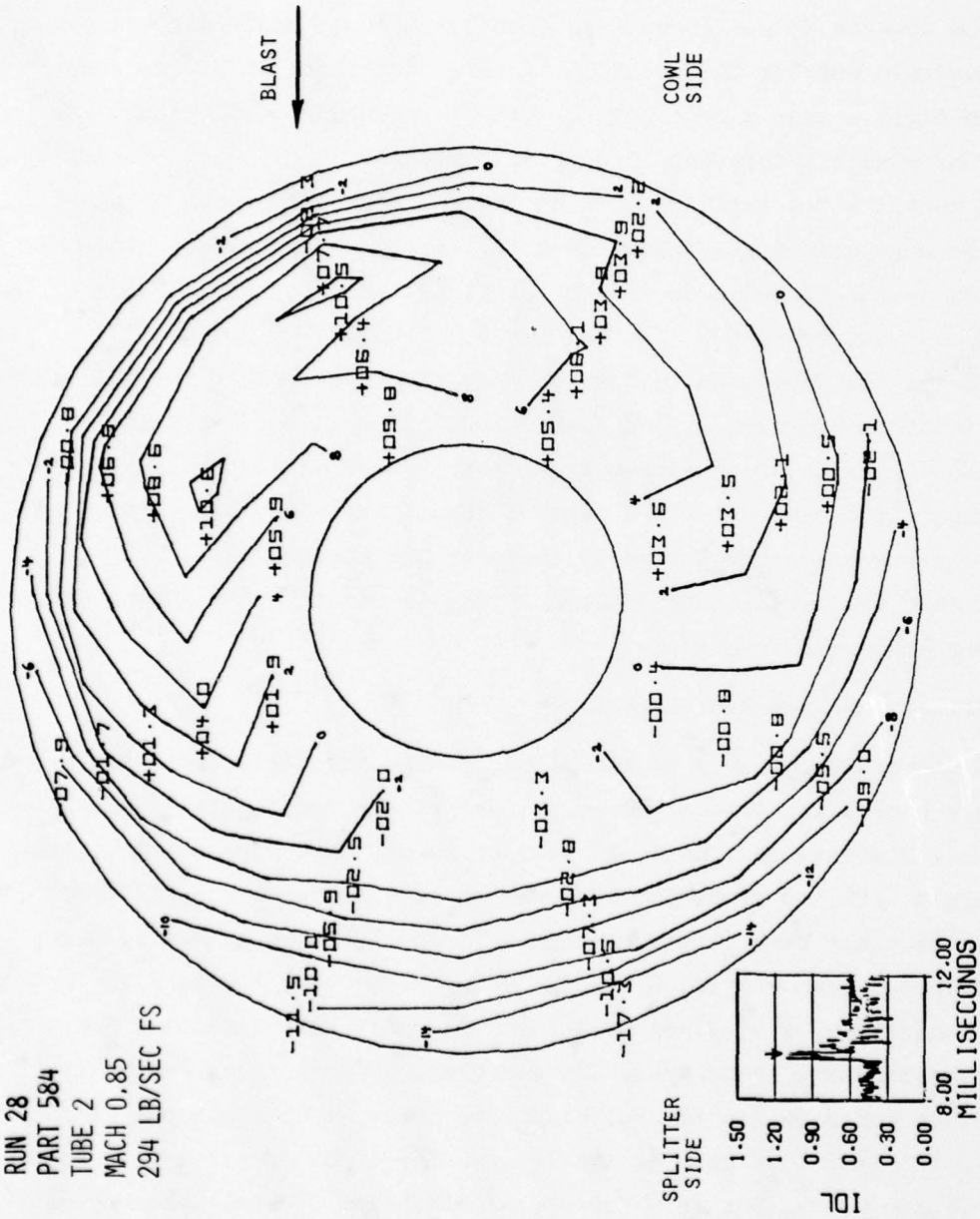


Figure 5.18. Outboard inlet total pressure contours for a large blast-induced distortion condition.

for some firings (e.g., for the blastward inlet at $\Delta p = 5.2$ psi at Mach 0.7 in Figure 5.8 and for blastward and leeward inlets at $\Delta p = 3.8$ psi at Mach 0.55 in Figure 5.13), but further study would be required to verify whether these late time data are relevant to the blast-inlet problem. Possible sources of late-time distortion are discussed in Section 9.

5.3.4 Mach Number Effects

No definite significant effects of Mach number on the distortion indices IDL, IDC and IDR were observed in the blast range (e.g., see Figures 5.13 and 5.14). This lack of observed effect is attributed primarily to the choking action of the vane system downstream of the simulated engine face, which tends to maintain the internal inlet flow at any location in the inlet at a constant Mach number condition, regardless of the state of the external flow conditions. Further more definite evidence indicating this apparent lack of Mach number effects on inlet pressures is given in Figure 5.19, which compares inlet ramp pressures for transducer 1980 (located about half-way down the inlet, see Figure 5.4) for four Mach number conditions. It may be noted that most fine details of the pressure histories in Figure 5.19 are almost identical for the different Mach numbers, especially for Mach 0.55 and 0.85.

5.3.5 Effects of Yaw Angle

No definite effects of yaw angle on distortion are readily evident from the results of the three yawed test firings (Figure 5.17). Appreciable increases in IDL occurred for both inlets in each firing, but the increases did not generally appear much greater than for similar unyawed firings (see Figs. 5.8 and 5.9). However, it should be noted that a significantly high level of distortion appears to have developed in the leeward inlet toward the end of the nominal blast event (at second arrow) of Run 25 (Fig. 5.17b).

5.3.6 Long Duration Distortion Effects

If the rate of decay of a blast wave is extremely small, as for a large nuclear burst, then the struck inlet-engine system will tend at late times to come to a quasi-steady equilibrium condition where the

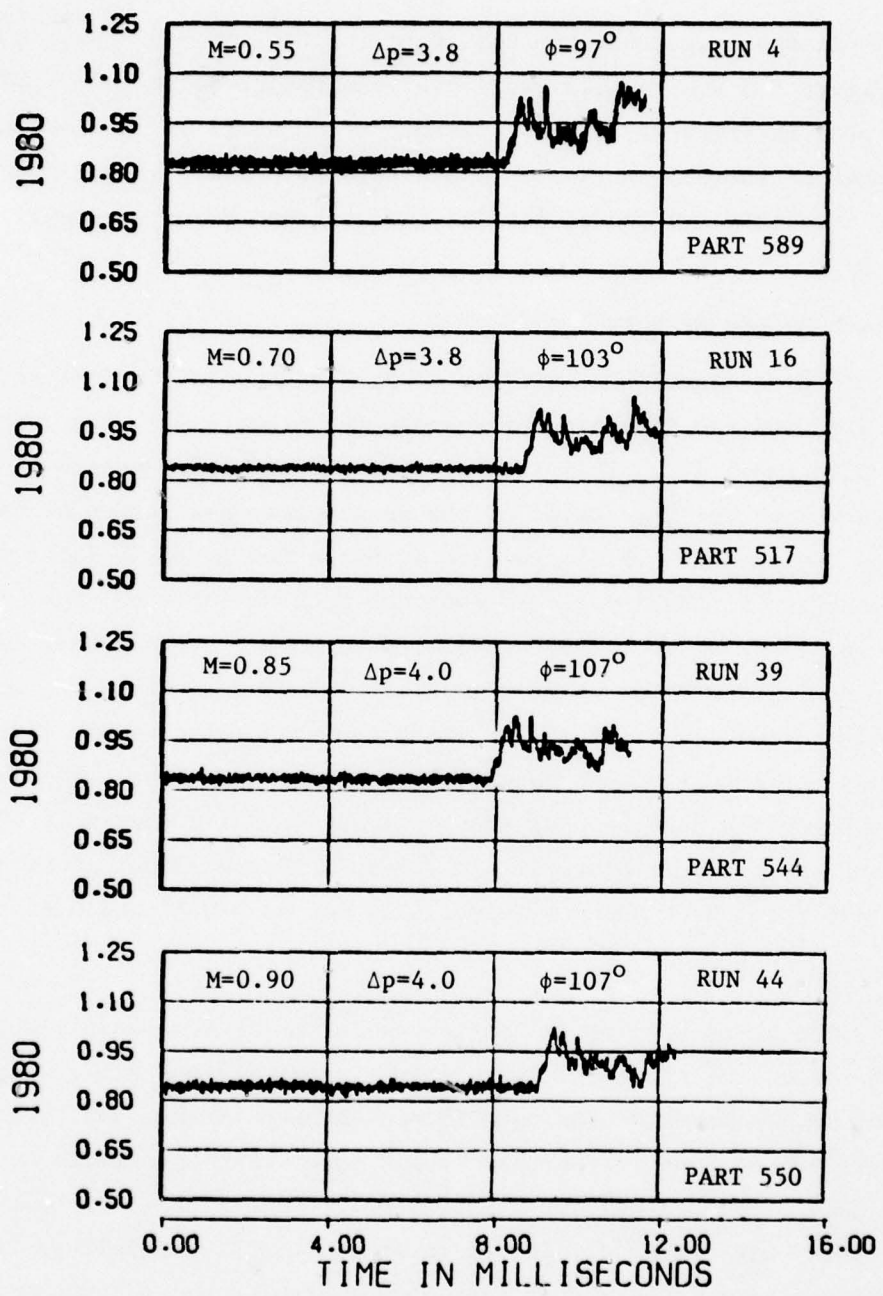


Figure 5.19. Comparison of ramp pressure time histories for four Mach numbers, tube 2, flow rate \approx 350 lb/sec.

effect of the blast wave will be essentially the same as would be produced by steady yawed flight at the side-slip angle and total pressure caused by the blast (as given by Figures 5.1 and 5.2. In regard to this point, it may be noted that our test results for steady yawed conditions generally indicate 10% or less increase, or decrease, in the distortion parameter IDL as the sideslip angle varies from the zero angle condition to angles anywhere in the range from -10° to $+10^{\circ}$. Hence, it might be expected that late-time blast distortions would be small for blast overpressures producing blast-induced sideslip angles up to at least 10° , as given by Figure 5.1 in Section 5. For example, for Mach 0.85 flight, Figure 5.1 indicates that blast overpressures up to about 3.3 psi would not produce sideslip angles over 10° and, hence, would not be expected to produce large late-time distortion effects.

The value of the above observations is, of course, of limited value since we cannot at this time specify what we mean by "late time" in a very definite manner. However, judging from BID code calculations for times up to about 6 milliseconds, presented later in Section 7 (Figure 7.2), it appears that quasi-steady equilibrium would not be reached for the test model until times considerably greater than 6 milliseconds (or 60 milliseconds for a full scale B-1 inlet).

5.3.7 Concluding Remarks on Distortion Effects

In concluding this discussion of distortion effects, it should be noted that while generally very few large distortion values were obtained during the early-time definitely blast-type flow periods of the present tests, the distortion criteria used above (IDC, IDR and IDL) are not necessarily completely reliable indices of whether an engine would stall under transient blast conditions. Other distortion criteria should also be considered (e.g., Ref. 5.2 and 5.3) and attention should also be directed to the actual contours of pressure distortion which are obtained under blast intercept conditions, such as is illustrated in Figure 5.18 for one run at a time shortly after blast intercept (see arrow in inset IDL plot) when appreciable distortion was experienced in the outboard inlet. Also attention should be directed to the durations of any large observed distortion levels, comparing them with duration results

from other tests (e.g., Ref. 5.4). Furthermore, attention should be directed also to effects of blast-induced longitudinal pressure variations (Sec. 9) and blast-fan interactions (Sec. 8) to assess more completely the possible stall inducing potential of blast waves.

These same types of questions should also be considered with respect to the large distortion values sometimes observed at times after the fairly definite blast type flow duration time of 3.3 milliseconds.

Most of the above topics are not explored in the present report because the reduced test data were not made available in a suitable form in time to permit such studies to be performed.

SECTION VI
COMPARISON OF THEORY AND EXPERIMENT

Concurrent with the performance of this experimental investigation, Kaman Avidyne developed a theoretical two-dimensional computer code, designated BID (blast-induced-distortion), for predicting the transient flow field produced in an inlet by a blast wave striking the inlet at an arbitrary angle of incidence (Reference 6.1). Calculations of inlet pressure time histories were made with this code for four conditions similar to those of the 16T experimental tests and the results of these calculations are compared with the test results in this section.

The specific conditions for which BID calculations were made are: constant shock overpressure of 5 psi at one atmosphere ambient pressure, inlet mass flow rate (full-scale) 350 lb/sec, tunnel Mach number of 0.70 for a blast intercept angle of $\phi=90^\circ$ and tunnel Mach number of 0.85 for intercept angles of $\phi=90^\circ$, 105° and 135° . Calculated BID pressure time histories for various locations in the inlets are presented in Figures 6.1 to 6.5 together with experimental data for those test runs corresponding most closely to the conditions of the theoretical calculations.

The reader is reminded here that in looking at the experimental data in Figures 6.1 to 6.3, attention should be directed on times between the two arrows above each curve; the data at later times are not considered necessarily representative of a blast type flow (See Sec. 4). Also it should be recognized that the theoretical calculations shown in Figures 6.1 to 6.4 are for a constant-strength (step) blast wave (5 psi overpressure), whereas the test data correspond to a time-varying blast wave characterized by an initial shock value (shown below each figure), and possible subsequent increases in pressure, followed by a tendency to decrease to zero in 4-6 milliseconds after initial shock arrival.

The reader is also advised to make comparisons of theory and experiment primarily on the basis of wave shape rather than on amplitude comparisons, since the calibration factors used for some of the shown

ramp and cowl data are either nominal or questionable values and a few appear to be significantly in error*.

Considering first the Mach 0.7 condition, it can be seen from the presentation of ramp and cowl time histories in Figure 6.1 that there is a great difference in the pressure waveforms for different locations in the inlet (see Figure 5.4 to identify the locations indicated in the figure), and that in almost every case the theoretical results follow well most of the details observed in the experimental data. For example, for location 1970, the BID calculation clearly delineates the first three shock arrivals and, at late time, delineates a large pressure increase resulting from reflection of the blast from the simulated engine throat of the inlet model.

A similar comparison is made for ramp pressures for Mach 0.85 in Figures 6.2 and 6.3 and for cowl pressures in Figure 6.4. Again the theoretical and experimental wave shapes are generally in good agreement. A few noticeable differences do appear to exist, such as the more rapid late time decays (say near the second arrow) of the experimental pressures for locations 1950 and 1970 in Figure 6.3 and for the cowl locations in Figure 6.4. These differences may be attributed in part to differences between the constant strength blast assumed for the calculations and the actual variable strength blast of the test.

A final comparison is made in Figure 6.5 between calculated and experimental total pressures at the simulated engine face location for a location near the ramp in the blastward (outboard) inlet. The two transducers shown are located vertically above one another in the inlet (see Figure 4.3) so that the theoretical (two-dimensional) BID prediction is the same for both transducers. Differences between the two experimental results are hence indicative of the importance of three-dimensional effects not covered by the theory in its present form.

* These calibration factor problems arose as a result of pre-test mechanical and electrical malfunctions of the transducers which could not be resolved in the very limited time available for the 16T tunnel tests. Preliminary examinations of the test data indicated that more reliable estimates for some of these factors can be obtained by considering some redundant features of the data, but this has not yet been done.

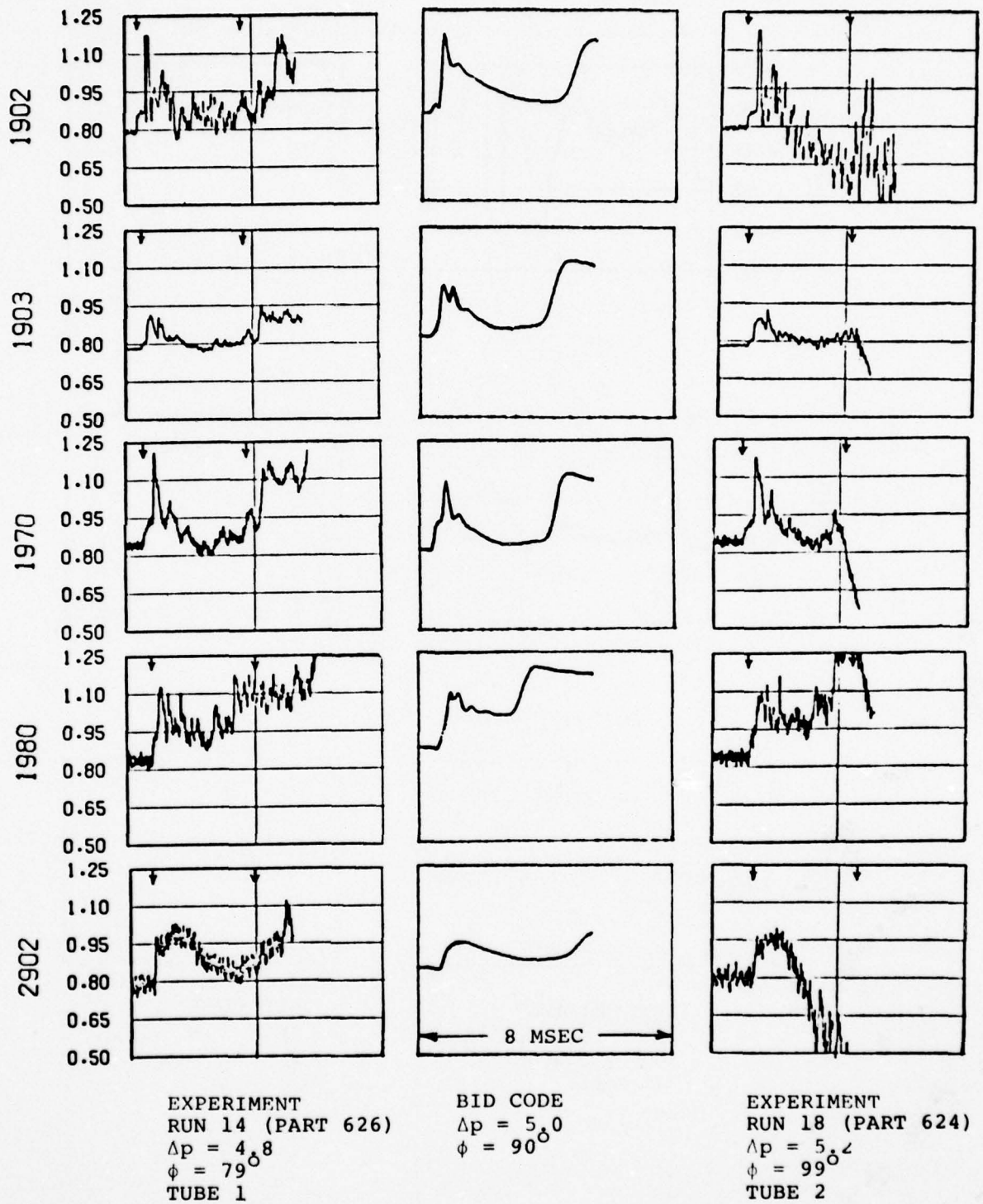


Figure 6.1. Comparison of theoretical and experimental time histories of ramp and cowl pressures at Mach 0.70, flow rate ≈ 350 lb/sec.

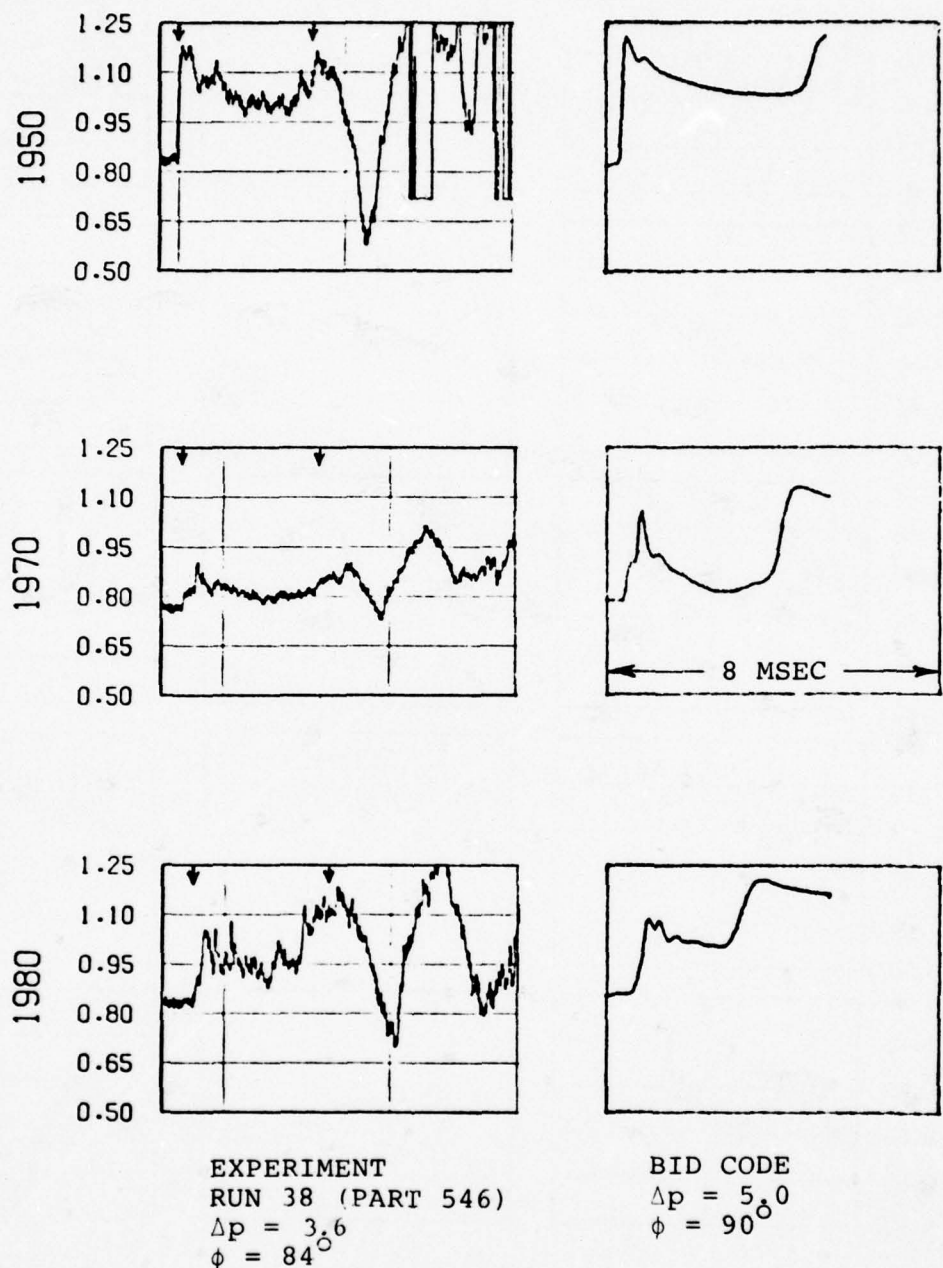


Figure 6.2. Comparison of theoretical and experimental time histories of ramp pressures in the blastward inlet at Mach 0.85, tube 1 data, flow rate ≈ 350 lb/sec.

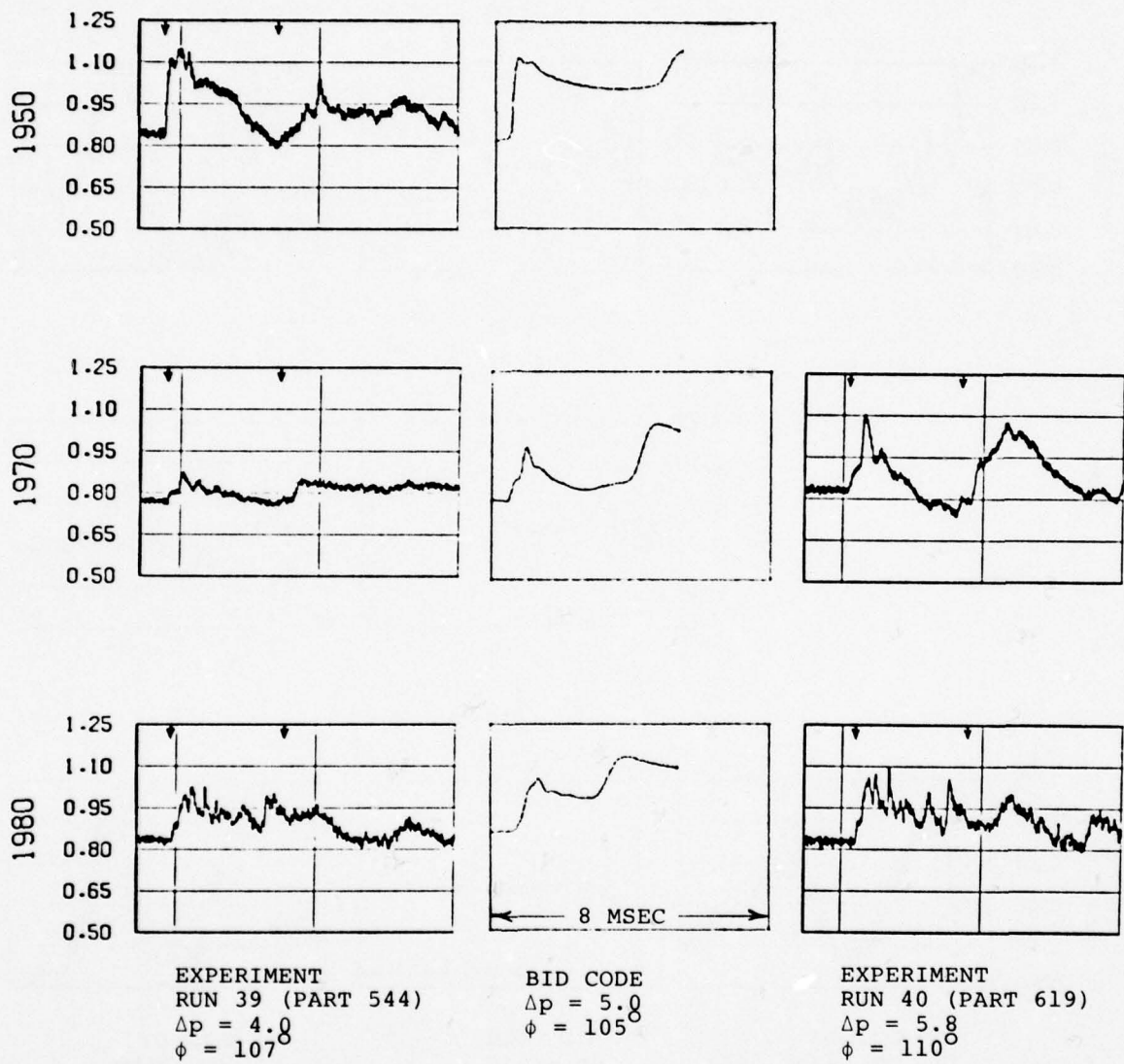


Figure 6.3. Comparison of theoretical and experimental time histories of ramp pressures in the blastward inlet at Mach 0.85, tube 2 data, flow rate ≈ 350 lb/sec.

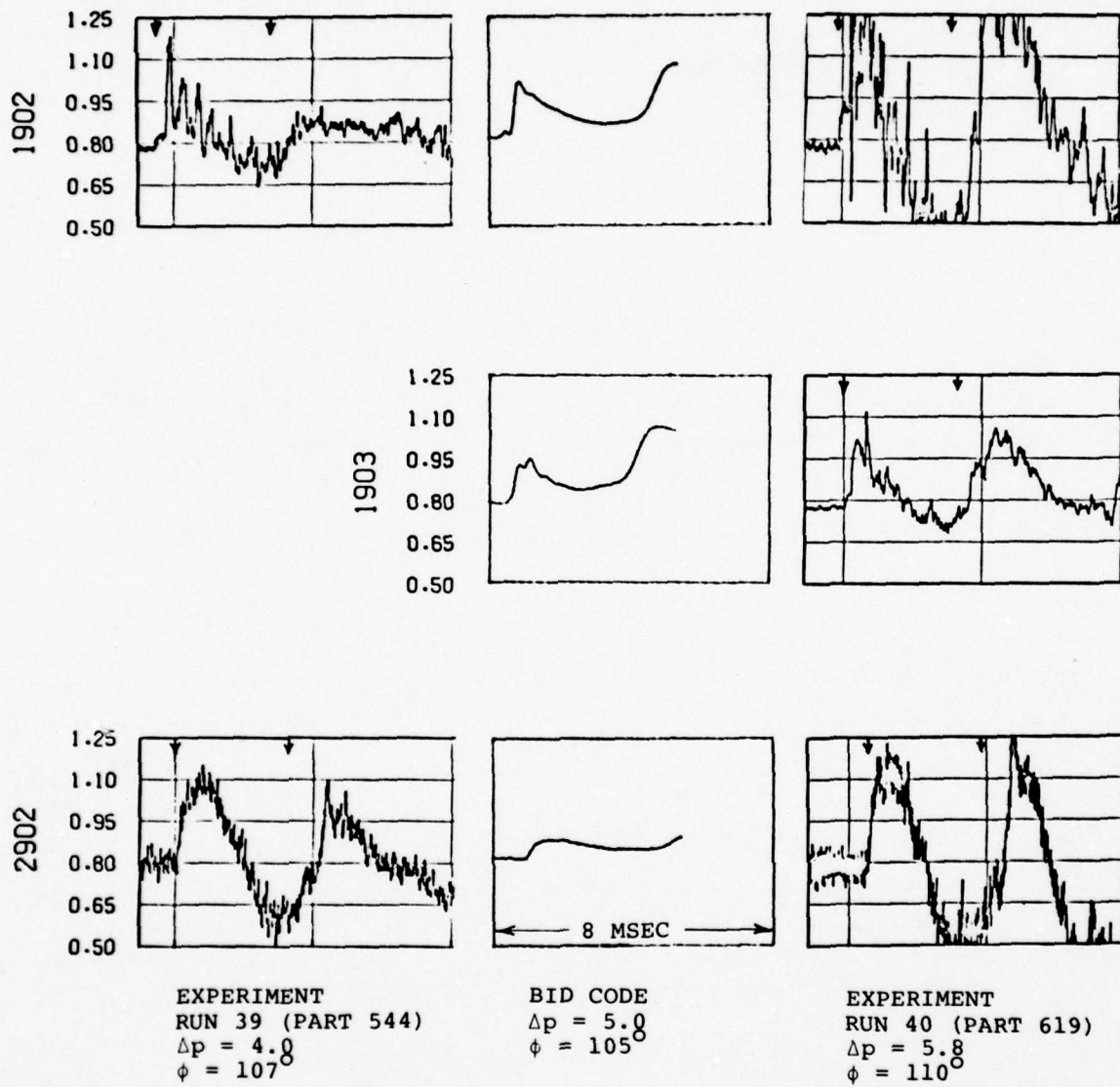


Figure 6.4. Comparison of theoretical and experimental time histories of cowl pressures at Mach 0.85, flow rate ≈ 350 lb/sec.

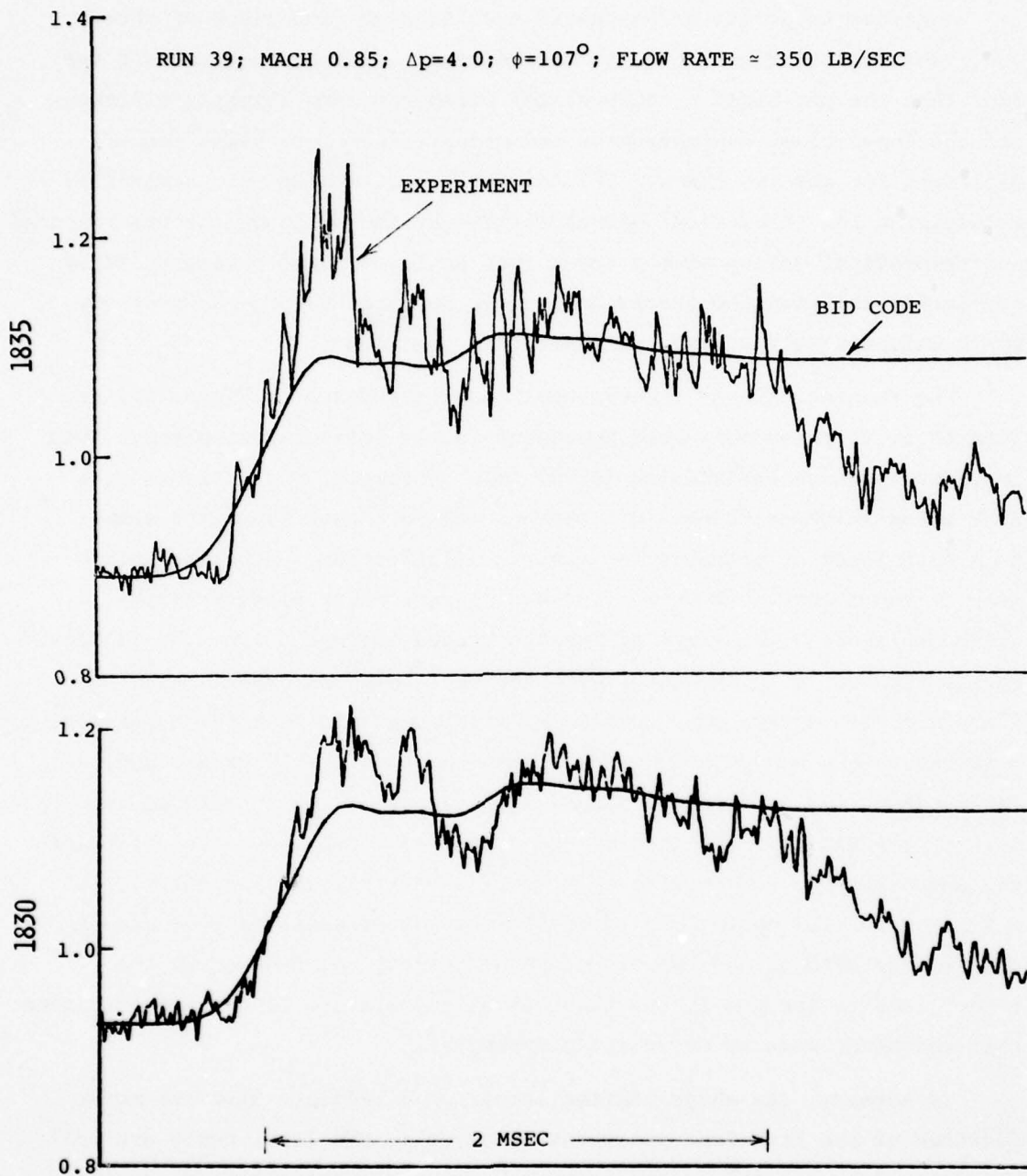


Figure 6.5. Comparison of theoretical and experimental total pressure time histories at the engine face for the blastward inlet.

In order to permit a reasonable quantitative comparison of theory and experiment in Figure 6.5, it was necessary to take into account the fact that the pre-blast (steady-state) pressures were slightly different and the input blast overpressures and orientations were significantly different for the two cases. This difference was taken into account by multiplying the theoretical BID code curve by the ratio of the experimental and theoretical values of the shock jump in input total pressure and by vertically shifting the theoretical curve so that the pre-blast steady-state values were the same for theory and experiment.

The theoretical and experimental total pressures in Figure 6.5 are seen to be in reasonably good agreement in the following respects. Both indicate a reasonably similar (slow) rate of rise of the pressure to a peak value in about 0.3-0.4 millisecond and both have about the same mean peak level of pressure for about 2 milliseconds. Also the third peak in the theoretical curve (at about 1 msec after blast arrival), which represents the return of the blast wave reflected from the simulated engine throat, is in agreement with the corresponding experimental time. There are, of course, some noticeable differences, in that the experimental peak values are appreciably greater than the theoretical values and, at later times, may be smaller. These differences may be attributed in part to the finite resolution of the numerical code, some attenuation of the shock for the code due to an effective "artificial viscosity", with a fixed-mesh cell system, to three-dimensional effects (as evidenced by differences between the two experimental traces) not covered by the theory, and to the use in the theoretical calculation of the approximation that the blast wave is of constant strength.

In summary, the above limited comparisons indicate that the major features of the transient pressures observed in the inlet tests are well represented by the BID code results. However, a more extensive comparative study of the 16T results would be desirable to more definitively establish the limitations of the code predictions. Such a correlation would require incorporation into the BID code of the actual time history of the blast wave incident on the inlet (instead of the constant over-

pressure value used here). This, in turn, requires evaluation of the input blast time history from the test data, which is a non-trivial task because of possible significant fuselage inlet and claw probe interference effects.

SECTION VII
SHOCK ORIENTATION EFFECTS

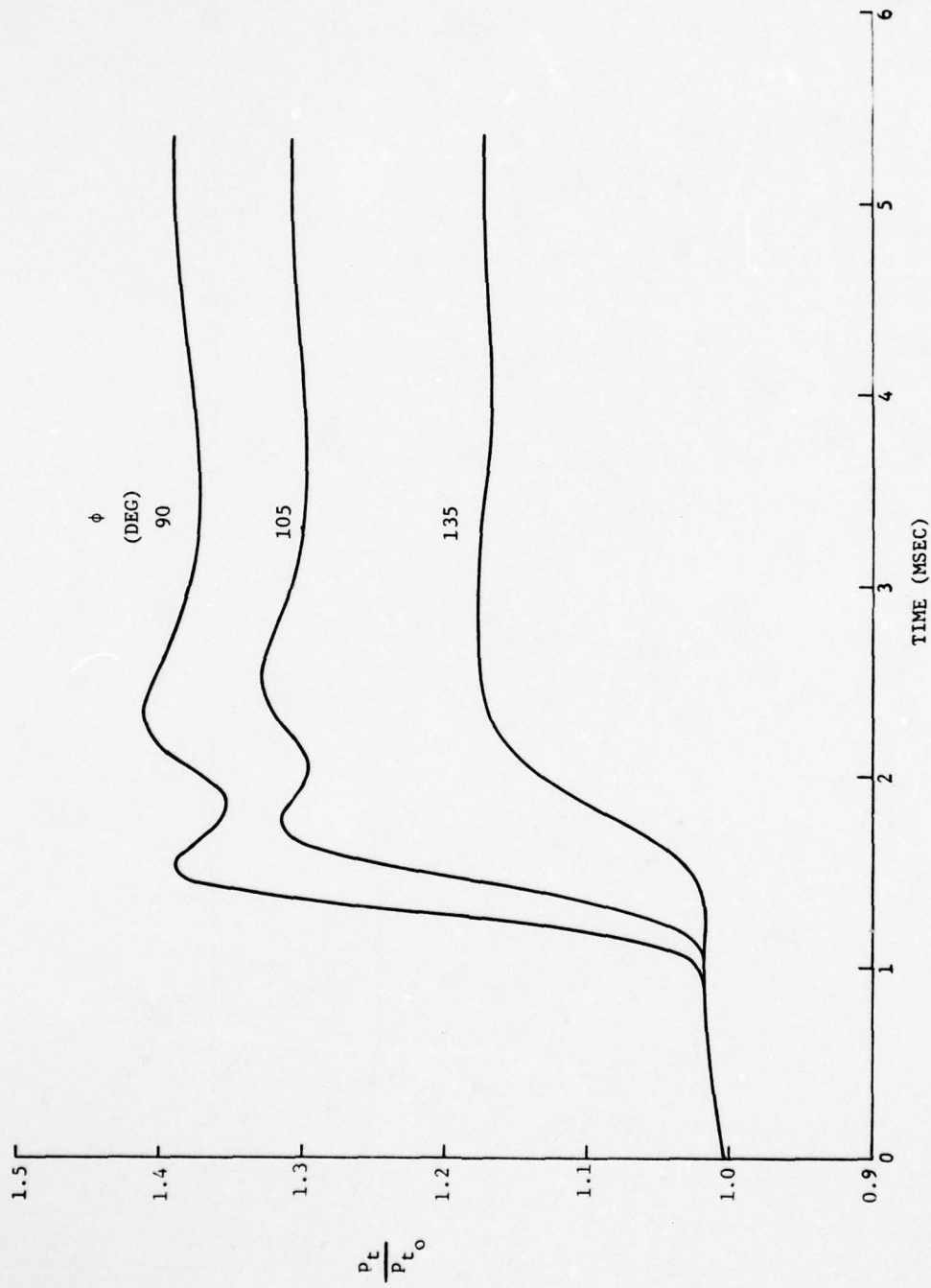
This section considers briefly some gross effects of the blast intercept angle, ϕ , on engine face total pressures for the test model as calculated from the BID code for Mach 0.85 flight conditions.

It was noted in Section 5 that for a blast wave of constant overpressure, the increase in blast total pressure in free space (before intercepting the inlet) is largest for zero intercept angle and decreases with increasing intercept angle, according to the curves of Figure 5.2. As might be expected, the same type of variation is obtained for the total pressure at the engine face, as is shown in Figure 7.1. This figure presents total-pressure time histories near the center of the blastward and leeward inlets as calculated with the BID code for a constant-strength 5-psi overpressure blast wave striking the inlets at intercept angles of 90° , 105° and 135° .

It may be noted in Figure 7.1 that, in addition to a decrease of face total pressure with increasing intercept angle, there is a noticeable reduction in the complexity of the pressure signature for the blastward inlet as the intercept angle increases from 90° to 135° . For the nearly side-on intercept angles of 90° and 105° there are two distinct peaks, the first representing the initial blast wave striking the face and the second representing the reflected shock from the choked section of the simulated engine. For the larger 135° intercept angle, where the blast wave overtakes the inlet from the rear, the distinction between the incident and reflected blast wave is hardly detectable.

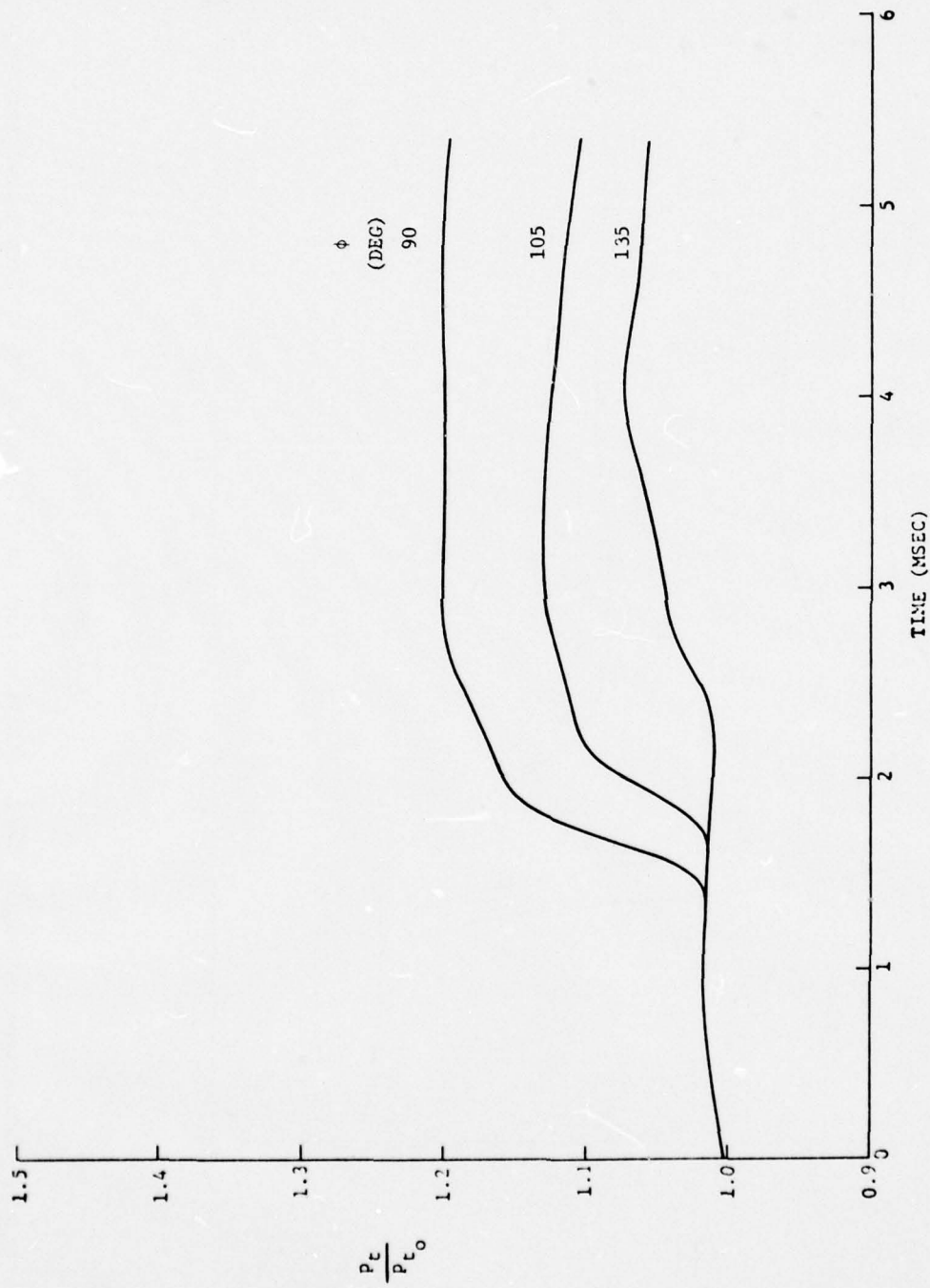
It can also be observed in Figure 7.1 that the rate of increase of face pressure to its maximum value decreases considerably as the intercept angle increases from 90° to 135° , both for the blastward and leeward inlets.

In order to better relate the face pressures to the incident blast conditions, the total-pressure curves from Figure 7.1 are also presented in Figure 7.2 in the form of the ratio of the change in total pressure (due to the blast) to the change in total pressure across the blast front before it encounters the inlet (from Figure 5.2). It is evident from



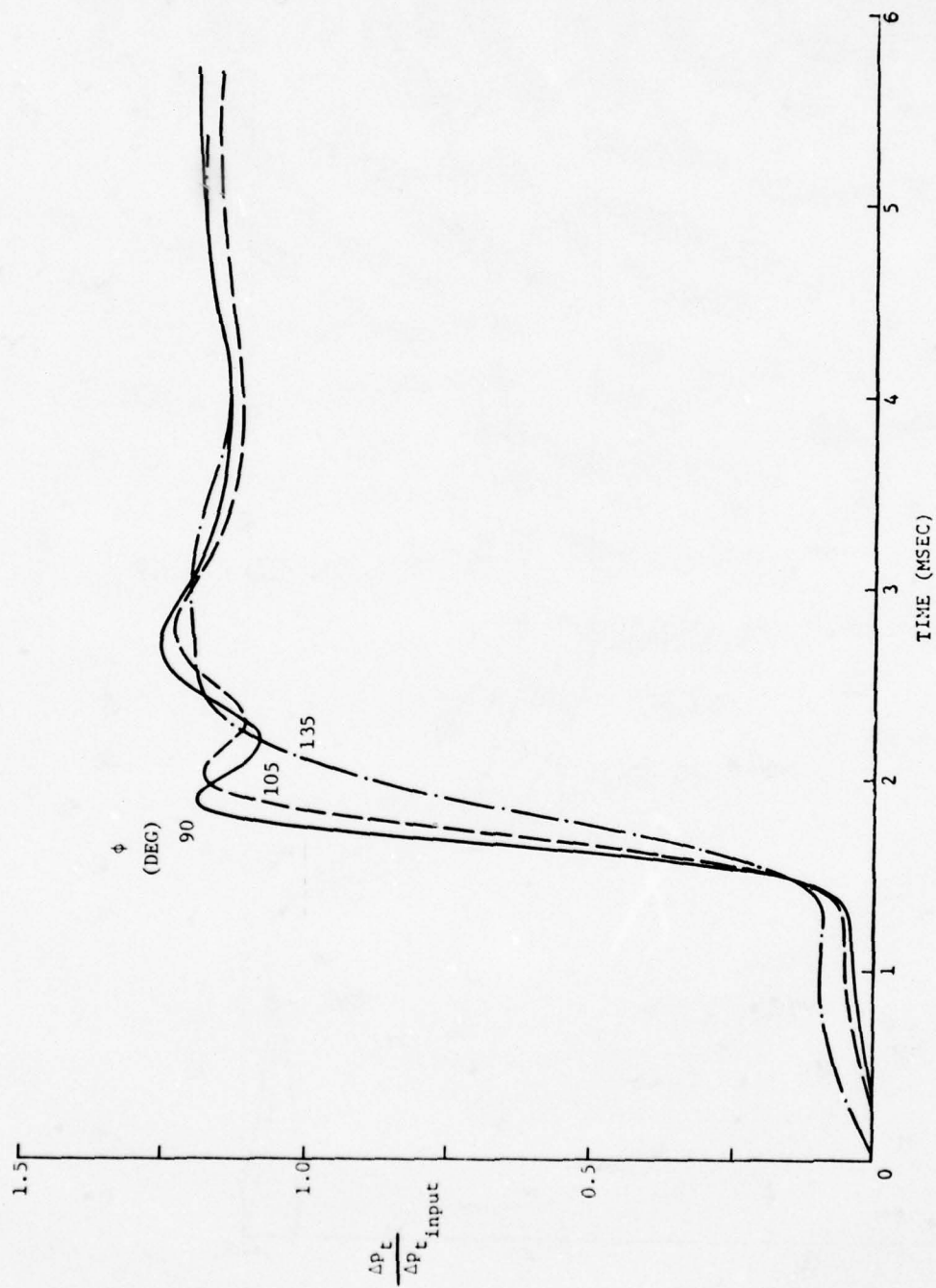
(a) Blastward inlet.

Figure 7.1. Comparison of engine face total pressure time histories for three blast intercept angles.



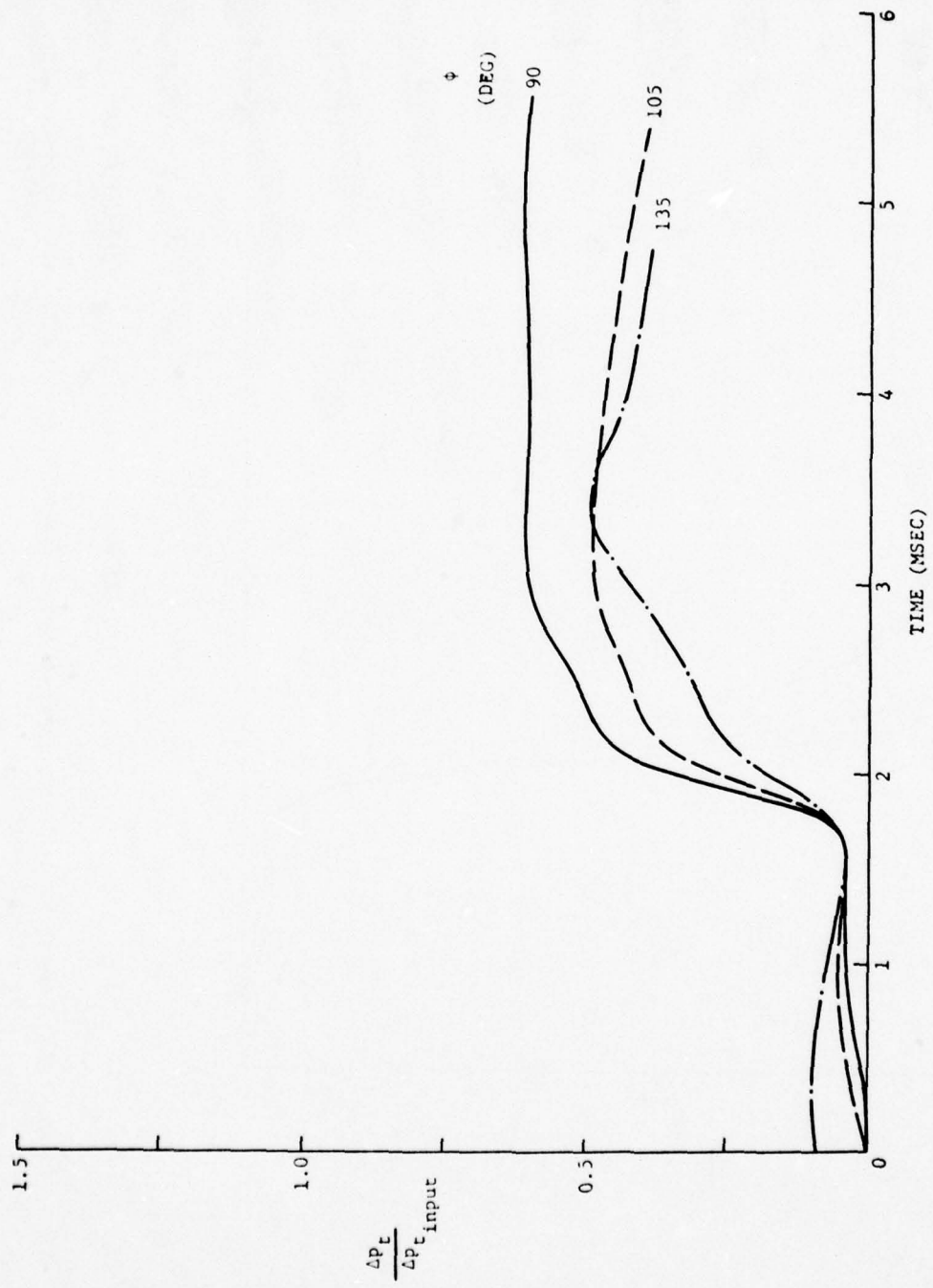
(b) Leeward inlet.

Figure 7.1. Concluded.



(a) Blastward inlet.

Figure 7.2. Comparison of engine face total pressure ratio time histories for three blast intercept angles.



(b) Leeward inlet.

Figure 7.2. Concluded.

Figure 7.2 that, for the blastward inlet, the average total-pressure change at the simulated engine face has about the same ratio to the incident total-pressure change for all three intercept angles, the ratio being about 1.17 for the time range shown. For the leeward inlet, this ratio is smaller and varies somewhat with the intercept angle.

The significance of the above observations with respect to engine performance has not yet been explored in detail. However, both the decreasing intensity and the decreasing rate of change of total pressure observed for increasing intercept angle in Figure 7.1 may imply a decrease in inlet distortion with increasing intercept angle, at least in the 90° to 135° range.

SECTION VIII
INTERACTION OF BLAST SHOCK WITH THE
ENGINE FAN

The principal question regarding blast wave interaction with the engine inlet, of course, is what effect this interaction would have upon the operation of the engine downstream.

The effect would depend upon the nature of the transient events that take place when the blast shock and blast-induced flow reach the engine. At present there is no means for analyzing this sequence of events nor are there test data available for its assessment. As an admittedly limited first step in understanding the problem, the interaction at the fan stage of a turbofan engine will be examined here on a quasi-steady basis.

8.1 QUASI-STEADY BLAST SHOCK INTERACTION WITH A FAN

The quasi-steady interaction of a blast shock leaving the inlet and entering a fan will be analyzed by making the assumption that the interaction reaches an equilibrium rapidly enough that a new steady-state fan point is reached essentially immediately after shock arrival. Of course, the transient interactions of the blast shock with the rotor and stator blades are expected to be important, but, until the means are available for analysis of these interactions, the analysis of a quasi-steady interaction will have to suffice for providing an assessment of some of the features of shock interaction with a fan.

The time sequence of events associated with the interaction of a shock wave with a fan is shown in Figure 8.1. Here the flow going into and out of the fan is treated on a one-dimensional basis. Region 2 contains the preblast flow entering the fan and region 3 contains the preblast flow leaving it. The fan is located at the origin of the coordinates.

The blast shock at the fan is assumed for this analysis to be a step-blast, i.e. to have uniform properties in region 2' behind the

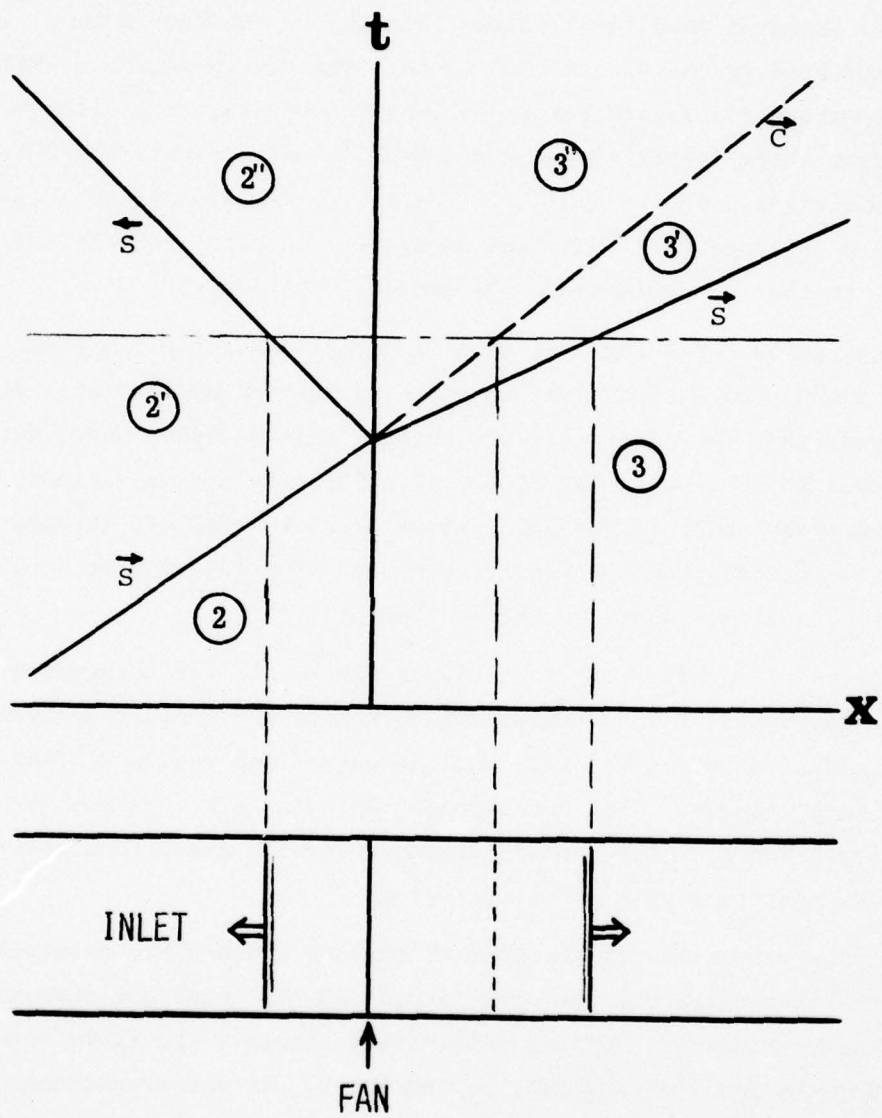


Figure 8.1. Shock interaction with fan.

shock. The shock wave is partially reflected upstream producing the flow in regions 2'' ahead of the fan. It also is transmitted through the fan producing the flow in regions 3' and 3'' downstream of the fan. The air in region 3' has first passed through the fan and is then shock compressed by the transmitted shock. The air in region 3'' has been twice shock compressed before passing through the fan, first by the incident shock (separating zones 2 and 2') and then by the reflected shock (separating zones 2' and 2''). The air in regions 3' and 3'' is separated by a contact surface; the pressures and particle velocities are equal in the two regions but the densities differ.

It should be noted that the shock interaction with a fan might possibly produce expansion waves in place of the transmitted or reflected shock waves. For the particular fan interactions analyzed here, which are believed to be typical for modern axial-flow turbo-fan engines, only shock waves would be possible, so only shock waves are assumed here for the transmitted and reflected waves. The addition of expansion waves to the analysis would be straightforward.

Prior to the arrival of the incident shock, the fan compresses region-2 flow upstream into region-3 flow downstream. After arrival of the incident shock at the fan, the fan compresses region-2'' flow upstream into region-3'' flow downstream. The fan therefore goes from a pre-interaction operating point between regions 2 and 3 to a post-interaction operating point between regions 2'' and 3''.

The flow properties in the initial regions 2 and 3 are determined by a match between the fan characteristics and the inlet and downstream engine characteristics. For typical current aircraft the flows entering and leaving the fan are subsonic, so the inlet, fan and downstream engine characteristics are interacting. The flow properties in region 2' are determined by knowing the strength of the incident shock. The properties in regions 2'', 3' and 3'' are determined by a match between the strengths of the transmitted and reflected shock waves and the characteristics of the fan. Results for a typical fan will be shown.

This quasi-steady interaction of the shock with a fan has been programmed into a FORTRAN IV code called QBIF (Quasi-steady Blast Interaction with a Fan). The fan characteristics are a code input.

The important questions stemming from the QBIF calculation are (a) what operating point the fan would arrive at, (b) what effect the reflected shock would have upon upstream flow within the inlet and (c) what effect the transmitted shock wave might have on the flow downstream at the compressor inlet or through the bypass duct to the afterburner and the turbine outlet.

8.2 BLAST SHOCK AT ENGINE FACE

In view of the large number of tests and variables in the 0.1-scale B-1 inlet tests at AEDC, calculations with the QBIF code have been concentrated in this study on the test conditions of a selected run in the test series at AEDC, Run 40 (Part 619). The pre-blast flow and blast conditions for this run are tabulated in Table 8.1.

The wind-tunnel Mach number for Run 40 (Part 619) was 0.85 and the mass flow at the engine faces was 351.9 and 351.0 lb/sec full-scale for the outboard and inboard inlets, respectively. The blast shock strength scaled to standard sea level conditions was 5.8 psi. The jump in average total pressure at the two engine faces when the blast shock arrived was 0.435 and 0.150 of the pre-blast free-stream total pressure, respectively, for the two inlets. The corresponding ratios of the static pressure behind the shock to the value ahead is 1.280 and 1.101 at the engine face for the respective inlets.

8.3 ENGINE FAN CHARACTERISTICS

For two-stage fan characteristics representative of current technology, the data of Reference 8.1 have been employed. A sketch of this fan and a tabulation of its passage dimensions are reproduced from Reference 8.1 in Figure 8.2. The fan was designed for a tip speed of 1450 ft/sec, an overall pressure ratio of 2.8 and a corrected mass flow of 184.2 lbm/sec. The efficiency at this design operating point was found to be 85.7 percent from tests (Reference 8.1). The overall performance maps for the fan are presented in Figure 8.3. An enlarged

TABLE 8.1

INLET DATA OF RUN 40 (PART 619) PERTINENT TO
BLAST SHOCK-FAN INTERACTION

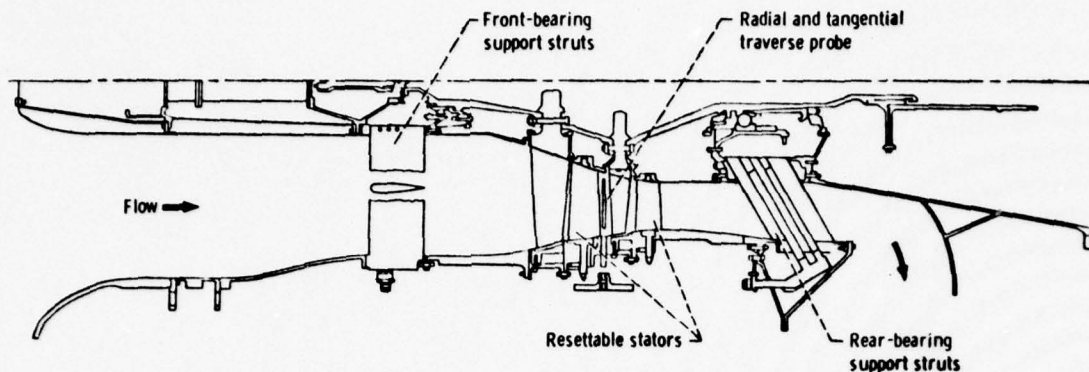
TUNNEL DATA

<u>PREBLAST</u>	<u>BLAST</u>
$M_o = 0.850$	$\Delta p = 5.8 \text{ psi}^*$
$p_{t_o} = 11.801 \text{ psia}$	
$p_o = 7.358 \text{ psia}$	
$T_{t_o} = 569^\circ\text{F}$	

ENGINE-FACE DATA

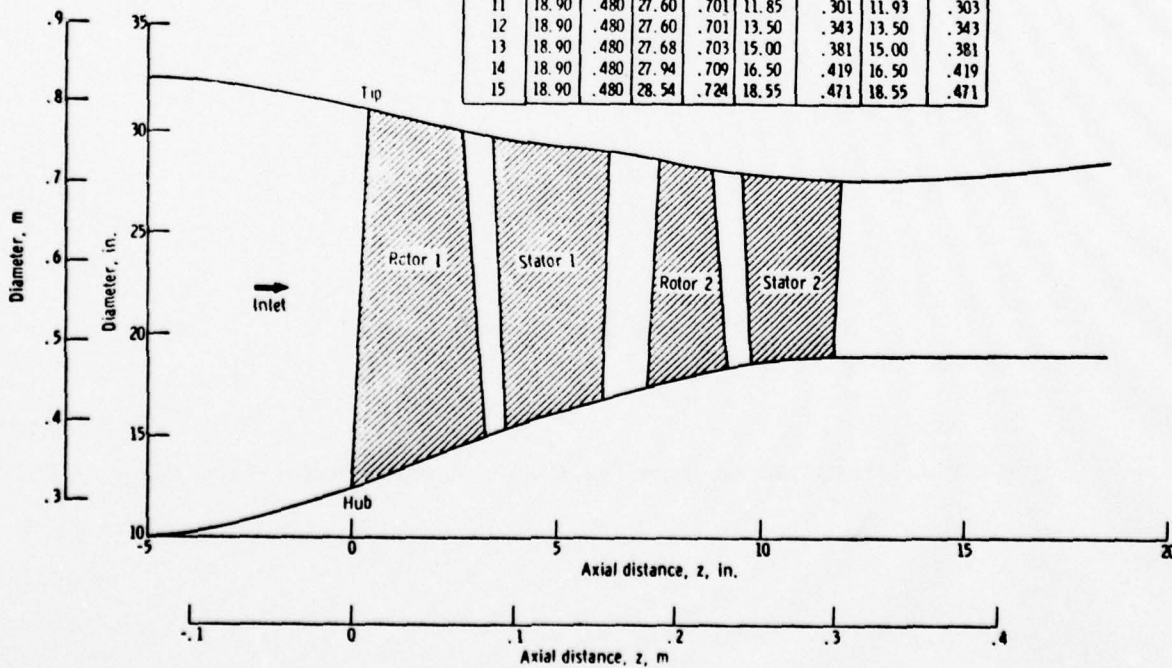
	<u>OB</u> <u>INLET</u>	<u>IB</u> <u>INLET</u>
<u>PREBLAST</u>		
M_2	0.519	0.511
$p_{t_{av}}/p_{t_o}$	0.979	0.980
WZR-FS (lb/sec)	351.9	351.0
<u>BLAST</u>		
$(p_{t_{av_s}} - p_{t_{av}})/p_{t_o}$	0.435	0.150
p_s/p	1.280	1.101

* Scaled to one atmosphere ambient pressure.



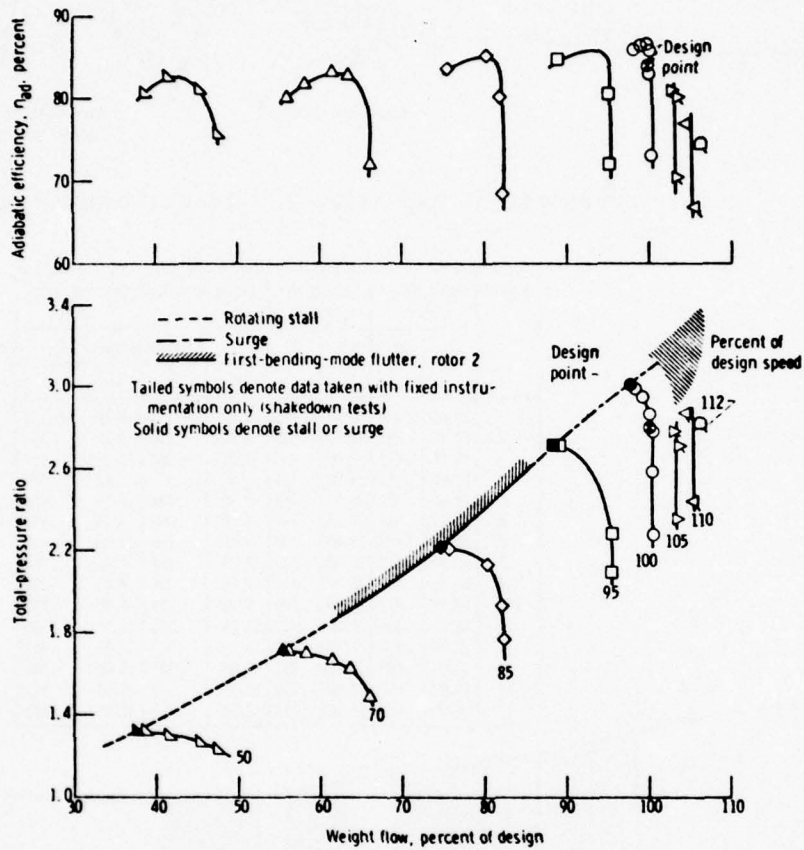
(b) Schematic of two-stage fan test arrangement.

Station	Inside diameter		Outside diameter		Axial distance, z			
	in.	m	in.	m	in.		m	
1	10.00	0.254	32.48	0.825	-5.20	-0.132	-5.20	-0.132
2	10.26	.261	32.33	.821	-3.70	-.094	-3.70	-.094
3	10.94	.278	31.96	.811	-2.245	-.057	-2.245	-.057
4	12.40	.315	31.00	.787	.0	.0	.42	.011
5	14.84	.377	29.93	.760	3.30	.084	2.75	.070
6	15.22	.387	29.67	.754	3.80	.097	3.45	.088
7	16.85	.428	28.96	.736	6.15	.156	6.33	.161
8	17.39	.442	28.58	.726	7.23	.184	7.57	.192
9	18.35	.467	28.12	.714	9.20	.234	8.82	.224
10	18.58	.472	27.90	.709	9.80	.249	9.59	.244
11	18.90	.480	27.60	.701	11.85	.301	11.93	.303
12	18.90	.480	27.60	.701	13.50	.343	13.50	.343
13	18.90	.480	27.68	.703	15.00	.381	15.00	.381
14	18.90	.480	27.94	.709	16.50	.419	16.50	.419
15	18.90	.480	28.54	.724	18.55	.471	18.55	.471



(a) Flow path.

Figure 8.2. Configuration of NASA two-stage axial-flow fan.



Two-stage fan overall performance

Figure 8.3. Performance maps for NASA two-stage axial-flow fan.

map is presented in Figure 8.4 for the fan total-pressure ratio. Four operational lines have been added to this map for fan exit Mach numbers of 0.45, 0.51, 0.64 and 1.00.

Six preblast operating points were calculated for the two engine-face Mach numbers of Table 8.1 and for three values of the stall margin — 8, 15 and 24 percent. The definition of stall margin, SM, used here is

$$SM = \frac{\left(\frac{p_{t_3}}{p_{t_2}}\right)_{\text{stall}} - \left(\frac{p_{t_3}}{p_{t_2}}\right)}{\left(\frac{p_{t_3}}{p_{t_2}}\right)_{\text{stall}}} \times 100, \text{ percent}$$

where p_{t_3}/p_{t_2} is the fan total-pressure ratio at the operating point and $\left(\frac{p_{t_3}}{p_{t_2}}\right)_{\text{stall}}$ is the value at stall or surge for the same equivalent mass flow.

8.4 Blast Effect on Fan Operation

Calculations with the QBIF code were carried out for the fan of Reference 8.1 for three initial conditions of the two inlets. The fan operating points that would result are presented in Figure 8.4 for the three initial stall margins for the two inlets. The shock pressure ratio at the engine face, p_2'/p_2 , is the parameter for the curves. The results show that increasing this shock strength reduces both the equivalent mass flow and the total pressure ratio.

The incident shock pressure ratio at the engine face for the inboard inlet in Part 619 was 1.101. The operating points resulting from this interaction with the fan for the three initial stall margins are joined in Figure 8.4 by the curve for $p_2'/p_2 = 1.10$. The points for double and half that shock overpressure, i.e. p_2'/p_2 equal 1.20 and 1.05, are joined similarly. These resulting operating points are all well within the area of the performance map where acceptable operation would be expected. Therefore the blast should produce no problem for the inboard fan according to the QBIF code calculations.

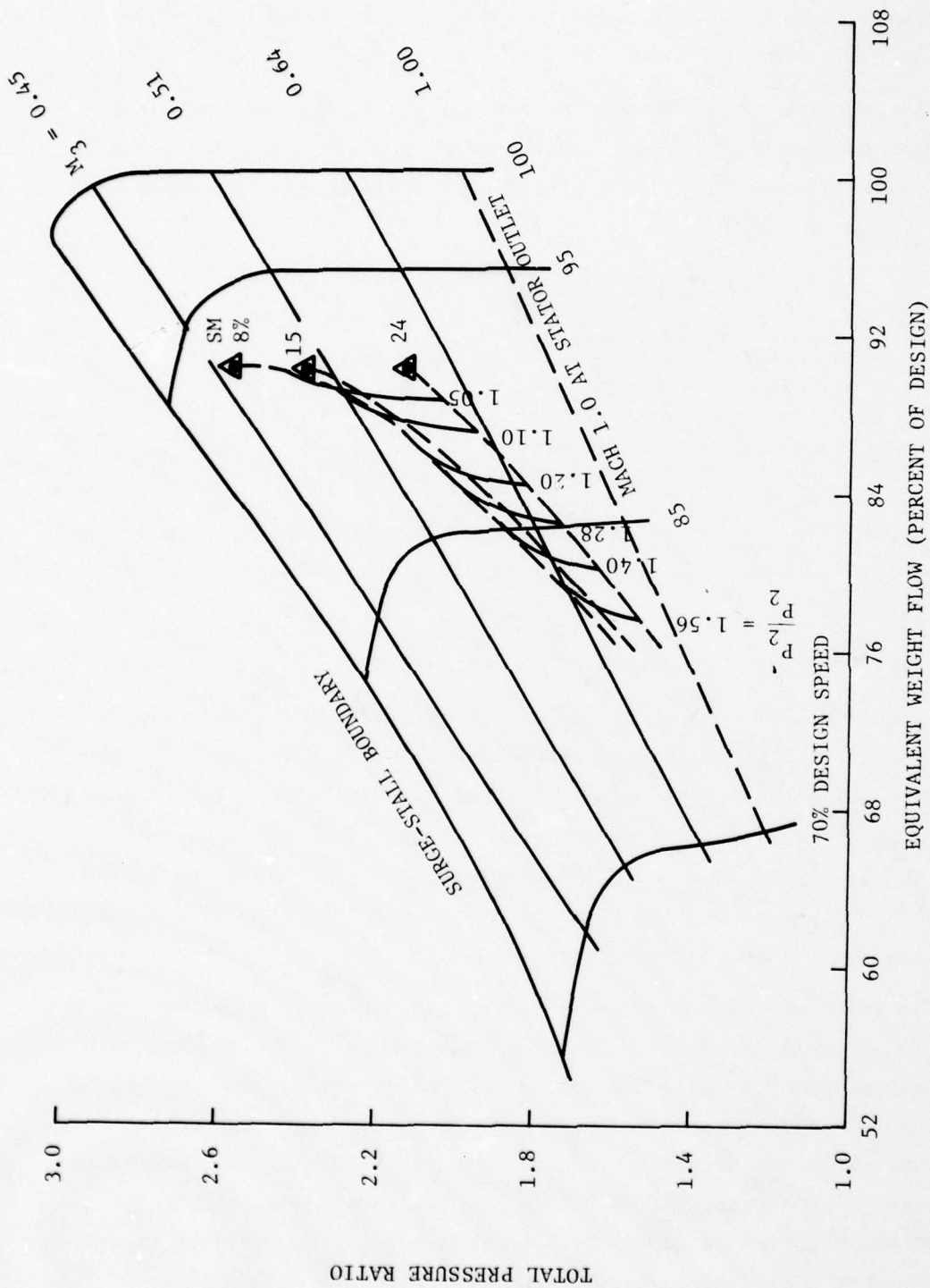


Figure 8.4. Two-stage-fan overall performance map.

The pressure ratio of the shock at the engine face in the outboard inlet in Run 40 was 1.28. The resulting three operating points for the three stall margins wind up much closer to the $M_3=1.0$ operating line. The flow in stator no. 2 of the fan would be expected to choke at about midway between the $M_3=0.64$ line and the $M_3=1.00$ line. Therefore the blast would be expected to choke the fan in the outboard inlet for this shock strength and an initial stall margin of 24 percent.

The resulting operating points are also shown for about a 42 and 100 percent increase in shock overpressure, i.e. $p_2'/p_2 = 1.40$ and 1.56 , and one-half the overpressure, $p_2'/p_2 = 1.14$. The higher overpressures would be expected to choke the fan for the initial 24 percent stall margin.

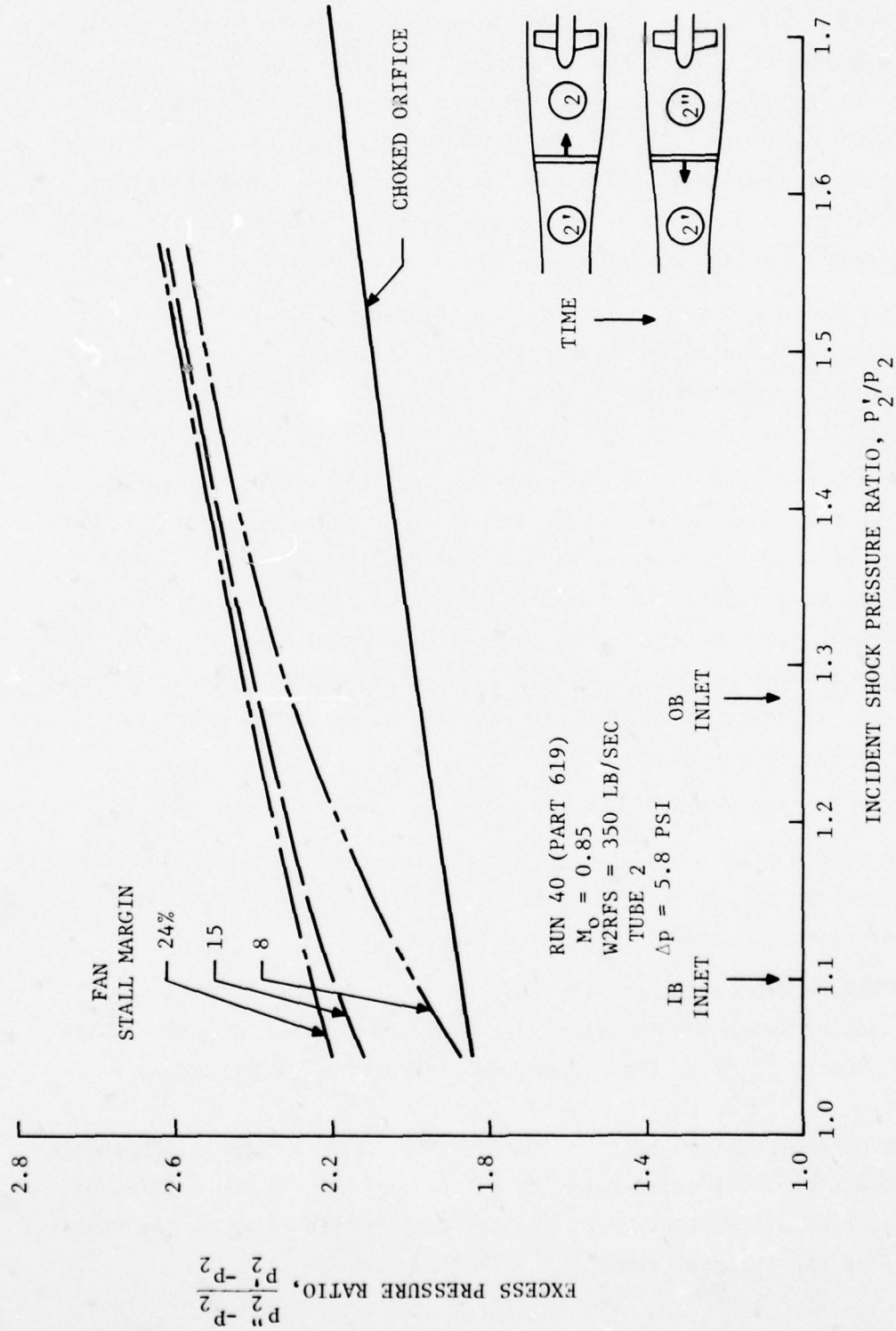
Choking of a fan for the short durations that would be experienced during penetration of a blast wave is not expected to be harmful to its operation on this quasi-steady basis. The problem for the fan would arise if it be driven to the surge-stall boundary. The effect of this initial shock from the blast wave for the cases run, however, is to increase the downstream Mach number, thereby driving the fan away from the surge-stall boundary. What the effect would be for other initial fan points remains to be explored.

8.5 FAN REFLECTED SHOCK

The properties of the shock reflected upstream from the fan, following the interaction of the incident shock with the fan, are presented in Figure 8.5 from the calculations with the QBIF code.

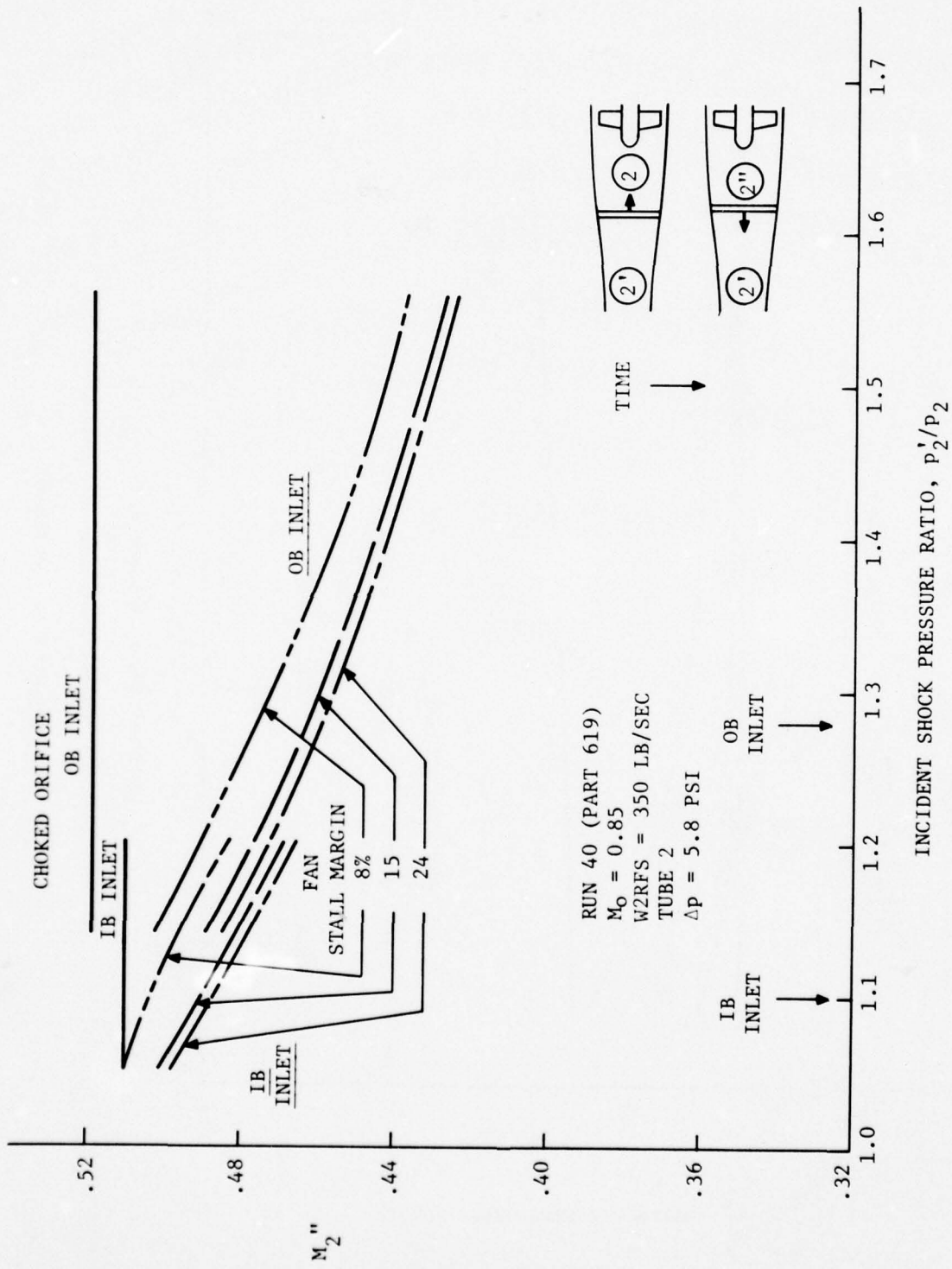
In Figure 8.5(a) the pressure of the reflected shock in excess of the initial pressure is presented as a ratio to the overpressure of the incident shock, $\frac{p_2''-p_2}{p_2'-p_2}$. This excess pressure ratio is plotted as a

function of the pressure ratio of the incident shock, p_2'/p_2 . A value of the ordinate of unity corresponds to no reflected shock and a value of two indicates an overpressure of the reflected shock equal to the overpressure of the incident shock.



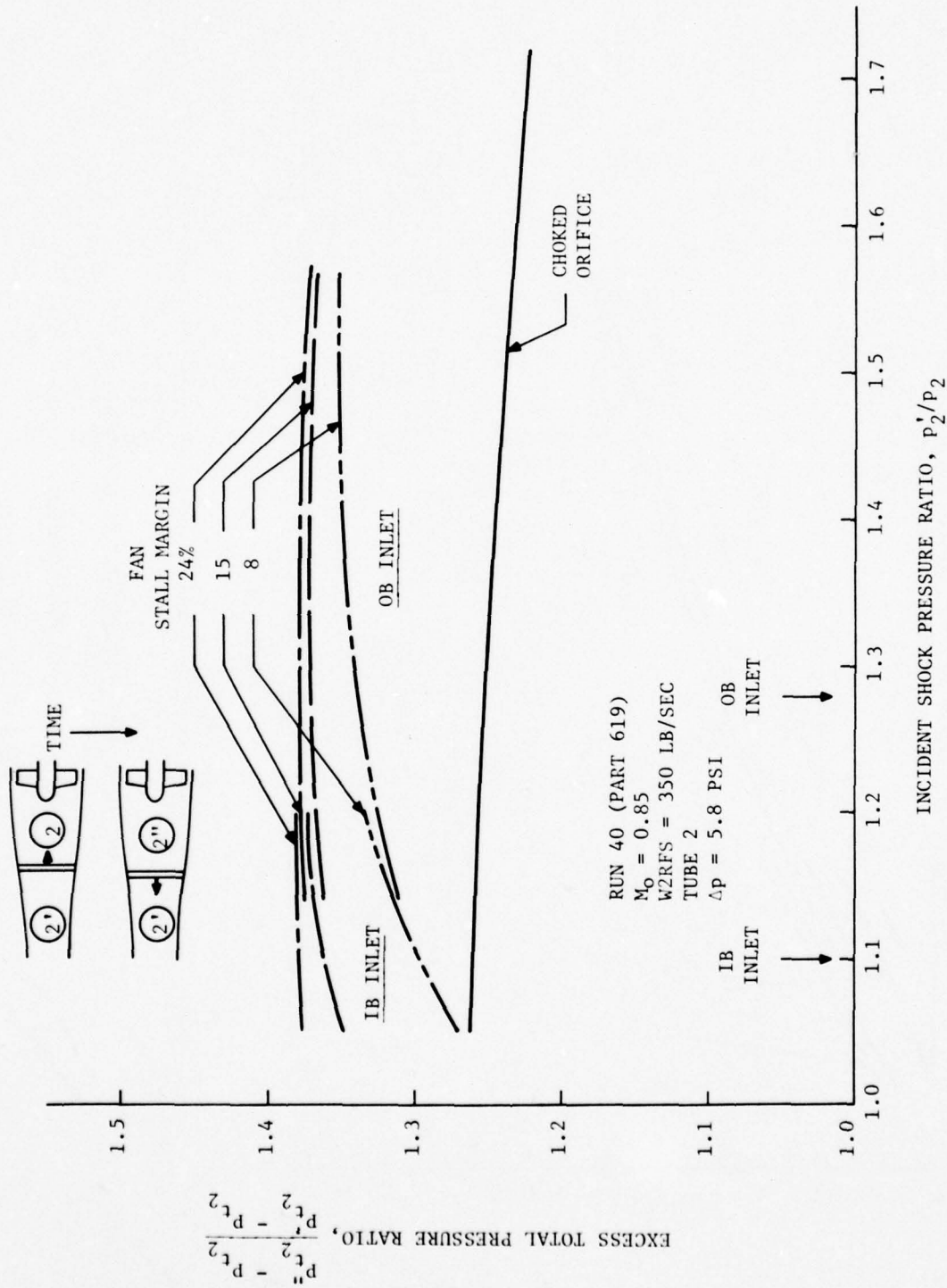
(a) Excess pressure ratio.

Figure 8.5. Variation of fan reflected shock properties with incident shock pressure ratio.



(b) Particle Mach number.

Figure 8.5. Continued.



(c) Excess total-pressure ratio.

Figure 8.5. Concluded.

A common method for simulating an engine in inlet testing is to choke the flow leaving the inlet at about the downstream location for the engine. This is done by using a fixed choked orifice or nozzle or adjustable vanes. The latter were employed with the 0.1-scale B-1 inlet and were located near the fan station.

The properties of shocks reflected upstream from a choked orifice (or nozzle or vanes) and fan are compared in Figure 8.5(a). The values of the incident shock pressure ratio at the engine face for Run 40 are indicated on the abscissa. The increment in excess pressure ratio of the reflected shock for the fan is markedly greater than for the choked orifice. Under the shock conditions of the outboard inlet in Run 40 it is 33 to 45 percent greater. This means that the strength of the shock reflected upstream from the fan would be that much greater with a turbofan engine than was experienced in the tests in the 0.1-scale B-1 inlet.

The partial Mach number, M_2'' , of the flow behind (downstream) the reflected shock and entering the fan or a choked orifice is shown in Figure 8.5(b). The inflow Mach number for a choked fan would be constant. The decrease for the fan is due primarily to the increase in temperature and speed of sound by the double shocking of the air, and only partially to the reduction, generally, in particle velocity.

Analyses of aircraft turbine engines are generally concerned with the total pressure. The excess total-pressure ratio,

$$\frac{p_{t2}'' - p_{t2}}{p_{t2}' - p_t},$$

is presented in Figure 8.5 (c). It is not as large for either the choked orifice or fan as was the excess static pressure. In other words, this means that the total pressure does not get incremented as much by the reflected shock relative to the increment by the incident shock as does the static pressure. However, the total pressure increment due to the reflected shock is markedly greater for the fan than for a choked orifice. For the outboard inlet and the shock conditions of Run 40 (Part 619), the increment would be 34 to 50 percent greater for the fan than for the choked orifice.

The variation of the properties of the shock transmitted downstream by the fan as a function of the incident shock strength are presented in Figure 8.6. The pressure ratio for the transmitted shock wave is shown in Figure 8.6(a). The ratio is always less than for the incident shock, but it is relatively large. The effect upon the downstream engine operation might be significant.

The particle Mach number M_3'' downstream of the fan for the transmitted shock is plotted in Figure 8.6(b). It increases with the strength of the incident shock in all cases. It is reasonable to expect that the second stator of the fan would choke at a downstream Mach number somewhere near 0.8, so the downstream Mach number would not increase beyond that point. In the absence of data on the choke Mach number, the curves have been continued as if there were no choking.

This condition for a choked second stator would be nearly reached for the fan operating at a stall margin of 24 percent and incident shock pressure ratios approaching 1.6. For lower initial stall margins the pressure ratio of the incident shock would need to be considerably greater for choking. In summary, the result of this analysis with the QBIF code is to indicate that this fan operating at the initial conditions of the Run 40 test would not experience any operational problems on a quasi-steady basis for (step) shocks at the engine face of the magnitude expected of Run 40 for the incidence angle, ϕ , of 100 degrees and shock overpressure of 5.8 psi scaled to 1 atm. The upstream reflected shock would be notably stronger, however, than for the choked control vanes used (as the simulated engine) in the tests.

The effect of the reflected shock on the flow within the inlet will be examined in Section 9. The strength of the transmitted wave is large, its effect on engine operation downstream is not known.

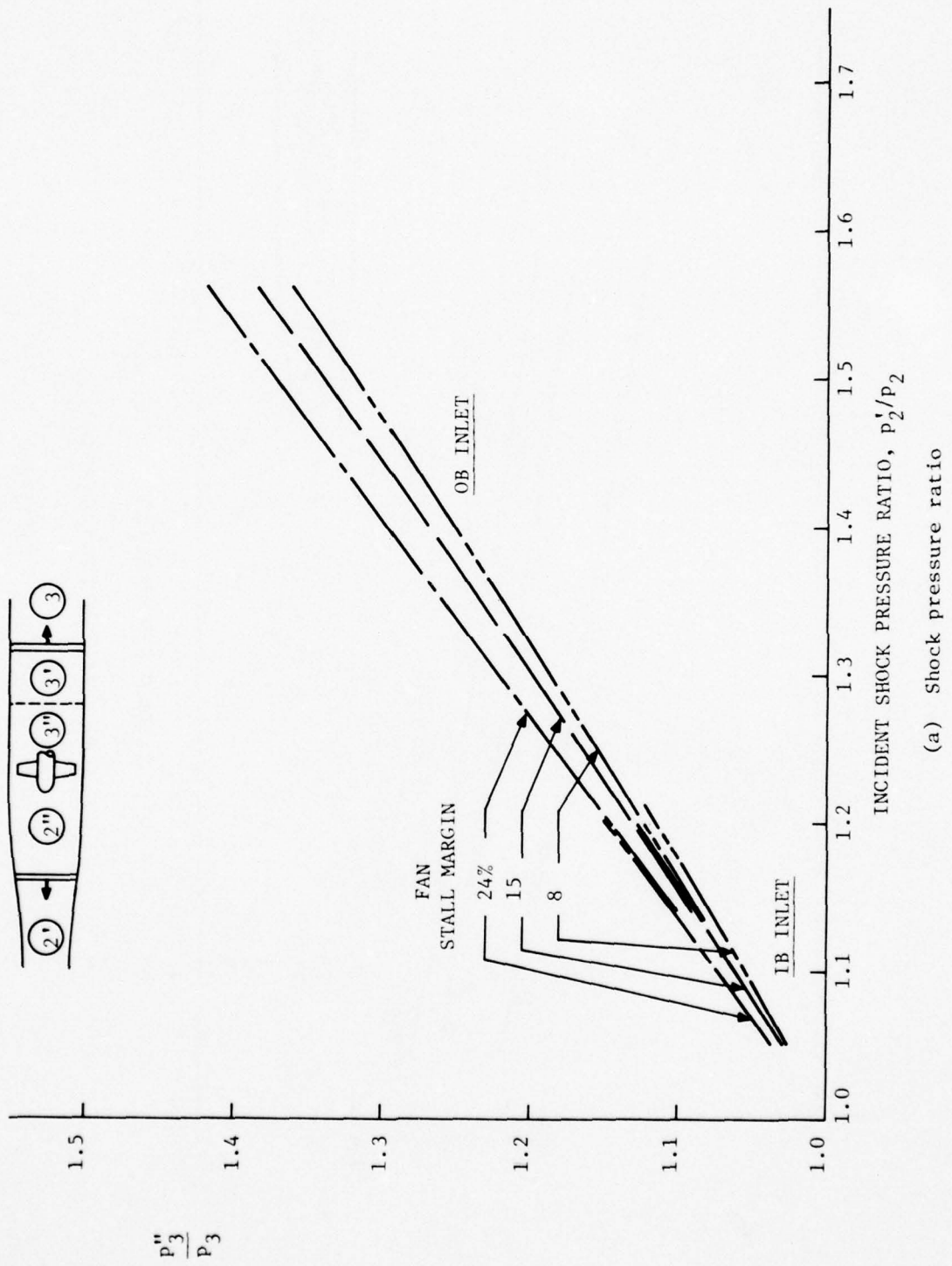
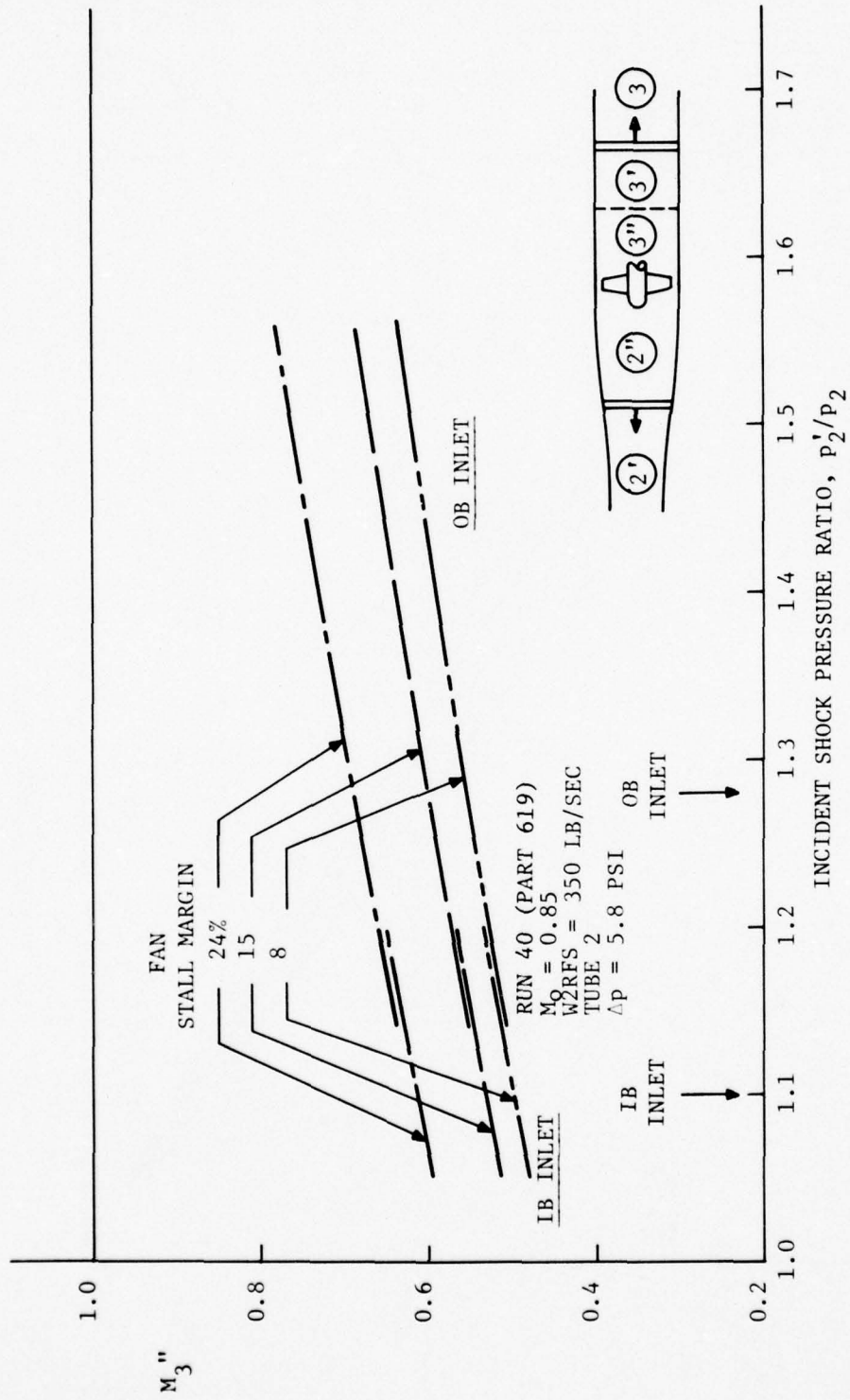


Figure 8.6. Variation of fan transmitted shock properties with incident shock pressure ratio.



(b) Particle Mach number.

Figure 8.6. Concluded

SECTION IX
REFLECTED SHOCK-BOUNDARY LAYER INTERACTION WITHIN INLET

Another important feature of the inlet-blast interaction problem is the interaction inside the inlet between the blast shock waves and the inlet boundary layer. The sketch in Figure 9.1 depicts the features of shock-boundary layer interaction that might occur on the walls of the inlets of the B-1 type due to the reflected shock from the fan. The flow in the boundary layers would be forced to negotiate the adverse pressure gradients associated with these shock waves moving upstream from the engine forces. If sufficiently strong, the adverse pressure gradients could cause the boundary layers to separate on the inlet walls, depending upon the boundary layer characteristics. This possibility will be assessed in this section.

The interaction is complicated by the variation of the "free-stream" properties within the inlet both in the flow direction and time-wise. The total pressure and total temperature in particular both vary longitudinally and with time as the reflected shock moves upstream. More data are required for this analysis than were measured in the tests with the 0.1-scale B-1 inlet, so calculations made of the flow with the BID code have been employed.

9.1 SHOCK-BOUNDARY LAYER CALCULATION

The development of the boundary layers was computed using the results of BID code calculations to provide the distributions of the free-stream properties of static pressure, total pressure and total temperature near each wall. The BID code models the fan as a choked orifice, in line with the 0.1-scale inlet model. The distributions for each wall of the inlets were selected corresponding to the time when the static pressure gradients appeared to be relatively steep within the blastward inlet. No systematic attempt was made to select the most adverse distributions for the boundary layers. These properties defined the conditions at the outer edge of each boundary layer.

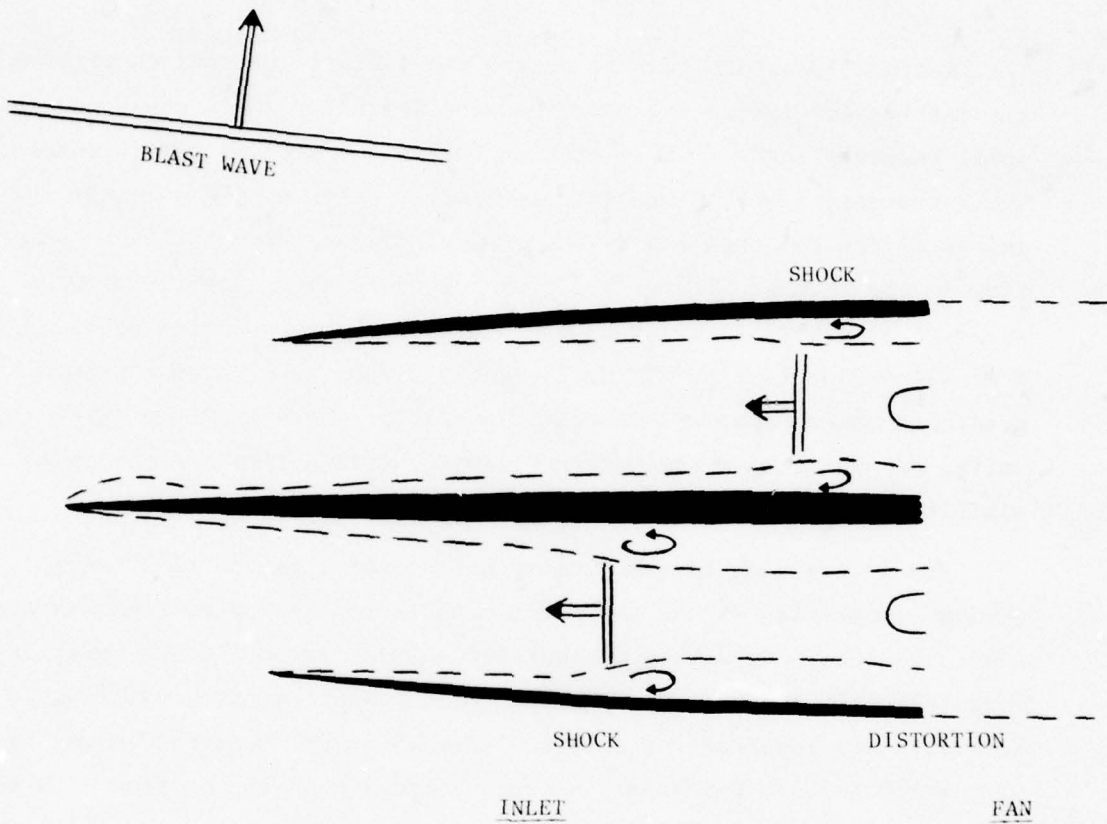


Figure 9.1. Boundary layer separation and distortion from fan reflected shock wave.

The growth and behavior of the boundary layers along the walls for these free-stream conditions were computed using the BLAYER code of NASA, presented in Reference 9.1. Since the Reynolds number of the boundary layers would be generally large relative to the transition value, the boundary layers were assumed to be turbulent from the leading edge of each surface.

The BLAYER code assumes a constant total pressure and total temperature outside of the boundary layer. Because they both generally vary significantly for the calculations made, the calculations were carried out piecewise taking the total pressure and total temperature as constant over each segment. This procedure was found to be significant to the values computed, but it is not believed to alter the general conclusions reached from the calculations.

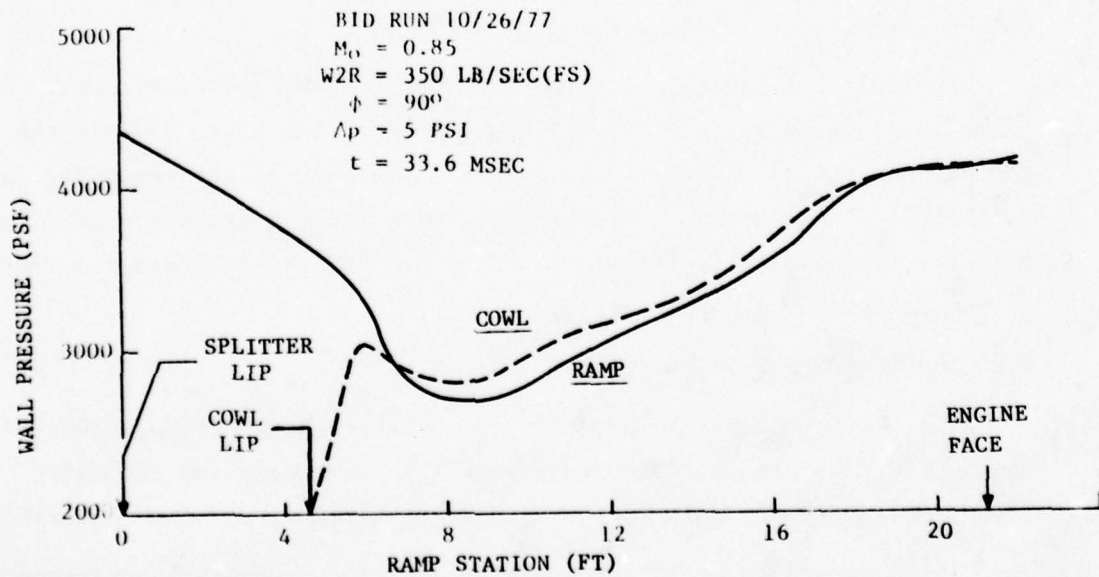
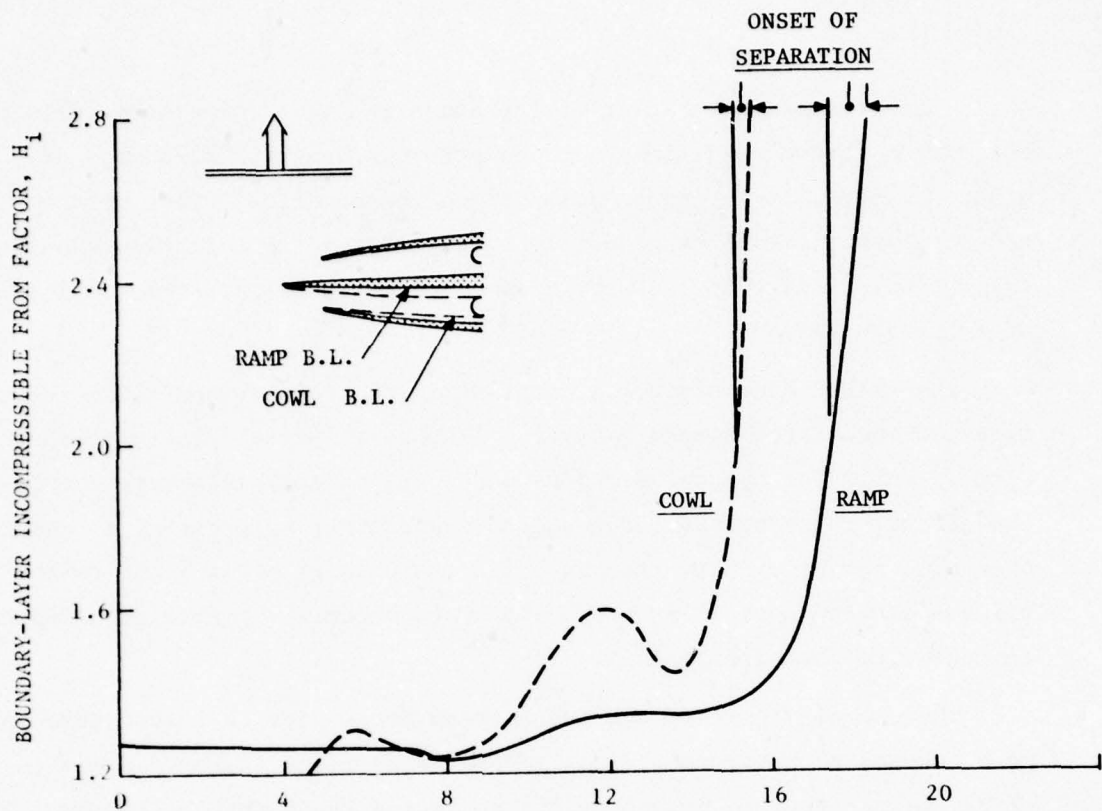
The distributions of the free-stream properties that were selected were assumed to be frozen. That is they were taken as non-varying in time, whereas they do change as the reflected shock moves upstream. The significance of this assumption is not readily assessable. The BLAYER code applies only for the frozen pressure distribution, so the question must be resolved at a later time.

The BLAYER calculations were performed for the full-scale B-1 inlets, as scaled up from the 0.1-scale model. The blast wave in the BID calculation is assumed to arrive from the side of the aircraft, that is $\phi = 90^\circ$ (0° is a head-on intercept), with a shock overpressure of 5.0 psi. The flight Mach number was taken to be 0.85 and the mass flow rate in the inlets to be 350 lb/sec.

9.2 SHOCK-BOUNDARY LAYER RESULTS

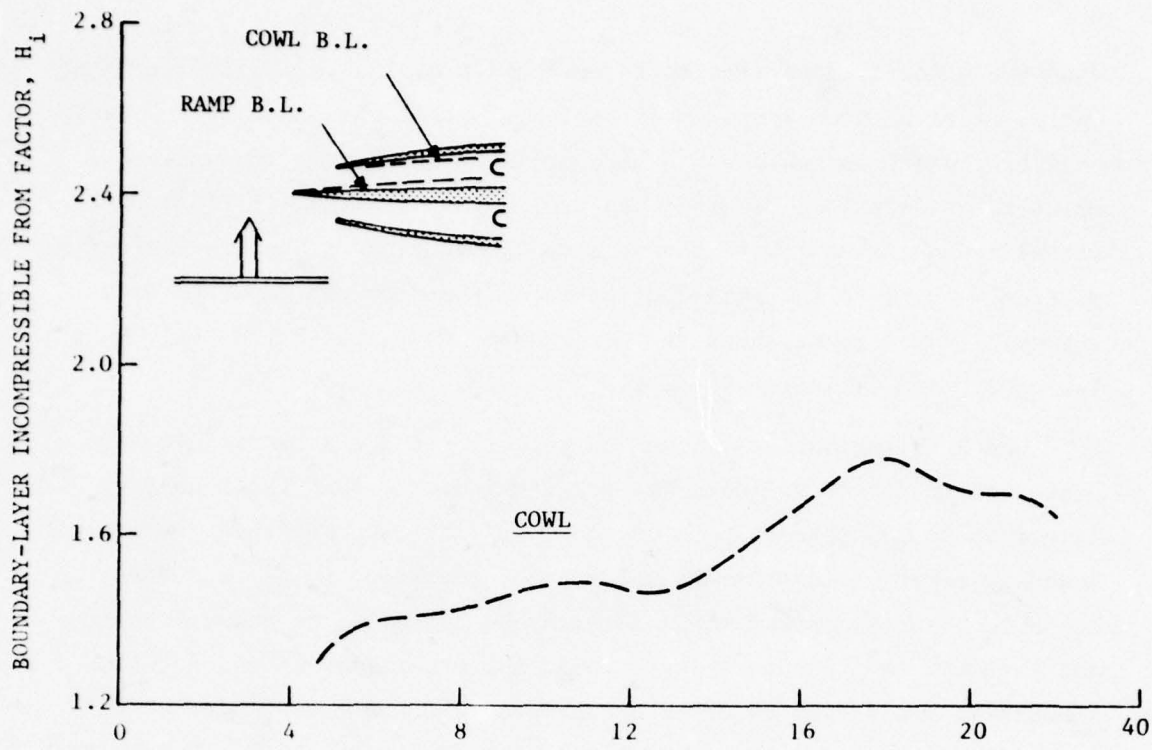
The pressure distributions for the boundary layer calculations with the BLAYER code are presented in Figure 9.2 along with the boundary-layer incompressible form factor H_i that resulted from these calculations.

The boundary-layer factor H_i is a parameter essentially representing the velocity distribution across the boundary layer (normal to the wall).

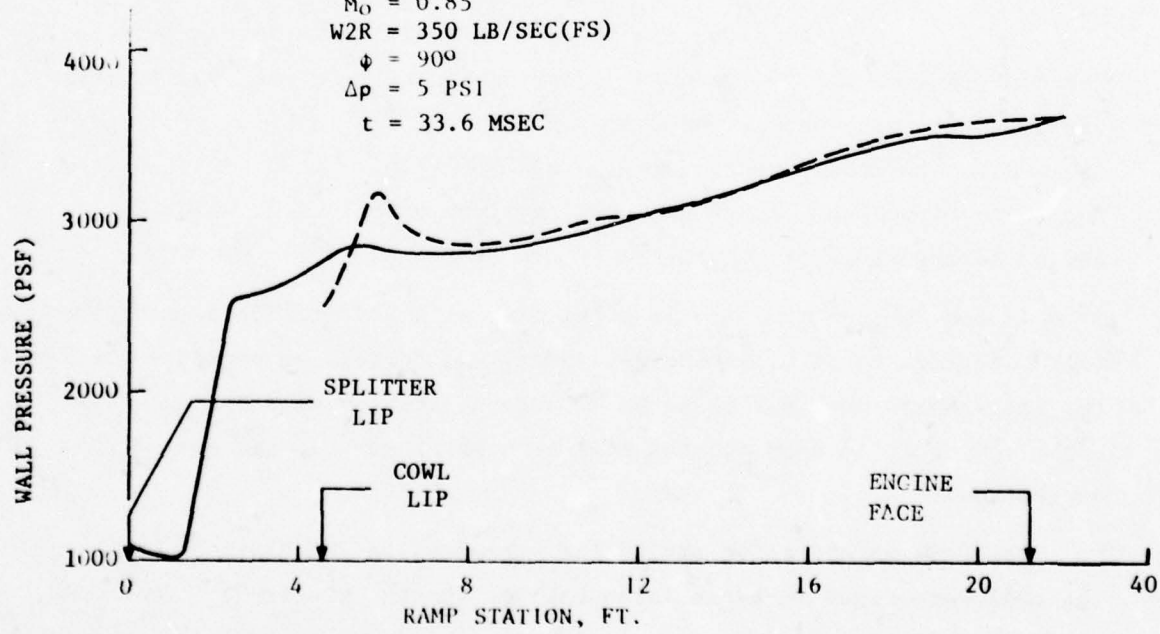


(a) Blastward inlet.

Figure 9.2. Effect of fan reflected shock on boundary layers of inlets.



BID RUN 10/26/77
 $M_0 = 0.85$
 $W2R = 350 \text{ LB/SEC(FS)}$
 $\phi = 90^\circ$
 $\Delta p = 5 \text{ PSI}$
 $t = 33.6 \text{ MSEC}$



(b) Leeward inlet.
 Figure 9.2. Concluded

When the velocity distribution is more uniform, the parameter approaches unity. A value of 1.2 to 1.4 is typical for a turbulent boundary layer on a flat plate in the absence of a pressure gradient. In an adverse pressure gradient (increasing pressure in the direction of flow) the velocities decrease toward the wall so H_i increases. When the velocity gradient normal to the wall goes to zero, the flow can separate from the wall. Experience shows that separation may occur for H_i values as low as 2.0 and definitely by 2.8.

The H_i distributions along the walls for the blastward inlet are presented in Figure 9.2(a). The results indicate that the boundary layers would separate on both the cowl and the ramp surfaces. The cowl boundary layer would separate upstream of the ramp, so it is quite probable that the stream would actually be deflected to the ramp side and that the ramp boundary layer would not separate. In any event, separation would take place on one side of the blastward inlet which would produce significant distortion at the engine face when the separated flow arrives there.

The H_i distribution for the leeward inlet is shown in Figure 9.2(b). The distribution for the ramp is not presented because the longitudinal variation in total pressure outside of the boundary layer is so large as to make conclusions from the results undependable. The H_i distribution for the cowl boundary layer reaches a maximum of only 1.8, which is below the threshold of separation.

In the BID code the fan is modeled as a choked orifice as mentioned (for matching to the 0.1-scale B-1 inlet model data), so pressure gradients for the leeward cowl may be 15 to 40 percent greater with a fan. This might be enough to separate the cowl boundary layer but the question is unresolved.

There is an effective artificial viscosity in the BID code because the cells are fixed in space (also called "shock capturing"). This has the effect of reducing pressure gradients, resulting in lower calculated values of H_i .

The question then arises as to why larger values of the distortion parameters were not measured during the test periods with the 0.1-scale B-1 inlet. Some rough estimates of the time-distance relationships of events within an inlet are useful in examining this question. Several are depicted in Figure 9.3 for Mach 0.85 flight conditions. The initial shock would reach the engine face in about 0.9 milliseconds and the vanes is about 1.1 milliseconds. The reflected shock from the vanes moves upstream more slowly, as shown. Somewhere within the inlet the boundary layer would separate. To estimate when the separated flow might reach the engine face, some other velocities must be considered.

The particle velocity within the duct is about one-third of the initial (incident) shock velocity. Vorticity shed from the leading edge of the cowl or splitter lips would first travel at about one half of the particle speed and slowly speed up as it moves out into the free stream. Assuming a step speed-up half way down the duct, the vortex would reach the engine face at 4.2 milliseconds.

The blast-type flow period produced by the shock tube exit flow at the inlet is terminated by the arrival of the shock-tube cold gas or the backward-facing shock or compression wave, observed as a sudden increase in the rate of pressure change at the inlet. In the case shown in Figure 9.3 this event would occur at the inlet entrance at about 3.3 milliseconds, and could arrive at the engine face by about 4.2 milliseconds.

The speed of the front of the separated boundary layer is not known, but it is reasonable to expect it to be significantly less than for the free-stream particles. For estimation purposes, if the reflected shock would separate the boundary layer midway down the inlet and the front of the separated flow travels at one-half of the particle velocity, the separation zone would reach the engine face at somewhat more than a millisecond after the termination of the test period.

Figure 5.8 shows that the distortion parameter IDC increased considerably for the blastward inlet for $\Delta p = 5.0$ and 5.2 psi beginning at about one millisecond after termination of the 3.3-millisecond nominal test period, indicated in the figure by the arrows. IDR increased at

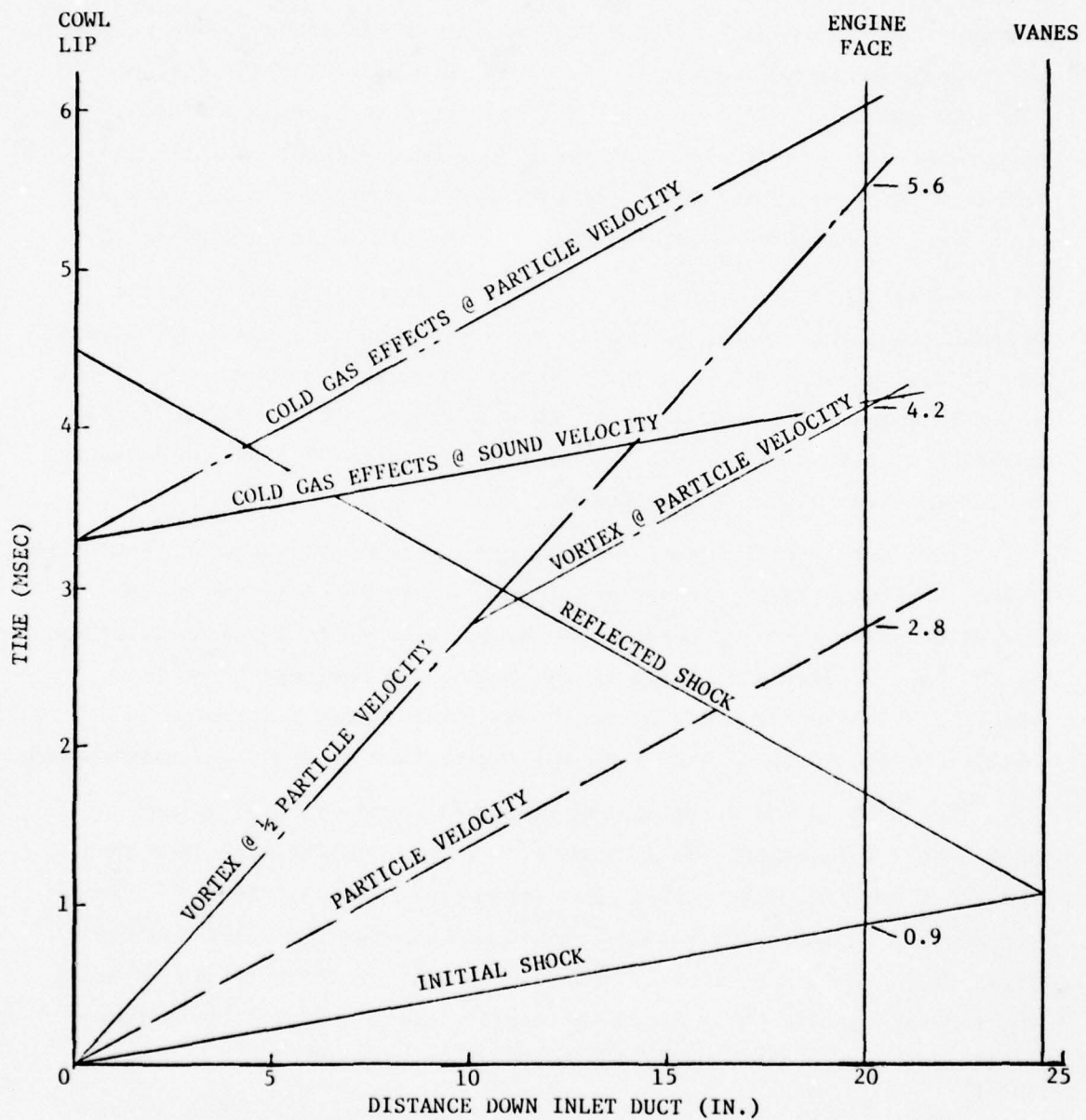


Figure 9.3. Inlet time-distance relationships for a flight Mach number of 0.85 and a mass flow rate of 350 lb/sec.

about the same time but not in as great a proportion, in comparison with the values during the test period. IDL increased apparently well beyond the full-scale value of 1.50.

For the leeward inlet, Figure 5.9, the distortion indicated is not as large. IDC and IDL appear to have increased beginning at about the end of the nominal test period, particularly for the 5.2 psi shock. IDR, on the other hand, decreased. IDL experiences only brief bursts above a value of about 1.1.

Because these large increases in distortion occurred after the expected arrival of the backward facing shock or compression wave, a question does arise as to what degree the high level of distortion may have been due to the character of the blast wave during the later period. This question should be examined to the extent possible for the present data.

SECTION X
DISCUSSION

This section presents a summary and discussion of some of the important aspects of the development and testing program, most of which are described in detail in previous sections, and indicates some recommendations for future developments. Topics discussed are the blast generator development, the 16T wind tunnel blast tests, the BID code for predicting inlet blast flows and blast-fan interactions.

10.1 BLAST GENERATORS

The blast generation development program began with theoretical REFLECT2/S2D code calculations for the firing of a shock tube into still air, followed by firings of two-in.-dia shock tubes into the AEDC 1T (one-foot-square) wind tunnel at Mach numbers from 0.6 to 0.9 (Sec. 2). Results of these tests, for the case of the shock tube firing perpendicular to the tunnel axis, gave useful blast type flows in this Mach number range for the overpressure range 2 - 5 psi (referred to sea-level ambient pressure) for distances from the tube exit of about 4.5 diameters, for polar angles from the tube axis from -15° to $+30^{\circ}$ downstream of the tube. Durations of nearly constant blast pressure (to 30% decay) were obtained for these conditions in the range of about 0.5 to 2 milliseconds per foot of tube diameter, with best results being obtained at a polar angle of 15° . At downstream polar angles from the tubes of 45° or more, the blast wave durations were generally much shorter and were not of interest. Also, it was found from the 1T tests that if the shock tube driver pressure was too low compared to the ambient pressure a non-constant pressure type of blast wave profile was produced, characterized by an extremely rapid decay.

Results of the above calculations and small shock tubes were found to be essential in selecting the shock-tube dimensions, locations and driver pressures for the subsequent development of large shock tubes for the AEDC 16T (16 foot square) wind tunnel tests.

The three large shock tube installation designed and constructed for the 16T wind tunnel tests had the following characteristics. Distances from the shock tube exits to the inlet were 3.8 to 4.3 tube

diameters, at polar angles from 11.2° to 28.3° . Shock tube driver pressures of 55 to 186 psia were used, usually at a tunnel ambient pressure of one-half atmosphere.

Definition of the properties of the blast waves produced at the inlet location in the 16T tests was made using both measured data from the tests as well as the test results from the 1T tests. The strength of the blast shock was well defined at probe locations by the 16T measurements, but interference from the inlet model degraded the definition of the flow following the shock somewhat. Firings in the 16T tunnel without a model would be useful for defining these blast properties, but they were precluded by limitations on tunnel time; as an alternative, an analysis of model interference on the blast measurements is recommended. The incidence angle of the blast shock was defined from comparative arrival times at several pressure transducers; shadowgraphs would be a useful alternative for this measurement in future tests for greater accuracy.

Shock-tube dimensions of a 22.6 in-ID and a 17-ft length were selected to provide the best combination of blast wave characteristics within space constraints of the wind tunnel for the three shock tubes. Commercial pre-scored, pre-stressed diaphragms (rupture discs) in a double-diaphragm arrangement provided fast, clean-opening diaphragm bursts free of any petal debris. By using three shock tubes the number of firings during the test period was essentially doubled over using a single tube.

10.2 THE 16T WIND TUNNEL TESTS AND ANALYSIS

The 0.1-scale B-1 inlet model used in the 16T tests had been mated previously to the tunnel sting support, so only some strengthening of the model and the 16T tunnel walls for loading by the shock-tube driver gas was required for testing.

Blast tests were performed at Mach 0.55, 0.70, 0.85 and 0.90 with inlet mass flow rates ranging from 235 to 350 lb/sec (full scale), shock overpressures from about 2 to 6 psi (referred to sea level) and model yaw angles of 0 and 5 degrees (nose away from shock tube).

Typically, blast type flows lasting about 3.3 milliseconds were achieved at the inlet, with corresponding nearly constant pressure durations (to 30% decay) of between 1 and 4 msec. This met test requirements amply. However, for future tests vortex and boundary-layer separation phenomena effects that are now believed to be important at later times make it desirable to double the test durations.

The test durations might be increased about 50 percent by moving the model about four feet off the centerline of tunnel, increasing the distance from the shock tubes and thereby the blast duration, but the shock-tube dimensions would need to be reexamined. Any additional increase in duration would require using a smaller-scale model (gaining thereby in scaled duration).

The blast interaction with the inlet as observed in the tests can be divided into three characteristic phases in terms of events at the engine face. During the first phase the blast shock travels down both inlets and reflects from the choked vanes (or fan for the full-scale engine), then returning to the engine face. In the second phase any vortex shed from the leading edge of the splitter, for example, would reach the engine face, and shock wave-boundary layer interaction within the inlet would take place and also reach the engine face. After these two stages, events are believed to happen relatively slowly, that is on a quasi-steady basis, so steady-state test results and analyses would be applicable — this is called the third stage. Attention here is focused primarily on the first two stages.

In the blastward inlet during the first period the multiple reflections of the shock result in a "staircase" of shocks arriving at the engine face over about a 0.3-msec period followed by some decay preceding the arrival of the reflected shock in about another millisecond. In the leeward inlet the shock diffracts around the splitter and enters the inlet more normal to the model centerline. It reaches the engine face as essentially a single shock, much weaker than for the blastward inlet.

When the shock in the blastward inlet reaches the engine face, distortion IDL values near unity are observed which might be of some concern during maneuvering or other stressful flight conditions. The distortion patterns examined have had high total pressures on the cowl side of the face. The distortions in the leeward inlet during this period were generally lower.

Calculations were made of the blast shock interaction with a fan typical of current technology for turbofan engines. Shock strengths measured at the engine face in the 16T tests were used. The interaction was assumed for simplification purposes to be quasi-steady with a step shock (no ramp or decay). For the blastward inlet the results indicate the fan would choke at the second stator for the lateral ($\phi \approx 90^\circ$) blast intercept. This presumably presents no operational problem, but the results are not believed to be general. The interaction should be studied for the range of conditions expected. Of clear concern to engine operation are effects produced downstream by the transmitted shock wave upon the afterburner and turbine rear stages and upstream by the reflected shock upon flow within the inlet.

Concerning the latter, boundary-layer calculations indicate that the reflected shock would definitely separate the upstream boundary layers within the blastward inlet for a 5-psi blast shock. This is expected to result in serious distortion at the engine face.

In the tests IDL values over 1.25 were observed at the engine face at about 4 milliseconds after shock arrival there. This is about one millisecond after the end of the validated duration of blast type flow, therefore it is possible the distortion at that late time was due to variations in the blast wave. In view of the significance of this effect to engine operation, it is recommended that the blast data be analyzed further to verify that the late-time distortions are relevant to the blast-inlet problem.

Interaction of the reflected shock with the boundary layers in the leeward inlet could only be analyzed to a limited extent, because of restrictions in the methods of analysis available. Separation on the cowl side might occur if calculations were refined, but not as carried out. Estimation of separation on the ramp side requires an assessment

of separation effects in BID calculations for the leading edge of the ramp and the improvement in the boundary-layer method, needed also for the blastward inlet.

Vortex formation at the splitter is another possible source of distortion for the leeward inlet. Distortion values in the leeward inlet did reach large values in the tests for times after the 3.3-msec blast flow period but whether the shedding of vortices is also a blast inlet problem depends on resolution of the late-time blast-wave data.

During the about 3.3-msec period of blast type flow the maximum IDL values were affected by the inlet mass flow rate. But there were no definite significant effects of either Mach number or inlet yaw angle on IDL.

The whole question of blast distortion relative to its effect upon engine operation is an open question at this point. The particular distortion indices used in work with the B-1 inlet (IDC, IDR, IDL and IDT) have been employed here, basically as parameters that have met with success for distortions of the type obtained in typical flight situations (maneuvering flight, throttle transients, etc.). There are many other distortion parameters in use. Also, there are factors involved in a blast interaction that are not reflected in these parameters, such as the rapidity of the changes due to the shocks, and features of the spatial distortions that are significantly different, etc. The effects of these differences on engine operation must be answered before the question can be resolved.

The BID code provides good predictions of the observed pressure histories in the inlet duct and at the engine face, particularly in reproducing the principal events, such as shock reflections. The pressures predicted at the engine face tend to be slightly low but the trends are generally good, so that a simple factor (accounting for numerical viscosity effects) would be expected to bring them into good agreement. The BID code at present does not include blast decay; this addition to the code would provide an improvement at late times. A second improvement that is recommended is to extend the code to three

dimensions; this would allow for modelling the hub and would account for differences in the vertical direction. Work is recommended to further correlate distortion predictions of the BID code with the test data.

BID code calculations have been made for intercept angles from 90 to 135 degrees from head on. The 90-deg intercept results in much larger total-pressure increment at the engine face with greater pressure-time variations than for the more rearward intercepts. Further studies extending the blast intercept angles are recommended.

Regarding the effects of the observed inlet pressures on an engine fan stage, the calculation of the quasi-steady interaction of the blast shock with a fan and with a choked flow for a 90-deg intercept indicates the reflected shock would be considerably stronger for a fan than for a choked-flow condition, as used in these tests, by as much as 43 percent for a typical case. Control of flow by means of a choked nozzle or vanes is a standard technique used in inlet testing. Consideration should be given to this problem of weaker reflected shocks in planning and analyzing results of similar blast-inlet testing.

SECTION XI
CONCLUSIONS

From the analyses and wind-tunnel tests carried out to simulate nuclear blast interaction on a B-1 type engine inlet, the following conclusions are reached.

1. Blast simulations capability has been developed and demonstrated in the AEDC 16T wind tunnel for blast strengths of 2 to 6 psi, scaled to sea-level conditions, and nearly constant blast pressures (with less than \pm 30-percent decay) lasting from 1 to 4 milliseconds.
2. A data bank of blast interaction data has been developed with the 0.1-scale B-1 inlet for lateral intercepts, varying wind-tunnel Mach number from 0.55 to 0.90, inlet mass flow rate from 235 to 350 lb/sec. (full scale), shock overpressures from 2 to 6 psi (sea level) and model yaw angles from 0 to 5 degrees.
3. The BID code predicts satisfactorily the principal features of the pressure time history within the inlet duct and at the engine face. Additional work is recommended for prediction of distortion at the engine face. Recommended additions to the code include accounting for blast decay and extending the code to three dimensions.
4. Four potentially adverse effects to engine operation from blast interaction were identified: blast-induced distortion, fan choking, afterburner blow out and shock-boundary layer induced distortion.
5. Blast-induced distortions during the time of definite blast-type flow in the inlet were usually smaller than but did sometimes reach normal inlet allocation levels for the B-1 airplane. Distortions at later times greatly exceeded the allocation. Boundary-layer separation in the inlet by simulated fan (vane) reflection of the blast shock is suspect for the latter distortion levels.

6. Distortion studies made here are severely limited by the unavailability of a parameter for judging the effect of transient distortions on gas-turbine engine operation. Blast tests with an inlet-engine combination are strongly recommended for meeting this need.

REFERENCES

- 1.1 Pierce, D., Simulation of Blast Waves in a Supersonic Wind Tunnel, British Royal Aircraft Establishment, Tech. Note No. Aero. 2665, January 1960.
- 1.2 Test Facilities Handbook (Tenth Edition), Arnold Engineering Development Center, Arnold Air Force Station, Tennessee, May 1974.
- 2.1 AEDC Reports, Data tabulations, Plots and Tapes on the Inlet Blast Effects Test, AEDC Project P41A-07A, Test TM 332, 1975.
- 4.1 Mitchell, C.E., and Powers, J.L. Jr., Pretest Information for the 0.10 Scale B-1 Inlet Development Model II Nuclear Blast Effects Test in the AEDC 16-Foot Transonic Propulsion Wind Tunnel, Rockwell International Report NA-76-593, August 1976.
- 4.2 AEDC Reports, Data Tabulations, Plots and Tapes on the DNA B-1 Blast Effects Test, AEDC Project P41T-D2A, Test TF-419, 1976-1977.
- 5.1 Haagenson, W.R., and Randall, L.M. Inlet Development for the B-1 Strategic Bomber, Rockwell International, AIAA Paper No. 74-1064, 1974.
- 5.2 Hercock, R.G., and Williams, D.D., Aerodynamic Response, in Distortion Induced Engine Instability, AGARD-LS-72, 1974.
- 5.3 Koch, K.E., and Rees, R.L., Analysis of Pressure Distortion Testing, NASA CR-2766, 1976.
- 5.4 Brimelow, B., Techniques for Establishing Propulsion System Stability, Technical Memorandum APTA-TM-69-12, April 1969.
- 6.1 Thompson, J.H., Tomayko M.A. and Ruetenik, J.R. BID Code for Computing Aircraft Engine-Inlet Response to Blast Disturbances, Kaman Avidyne TR-130. (In preparation).
- 8.1 Ruggeri, R.S., and Benser, W.A., Performance of a Highly Loaded Two-Stage Axial-Flow Fan, NASA Technical Memorandum X-3076, August 1974.
- 9.1 McNally, W.D., FORTTRAN Program for Calculating Compressible Laminar and Turbulent Boundary Layers in Arbitrary Pressure Gradients, NASA Technical Note D-5681, May 1970.

REFERENCES (CONT'D)

- A.1 Ruetenik, J.R., Analysis of Godunov Method with Fixed Mesh for Hydrodynamic Calculations, Sponsored by Kaman Avidyne Internal Research and Development Program, Proprietary, 1973.
- A.2 Lee, W.N., Smiley, R., Ruetenik, J.R. and Hobbs, N.P., Evaluation of Back-Blast Pressures Produced by a Wing-Mounted 105-MM Recoilless Rifle, Kaman Avidyne Report TR-97, Watervliet Arsenal Technical Report WVT-CR-74023, 1974.
- A.3 Thompson, J.H., REFLECT2 Computer Code for Ground-Reflected Blast Waves and Shock Tube Jet Simulation, Kaman Avidyne TM-98, 1976.
- A.4 Thompson, J.H. REFLECT Computer Code for Ground-Reflected Blast Waves, Vol. II, Computer Program Description, Kaman Avidyne Report TR-96, Defense Nuclear Agency Report 3470F-2, 1975.

APPENDIX A
THEORETICAL STUDIES OF THE FLOW FIELD PRODUCED BY
FIRING A SHOCK TUBE INTO A STATIONARY FLUID

A.1 INTRODUCTION

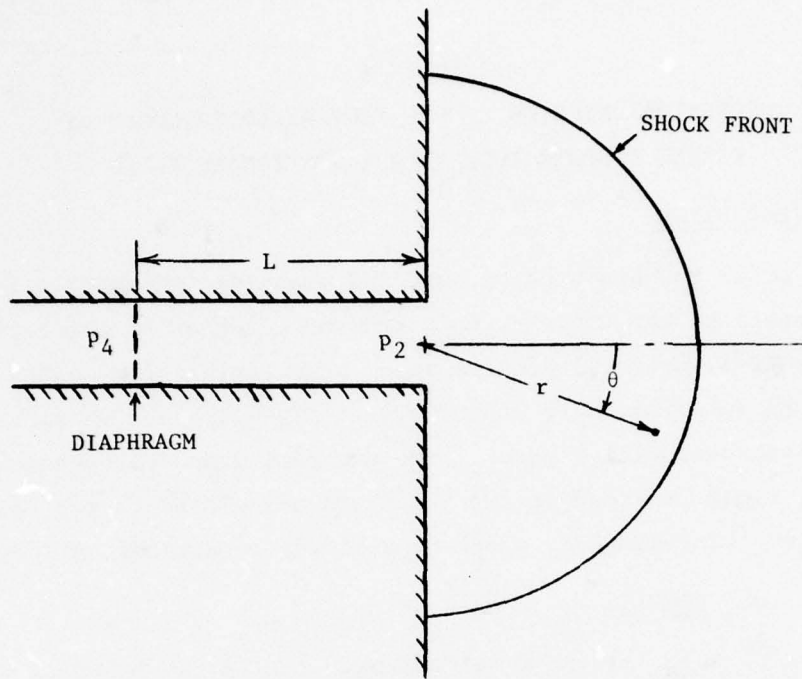
In order to obtain background and planning information for the wind tunnel tests of this report, KA performed a series of theoretical studies for the axi-symmetrical problem where a prescribed flow exits from a shock tube into initially stationary air ($\gamma = 1.4$) at an ambient pressure of one atmosphere (14.7 psia). The external transient pressure disturbance or blast field produced in the fluid was calculated by two KA computer codes for a wide range of shock tube firing conditions, as described below.

A.2 S2D CODE STUDIES

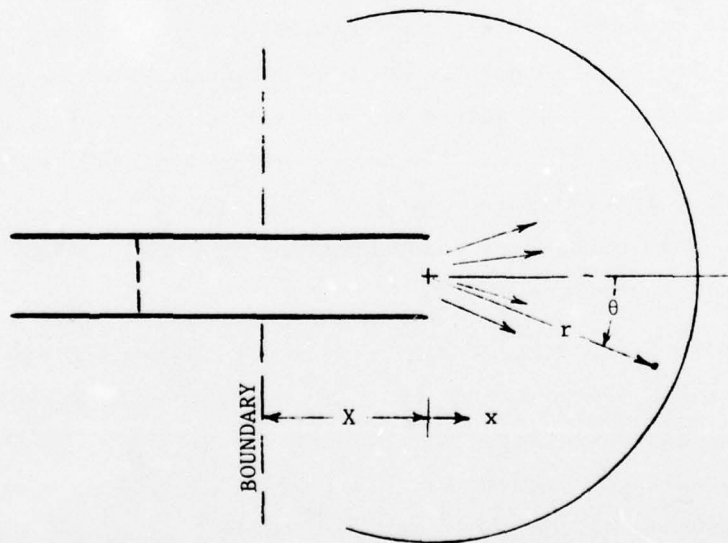
Initial calculations were made with the KA S2D Eulerian computer code (References A.1 and A.2), with several different representations of the geometry of the exit end of the tube. In one representation, shown in Figure A.1a, the shock tube was assumed to be fired into a half-space bounded by a rigid wall. In a second representation, the shock tube was assumed to protrude into the flow from a boundary by various distances, X , as shown in Figure A.1b, with a non-reflecting boundary condition being assumed to apply at this "boundary" distance behind the end of the shock tube. More specifically, the flow field for $x < -X$ in Figure A.1b was assumed to have properties independent of x , with X being varied from about 0.3 to 1.5 tube diameters.

These particular S2D solutions were used to determine the sensitivity of the external flow field to the boundary conditions as described above. In general, it was found that, for the range of exit pressures considered, from 37 to 103 psia, the pressures at all distances two or more tube diameters downstream of the tube exit were essentially independent of the assumed boundary conditions.

Since our interest was primarily in large downstream distances, the above observations indicated that we could more profitably study this shock-tube fluid flow problem by making use of the REFLECT2 computer code described below, which permits better resolution of pressure transients,



(a) Wall boundary.



(b) No wall boundary.

Figure A.1. Problem of a shock tube firing into a stationary fluid.

but is presently less capable than the S2D code for handling complex boundary conditions.

A.3 REFLECT2 CODE STUDIES

Calculations were made with the KA REFLECT2 Lagrangian computer code (References A.3 and A.4) for the shock tube exit flow conditions of Figure A.1a for a range of exit pressures (p_2) from 24 to 103 psia.

Geometrical properties of the shock tube were taken as : inside diameter of 2 inches, driver length (LR) of 4.5 inches and driven length (LN) of 9 inches.

The shock tube exit flow conditions of pressure, density and velocity were taken to be the same as for a perfect one-dimensional shock tube flow with a specific heat ratio of $\gamma = 1.4$. In some solutions the exit flow conditions were assumed to be constant corresponding to the initial blast field behind the shock front. In other solutions, account was taken of the change in density produced when the contact surface originally at the tube diaphragm position reached the exit end of the shock tube. Consideration of this contact surface change appeared to have little effect on the initial blast phenomena discussed below and is not discussed herein.

Figure A.2 presents sample time histories of pressure time histories at several positions along the axis of symmetry ($r =$ radial distance from tube exit, $d =$ diameter) for several firing pressures ($p_{41} = p_4/p_o$, $p_{21} = p_2/p_o$, $p_4 =$ driver pressure, $p_2 =$ shock (exit) pressure, $p_o =$ ambient pressure).

The following important features may be seen in Figure A.2. For the lowest shown driver pressure ratio, $p_{41} = 2.8$, the blast overpressure decays very rapidly after shock arrival reaching zero in less than 0.2 msec for the two inch-diameter shock tube. This waveform has a too rapid decay to be of interest for the present program. For the intermediate pressure ratio, $p_{41} = 10.4$, a much longer positive overpressure duration is obtained, about 0.4 msec and the overpressure is much more nearly constant during the positive phase than for $p_{41} = 2.8$. Finally, for the largest pressure ratio, $p_{41} = 15.3$, the positive phase duration is again about 0.4 msec, and the overpressure remains nearly constant for over 0.3 msec.

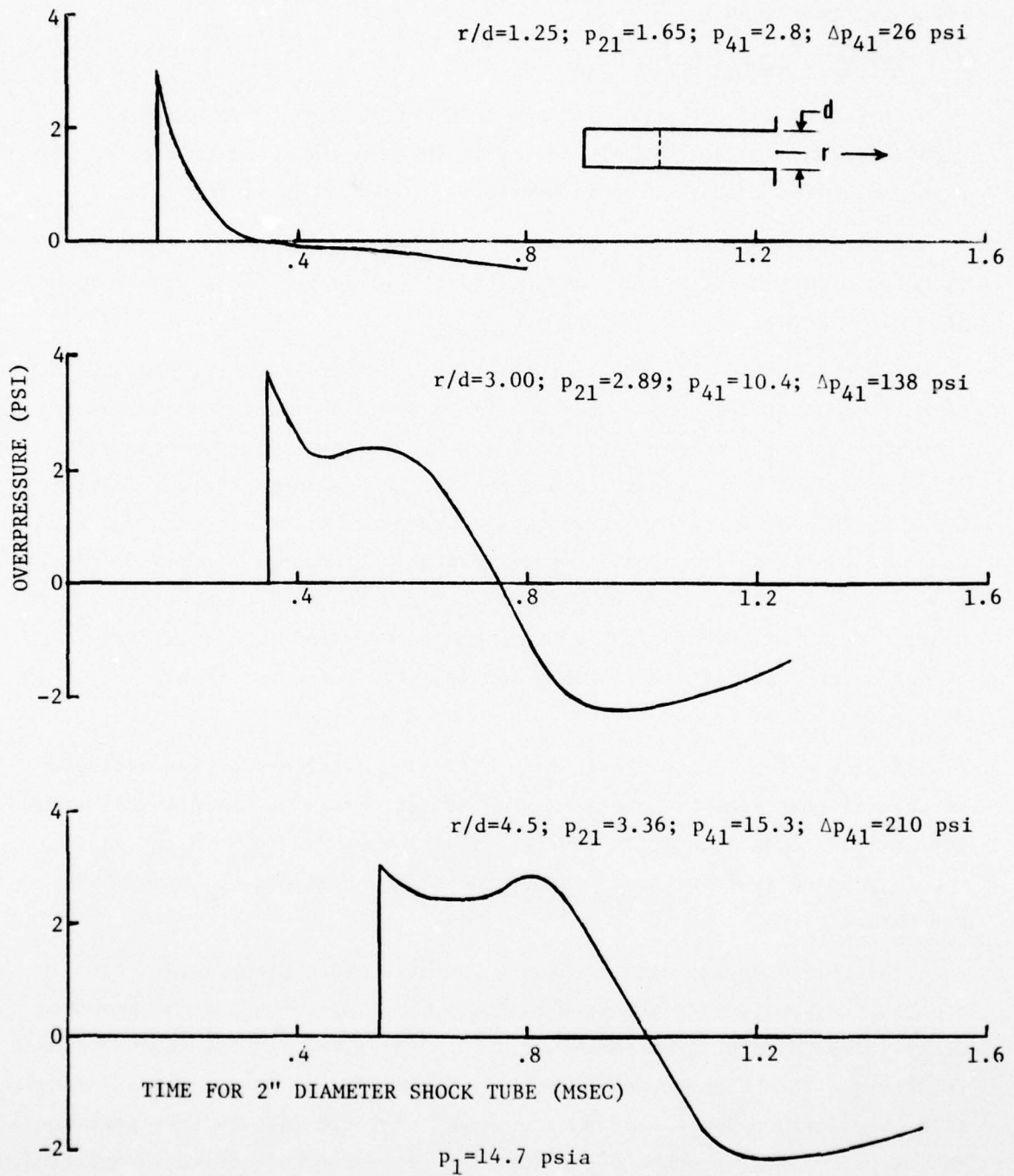


Figure A.2. Theoretical blast pressures outside of a shock tube.

Figure A.3 presents the calculated initial peak or transient blast overpressure, Δp , in the fluid along the axis of the shock tube, as a function of driver pressure ratio p_{41} , and exit pressure ratio, p_{21} and radial distance in tube diameters from the tube exit, r/d .

The initial blast pressure is observed to increase nonlinearly with increasing pressure ratio and to vary roughly inversely with distance from the tube exit in the range of interest ($0.1 < \Delta p/p_o < 0.4$).

These theoretical results can be represented fairly well by the empirical equation:

$$\Delta p/p_o = 1.5 (6.39(r/d)p_{21}^{-1.75} + 0.4)^{-1.5} \quad (A.1)$$

for the range $0.1 < \Delta p/p_o < 1.0$ where $1 < r/d < 10$ and $2 < p_{21} < 7$.

A.4 CONCLUSIONS

The above results of these studies indicated that for reasonable shock tube driving pressure (under 600 psia) external shock overpressures in the desired range of 2 - 5 psi could be obtained at distances from the tube exit in the range of 3 - 10 diameters. Also the calculated durations of the shock overpressure appeared to be long enough to be useful for simulating a nuclear blast on a small inlet model. For example, at a driver pressure of 225 psia, at 4.5 diameters from the shock tube along the tube axis, the shock overpressure along the axis of the tube was calculated to be about 3.0 psi and the duration of nearly constant overpressure to be about 2.5 milliseconds per foot of tube diameter.

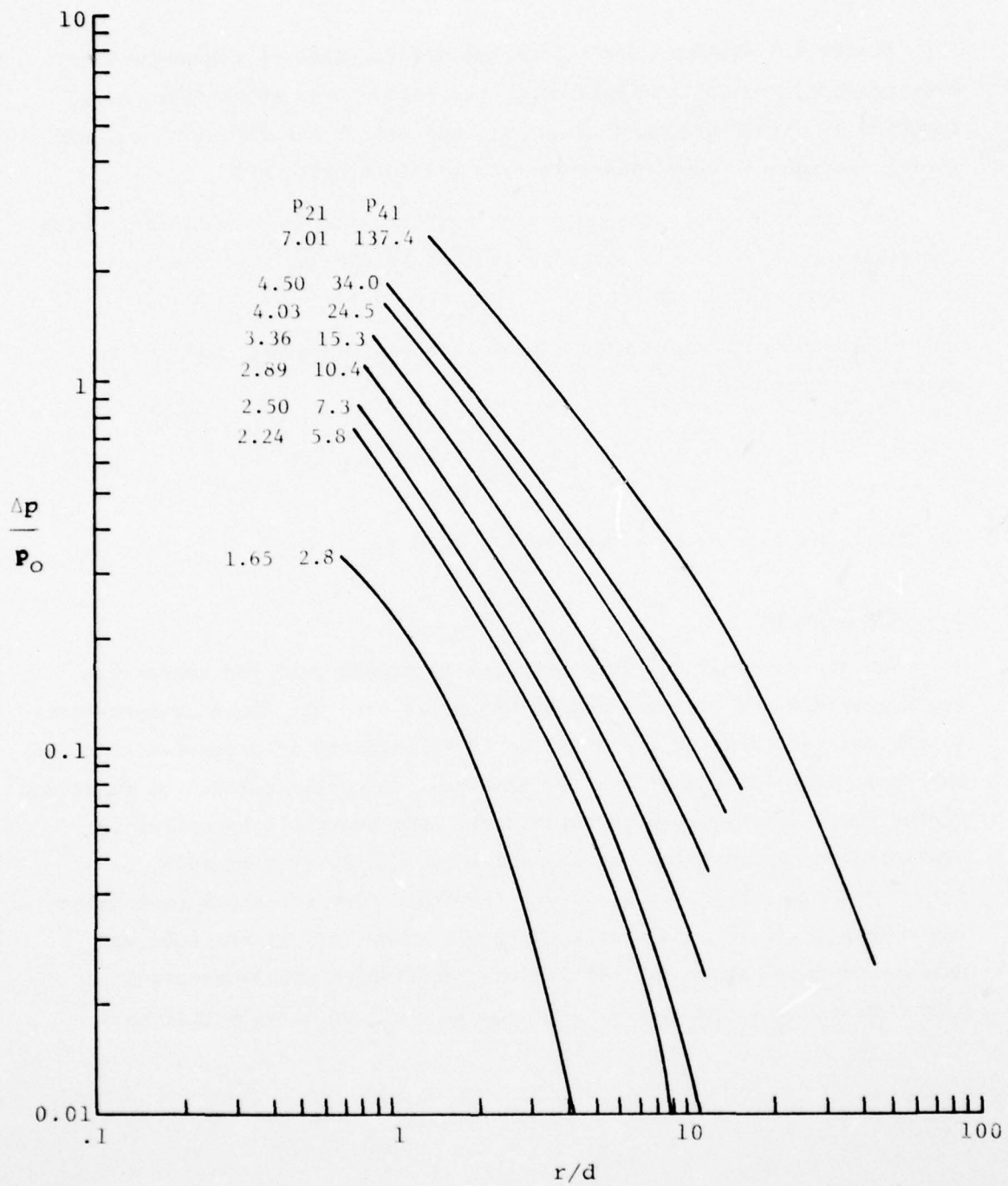


Figure A.3. Variation of overpressure with distance from shock tube.

APPENDIX B

STEADY-STATE PRE-BLAST TEST CONDITIONS IN THE AEDC 16T TUNNEL

This appendix presents AEDC tabulations of the steady-state wind tunnel and inlet operating conditions and inlet pressures and distortions existing immediately before the firing of each shock tube. The data are presented in the chronological order of the firings, by Part number, and are preceded by a table of nomenclature.

In these tables the following parameters are in error: IDCO, IDCI, IDLO and IDLI for data set 2 and PDO, PDI, PDPO and PDPI for both data sets 1 and 2. Corrected values of these parameters are available, but are not included here since they are not essential for the present study.

Steady-State Printout Nomenclature

DNA B-1 Blast Effects Test

P41T-D2A (TF-419)

<u>Parameter</u>	<u>Description</u>
AB1 ϕ -I	Outboard and inboard total bleed zone I areas, in. ²
AB2 ϕ -I	Outboard and inboard total bleed zone II areas, in. ²
ALPHA	Model angle of attack defined positive nose up, deg
BETA(SIC)	The angle of yaw defined positive pilot's right, deg
B5-1	Fuselage configuration
C	Structural mode control fin's angle relative to the model axis
C3	Structural mode control fin configuration
CP1SS	Claw probe one static pressure ratioed to free-stream total pressure
CP2SS	Claw probe two static pressure ratioed to free-stream total pressure
CP3SS	Claw probe three static pressure ratioed to free-stream total pressure
Date	The date the data were taken
Day	The day the data were taken, deg
ERCODE	Tunnel error code
E10	Boundary layer control system configuration
G34-2	Wing gutter configuration
H1I	Inboard lip height, in.
HL ϕ	Outboard lip height, in.
H16-1	Wind hood configuration
HR	The hour the data were taken, hr

<u>Parameter</u>	<u>Description</u>
IDA	Average engine-face distortion index
IDC	Engine-face total circumferential distortion index
IDL	Fan stall margin ratio
IDR	Engine-face total radial distortion index
IDT	Engine-face overall total pressure distortion
I40	Inlet configuration
IDC12	Engine-face total circumferential distortion index at the hub
IDC45	Engine-face total circumferential distortion index at the tip
J27	Porous bleed hole configuration
L7	Cowl configuration
M	Free-stream Mach number
MA	First ramp Mach number
MB	Mach number constants box
MIN	The minute the data were taken, min.
MFR2	Engine-face mass flow ratio
MFR100	Engine-face mass flow ratio corrected to 100% recovery
MODE	Mode code
M2	Engine-face Mach number based on engine-face static to total pressure ratio
M2S	Engine-face Mach number based on weight flow
M6	Flow meter configuration
NCN	Nozzle contour number
NSP	Normal shock parameter
N30-1	Nacelle configuration

<u>Parameter</u>	<u>Description</u>
P	Tunnel static pressure, psfa
Part	Part number
PCA-1	Primary plenum pressure, psfa
PCB-2	Back-up plenum pressure, psfa
PD	Back-up prediction of peak instantaneous fan stall margin ratio
PDP	Primary prediction of peak instantaneous fan stall margin ratio
PLX	Model measured pressure ratioed to free-stream total pressure where L refers to outboard (L=1) and inboard (L=2) and X refers to the pressure designation (X=020, 030, 035, etc.)
PMIN	The minimum engine-face total pressure ratioed to free-stream total pressure
PMAX	The maximum engine-face total pressure ratioed to free-stream total pressure
PTI	Tunnel compressor inlet total pressure, psfa
PTA-1	Primary tunnel total pressure, psfa
PTB-2	Back-up tunnel total pressure, psfa
PSTCE1	Exit control pressure for shock tube number one, psia
PSTCE2	Exit control pressure for shock tube number two, psia
PSTCE3	Exit control pressure for shock tube number three, psia
PSTCD1	Driver control pressure for shock tube number one, psia
PSTCD2	Driver control pressure for shock tube number two, psia
PSTCD3	Driver control pressure for shock tube number three, psia
PSTCI1	Interstage control pressure for shock tube number one, psia

<u>Parameter</u>	<u>Description</u>
PSTCI2	Interstage control pressure for shock tube number two, psia
PSTCI3	Interstage control pressure for shock tube number three, psia
PSTRD1	Driver pressure for shock tube one, psia
PSTRD2	Driver pressure for shock tube two, psia
PSTRD3	Driver pressure for shock tube three, psia
PSTRI1	Interstage pressure for shock tube one, psia
PSTRI2	Interstage pressure for shock tube two, psia
PSTRI3	Interstage pressure for shock tube three, psia
P1700	MA total pressure ratioed to free-stream total pressure
P1701	MA static pressure ratioed to free-stream total pressure
Q	Free-stream dynamic pressure
R2	Engine-face total pressure recovery
RB ϕ -I	Outboard and inboard second ramp angle, deg
RC ϕ -I	Outboard and inboard third ramp angle, deg
REX10 ⁻⁶	Free-stream unit Reynolds number times ten to the minus six, ft ⁻¹
SCHED	Tunnel parameter
Sec	The second the data were taken, sec
SHOCK TUBE SELECT	Shock tube select code with the last two digits referring to the volumetric size, cu.ft.
S19	Sideplate configuration
TAVG	Engine-face tip average static pressure ratioed to free-stream total pressure
Test	Test number
TI2	Average engine-face turbulence factor

<u>Parameter</u>	<u>Description</u>
TPR	Tunnel pressure ratio
TT	Free-stream total temperature, °R
TTA-1	Primary tunnel total temperature, °R
TTB-2	Back-up tunnel total temperature, °R
U	Bypass door position
U1	Bypass configuration
VANEI	Inboard flow throttling vane angle, deg
VANE ϕ	Outboard flow throttling vane angle, deg
WAE	East wall angle, deg
WAW	West wall angle, deg
WA/WT	Mass flow ratio of tunnel make-up air
W8-1	Wing configuration
Wind-off	Part and point number of current wind-off
W2	Engine-face weight flow, lb/sec
W2R	Engine-face weight flow corrected to standard conditions, lb/sec
W2R-FS	Full scale engine-face weight flow corrected to standard conditions, lb/sec

THIS PAGE IS BEST QUALITY PRACTICABLE
FROM COPY FURNISHED TO DDC

*** STEADY STATE ***

PART POINT	PROJECT	TEST	DATE	DAY	HR	MIN	SEC	ERCODE	MODE	SET/DATE	WIND-OFF	AEDC	PROPULSION	WIND TUNNEL						
512	3411-D2A	TE4-9	9/25/76	2691	11	391	59	0	0	3110/27/76	5027	-1	TRANSONIC	161						
W-PT	P	0	REX10-6	II	PIA-1	PIR-2	PCA-1	PCB-2	IIA-1	IIB-0	PTL	NCN	MAE	WAW	TPR	WAW	MI	MB	SCHED	
0.700	1455.7	1056.6	362.5	2.478	570	1465.7	1466.3	1066.1	1066.4	110	116	1166.6	0-0.00	0.00	1.256	0.0098	0.700	1		
ALPHA BETA VANE0 VANE1 SHOCK TUBE SELECT 14C S19 L7 J27 E10 U1 M6 G34-2 W8-1 H10-1 N30-1 B5-1 C3																				
X.O 0.001 12.21 15.58 5015 RBC-1E7.RCC-1s2.1.AB10-1s.5.AB20-1s0.HL0s2.733.HL1s2.726.C80.URS																				
WFR2	MFR100	W2R	W2R-FS	TI2	IDT	IDR	IDC	IDL	PD	PDP										
OUTWARD	0.19789	0.7498	0.7660	3.513	351.26	0.0077	0.0393	0.0331	0.5079	1.0007	1.2611	0.0748								
INBOARD	0.19782	0.7341	0.7502	3.441	34.15	0.0053	0.0430	0.0238	0.5203	1.0001	1.2413	0.0668								
S2S	M2	MA	NSP	TAVG	W2	CPASS	CP2SS	CP3SS												
OUTWARD	0.1447	0.510	0.596	0.8100	0.8195	2.273	0.736	0.768	0.737											
INBOARD	0.1475	0.465	0.000	0.6349	0.8321	2.225														
*** RAMP PRESSURES ***																				
*** CONL INTERNAL PRESSURES ***																				
*** BLC PLENUM ***																				
PL435	PL452	PL473	PL480	PL490	PL500	PL530	PL535	PL545	PL543	PL573										
OUTWARD	0.7085	0.8479	0.7738	0.8357	0.8408	0.7893	0.7815	0.8153	0.6413	0.7775	0.6050									
INBOARD	0.16095	0.6407	0.7612	0.8526	0.8568	0.6111	0.7915	0.8330	0.8728	0.17753	0.8139									
*** FLOWMETER PRESSURE ***																				
*** CONTROL PARAMETERS ***																				
*** INBOARD PT2/PTS ***																				
PL680	PL681	PL682	PL683	PL690	PL691	PL692	PL693	PL702	PL703	PL704	PL700	PL701								
OUTWARD	0.15677	0.5867	0.5868	0.5884	0.4671	0.4662	0.4620	0.4677	0.8960	0.7987	0.7761	1.0010	0.7873							
INBOARD	0.15245	0.5843	0.5841	0.5846	0.4696	0.4664	0.4670	0.4699	0.9646	0.8053	0.7913									
*** OUTBOARD PT2/PTS ***																				
*** INBOARD RMS2 ***																				
RING	22.5256	67.5	112.5	157.5	202.5	247.5	292.5	337.5	22.5	67.5	112.5	157.5	202.5	247.5	292.5	337.5	337.5			
1	1.000	1.000	1.001	1.001	1.001	1.001	1.000	1.000	1.000	1.000	1.001	1.001	1.001	1.001	1.000	1.000	1.000	1.000	1.000	
2	1.002	0.996	1.001	1.002	1.002	0.998	1.001	1.002	1.001	1.000	1.001	1.001	1.001	1.001	1.001	0.997	0.991	1.001	1.001	
3	1.995	0.973	0.952	1.000	1.001	0.970	0.975	0.992	0.999	0.979	0.954	1.001	1.000	1.000	0.997	0.969	0.994	0.994	0.994	
4	0.991	0.952	0.975	0.990	0.989	0.948	0.936	0.949	0.961	0.942	0.958	0.990	0.969	0.976	0.945	0.956	0.956	0.956	0.956	
5	0.907	0.929	0.948	0.970	0.944	0.936	0.906	0.923	0.923	0.913	0.941	0.946	0.953	0.963	0.927	0.924	0.924	0.924	0.924	
*** OUTBOARD RMS2 ***																				
RING	22.5256	67.5	112.5	157.5	202.5	247.5	292.5	337.5	22.5	67.5	112.5	157.5	202.5	247.5	292.5	337.5	337.5			
1	1.004	0.904	0.903	0.900	0.903	0.903	0.905	0.903	0.903	0.903	0.900	0.900	0.900	0.903	0.903	0.903	0.903	0.903	0.903	
3	0.909	0.912	0.907	0.904	0.905	0.905	0.909	0.909	0.911	0.900	0.901	0.901	0.901	0.901	0.906	0.914	0.909	0.909	0.909	
5	1.004	0.913	0.913	0.911	0.909	0.911	0.911	0.911	0.913	0.910	0.904	0.904	0.904	0.904	0.911	0.910	0.904	0.904	0.904	
DATA SET 1																				
JTBWARD	0.10980	0.0748	0.0331	0.0393	0.5079	0.0077	1.0007	1.2611	0.9789	0.0022	0.0331	0.9057	1.0016							
I-B-ARD	0.13901	0.0668	0.0238	0.0430	0.8203	0.0053	1.0003	1.2613	0.9782	0.0045	0.0238	0.9129	1.0010							
DATA SET 2																				
JTBWARD	0.10983	0.0748	0.0393	0.0430	0.8452	1.0110	1.2428	0.9789	0.9967	0.0486	0.9057	1.0014								
INBOARD	0.10901	0.0668	0.0880	0.0430	0.8193															
DATA SET 3																				
PSTC1	PSTC2	PSTC3	PSTC4	PSTC5	PSTC6	PSTC7	PSTC8	PSTC9	PSTC10	PSTC11	PSTC12	PSTC13	PSTC14	PSTC15	PSTC16	PSTC17	PSTC18	PSTC19	PSTC20	
7.82	7.131	26.95	0.00	0.00	0.00	0.00	0.00	0.00	0.00	0.00	0.00	15.05	59.40	14.40	14.40	32.80	14.55	14.55	14.55	

THIS PAGE IS BEST QUALITY PRACTICABLE
 FROM COPY FURNISHED TO DDC

*** STEADY STATE ***

PARY POINT PROJECT TEST DATE DAY HR MIN SEC ERCODE MODE SETIDATE WIND-OFF AEDC PROPELLSION WIND TUNNEL
 513 2.441-02A TF419 9/25/76 2691 11 561 15 0 3110/27/76 5024 -1 TRANSONIC 16T

 V ST 0 REX10-6 TT PTA-1 PTH-2 PTA-1 PTH-2 PTA-1 PTH-2 PTA-1 PTH-2 PTA-1 PTH-2 PTA-1 PTH-2 PTA-1 PTH-2 PTA-1 PTH-2
 C.700 1473.1 1060.5 363.8 2.490 569 1471.1 1471.6 1070.4 109 118 1171.9 0-0.00 0.00 1.255 0.0062 0.700 1

 ALPHA BEA VANE0 VANE1 SHOCK TUBE SELECT 14F S19 L7 J27 E10 U1 M6 G34-2 M8-1 H16-1 N30-1 85-1 G3
 X.0 20.000 19.00 15.58 5817 RB-1E7,RC-1E2,AB1E1E,5,AB2E-1E0,HL0E2,7,3,HL1E2,7,2A,CE0,URS

 W2 WFR2 MFR100 W2R W2R-FS T12 IDT IDR IDC IDL PD PDP IDA
 CUTBOARD 0.7287 0.7494 0.7657 3.511 351.10 0.076 0.0973 0.0390 0.0330 0.5045 1.0006 1.2613 0.0744
 INBOARD 0.9781 0.7334 0.7498 3.438 343.82 0.0053 0.0901 0.0343 0.0236 0.5204 1.0001 1.2613 0.0667

 W25 W2 WA NSP JAVG W2 CPASS CP255 CP355
 CUTBOARD 0.546 0.511 0.596 0.2102 0.8189 2.280 0.736 0.768 0.737
 INBOARD 0.474 0.487 0.000 0.8349 0.8318 2.232

*** RAMP PRESSURES ***

PL435 PL450 PL470 PL480 PL490 PL020 PL030 PL035 PL045 PL543 PL573
 0.7991 0.8478 0.7737 0.8381 0.8405 0.7889 0.7812 0.8149 0.8650 0.7773 0.8039
 0.5098 0.8403 0.7806 0.8522 0.8566 0.8102 0.7908 0.8331 0.8739 0.7751 0.8158

*** FLOWMETER PRESSURE ***

PL680 PL681 PL682 PL683 PL690 PL691 PL692 PL693 PL702 PL703 PL704 PL700 PL701
 0.5459 0.5853 0.5843 0.5856 0.4619 0.4619 0.4586 0.4643 0.9854 0.7983 0.7759 1.0008 0.7870
 0.2319 0.5810 0.5812 0.5824 0.4625 0.4625 0.4634 0.4664 0.9640 0.8048 0.7908

*** OUTBOARD PT2/PT0 ***

RING 22-5DEG 67.5 112.5 157.5 202.5 247.5 292.5 337.5 22.5 67.5 112.5 157.5 202.5 247.5 292.5 337.5
 1 1.000 1.000 1.001 1.001 1.001 1.001 1.001 1.000 1.000 1.000 1.001 1.001 1.001 1.000 1.000 1.001
 2 1.000 0.995 1.000 1.001 1.000 1.000 1.000 1.000 1.000 1.000 1.000 1.000 1.000 1.000 1.000 1.000
 3 0.995 0.973 0.991 1.000 1.001 0.999 0.999 0.999 0.999 0.999 0.999 0.999 0.999 0.999 0.999 0.999
 4 0.991 0.952 0.974 0.991 0.991 0.991 0.991 0.991 0.991 0.991 0.991 0.991 0.991 0.991 0.991 0.991
 5 0.967 0.929 0.948 0.971 0.944 0.936 0.906 0.923 0.923 0.941 0.941 0.946 0.952 0.962 0.928 0.924

*** CUTBOARD RMS2 ***

RING 22-5DEG 67.5 112.5 157.5 202.5 247.5 292.5 337.5 22.5 67.5 112.5 157.5 202.5 247.5 292.5 337.5
 1 0.004 0.504 0.003 0.000 0.003 0.003 0.003 0.003 0.003 0.000 0.000 0.000 0.003 0.003 0.003 0.001
 2 0.009 0.012 0.007 0.004 0.005 0.014 0.009 0.011 0.006 0.011 0.000 0.000 0.001 0.001 0.008 0.008
 3 0.004 0.012 0.013 0.013 0.013 0.011 0.009 0.011 0.004 0.011 0.004 0.004 0.004 0.004 0.011 0.011
 4 0.004 0.012 0.013 0.013 0.013 0.011 0.009 0.011 0.004 0.011 0.004 0.004 0.004 0.004 0.011 0.011
 5 0.004 0.012 0.013 0.013 0.013 0.011 0.009 0.011 0.004 0.011 0.004 0.004 0.004 0.004 0.011 0.011

CATA SET 2

CUTBOARD 0.973 0.074 0.0330 0.0330 0.5245 1.0006 1.2613 0.9787 0.0022 0.0330 0.9058 1.0010
 INBOARD 0.9901 0.0667 0.0236 0.0430 0.5204 0.8253 1.0001 0.9781 0.0047 0.0236 0.9129 1.0010
 CATA SET 2
 CUTBOARD 0.973 0.074 0.0330 0.0330 0.5245 1.0006 1.2613 0.9787 0.0022 0.0330 0.9058 1.0010
 INBOARD 0.9901 0.0667 0.0236 0.0430 0.5204 0.8253 1.0001 0.9781 0.0047 0.0236 0.9129 1.0010

PSTCE1 PSTCE2 PSTCE3 PSTCD1 PSTCD2 PSTCD3 PSTC11 PSTC12 PSTC13 PSTRD1 PSTRD2 PSTRD3 PSTRI1 PSTRI2 PSTRI3
 7.85 7.39 7.31 0.00 0.00 0.00 0.00 0.00 0.00 7.55 69.70 14.40 7.50 39.40

AD-A065 388

KAMAN AVIDYNE BURLINGTON MASS
WIND-TUNNEL SHOCK-TUBE SIMULATION AND EVALUATION OF BLAST EFFEC--ETC(U)
MAR 78 J R RUETENIK, R F SMILEY

F/G 21/5

DNA001-76-C-0107

UNCLASSIFIED

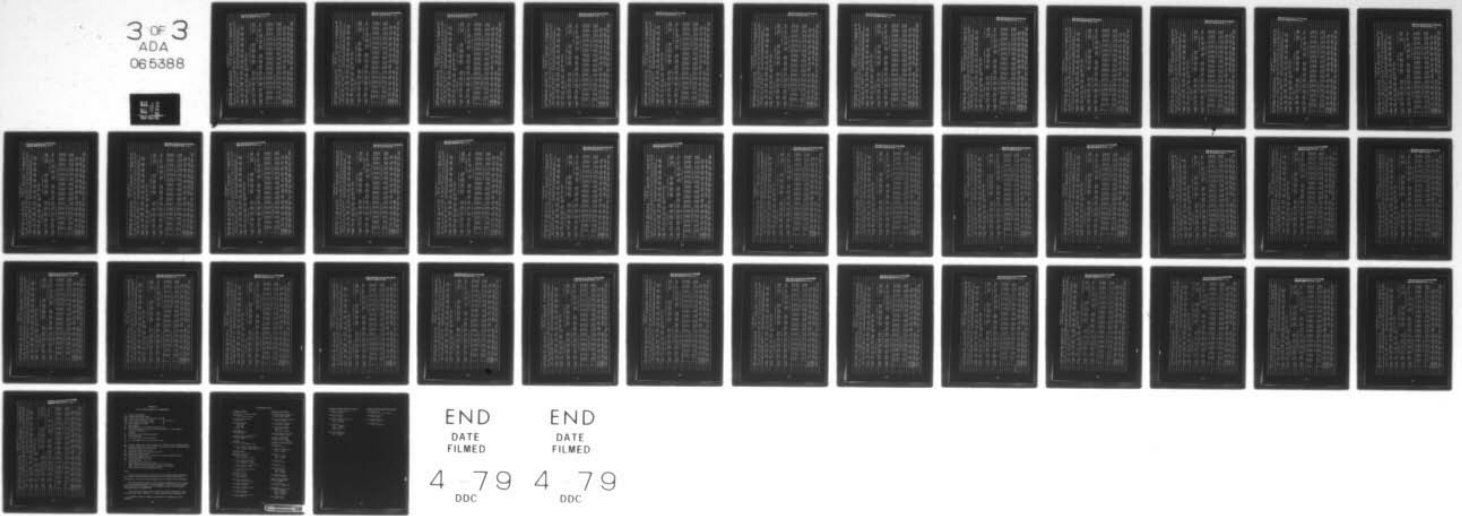
KA-TR-147

DNA-4590F

NL

3 OF 3
ADA
065388

ALL
OUT



END
DATE
FILMED

4 79
DDC

END
DATE
FILMED

4 79
DDC

*** STEADY STATE ***

PART	POINT	PROJECT	TEST	DATE	DAY	HR	MIN	SEC	ERCODE	MODE	SETDATE	WIND-OFF	AEDC	PROPULSION	WIND	TUNNEL
518	2	PLAT-D2A	YF419	9/25/76	2621	51	41	14	0	0	31102277A	5167	-1	TRANSONIC	167	
M	PT	P	0	REX10-6	TT	PTA-1	PTB-2	PCA-1	PCB-2	ITA-1	JTB-0	PTI	MCN	WAE	HAN	TPR
0.700	148.1	1758.3	363.1	2.484	569	1466.1	1468.5	1067.9	1068.2	110	117	1167.7	0-0.00	0.00	1.257	0.0062
0.700	1	1	1	1	1	1	1	1	1	1	1	1	1	1	1	1
ALPHA	BETA	VANE0	VANE1	SHOCK	TUBE	SELECT										
1.0	0.000	19.01	15.25	5017												
RBC=187,RC0=182,1,AR10=185,5,AB20=180,HL02=733,HL12=726,CR0,URS																
R2	MFR100	MFR100	MFR100	MFR100	MFR100	MFR100	MFR100	MFR100	MFR100	MFR100	MFR100	MFR100	MFR100	MFR100	MFR100	MFR100
0.9795	0.7430	0.7586	3.478	347.83	0.0076	0.0962	0.0387	0.0323	0.4983	1.0004	1.2617	0.0732	0.0000	0.0000	0.0000	0.0000
0.9780	0.7318	0.7483	3.431	343.11	0.0067	0.0904	0.0432	0.0238	0.5225	1.0008	1.2606	0.0670	0.0000	0.0000	0.0000	0.0000
ALPHA BETA VANE0 VANE1 SHOCK TUBE SELECT I4C S19 L7 J27 E10 U1 M6 G34-2 W8-1 H10-1 N30-1 B5-1 C3																
RBC=187,RC0=182,1,AR10=185,5,AB20=180,HL02=733,HL12=726,CR0,URS																
J25	M2	M4	MSP	TAVG	M2	CP155	CP255	CP355								
0.491	0.506	0.594	0.6115	0.8226	2.256	0.736	0.768	0.737								
0.473	0.488	0.600	0.6346	0.8312	2.222											
*** RAMP PRESSURES ***																
PL435	PL450	PL470	PL480	PL490	PL020	PL030	PL035	PL045	PL543	PL573						
0.6715	0.8495	0.7786	0.8389	0.8432	0.7929	0.7873	0.8185	0.8635	0.7771	0.8096						
0.8095	0.8407	0.7795	0.8511	0.8560	0.8099	0.7898	0.8325	0.8723	0.7748	0.8127						
*** CONL INTERNAL PRESSURES ***																
PL690	PL681	PL682	PL683	PL690	PL691	PL692	PL693	PL702	PL703	PL704	PL700	PL701				
0.5533	0.5533	0.5532	0.5542	0.5198	0.4209	0.4167	0.4177	0.9896	0.8030	0.7802	1.0000	0.7870				
0.5531	0.5530	0.5506	0.5504	0.4217	0.4192	0.4205	0.4228	0.9640	0.8045	0.7899						
*** FLOWMETER PRESSURE ***																
RING 22-50EG	67.5	112.5	157.5	202.5	247.5	292.5	337.5	22.5	67.5	112.5	157.5	202.5	247.5	292.5	337.5	
1	1.001	1.000	1.001	1.001	1.001	1.001	1.001	1.001	1.001	1.001	1.001	1.001	1.001	1.001	1.001	
2	1.001	0.997	1.001	1.001	1.001	1.001	1.001	1.001	1.001	1.001	1.001	1.001	1.001	1.001	1.001	
3	0.996	0.977	0.993	1.000	1.001	0.969	0.978	0.999	0.979	0.994	1.000	1.000	0.987	0.969	0.994	
4	0.992	0.955	0.977	0.987	0.989	0.949	0.938	0.950	0.941	0.941	0.957	0.991	0.987	0.945	0.957	
5	0.963	0.932	0.950	0.963	0.945	0.937	0.908	0.924	0.923	0.941	0.946	0.951	0.962	0.927	0.924	
*** OUTBOARD PT2/PTC ***																
RING 22-50EG	67.5	112.5	157.5	202.5	247.5	292.5	337.5	22.5	67.5	112.5	157.5	202.5	247.5	292.5	337.5	
1	0.004	0.003	0.000	0.003	0.003	0.003	0.003	0.003	0.003	0.000	-1.000	0.003	0.003	0.003	0.003	
2	0.041	0.012	0.007	0.004	0.004	0.014	0.009	0.011	0.008	0.011	0.000	0.001	0.001	0.008	0.015	0.009
3	0.004	0.012	0.012	0.014	0.011	0.009	0.011	0.013	-1.000	0.010	0.009	0.009	0.012	0.011	0.010	0.012
*** INBOARD RMS2 ***																
DATA SET 1	IDT	IDA	IDC	IDR	IDL	T12	PD	PDP	R2	IDC12	JDC45	PMIN	PHAX			
	0.0962	0.0732	0.0323	0.0387	0.4983	0.0076	1.0004	1.2617	0.9795	0.0019	0.0323	0.9078	1.0021			
	0.0904	0.0670	0.0238	0.0432	0.5225	0.0067	1.0009	1.2606	0.9780	0.0044	0.0238	0.9125	1.0009			
DATA SET 2																
	0.0962	0.0732	0.0945	0.0387	0.8272	1.0118	1.2420	0.9780	0.0092	0.0385	0.9125	1.0009				
	0.0904	0.0670	0.0892	0.0432	0.8226											
*** CONTROL PARAMETERS ***																
PSTCE1	PSTCE2	PSTCE3	PSTCD1	PSTCD2	PSTCD3	PSTC11	PSTC12	PSTC13	PSTRD1	PSTRD2	PSTRD3	PSTR11	PSTR12	PSTR13		
7.87	7.54	7.23	0.00	0.00	0.00	0.00	0.00	0.00	14.20	7.50	101.85	14.10	7.50	54.00		

THIS PAGE IS BEST QUALITY PRACTICABLE FROM COPY FURNISHED TO DDC

THIS PAGE IS BEST QUALITY PRACTICABLE
FROM COPY FURNISHED TO DDC

*** STEADY STATE ***

PART POINT PROJECT TEST DATE DAY HR MIN SEC ERGODE MODE SETID DATE WIND-OFF AEDC PROPULSION WIND TUNNEL													
519 2 P41-02A F419 9/25/76 2681 51 151 33 0 0 3130/2776 5167 -1 TRANSONIC 167													
W PI 0 0 REX10-6 TT PTA-1 PTR-2 PCA-1 PCR-2 TTA-1 ITB-0 PTI CN WAE MAW TPR MAWHT MB SCHED													
3.699 140.8 1059.2 362.5 2.482 569 1468.2 1468.8 1068.7 1069.0 110 117 1170.3 0-0.00 0.00 1.254 0.0089 0.700 1													
ALPHA BETA VANE VANE: SHOCK TUBE SELECT 140 S19 L7 J27 E10 U1 M6 G34-2 M0-1 H16-1 N30-1 B5-1 C3													
3.0 -2.200 19.01 15.55 5020 RB-1E7,RC0-1R2.1,AB10-1R,5,AB20-JE0,HLCR2.733,HLI2.726,CES,UPS													
R2	WFR2	MFR100	W2R	W2R-FS	J12	ID1	IDR	IDC	IDL	PD	PDP	IDA	
MUTEWARD	0.9793	0.7444	0.7604	3.484	348.45	0.0952	0.0383	0.0325	0.4955	1.0003	1.2619	0.0732	
INBOARD	0.9778	0.7339	0.7505	3.440	343.95	0.0967	0.0909	0.0431	0.0241	0.5227	1.0008	1.2606	
M2S	M2	MA	NSP	JAVG	M2	CP1SS	CP2SS	CP3SS					
MUTEWARD	0.492	0.505	0.593	0.8318	0.8227	2.259	0.736	0.768	0.737				
INBOARD	0.474	0.486	0.000	0.8349	0.8317	2.227							
*** 3AMP PRESSURES ***													
PL435	PL452	PL470	PL480	PL490	PL020	PL030	PL035	PL045	PL543	PL573			
MUTEWARD	0.8031	0.6493	0.7721	0.8383	0.7927	0.7871	0.8181	0.8637	0.7774	0.6095			
INBOARD	0.8078	0.6405	0.7796	0.8559	0.8100	0.7897	0.8330	0.8748	0.7750	0.6127			
*** FLOWMETER PRESSURE ***													
PL680	PL681	PL682	PL683	PL690	PL691	PL692	PL693	PL702	PL703	PL704	PL700	PL731	
MUTEWARD	0.5476	0.5472	0.5468	0.5474	0.4304	0.4057	0.4069	0.9690	0.8028	0.7603	1.0000	0.7883	
INBOARD	0.5443	0.5448	0.5443	0.5440	0.4305	0.4097	0.4119	0.9635	0.8045	0.7902			
*** INBOARD PT2/PT0 ***													
RI-0	22.5 DEG	47.5	112.5	157.5	202.5	247.5	292.5	337.5	22.5	67.5	112.5	157.5	
1	1.000	1.000	1.000	1.000	1.000	1.000	1.000	1.000	1.000	1.000	1.000	1.000	
2	1.000	0.995	0.999	1.000	0.996	0.999	1.000	1.000	1.000	1.000	1.000	1.000	
3	1.000	0.978	0.993	1.000	0.970	0.976	0.992	0.999	0.978	0.994	1.000	1.000	
4	1.000	0.954	0.977	0.988	0.959	0.937	0.950	0.962	0.941	0.957	0.977	0.945	
5	0.968	0.932	0.950	0.969	0.945	0.937	0.907	0.924	0.923	0.941	0.946	0.962	
*** INBOARD RMS2 ***													
RI-0	22.5 DEG	47.5	112.5	157.5	202.5	247.5	292.5	337.5	22.5	67.5	112.5	157.5	
1	1.000	1.000	1.000	1.000	1.000	1.000	1.000	1.000	1.000	1.000	1.000	1.000	
2	1.000	0.995	0.999	1.000	0.996	0.999	1.000	1.000	1.000	1.000	1.000	1.000	
3	1.000	0.978	0.993	1.000	0.970	0.976	0.992	0.999	0.978	0.994	1.000	1.000	
4	1.000	0.954	0.977	0.988	0.959	0.937	0.950	0.962	0.941	0.957	0.977	0.945	
5	0.968	0.932	0.950	0.969	0.945	0.937	0.907	0.924	0.923	0.941	0.946	0.962	
*** OUTBOARD RMS2 ***													
RI-0	22.5 DEG	47.5	112.5	157.5	202.5	247.5	292.5	337.5	22.5	67.5	112.5	157.5	
1	1.000	0.995	0.999	1.000	0.996	0.999	1.000	1.000	1.000	1.000	1.000	1.000	
2	1.000	0.978	0.993	1.000	0.970	0.976	0.992	0.999	0.978	0.994	1.000	1.000	
3	1.000	0.954	0.977	0.988	0.959	0.937	0.950	0.962	0.941	0.957	0.977	0.945	
4	1.000	0.932	0.950	0.969	0.945	0.937	0.907	0.924	0.923	0.941	0.946	0.962	
*** INBOARD RMS2 ***													
DATA SET 1	ID1	IDC	IDR	IDL	J12	PD	PDP	R2	IDC12	IDC45	PMIN	PMAX	
MUTEWARD	0.0952	0.0732	0.0325	0.0383	0.4955	0.0076	1.0003	1.2619	0.9790	0.0036	0.0325	0.9074	
INBOARD	0.0902	0.0671	0.0241	0.0431	0.0227	0.0067	1.0008	1.2606	0.9779	0.0048	0.0241	0.9122	
DATA SET 2													
MUTEWARD	0.0952	0.0732	0.0325	0.0383	0.4955	0.0076	1.0003	1.2619	0.9790	0.0036	0.0325	0.9074	
INBOARD	0.0902	0.0671	0.0241	0.0431	0.0227	0.0067	1.0008	1.2606	0.9779	0.0048	0.0241	0.9122	
DATA SET 3													
MUTEWARD	0.0952	0.0732	0.0325	0.0383	0.4955	0.0076	1.0003	1.2619	0.9790	0.0036	0.0325	0.9074	
INBOARD	0.0902	0.0671	0.0241	0.0431	0.0227	0.0067	1.0008	1.2606	0.9779	0.0048	0.0241	0.9122	
DATA SET 4													
MUTEWARD	0.0952	0.0732	0.0325	0.0383	0.4955	0.0076	1.0003	1.2619	0.9790	0.0036	0.0325	0.9074	
INBOARD	0.0902	0.0671	0.0241	0.0431	0.0227	0.0067	1.0008	1.2606	0.9779	0.0048	0.0241	0.9122	
DATA SET 5													
MUTEWARD	0.0952	0.0732	0.0325	0.0383	0.4955	0.0076	1.0003	1.2619	0.9790	0.0036	0.0325	0.9074	
INBOARD	0.0902	0.0671	0.0241	0.0431	0.0227	0.0067	1.0008	1.2606	0.9779	0.0048	0.0241	0.9122	
DATA SET 6													
MUTEWARD	0.0952	0.0732	0.0325	0.0383	0.4955	0.0076	1.0003	1.2619	0.9790	0.0036	0.0325	0.9074	
INBOARD	0.0902	0.0671	0.0241	0.0431	0.0227	0.0067	1.0008	1.2606	0.9779	0.0048	0.0241	0.9122	
DATA SET 7													
MUTEWARD	0.0952	0.0732	0.0325	0.0383	0.4955	0.0076	1.0003	1.2619	0.9790	0.0036	0.0325	0.9074	
INBOARD	0.0902	0.0671	0.0241	0.0431	0.0227	0.0067	1.0008	1.2606	0.9779	0.0048	0.0241	0.9122	
DATA SET 8													
MUTEWARD	0.0952	0.0732	0.0325	0.0383	0.4955	0.0076	1.0003	1.2619	0.9790	0.0036	0.0325	0.9074	
INBOARD	0.0902	0.0671	0.0241	0.0431	0.0227	0.0067	1.0008	1.2606	0.9779	0.0048	0.0241	0.9122	
DATA SET 9													
MUTEWARD	0.0952	0.0732	0.0325	0.0383	0.4955	0.0076	1.0003	1.2619	0.9790	0.0036	0.0325	0.9074	
INBOARD	0.0902	0.0671	0.0241	0.0431	0.0227	0.0067	1.0008	1.2606	0.9779	0.0048	0.0241	0.9122	
DATA SET 10													
MUTEWARD	0.0952	0.0732	0.0325	0.0383	0.4955	0.0076	1.0003	1.2619	0.9790	0.0036	0.0325	0.9074	
INBOARD	0.0902	0.0671	0.0241	0.0431	0.0227	0.0067	1.0008	1.2606	0.9779	0.0048	0.0241	0.9122	

*** STEADY STATE ***																			
PART POINT PROJECT TEST	DATE	DAY HP	MIN SEC	ERCODE	MODE	SET/DATE	WIND-OFF	AEDC	PROPULSION	WIND TUNNEL									
52A	2-2411-02A	IF419	9/25/76	2491	71	71	37	0	3110/27/76	524/-1				TRANSONIC	16T				

REX10-6 TT PTA-1 PTB-2 PCA-1 PCB-2 JTA-1 JTB-0 PTI MCH WAE MAH TPR WJMT MB SCHED																			
730	1463	4	1.50,2	363,4	2,489	569	1469,4	1470,0	1048,6	1009,1	109	114	1170,2	0-0,00	0,00	1,256	0,0078	0,700	1
ALPHA BETA VANE0 VANE1 SHOCK TUBE SELECT																			
1,0	2,502	18,99	45,53	5317	140	S19	L7	J27	E10	U1	M6	G34-2	W8-1	M16-1	N3U-1	85-1	G3		
R82-187,R80-182,1,AB10-18,5,AB26-18,0,HL082,733,HL142,726,CS0,JWS																			
R2	WFR2	MFR100	M28	M2R-FS	I12	IDT	IDR	IDC	IDL	PD	PDR	IDA							
PL70	0,9791	0,7444	0,7802	3,486	348,61	0,0076	0,0942	0,0382	0,0318	0,4923	1,0001	1,2621	0,0723						
PL30	0,9778	0,7342	0,7508	3,443	344,28	0,0065	0,0907	0,0432	0,0241	0,5234	1,000A	1,2606	0,0673						
Z2S	M2	W2	M2P	W2	CP1SS	CP2SS	CP3SS												
PL10	0,492	0,502	0,593	0,8113	0,8241	2,263	0,756	0,768	0,737										
PL20	0,475	0,467	0,600	0,8352	0,8315	2,232													
*** RAMP PRESSURES ***																			
*** COHL INTERNAL PRESSURES ***																			
PL435	PL450	PL470	PL480	PL490	PL020	PL030	PL035	PL045											
PL10	0,612	0,6494	0,7754	0,8392	0,8434	0,7926	0,7871	0,8182	0,6632										
PL20	0,6082	0,6436	0,7793	0,8510	0,8556	0,8094	0,7893	0,8322	0,8733										
*** FLOWMETER PRESSURE ***																			
PL690	PL661	PL682	PL683	PL691	PL692	PL693	PL702	PL703	PL704	PL700	PL701								
PL10	0,5591	0,5536	0,5595	0,5592	0,4275	0,4282	0,4238	0,4250	0,9893	0,8026	0,7600	0,9993	0,7875						
PL20	0,5570	0,5563	0,5566	0,5563	0,4267	0,4266	0,4279	0,4303	0,9833	0,8045	0,7896								
*** OUTBOARD PT2/PTD ***																			
R1/G	22,5DEC	67,5	112,5	157,5	202,5	247,5	292,5	337,5	377,5	22,5	67,5	112,5	157,5	202,5	247,5	292,5	337,5		
1	1,000	1,000	1,000	1,000	1,000	1,000	1,000	1,000	1,000	1,000	1,000	1,000	1,000	1,000	1,000	1,000	1,000		
2	1,992	0,999	0,999	0,999	0,999	1,000	1,001	1,000	1,001	1,001	1,000	1,000	0,996	0,989	1,000	1,000	0,994		
3	1,996	0,997	0,994	0,999	1,001	0,999	0,977	0,992	0,999	0,978	0,994	1,001	1,000	0,986	0,948	0,994	0,957		
4	1,992	0,995	0,977	0,988	0,989	0,940	0,938	0,950	0,962	0,941	0,957	0,991	0,987	0,972	0,945	0,957	0,922		
5	1,968	0,932	0,950	0,965	0,944	0,937	0,908	0,924	0,922	0,912	0,940	0,947	0,952	0,962	0,927	0,922			
*** OUTBOARD RMS2 ***																			
R1/G	22,5DEC	67,5	112,5	157,5	202,5	247,5	292,5	337,5	377,5	22,5	67,5	112,5	157,5	202,5	247,5	292,5	337,5		
1	2,504	0,003	0,003	0,003	0,003	0,003	0,003	0,003	0,003	0,003	0,003	0,003	0,003	0,003	0,003	0,003	0,003		
3	2,010	0,012	0,007	0,004	0,004	0,004	0,004	0,004	0,004	0,011	0,008	0,011	0,000	0,001	0,003	0,008	0,015		
5	2,024	0,012	0,014	0,011	0,009	0,011	0,013	0,012	0,010	0,009	0,009	0,009	0,009	0,009	0,011	0,011	0,010		
DATA SET 1																			
PL20	0,0942	0,0723	0,0318	0,0362	0,0432	0,0432	0,0432	0,0432	0,0432	0,0432	0,0432	0,0432	0,0432	0,0432	0,0432	0,0432	0,0432		
PL30	0,0907	0,0673	0,0241	0,0432	0,0432	0,0432	0,0432	0,0432	0,0432	0,0432	0,0432	0,0432	0,0432	0,0432	0,0432	0,0432	0,0432		
DATA SET 2																			
PL30	0,0942	0,0723	0,0318	0,0362	0,0432	0,0432	0,0432	0,0432	0,0432	0,0432	0,0432	0,0432	0,0432	0,0432	0,0432	0,0432	0,0432		
PL30	0,0907	0,0673	0,0241	0,0432	0,0432	0,0432	0,0432	0,0432	0,0432	0,0432	0,0432	0,0432	0,0432	0,0432	0,0432	0,0432	0,0432		
*** INBOARD PT2/PTD ***																			
PL20	0,0942	0,0723	0,0318	0,0362	0,0432	0,0432	0,0432	0,0432	0,0432	0,0432	0,0432	0,0432	0,0432	0,0432	0,0432	0,0432	0,0432		
PL30	0,0907	0,0673	0,0241	0,0432	0,0432	0,0432	0,0432	0,0432	0,0432	0,0432	0,0432	0,0432	0,0432	0,0432	0,0432	0,0432	0,0432		
*** INBOARD RMS2 ***																			
PL20	0,0942	0,0723	0,0318	0,0362	0,0432	0,0432	0,0432	0,0432	0,0432	0,0432	0,0432	0,0432	0,0432	0,0432	0,0432	0,0432	0,0432		
PL30	0,0907	0,0673	0,0241	0,0432	0,0432	0,0432	0,0432	0,0432	0,0432	0,0432	0,0432	0,0432	0,0432	0,0432	0,0432	0,0432	0,0432		
*** CONTROL PARAMETERS ***																			
PL543	PL573																		
0,7772	0,8078																		
0,7750	0,8122																		

THIS PAGE IS BEST QUALITY PRACTICABLE FROM COPY FURNISHED TO DOC

THIS PAGE IS BEST QUALITY PRACTICABLE
FROM COPY FURNISHED TO DDC

*** STEADY STATE ***														
PART POINT	PROJECT	TEST	DATE	DAY	HR	MIN	SEC	ERCODE	MODE	SET/DATE	WIND-OFF	AEDC	PROPULSION	WIND TUNNEL
527	2-6411-02A	TF419	9/25/78	2681	71	341	34	0	0	3110/27/78	524/ -3			TRANSONIC 147
*** RAMP PRESSURES ***														
*** CONVL INTERNAL PRESSURES ***														
*** BLC PLENUM ***														
*** FLOWMETER PRESSURE ***														
*** CONTROL PARAMETERS ***														
*** INBOARD PT2/PTO ***														
*** OUTBOARD PT2/PTO ***														
*** INBOARD RMS2 ***														
*** OUTBOARD RMS2 ***														
DATA SET 1														
DATA SET 2														
PSTCE1 PSTCE2 PSTCE3 PSTC01 PSTC02 PSTC03 PSTC11 PSTC12 PSTC13 PSTC21 PSTC22 PSTC23 PSTC31 PSTC32 PSTC33 PSTI01 PSTI02 PSTI03 PSTI11 PSTI12 PSTI13 PSTI21 PSTI22 PSTI23 PSTI31 PSTI32 PSTI33														

THIS PAGE IS BEST QUALITY PRACTICABLE
FROM COPY FURNISHED TO DDC

*** STEADY STATE ***																			
PART PROJ	TEST	DATE	DAY	HR	MIN	SEC	ENCODE	MODE	SETDATE	WIND-OFF	AEDC	PROCPULSION	WIND TUNNEL						
544	1	27/76	27	12	1	231	55	0	311022/76	5427	-2	IRANSONIC	18T						
*** CONTROL PARAMETERS ***																			
U	PT	P	0	REX10-6	JT	PJA-1	PTR-2	PCA-1	PCB-2	TJA-1	TTB-0	PTI	NCN	WAE	HAW	TYP	WAW/HT	MB	SCHED
0.647	1693.6	1059.3	531.9	3.169	569	1693.6	1694.4	1072.5	1072.7	110	110	1363.1	0-0.00	0.00	0.00	1.261	0.0261	0.850	1
*** FLOWMETER PRESSURE ***																			
ALPHA BETA VAVEC VANEI SHOCK TUBE SELECT 140 519 L7 J27 E10 U1 M6 G34-2 W8-1 H16-1 N30-1 B5-1 C3																			
3.0	2.232	18.49	-4.33	5015	RBC	-167.8CC	-162.1	AB10-1	5.5	AB20-1	6.0	HL02-2	333.0	HL12-726	630.0	UBS			
*** RAMP PRESSURES ***																			
R2	MFR2	MFR100	H2R	H2R-FS	T12	JDY	IDR	IDC	IDL	PD	PDP	IDA							
PUTWARD	0.9795	0.6919	0.7062	3.469	346.90	0.0080	0.1003	0.0377	0.0375	0.5121	1.0010	1.2607	0.0773						
INBOARD	0.19805	0.6919	0.7057	3.466	346.62	0.0022	0.0951	0.0436	0.0313	0.5470	0.9996	1.2614	0.0763						
*** INTERNAL PRESSURES ***																			
H2S	H2	MA	NSP	IAVG	W2	CPASS	CP2SS	CP3SS											
PUTWARD	0.479	0.516	0.688	0.7965	0.6170	2.596	0.650	0.698	0.650										
INBOARD	0.479	0.507	0.000	0.6018	0.6225	2.596													
*** BLC PLENUM ***																			
PL435	PL450	PL470	PL480	PL490	PL022	PL070	PL035	PL045	PL543	PL523									
PUTWARD	0.7815	0.8381	0.7687	0.8336	0.8373	0.7815	0.7788	0.8134	0.8614	0.7433	0.7965								
INBOARD	0.7867	0.8288	0.7654	0.8419	0.8484	0.7922	0.7759	0.8210	0.8669	0.7348	0.7991								
*** CONTROL PARAMETERS ***																			
*** INBOARD PT2/PTC ***																			
PL650	PL621	PL682	PL683	PL690	PL691	PL692	PL693	PL702	PL703	PL704	PL700	PL701							
PUTWARD	0.4972	0.4955	0.4968	0.4973	0.5079	0.5094	0.2947	0.2989	0.6983	0.7951	0.7714	0.9996	0.7284						
INBOARD	0.4973	0.4985	0.4959	0.5017	0.5000	0.5028	0.5024												
*** OUTBOARD PT2/PTC ***																			
RING	22.6566	67.5	112.5	157.5	202.5	247.5	292.5	337.5	221.5	67.5	112.5	157.5	202.5	247.5	292.5	247.5	292.5	337.5	
1	1.001	1.001	1.001	1.001	1.001	1.001	1.001	1.001	1.001	1.001	1.001	1.001	1.001	1.001	1.001	1.001	1.001	1.001	
2	1.000	1.000	1.001	1.001	1.001	1.001	1.001	1.001	1.001	1.001	1.001	1.001	1.001	1.001	1.001	1.001	1.001	1.001	
3	1.000	0.990	1.001	0.992	1.001	0.983	0.970	0.987	0.997	0.977	0.995	1.001	1.001	1.001	1.001	1.001	0.986	0.999	
4	1.005	0.973	1.000	0.961	0.965	0.944	0.933	0.946	0.957	0.937	0.957	0.986	0.997	0.996	0.957	0.957	0.961	0.961	
5	0.975	0.953	0.969	0.939	0.941	0.936	0.904	0.923	0.919	0.908	0.939	0.940	0.959	0.974	0.935	0.935	0.928	0.928	
*** INBOARD RMS2 ***																			
RING	22.6566	67.5	112.5	157.5	202.5	247.5	292.5	337.5	221.5	67.5	112.5	157.5	202.5	247.5	292.5	292.5	337.5		
1	1.004	0.004	0.003	0.003	0.004	0.004	0.004	0.004	0.003	0.001	0.001	0.001	0.001	0.001	0.001	0.001	0.001		
2	1.004	0.004	0.003	0.003	0.003	0.003	0.003	0.003	0.003	0.003	0.003	0.003	0.002	0.002	0.001	0.001	0.001		
3	1.004	0.004	0.003	0.003	0.003	0.003	0.003	0.003	0.003	0.003	0.003	0.003	0.003	0.003	0.003	0.003	0.003		
4	1.004	0.004	0.003	0.003	0.003	0.003	0.003	0.003	0.003	0.003	0.003	0.003	0.003	0.003	0.003	0.003	0.003		
5	1.004	0.004	0.003	0.003	0.003	0.003	0.003	0.003	0.003	0.003	0.003	0.003	0.003	0.003	0.003	0.003	0.003		
*** OUTBOARD RMS2 ***																			
DATA SET 1																			
PUTWARD	0.1003	0.0773	0.0375	0.0377	0.5121	0.0080	1.0010	1.2607	0.9796	0.0030	0.0030	0.0375	0.9039	1.0022					
INBOARD	0.10951	0.0743	0.0313	0.0345	0.5470	0.0022	0.9996	1.2614	0.9802	0.0003	0.0003	0.0313	0.9077	1.0009					
DATA SET 2																			
PUTWARD	0.1003	0.0773	0.0375	0.0377	0.5121	0.0080	1.0010	1.2607	0.9796	0.0030	0.0030	0.0375	0.9039	1.0022					
INBOARD	0.10951	0.0743	0.0313	0.0345	0.5470	0.0022	0.9996	1.2614	0.9802	0.0003	0.0003	0.0313	0.9077	1.0009					
*** INBOARD RMS2 ***																			
PUTWARD	0.1003	0.0773	0.0375	0.0377	0.5121	0.0080	1.0010	1.2607	0.9796	0.0030	0.0030	0.0375	0.9039	1.0022					
INBOARD	0.10951	0.0743	0.0313	0.0345	0.5470	0.0022	0.9996	1.2614	0.9802	0.0003	0.0003	0.0313	0.9077	1.0009					
*** INBOARD RMS2 ***																			
PUTWARD	0.1003	0.0773	0.0375	0.0377	0.5121	0.0080	1.0010	1.2607	0.9796	0.0030	0.0030	0.0375	0.9039	1.0022					
INBOARD	0.10951	0.0743	0.0313	0.0345	0.5470	0.0022	0.9996	1.2614	0.9802	0.0003	0.0003	0.0313	0.9077	1.0009					

THIS PAGE IS BEST QUALITY PRACTICABLE
FROM COPY FURNISHED TO DDG

*** STEADY STATE ***

PART POINT PROJECT TEST DATE DAY HR MIN SEC ERCODE MODE SET/DATE WIND-OFF AEDC PROPUSSION WIND TUNNEL
545 2 041I-22A JF419 9/27/76 22:21:41 2A 0 0 3:10/27/76 542/ -2 TRANSONIC 167

W PT 0 0 REX10-6 TT PTA-1 P1B-2 PCA-1 PCR-2 JTA-1 TTB-0 PTLNCN HAE HAN TPR MA/WT MB SCHED
0.967 1654.4 1059.5 532.4 3.370 569 1694.4 1694.7 1072.7 1072.9 110 116 1343.0 0-0.00 0.00 1.262 0.0266 0.850 1

ALPHA BETA VANE0 VANE1 SHOCK TUBE SELECT 140 S19 L7 J27 E10 U1 M6 G34-2 W0-1 H16-1 N30-1 85-1 C3
3.0 -0.004 10.49 14.30 5017 RB2-1B7AR2-1R2.1.8B10-1R.2. AR20-1B0.H182.2.33.H182-726.CED.U85

R2 MFR2 MFR100 M2R-F5 T12 IDT IDR IDC IDL PDP JDA
OUTWARD 0.9795 0.6920 0.7064 3.470 347.00 0.0079 0.1002 0.0379 0.0373 0.5131 1.0010 1.2607 0.0772
INBOARD 0.9805 0.6926 0.7064 3.470 346.99 0.0021 0.0933 0.0435 0.0314 0.2371 0.9996 1.2615 0.0742

W25 W2 MA MSP JAV5 W2 CP155 CP255 CP355
OUTWARD 0.479 0.515 0.667 0.7560 0.8176 2.598 0.650 0.698 0.650
INBOARD 0.475 0.507 0.600 0.6021 0.6227 2.800

*** RAMP PRESSURES ***

*** COMB. INTERNAL PRESSURES ***

*** BLC. PLENUM ***

PL435 PL453 PL470 PL480 PL490 PL020 PL030 PL045 PL045 PL543 PL573
OUTWARD 0.741 0.8353 0.7689 0.8337 0.8374 0.7812 0.7785 0.8130 0.8610 0.7428 0.7961
INBOARD 0.7584 0.8285 0.7646 0.8413 0.8476 0.7945 0.7752 0.8224 0.8671 0.7347 0.7983

*** FLOWMETER PRESSURE ***

*** CONTROL PARAMETERS ***

PL680 PL681 PL682 PL683 PL690 PL691 PL692 PL693 PL702 PL703 PL704 PL700 PL701
OUTWARD 0.4931 0.4929 0.4912 0.4939 0.4293 0.2792 0.2686 0.2747 0.9982 0.7946 0.7713 0.9991 0.7284
INBOARD 0.4934 0.4944 0.4926 0.4925 0.42746 0.2733 0.2763 0.2792 0.9905 0.7945 0.7752

*** OUTBOARD P12/P10 ***

*** INBOARD PT2/PTC ***

R1.5 22.5 DEG 67.5 112.5 157.5 202.5 247.5 292.5 337.5 22.5 67.5 112.5 157.5 202.5 247.5 292.5 337.5
1 1.001 1.001 1.001 1.001 1.001 1.001 1.001 1.001 1.001 1.001 1.001 1.001 1.001 1.001 1.001 1.001
2 1.001 1.001 1.001 1.001 1.001 1.001 1.001 1.001 1.001 1.001 1.001 1.001 1.001 1.001 1.001 1.001
3 0.999 0.999 1.001 0.992 1.001 0.993 0.970 0.988 0.997 0.977 1.001 1.001 1.001 1.001 1.001 1.001
4 0.996 0.973 0.999 0.961 0.985 0.944 0.933 0.946 0.957 0.937 0.958 0.986 0.998 0.996 0.957 0.961
5 0.076 0.952 0.969 0.939 0.941 0.936 0.904 0.924 0.919 0.908 0.940 0.940 0.959 0.974 0.935 0.928

*** OUTBOARD RMS2 ***

*** INBOARD RMS2 ***

R1.5 22.5 DEG 67.5 112.5 157.5 202.5 247.5 292.5 337.5 22.5 67.5 112.5 157.5 202.5 247.5 292.5 337.5
1 0.004 0.004 0.003 0.003 0.004 0.004 0.004 0.004 0.001 0.001 0.001 0.001 0.001 0.001 0.001 0.001
3 0.000 0.011 0.004 0.009 0.005 0.015 0.010 0.013 0.000 0.004 0.002 0.001 0.001 0.001 0.001 0.001
5 0.004 0.012 0.013 0.013 0.011 0.009 0.011 0.013 0.004 0.003 0.003 0.003 0.003 0.003 0.003 0.004

DATA SET 1 JDI IDA JDC IDR JDL J12 PD PDP R2 IDC12 IDC45 PMIN PMAX
OUTWARD 0.1002 0.0772 0.0373 0.0379 0.5131 0.0079 1.0010 1.2607 0.9796 0.0030 0.0373 0.9040 1.0022
INBOARD 0.0953 0.0742 0.0314 0.0343 0.2471 0.0021 0.9998 1.2615 0.9905 0.0002 0.0314 0.9077 1.0011

DATA SET 2
OUTWARD 0.1002 0.0772 0.0373 0.0379 0.5131 0.0079 1.0010 1.2607 0.9796 0.0030 0.0373 0.9040 1.0022
INBOARD 0.0953 0.0742 0.0314 0.0343 0.2471 0.0021 0.9998 1.2615 0.9905 0.0002 0.0314 0.9077 1.0011

PSTCE1 PSTCE2 PSTCE3 PSTCD1 PSTCD2 PSTCD3 PSTC11 PSTC12 PSTC13 PSTD1 PSTD2 PSTD3 PSTR11 PSTR12 PSTR13
7.82 7.38 7.37 0.00 0.00 0.00 0.00 0.00 14.55 7.55 113.35 14.55 7.70 61.30

THIS PAGE IS BEST QUALITY PRACTICABLE
FROM COPY FURNISHED TO DDC

*** STEADY STATE ***

PART PRINT PROJECT TEST DATE DAY HR MIN SEC ERCODE MODE SETDATE WIND-OFF AEDC PROPULSION WIND TUNNEL
 564 2 P511-02A JF419 9/27/76 221211 501 52 0 0 311027/7A 542/ -2 TRANSONIC 167

M - PT P Q REX10-6 JI PJA-1 PIB-2 PCA-1 PCB-2 IYA-1 IIB-2 PIJ MCH MAE MAM TPR WAWMT MB SCHED
 C.947 1693.7 1.59.5 531.9 3.168 569 1693.7 1694.0 1072.7 1072.6 110 110 1343.1 0.0.00 0.00 1.261 0.0262 0.850 1

ALPHA BETA VANE0 VANE1 SHOCK TUBE SELECT 14R S19 L7 J27 E10 U1 M6 G34-2 W6-1 M16-1 N30-1 B5-1 C3
 1.0 -J.007 18.49 14.29 5620 RB0-1e7.RCC-1e2.1.AB10-1e.5.AB20-1e0.HL0e2.733.HL1e2.726.Ce0.UBS

R2 MFR2 MFR100 W2R W2R-FS T12 IDT IDR IDC IDL PD PDP JDA
 PUT3ARD 0.9795 0.5936 0.7081 3.478 347.81 0.0780 0.0989 0.0378 0.0374 0.5131 1.0010 1.2606 0.0773
 I.3EARD 0.9795 0.5933 0.7071 3.473 347.31 0.0721 0.0924 0.0437 0.0315 0.5488 0.9996 1.2614 0.0745

M2S M2 MA MSP JAVG W2 CP1SS CR2SS CP3SS
 PUT3ARD 0.481 0.515 0.687 0.7974 0.8172 2.603 0.650 0.698 0.650
 I.3EARD 0.460 0.509 0.000 0.6020 0.9210 2.602

*** CONL INTERNAL PRESSURES *** *** BLC PLENUM ***
 PL435 PL457 PL470 PL480 PL490 PL020 PL030 PL035 PL045 PL543 PL573
 PUT3ARD 0.7913 0.8388 0.7693 0.8342 0.8378 0.7814 0.7784 0.8128 0.8610 0.7426 0.7963
 I.3EARD 0.7565 0.8280 0.7647 0.8415 0.8477 0.7914 0.7748 0.8226 0.8670 0.7345 0.7972

*** FLOWMETER PRESSURE *** *** CONTROL PARAMETERS ***
 PL680 PL681 PL682 PL683 PL690 PL691 PL692 PL693 PL702 PL703 PL704 PL700 PL701
 PUT3ARD 0.4942 0.4937 0.4936 0.4945 0.2810 0.2810 0.2723 0.2766 0.9967 0.7948 0.7711 0.9991 0.7289
 I.3EARD 0.4645 0.4952 0.4928 0.4928 0.2772 0.2760 0.2780 0.2814 0.9907 0.7945 0.7752

*** OUTBOARD PT2/PT0 *** *** INBOARD PT2/PT0 ***
 RING 22.5253 67.5 112.5 157.5 202.5 247.5 292.5 337.5 22.5 67.5 112.5 157.5 202.5 247.5 292.5 337.5
 1 1.001 1.001 1.001 1.001 1.001 1.001 1.001 1.001 1.001 1.001 1.001 1.001 1.001 1.001 1.001 1.001
 2 1.000 1.000 1.001 1.001 1.001 1.001 1.001 1.001 1.001 1.001 1.001 1.001 1.001 1.001 1.001 1.001
 3 0.999 0.991 1.001 1.001 1.001 1.001 1.001 1.001 1.001 1.001 1.001 1.001 1.001 1.001 1.001 1.001
 4 0.995 0.973 0.959 0.962 0.965 0.944 0.933 0.946 0.957 0.937 0.957 0.957 0.987 0.998 0.996 0.957 0.962
 5 0.975 0.952 0.969 0.939 0.941 0.936 0.904 0.923 0.919 0.907 0.940 0.940 0.959 0.974 0.935 0.928

*** OUTBOARD RMS2 *** *** INBOARD RMS2 ***
 RING 22.5060 67.5 112.5 157.5 202.5 247.5 292.5 337.5 22.5 67.5 112.5 157.5 202.5 247.5 292.5 337.5
 1 0.004 0.004 0.003 0.003 0.004 0.004 0.004 0.004 0.001 0.001 0.001 0.001 0.001 0.001 0.001 0.001
 2 1.000 0.011 0.004 0.009 0.005 0.025 0.010 0.013 0.010 0.004 0.004 0.002 0.001 0.001 0.001 0.001 0.001
 3 1.004 0.012 0.013 0.013 0.011 0.009 0.011 0.013 0.011 0.003 0.003 0.003 0.003 0.003 0.003 0.003 0.004
 4 0.999 0.0773 0.0745 0.0951 0.0378 0.0378 0.0378 0.0378 0.0378 0.0378 0.0378 0.0378 0.0378 0.0378 0.0378 0.0378
 5 1.004 0.012 0.013 0.013 0.011 0.009 0.011 0.013 0.011 0.003 0.003 0.003 0.003 0.003 0.003 0.004

DATA SET 1 IDT JDA IDC JDR IDL T12 T12 PDP R2 IDC12 IDC45 PMIN PHAX
 OUT3ARD 0.0949 0.0773 0.0374 0.0378 0.5131 0.0080 1.2606 0.9795 0.0030 0.0374 0.9038 1.0008
 I.3EARD 0.10954 0.0745 0.0315 0.0437 0.5488 0.10021 0.1998 1.2614 0.9805 0.0001 0.0315 0.9075 1.0010
 DATA SET 2
 PUT3ARD 0.0989 0.0773 0.0983 0.0378 0.0749 1.0143 1.2382 0.9795 0.0983 0.0521 0.9038 1.0008
 I.3EARD 0.10954 0.0745 0.0951 0.0437 0.6869 1.0120 1.2404 0.9805 0.0951 0.0467 0.9075 1.0010

PSTCE1 PSTCE3 PSTCE2 PSTC01 PSTC02 PSTC03 PSTC11 PSTC12 PSTC13 PSTRD1 PSTRD2 PSTRD3 PSTRI1 PSTRI2 PSTRI3
 7.34 7.38 7.37 0.00 0.00 0.00 0.00 0.00 0.00 0.00 120.60 7.85 6.55 63.90 7.75 6.40

THIS PAGE IS BEST QUALITY PRACTICALLY
FROM COPY FURNISHED TO DDC

*** STEADY STATE ***
PART PRINT PROJECT TEST DATE DAY HR MIN SEC ERCODE MODE SET/DATE WIND-OFF AEDC PROPUSSION WIND TUNNEL
550 2 2412 022A TE419 9/27/76 2711231 111 24 0 3110/2776 5487 -5 TRANSONIC 161

M OT P C Q REX10-6 TT PTA-1 PTR-2 PCA-1 PCB-2 TPA-1 TTB-0 PTLNCH MAE MAH TPR MAYHT MB SCHED
0.899 1785.6 1058.7 598.9 3.429 569 1788.6 1789.4 1073.2 1073.4 110 110 1449.1 0-0.00 0.00 1.238 0.0391 0.900 1
ALPHA 5-TA VANE9 VANE1 SHOCK TUBE SELECT 140 S19 L7 J27 E10 U1 M6 G34-2 M8-1 M16-1 M30-1 B5-1 C3
3.0 0.238 17.00 12.99 5015 R85-147,REC-102,1,AB10-1R,5,AB2R-1E0,H1052,733,H112,726,EO0,UES

R2 WFR2 WFR100 WFR W2R W2R-FS T12 IDT IDR IDC IDL PDP IDA
OUTBOARD 0.9908 0.6686 0.7021 3.491 349.14 0.078 0.0356 0.0371 0.4857 1.0000 1.2624 0.0742
INBOARD 0.9622 0.5990 0.7117 3.539 353.92 0.023 0.0929 0.0414 0.0333 0.5315 0.9991 1.2622 0.0736
OUTBOARD 0.453 0.598 0.711 0.8067 0.8277 2.762 0.620 0.676 0.621
INBOARD 0.491 0.502 0.500 0.9006 0.8269 2.804

*** RAMP PRESSURES ***
PL435 PL450 PL470 PL482 PL492 PL020 PL030 PL035 PL045 PL543 PL573
0.7839 0.8420 0.7807 0.8419 0.8443 0.7841 0.7900 0.8211 0.8721 0.7384 0.8017
INBOARD 0.7862 0.7856 0.7862 0.7873 0.7856 0.7952 0.7804 0.8268 0.8745 0.7266 0.7999

*** FLOWMETER PRESSURE ***
PL680 PL681 PL682 PL683 PL690 PL691 PL692 PL693 PL702 PL703 PL704 PL705 PL701
OUTBOARD 0.7847 0.7844 0.7837 0.7847 0.7870 0.7877 0.7862 0.7874 0.9883 0.8053 0.7824 0.9987 0.7128
INBOARD 0.7862 0.7856 0.7862 0.7873 0.7856 0.7952 0.7804 0.8268 0.8745 0.9989 0.7998 0.7804

*** INBOARD PT2/PT0 ***
R1-G 221550 67.5 112.5 157.5 202.5 247.5 292.5 337.5 22.5 67.5 112.5 157.5 202.5 247.5 292.5 337.5
1 1.001 1.001 1.001 1.001 1.001 1.001 1.001 1.001 1.001 1.001 1.001 1.001 1.001 1.001 1.001
2 1.022 1.003 1.001 1.001 1.001 0.994 0.999 1.001 1.001 1.001 1.001 1.001 1.001 1.001 1.001
3 1.030 0.995 1.001 0.988 1.002 0.984 0.989 0.986 0.997 0.977 0.996 1.001 1.001 1.001 0.992 1.000
4 1.096 0.991 1.000 0.961 0.984 0.986 0.935 0.948 0.957 0.939 0.959 0.985 0.998 0.999 0.969 0.973
5 1.077 0.958 0.972 0.948 0.943 0.939 0.908 0.926 0.921 0.910 0.942 0.940 0.961 0.980 0.948 0.930

*** OUTBOARD PT2/PT0 ***
R1-G 221550 67.5 112.5 157.5 202.5 247.5 292.5 337.5 22.5 67.5 112.5 157.5 202.5 247.5 292.5 337.5
1 1.001 1.001 1.001 1.001 1.001 1.001 1.001 1.001 1.001 1.001 1.001 1.001 1.001 1.001 1.001
2 1.022 1.003 1.001 1.001 1.001 0.994 0.999 1.001 1.001 1.001 1.001 1.001 1.001 1.001 1.001
3 1.030 0.995 1.001 0.988 1.002 0.984 0.989 0.986 0.997 0.977 0.996 1.001 1.001 1.001 0.992 1.000
4 1.096 0.991 1.000 0.961 0.984 0.986 0.935 0.948 0.957 0.939 0.959 0.985 0.998 0.999 0.969 0.973
5 1.077 0.958 0.972 0.948 0.943 0.939 0.908 0.926 0.921 0.910 0.942 0.940 0.961 0.980 0.948 0.930

*** INBOARD RMS2 ***
R1-G 221550 67.5 112.5 157.5 202.5 247.5 292.5 337.5 22.5 67.5 112.5 157.5 202.5 247.5 292.5 337.5
1 1.001 1.001 1.001 1.001 1.001 1.001 1.001 1.001 1.001 1.001 1.001 1.001 1.001 1.001 1.001
2 1.022 1.003 1.001 1.001 1.001 0.994 0.999 1.001 1.001 1.001 1.001 1.001 1.001 1.001 1.001
3 1.030 0.995 1.001 0.988 1.002 0.984 0.989 0.986 0.997 0.977 0.996 1.001 1.001 1.001 0.992 1.000
4 1.096 0.991 1.000 0.961 0.984 0.986 0.935 0.948 0.957 0.939 0.959 0.985 0.998 0.999 0.969 0.973
5 1.077 0.958 0.972 0.948 0.943 0.939 0.908 0.926 0.921 0.910 0.942 0.940 0.961 0.980 0.948 0.930

*** OUTBOARD RMS2 ***
R1-G 221550 67.5 112.5 157.5 202.5 247.5 292.5 337.5 22.5 67.5 112.5 157.5 202.5 247.5 292.5 337.5
1 1.001 1.001 1.001 1.001 1.001 1.001 1.001 1.001 1.001 1.001 1.001 1.001 1.001 1.001 1.001
2 1.022 1.003 1.001 1.001 1.001 0.994 0.999 1.001 1.001 1.001 1.001 1.001 1.001 1.001 1.001
3 1.030 0.995 1.001 0.988 1.002 0.984 0.989 0.986 0.997 0.977 0.996 1.001 1.001 1.001 0.992 1.000
4 1.096 0.991 1.000 0.961 0.984 0.986 0.935 0.948 0.957 0.939 0.959 0.985 0.998 0.999 0.969 0.973
5 1.077 0.958 0.972 0.948 0.943 0.939 0.908 0.926 0.921 0.910 0.942 0.940 0.961 0.980 0.948 0.930

DATA SET 1 IDY IDA IDC IDR IDL PDP PDP R2 IDC12 IDC45 PMIN PMAX
OUTBOARD 0.3056 0.0742 0.0371 0.0350 0.4857 1.0000 1.2624 0.9808 0.0034 0.0371 0.9060 1.0018
INBOARD 0.3029 0.0735 0.0333 0.0314 0.5315 0.0223 0.9991 1.2622 0.9822 0.0039 0.9399 1.0011
DATA SET 2
OUTBOARD 0.3056 0.0742 0.0350 0.0350 0.8304 1.0126 1.2410 0.9608 0.0940 0.0506 0.9080 1.0018
INBOARD 0.3029 0.0736 0.0325 0.0414 0.8563 1.0110 1.2421 0.9622 0.0925 0.0480 0.9099 1.0011

PSTC1 PSTC2 PSTC3 PSTC11 PSTC12 PSTC13 PSTC14 PSTC15 PSTC16 PSTC17 PSTC18
0.02375 7.34 7.50 0.00 0.00 0.00 0.00 0.00 0.00 0.00 14.15 85.75 14.25 14.05 45.50 14.05

THIS PAGE IS BEST QUALITY PRACTICABLE
FROM COPY FURNISHED TO DDC

```

*** STEADY STATE ***
PART POINT PROJECT TEST DATE DAY HR MIN SEC ERCODE MODE SETIDATE WIND-OFF AEDC PROPULSION WIND TUNNEL
553 2 641-D2A TF4.9 9/27/76 2711231 461 J5 0 3110/2776 548/ -1 TRANSONIC 161

V ST P 2 REX10-6 TT PTA-1 PTB-2 PCA-1 PCB-2 TTA-1 ITB-0 PTI-NCN MAE HAM TPR MA/MT MB SCHED
1.90 1788.5 1055.0 599.3 3.428 970 1786.5 1789.2 1072.5 1072.9 110 1496.4 0-0.00 0.00 1.237 0.0392 0.900 1

ALPHA BETA VANE0 VANE1 SHOCK TUBE SELECT 14C S19 L7 J27 E10 U1 M6 G34-2 M8-1 H10-1 N30-1 85-1 C3
3.0 0.327 13.3A 14.57 5020 RB2-1eZ,RCB-1e2,1,AB1C=1e,5,AB2D=1eD,HLG=2,733,HL1e2,726,CRO-URS

R2 MFR2 MFR100 W2R W2A-FS T12 IDT JDR IDC IDL PD PDP IDA
0.9801 0.9801 0.6896 0.7036 3.499 349.93 0.0076 0.0973 0.0357 0.0377 0.4949 1.0002 1.2619 0.0754
1.9826 0.6895 0.7007 3.485 348.47 0.0006 0.0906 0.0404 0.0328 0.5198 0.9985 1.2832 0.0721

M2S M2 MA MSP IAVG W2 CB1SS CP2SS CP3SS
OUTBOARD 0.484 0.505 0.714 0.8006 0.8235 2.766 0.619 0.676 0.620
INS-ARD 0.492 0.497 0.000 0.8040 0.8298 2.761

*** RAYD PRESSURES *** *** COML INTERNAL PRESSURES *** *** BLC PLENUM ***
PL435 PL457 PL470 PL480 PL490 PL020 PL030 PL035 PL045 PL543 PL573
OUTBOARD 0.7803 0.8389 0.7754 0.8361 0.8408 0.7883 0.7861 0.8174 0.8727 0.7883 0.8174 0.8727 0.7352 0.7985
INS-ARD 0.7802 0.8335 0.7745 0.8476 0.8540 0.7992 0.7846 0.8295 0.8736 0.7884 0.8174 0.8736 0.7284 0.8035

*** FLOWMETER PRESSURE *** *** CONTROL PARAMETERS ***
PL680 PL681 PL682 PL683 PL690 PL691 PL692 PL693 PL702 PL703 PL704 PL700 PL701
OUTBOARD 0.6547 0.6532 0.6533 0.6551 0.5552 0.5546 0.5521 0.5547 0.9988 0.7997 0.7778 0.9991 0.7109
INS-ARD 0.6544 0.6547 0.6546 0.6544 0.5544 0.5532 0.5543 0.5545 0.9988 0.8030 0.7843

*** OUTBOARD PT2/PT0 *** *** INBOARD PT2/PT0 ***
R1.0 22.5DEG 67.5 112.5 157.5 202.5 247.5 292.5 337.5 22.5 67.5 112.5 157.5 202.5 247.5 292.5 337.5
1 1.001 1.001 1.001 1.000 1.000 1.001 1.001 1.001 1.001 1.001 1.001 1.001 1.001 1.001 1.001 1.001
2 1.000 1.000 1.000 1.000 1.000 0.993 0.999 1.000 1.000 1.000 1.000 1.000 1.000 1.000 1.000 1.000
3 1.000 0.994 1.001 0.988 1.002 0.964 0.968 0.986 0.986 0.978 0.996 1.001 1.000 1.000 1.001 0.992 1.000
4 0.996 0.990 1.000 0.958 0.984 0.945 0.933 0.947 0.958 0.940 0.960 0.925 0.998 0.998 0.999 0.971 0.976
5 0.977 0.956 0.972 0.945 0.941 0.938 0.906 0.925 0.922 0.912 0.943 0.941 0.962 0.962 0.981 0.951 0.931

*** OUTBOARD RMS2 *** *** INBOARD RMS2 ***
R1.0 22.5DEG 67.5 112.5 157.5 202.5 247.5 292.5 337.5 22.5 67.5 112.5 157.5 202.5 247.5 292.5 337.5
1 0.003 0.003 0.003 0.003 0.003 0.003 0.003 0.003 0.003 0.003 0.003 0.003 0.003 0.003 0.003 0.003
2 0.000 0.000 0.000 0.000 0.000 0.000 0.000 0.000 0.000 0.000 0.000 0.000 0.000 0.000 0.000 0.000
3 0.000 0.000 0.000 0.000 0.000 0.000 0.000 0.000 0.000 0.000 0.000 0.000 0.000 0.000 0.000 0.000
4 0.000 0.000 0.000 0.000 0.000 0.000 0.000 0.000 0.000 0.000 0.000 0.000 0.000 0.000 0.000 0.000
5 0.000 0.000 0.000 0.000 0.000 0.000 0.000 0.000 0.000 0.000 0.000 0.000 0.000 0.000 0.000 0.000

DATA SET 1 IDT JDA IDC IDB IDL T12 PD PDP R2 IDC32 IDC45 PHIN PHAX
OUTBOARD 0.0973 0.0754 0.0377 0.0357 0.4949 0.0076 1.0002 1.2619 0.9901 0.0033 0.0377 0.9962 1.0015
INS-ARD 0.0905 0.0731 0.0328 0.0404 0.5198 0.0019 0.9985 1.2632 0.9826 0.0003 0.0328 0.9118 1.0008

DATA SET 2 IDT JDA IDC IDB IDL T12 PD PDP R2 IDC32 IDC45 PHIN PHAX
OUTBOARD 0.0973 0.0734 0.0357 0.0357 0.4949 0.0076 1.0013 1.2402 0.9801 0.0033 0.0357 0.9062 1.0015
INS-ARD 0.0906 0.0721 0.0353 0.0404 0.5198 0.0019 0.9985 1.2632 0.9826 0.0003 0.0328 0.9118 1.0008

PSTCE1 PSTCE2 PSTCE3 PSTCD1 PSTCD2 PSTCD3 PSTC11 PSTC12 PSTC13 PSTD1 PSTD2 PSTD3 PSTRI1 PSTRI2 PSTRI3
7.33 7.32 7.55 0.00 0.00 0.00 0.00 0.00 0.00 116.55 7.35 6.40 62.00 7.30 6.20

```

*** STEADY STATE ***

PART POINT	PROJECT TEST	DATE	DAY	HR	MIN	SEC	ENCODE	MODE	SET/DATE	WIND-OFF	AEDC	PROPULSION	WIND TUNNEL							
557	2-P41-02A	7-19	9/20	76	2721	11 431 37	0	0	3110/277A	5597 -1			TRANSONIC 167							
M	PT	P	O	REX10-6	TT	PTA-1	PTB-2	PCA-1	PCB-2	VIA-1	ITB-0	PTI	NCN	WAE	MAH	TPR	MA/WT	MB	SCHED	
C.251	1097.5	1057.8	535.7	3.178	570	1097.5	1098.1	1071.0	1071.7	110	111	1377.3	0-0.00	0.00	1.232	0.0310	0.890	1		
ALPHA	BETA	VANEO	VANET	SNOCK	TUBE	SELECT	14C	S19	L7	J27	E10	U1	M6	G34-2	MB-1	H16-1	N30-1	B5-1	C3	
3.0	0.012	25.07	21.22	5015			RAE-187	RCO-1a2	1.0	AB10-1	5.5	AB20-1	10.0	HL02-1	7.33	HL12-1	7.24	CG0	URS	
Q2	WFR2	MFR100	W2R	W2R-FS	T12	IDT	IDR	IDC	IDL	PD	PPD	IDA								
UTBOARD	0.2652	0.6001	0.6092	2.995	299.53	0.0761	0.0710	0.0281	0.0285	0.3845	0.9955	1.2694	0.0547							
INBOARD	0.2893	0.5973	0.6038	2.989	296.89	0.0623	0.0624	0.0271	0.0248	0.3596	0.9928	1.2729	0.0506							
M2S	M2	MA	NSP	YAVG	M2	CP3SS	CP2SS	CP3SS												
OUTBOARD	0.500	0.615	0.671	0.8594	0.8751	2.258	0.644	0.699	0.645											
INBOARD	0.596	0.607	0.000	0.0707	0.0826	2.248														
	*** RAMP PRESSURES ***																			
	*** COML INTERNAL PRESSURES ***																			
	*** BLC PLENUM ***																			
PL335	PL450	PL470	PL490	PL490	PL490	PL020	PL030	PL035	PL045											
0.307	0.8769	0.8441	0.8854	0.8855	0.8526	0.8525	0.8717	0.9041												
INBOARD	0.6424	0.8777	0.8476	0.8954	0.8975	0.8615	0.8546	0.8816	0.9124											
	*** FLOWMETER PRESSURE ***																			
	*** CONTROL PARAMETERS ***																			
PL680	PL661	PL682	PL683	PL690	PL691	PL692	PL693	PL702	PL703	PL704	PL700	PL701								
0.4721	0.4714	0.4714	0.4717	0.3520	0.3518	0.3482	0.3492	0.9982	0.8578	0.8471	0.9989	0.7385								
INBOARD	0.4705	0.4711	0.4705	0.3500	0.3498	0.3510	0.3515	0.9985	0.8694	0.8536										
	*** OUTBOARD PT2/PT0 ***																			
	*** INBOARD PT2/PT0 ***																			
PTG	22.5DEC	67.5	112.5	157.5	202.5	247.5	292.5	337.5	22.5	67.5	112.5	157.5	202.5	247.5	292.5	337.5				
1	1.001	1.001	1.001	1.001	1.001	1.001	1.001	1.001	1.001	1.001	1.001	1.001	1.001	1.001	1.001	1.001				
2	1.001	1.001	1.001	1.001	1.001	1.001	1.001	1.001	1.001	1.001	1.001	1.001	1.001	1.001	1.001	1.001				
3	1.001	1.001	1.001	1.001	1.001	1.001	1.001	1.001	1.001	1.001	1.001	1.001	1.001	1.001	1.001	1.001				
4	1.001	1.001	1.001	1.001	1.001	1.001	1.001	1.001	1.001	1.001	1.001	1.001	1.001	1.001	1.001	1.001				
5	1.001	1.001	1.001	1.001	1.001	1.001	1.001	1.001	1.001	1.001	1.001	1.001	1.001	1.001	1.001	1.001				
	*** OUTBOARD RMS2 ***																			
	*** INBOARD RMS2 ***																			
CAZA	SET 1	IST	IDA	IDC	IDR	IDL	I12	I12	PD	PPD	R2	IDC12	IDC45	PMIN	PMAX					
UTBOARD	0.0710	0.0547	0.0285	0.0281	0.3845	0.0761	0.9955	1.2694	0.9852	0.0028	0.0285	0.9312	1.0011							
INBOARD	0.0724	0.0516	0.0248	0.0211	0.3596	0.0723	0.9928	1.2729	0.9893	0.0004	0.0248	0.9392	1.0009							
CAZA	SET 2																			
INBOARD	0.0710	0.0547	0.0285	0.0281	0.3845	0.0761	0.9955	1.2694	0.9852	0.0028	0.0285	0.9312	1.0011							
INBOARD	0.0724	0.0516	0.0248	0.0211	0.3596	0.0723	0.9928	1.2729	0.9893	0.0004	0.0248	0.9392	1.0009							
PSTCE1	PSTCE2	PSTCE3	PSTCE01	PSTCE02	PSTCE03	PSTCE11	PSTCE12	PSTCE13	PSTCE01	PSTCE02	PSTCE03	PSTCE11	PSTCE12	PSTCE13						
0.012	7.09	7.09	0.000	0.000	0.000	0.000	0.000	0.000	0.000	0.000	0.000	0.000	0.000	0.000	0.000	0.000	0.000	0.000	0.000	

THIS PAGE IS BEST QUALITY PRACTICABLE
FROM COPY FURNISHED TO DDC

THIS PAGE IS BEST QUALITY PRACTICABLE
FROM COPY FURNISHED TO DDD

```

*** STEADY STATE ***

PART POINT PROJECT TEST DATE DAY HR MIN SEC ERICODE MODE SETDATE WIND-OFF AEDC PROPULSION WIND TUNNEL
558 2 P41E02A TF419 9/28/76 2221 1 231 1 0 3110/27/76 555/ 51 TRANSONIC 1A1

M DT 0 REX10-6 IT PTA-1 PTB-2 PCA-1 PCB-2 TTA-1 TTB-0 PTL NCN MAE MAW JPR WA/HT MB SCHED
C.650 1066.0 1057.3 534.9 3.178 569 1696.0 1696.6 1070.5 1070.9 110 111 1376.1 0-0.00 0.00 1.232 0.9321 0.850 1

ALPHA BETA VANE0 VANE1 SHOCK TUBE SELECT I40 S19 L7 J27 E10 U1 M6 G34-2 W6-1 H16-1 N30-1 85-1 C3
3.0 20212 25.06 21.22 5817 RB1-1E7,RC0-1E2,1,AB1A0-1E.5,AB20-1E0,HL1B1E2,731,HL1E2,72A,CED,URS

R2 WFR2 MFR100 W2R K2R-F5 T12 IDT IDR IDC IDL PD PDP IDA
OUTBOARD 0.9851 0.6000 0.6090 2.994 299.44 0.0559 0.0708 0.0281 0.0284 0.3838 0.9954 1.2695 0.0546
INBOARD 3.8293 3.5991 0.6092 2.978 297.77 0.0619 0.0629 0.0274 0.0247 0.3617 0.9927 1.2731 0.0310

M2S M2 MA MSP TAVG W2 CP155 CP255 CP355
OUTBOARD 0.900 0.414 0.669 0.8586 0.8756 2.256 0.645 0.899 0.645
INBOARD 3.397 0.408 0.300 0.6653 0.8022 2.253

*** RAMP PRESSURES ***
*** COHL INTERNAL PRESSURES ***
*** BLC PLENUM ***

PL35 PL45J PL47J PL480 PL490 PL020 PL030 PL045 PL045 PL543 PL573
OUTBOARD 0.5308 0.6770 0.6441 0.8855 0.8858 0.8529 0.8525 0.8718 0.9041 0.7877 0.8546
INBOARD 0.6424 0.8780 0.8478 0.8948 0.8980 0.8618 0.8547 0.8815 0.9123 0.7798 0.9595

*** FLOWMETER PRESSURE ***
*** CONTROL PARAMETERS ***

PL690 PL691 PL682 PL683 PL690 PL691 PL692 PL693 PL702 PL703 PL704 PL700 PL701
OUTBOARD 0.4701 0.4696 0.4703 0.4705 0.3497 0.3496 0.3457 0.3467 0.9995 0.8561 0.8472 0.9991 0.7403
INBOARD 0.4597 0.4705 0.4701 0.4693 0.3471 0.3472 0.3490 0.3493 0.9991 0.8645 0.8541

*** OUTBOARD PT2/PT0 ***
*** INBOARD PT2/PT0 ***

RING 22.5DEC 67.5 112.5 157.5 202.5 247.5 292.5 337.5 377.5 421.5 467.5 517.5 577.5 622.5 672.5 720.5 767.5 817.5
1 1.001 1.001 1.001 1.001 1.000 1.000 1.001 1.001 1.001 1.001 1.001 1.001 1.000 1.000 1.000 1.001 1.001
2 1.001 1.001 1.001 1.001 1.001 1.001 1.001 1.001 1.001 1.000 1.000 1.001 1.001 1.001 1.001 1.001 1.001
3 1.997 1.000 1.001 1.001 1.001 0.976 0.968 0.986 0.986 0.986 0.986 0.986 0.986 0.986 0.986 1.001 1.001
4 1.977 0.994 0.996 0.996 0.984 0.961 0.948 0.960 0.972 0.959 0.975 0.987 1.000 1.001 0.991 0.996
5 1.947 0.974 0.979 0.974 0.956 0.955 0.931 0.943 0.944 0.939 0.962 0.956 0.976 1.000 1.001 0.987 0.996

*** OUTBOARD RMS2 ***
*** INBOARD RMS2 ***

RING 22.5DEC 67.5 112.5 157.5 202.5 247.5 292.5 337.5 377.5 421.5 467.5 517.5 577.5 622.5 672.5 720.5 767.5 817.5
1 0.004 0.003 0.003 0.003 0.003 0.003 0.003 0.003 0.003 0.001 0.001 0.001 0.001 0.001 0.001 0.001 0.001
3 -1.000 0.004 0.004 0.004 0.005 0.011 0.008 0.010 0.007 -1.000 0.000 0.000 0.000 0.001 0.001 0.001 0.001
5 0.025 0.026 0.026 0.026 0.029 0.029 0.027 0.027 0.027 0.027 0.027 0.027 0.027 0.027 0.027 0.027 0.027

DATA SET 1 IDT IDA IDC IDR IDL IDL T12 PDP R2 1DC12 1DC45 PMIN PHAX
OUTBOARD 0.9708 0.0546 0.0284 0.0281 0.3636 0.0059 0.9954 1.2695 0.9851 0.0028 0.0284 0.9314 1.0011
INBOARD 0.9629 0.0510 0.0247 0.0274 0.3617 0.0019 0.9927 1.2731 0.9893 0.0003 0.0247 0.9388 1.0010

DATA SET 2
OUTBOARD 0.8708 0.0546 0.0696 0.0281 0.9296 1.0043 1.2545 0.9851 0.0696 0.0364 0.9314 1.0011
INBOARD 0.9629 0.0510 0.0625 0.0274 0.5747 1.0005 1.2599 0.9893 0.0625 0.0351 0.9388 1.0010

PSTCE1 PSTCE2 PSTCE3 PSTC01 PSTC02 PSTC03 PSTC11 PSTC12 PSTC13 PSTC01 PSTC02 PSTC03 PSTR11 PSTR12 PSTR13
7.67 7.60 0.00 0.00 0.00 0.00 0.00 0.00 0.00 0.00 0.00 0.00 0.00 0.00 0.00 0.00 0.00 0.00 0.00 0.00 0.00 0.00 0.00 0.00 0.00 0.00 0.00 0.00

```

*** STEADY STATE ***

PART PROJECT TEST DATE DAY HR MIN SEC ENCODE MODE SETIDATE WIND-OFF AEDC PROPUSSION HIND TUNNEL
 559 I P41-D2A Y419 9/29/76 2721 31 291 41 0 3150/27/76 558/ -1 TRANSONIC 16T

 W FT P D REX10-6 TT PTA-1 PTR-2 PCA-1 PCB-2 JTA-1 JTB-0 PT1 MCN WAE MAH YPR WAHMT M8 SCHED
 0.850 1695.7 1.572 534.8 3.177 569 1695.7 1696.2 1070.4 1070.7 110 111 1375.6 0-0-0 0.00 0.00 1.233 0.0326 0.850 1

 ALPHA BETA VANEI VANET SMCK TUBE SELECT 140 S19 L7 J27 E10 U1 M6 G34-2 H6-1 H16-1 N30-1 B9-1 C3
 3.0 2.023 25.04 21.21 5020 RBC-15Z,RC0-1a2,1,AB10-1a,5,AB20-1a,0,HL0a2,733,HL1a2,726,Ca0,UBS

 R2 MFR2 MFR100 M8R M2R-FS T12 IDR IDL IDC IDR IDL PD PDP IDA
 M1079ARD 0.8750 0.6000 0.6094 2.995 299.45 0.060 0.0703 0.0280 0.0281 0.3822 0.9954 1.2696 0.0543
 L1B2ARD 0.7692 0.6099 0.6095 2.977 297.67 0.0217 0.0634 0.0274 0.0248 0.3620 0.9926 1.2732 0.0512

 M2S M2 MA NS2 TAVG M2 CP2SS CP2SS
 M1079ARD 0.4-0 0.613 0.671 0.4588 0.8758 2.256 0.645 0.699 0.645
 L1B2ARD 0.397 0.408 0.400 0.4950 0.8821 2.252

 *** RAMP PRESSURES ***
 PL435 PL450 PL470 PL480 PL490 PL691 PL692 PL693 PL702 PL703 PL704 PL700 PL701
 M1079ARD 0.8315 0.8776 0.8449 0.8861 0.8528 0.8522 0.8714 0.9040 PL543 PL573
 L1B2ARD 0.8424 0.8775 0.8477 0.8945 0.8577 0.8615 0.8547 0.8819 0.9131 0.7873 0.8543
 0.7798 0.8600

*** CONTROL PARAMETERS ***

*** INBOARD PT2/PTC ***
 RING 22.5526 47.5 112.5 157.5 202.5 247.5 292.5 337.5 382.5 427.5 472.5 517.5 562.5 607.5 652.5
 1 1.001 1.001 1.001 1.001 1.001 1.001 1.001 1.001 1.001 1.001 1.001 1.001 1.001 1.001 1.001
 2 1.001 1.000 1.000 1.000 1.000 1.000 1.000 1.000 1.000 1.000 1.000 1.000 1.000 1.000 1.000
 3 1.000 1.000 1.000 1.000 1.000 1.000 1.000 1.000 1.000 1.000 1.000 1.000 1.000 1.000 1.000
 4 1.000 1.000 1.000 1.000 1.000 1.000 1.000 1.000 1.000 1.000 1.000 1.000 1.000 1.000 1.000
 5 1.000 1.000 1.000 1.000 1.000 1.000 1.000 1.000 1.000 1.000 1.000 1.000 1.000 1.000 1.000

 *** OUTBOARD PT2/PTC ***
 RING 22.5526 47.5 112.5 157.5 202.5 247.5 292.5 337.5 382.5 427.5 472.5 517.5 562.5 607.5 652.5
 1 1.001 1.001 1.001 1.001 1.001 1.001 1.001 1.001 1.001 1.001 1.001 1.001 1.001 1.001 1.001
 2 1.001 1.000 1.000 1.000 1.000 1.000 1.000 1.000 1.000 1.000 1.000 1.000 1.000 1.000 1.000
 3 1.000 1.000 1.000 1.000 1.000 1.000 1.000 1.000 1.000 1.000 1.000 1.000 1.000 1.000 1.000
 4 1.000 1.000 1.000 1.000 1.000 1.000 1.000 1.000 1.000 1.000 1.000 1.000 1.000 1.000 1.000
 5 1.000 1.000 1.000 1.000 1.000 1.000 1.000 1.000 1.000 1.000 1.000 1.000 1.000 1.000 1.000

 *** INBOARD RMS2 ***
 RING 22.5526 47.5 112.5 157.5 202.5 247.5 292.5 337.5 382.5 427.5 472.5 517.5 562.5 607.5 652.5
 1 1.001 1.001 1.001 1.001 1.001 1.001 1.001 1.001 1.001 1.001 1.001 1.001 1.001 1.001 1.001
 2 1.001 1.000 1.000 1.000 1.000 1.000 1.000 1.000 1.000 1.000 1.000 1.000 1.000 1.000 1.000
 3 1.000 1.000 1.000 1.000 1.000 1.000 1.000 1.000 1.000 1.000 1.000 1.000 1.000 1.000 1.000
 4 1.000 1.000 1.000 1.000 1.000 1.000 1.000 1.000 1.000 1.000 1.000 1.000 1.000 1.000 1.000
 5 1.000 1.000 1.000 1.000 1.000 1.000 1.000 1.000 1.000 1.000 1.000 1.000 1.000 1.000 1.000

 *** OUTBOARD RMS2 ***
 RING 22.5526 47.5 112.5 157.5 202.5 247.5 292.5 337.5 382.5 427.5 472.5 517.5 562.5 607.5 652.5
 1 1.001 1.001 1.001 1.001 1.001 1.001 1.001 1.001 1.001 1.001 1.001 1.001 1.001 1.001 1.001
 2 1.001 1.000 1.000 1.000 1.000 1.000 1.000 1.000 1.000 1.000 1.000 1.000 1.000 1.000 1.000
 3 1.000 1.000 1.000 1.000 1.000 1.000 1.000 1.000 1.000 1.000 1.000 1.000 1.000 1.000 1.000
 4 1.000 1.000 1.000 1.000 1.000 1.000 1.000 1.000 1.000 1.000 1.000 1.000 1.000 1.000 1.000
 5 1.000 1.000 1.000 1.000 1.000 1.000 1.000 1.000 1.000 1.000 1.000 1.000 1.000 1.000 1.000

 DATA SET 1 IDY IDA IDC IDR IDL T12 PD PDP R2 IDC12 IDC45 PMIN PMAX
 M1079ARD 0.0703 0.0543 0.0281 0.0280 0.3822 0.0660 0.9954 1.2696 0.9650 0.0026 0.0026 0.0026 0.9315 1.0008
 L1B2ARD 0.0512 0.0248 0.0274 0.3620 0.0217 0.9926 1.2732 0.9892 0.0005 0.0248 0.9385 1.0013

 DATA SET 2
 M1079ARD 0.0543 0.0692 0.0280 0.6237 1.0042 1.2546 0.9850 0.0692 0.0364 0.9315 1.0008
 L1B2ARD 0.0634 0.0512 0.0637 0.0274 0.5765 1.0005 1.2599 0.9892 0.0627 0.0354 0.9385 1.0013

 PSTC12 PSTC22 PSTC32 PSTC42 PSTC52 PSTC11 PSTC21 PSTC31 PSTC41 PSTC51 PSTR12 PSTR22 PSTR32 PSTR11 PSTR21 PSTR31
 7.87 7.486 7.41 6.00 0.00 0.00 0.00 61.45 7.80 6.45 33.9A 7.75 6.30

THIS PAGE IS BEST QUALITY PRACTICABLE FROM COPY FURNISHED TO DDG

*** STEADY STATE ***

PART POINT PROJECT TEST		DATE	DAY	HR	MIN	SEC	ERCODE	MODE	SETIDATE	WIND-OFF	AEDC	PROPULSION	WIND	TUNNEL
519	2	PA1-D2A	TF49	9/28/76	271	5	1	16	0	310/27/76	5477	-1	TRANSONIC	161

M	DT	P	0	REX10=6	TT	PTA-1	PTB-2	PCA-1	PCB-2	JTA-1	JTB-0	PTI	NCN	WAE	WAK	TPR	WAWT	WB	SCHED
0.703	148.9	1.557	365.7	2.493	509	1468.9	1469.5	1065.3	1065.8	110	110	1170.6	0.000	0.000	0.000	1.255	0.0063	0.700	1

ALPHA	SETA	VANE	SHOCK	TUBE	SELECT	14*	519	L7	J27	E10	U1	M6	G34-2	M8P1	H16-1	N30-1	B5-1	C3
1.0	1.0	1.0	1.0	1.0	1.0	1.0	1.0	1.0	1.0	1.0	1.0	1.0	1.0	1.0	1.0	1.0	1.0	1.0

M2S	M2	M1	MSP	TAVG	M2	CP155	CP255	CP355
0.487	0.503	0.726	0.7665	0.8102	2.241	0.720	0.761	0.751

*** RAMP PRESSURES ***

R1	R2	R3	R4	R5	R6	R7	R8	R9	R10
0.943	0.7361	0.7644	3.513	351.28	0.0111	0.1050	0.0364	0.0298	0.4674

*** CWL INTERNAL PRESSURES ***

PL435	PL451	PL470	PL480	PL490	PL020	PL030	PL035	PL045
0.7787	0.8149	0.7648	0.8232	0.6292	0.7786	0.7736	0.8071	0.8492

*** BLC PLENUM ***

PL543	PL573	PL703	PL704	PL700	PL701
0.7591	0.7914	0.9869	0.7664	0.9289	0.6541

*** CONTROL PARAMETERS ***

PL702	PL703	PL704	PL700	PL701
0.9869	0.7857	0.7664	0.9289	0.6541

*** FLOWMETER PRESSURE ***

PL690	PL682	PL683	PL690	PL691	PL692	PL693
0.4541	0.5435	0.4088	0.4042	0.4054	0.9869	0.7857

*** OUTBOARD PT2/PTC ***

R1	R2	R3	R4	R5	R6	R7	R8	R9	R10
0.912	0.968	0.968	0.948	0.922	0.918	0.944	0.955	0.935	0.954

*** INBOARD PT2/PTC ***

R1	R2	R3	R4	R5	R6	R7	R8	R9	R10
0.912	0.968	0.968	0.948	0.922	0.918	0.944	0.955	0.935	0.954

*** OUTBOARD RMS2 ***

R1	R2	R3	R4	R5	R6	R7	R8	R9	R10
0.912	0.968	0.968	0.948	0.922	0.918	0.944	0.955	0.935	0.954

*** INBOARD RMS2 ***

R1	R2	R3	R4	R5	R6	R7	R8	R9	R10
0.912	0.968	0.968	0.948	0.922	0.918	0.944	0.955	0.935	0.954

*** CONTROL PARAMETERS ***

PL702	PL703	PL704	PL700	PL701
0.9869	0.7857	0.7664	0.9289	0.6541

*** INBOARD RMS2 ***

R1	R2	R3	R4	R5	R6	R7	R8	R9	R10
0.912	0.968	0.968	0.948	0.922	0.918	0.944	0.955	0.935	0.954

*** CONTROL PARAMETERS ***

PL702	PL703	PL704	PL700	PL701
0.9869	0.7857	0.7664	0.9289	0.6541

*** INBOARD RMS2 ***

R1	R2	R3	R4	R5	R6	R7	R8	R9	R10
0.912	0.968	0.968	0.948	0.922	0.918	0.944	0.955	0.935	0.954

*** CONTROL PARAMETERS ***

PL702	PL703	PL704	PL700	PL701
0.9869	0.7857	0.7664	0.9289	0.6541

*** INBOARD RMS2 ***

R1	R2	R3	R4	R5	R6	R7	R8	R9	R10
0.912	0.968	0.968	0.948	0.922	0.918	0.944	0.955	0.935	0.954

*** CONTROL PARAMETERS ***

PL702	PL703	PL704	PL700	PL701
0.9869	0.7857	0.7664	0.9289	0.6541

*** INBOARD RMS2 ***

R1	R2	R3	R4	R5	R6	R7	R8	R9	R10
0.912	0.968	0.968	0.948	0.922	0.918	0.944	0.955	0.935	0.954

THIS PAGE IS BEST QUALITY PRACTICABLE FROM COPY FURNISHED TO DDC

THIS PAGE IS BEST QUALITY PRACTICABLE
FROM COPY FURNISHED TO DDG

*** STEADY STATE ***

PART POINT PROJECT TEST DATE DAY HR MIN SEC ERCODE MODE SETIDATE WIND-OFF AEDC PROPUSSION WIND TUNNEL
 57C 1.P41J-D2A TE419 9/28/76 2221.61 111 37 0 0 J11022726 567/ -1 TRANSSONIC 167

M PT P 0 REX10-6 TT PTA-1 P18-2 PCA-1 PCB-2 TTA-1 TTB-0 PTTI CN HAE HAN TPR WA/WI MB SCHED
 0.599 1471.1 1661.1 363.3 2.489 569 1471.1 1471.9 1070.7 1070.9 109 110 1169.7 0-0.00 0.00 1.258 0.0063 0.700 1

ALPHA BETA VAWO VANEI SHOCK TUBE SELECT 140 S19 L7 J27 E10 U1 M6 G34-2 W8-1 H16-1 N30-1 85-1 C3
 1.00 4.099 18.85 14.65 5020 RB2-187.RCD-182.1.181818.1.5.AB20-150.HL012.733.HL182.726.C.R.U.BS

R2 MFR100 M2R M2R-FS J12 IDR IDC IDL PD PDP IDA
 *OUTBOARD 0.9756 0.7453 0.7649 3.506 350.59 0.0076 0.0907 0.0388 0.0315 0.4966 1.0003 1.2618 0.0647
 INBOARD 0.9747 0.7433 0.7626 3.495 349.54 0.0024 0.1100 0.0422 0.0419 0.5691 1.0005 1.2599 0.0631

M25 M2 HA ASP TAVG M2 CP155 CP255 CP355
 *OUTBOARD 0.485 0.504 0.508 0.8483 0.9201 2.270 0.752 0.765 0.719
 INBOARD 0.494 0.502 0.000 0.8068 0.8208 2.261

*** CONL INTERNAL PRESSURES *** *** BLC PLENUM ***

PL435 PL453 PL470 PL480 PL490 PL020 PL030 PL035 PL045 PL543 PL573
 *OUTBOARD 0.076 0.8512 0.7733 0.8362 0.8407 0.7940 0.7832 0.8556 0.8598 0.7833 0.8052
 INBOARD 0.792 0.8256 0.7664 0.8385 0.8447 0.7930 0.7784 0.8208 0.8629 0.7800 0.8008

*** FLG-METER PRESSURE *** *** CONTROL PARAMETERS ***

PL630 PL681 PL682 PL683 PL690 PL691 PL692 PL693 PL702 PL703 PL704 PL700 PL701
 *OUTBOARD 0.5409 0.5406 0.5406 0.5387 0.5397 0.5398 0.5399 0.5325 0.5340 0.7923 0.7760 0.9996 0.8379
 INBOARD 0.5159 0.5394 0.5394 0.5394 0.5394 0.5399 0.5399 0.5365 0.9886 0.7976 0.7773

*** OUTBOARD PT2/PTC *** *** INBOARD PT2/PTC ***

RING 22.5359 67.5 112.5 157.5 202.5 247.5 292.5 337.5 377.5 422.5 467.5 512.5 557.5 602.5 647.5 692.5 737.5 782.5 827.5 872.5
 1 1.030 0.980 0.999 1.000 1.000 1.001 1.001 1.000 1.000 1.001 1.001 1.001 1.001 1.001 1.001 1.001 1.001 1.001 1.001
 2 0.932 0.923 0.986 1.001 1.001 0.994 1.001 1.001 1.002 0.993 1.000 1.001 1.000 0.994 0.999 1.000
 3 0.931 0.922 0.977 1.001 1.001 0.995 0.957 0.957 0.995 0.952 0.979 1.000 1.000 0.950 0.982 0.997
 4 0.987 0.937 0.972 0.991 0.991 0.991 0.928 0.928 0.964 0.917 0.928 0.992 1.000 0.941 0.954 0.958
 5 0.993 0.919 0.954 0.953 0.944 0.936 0.913 0.913 0.926 0.931 0.894 0.934 0.943 0.979 0.943 0.933 0.912

*** OUTBOARD RMS2 *** *** INBOARD RMS2 ***

RING 22.5359 67.5 112.5 157.5 202.5 247.5 292.5 337.5 377.5 422.5 467.5 512.5 557.5 602.5 647.5 692.5 737.5 782.5 827.5 872.5
 1 0.035 0.039 0.004 0.003 0.003 0.003 0.003 0.003 0.003 0.004 0.001 0.001 0.001 0.001 0.001 0.001 0.001 0.001 0.001
 2 0.030 0.031 0.011 0.003 0.005 0.007 0.009 0.006 0.006 0.006 0.006 0.003 0.003 0.003 0.003 0.003 0.003 0.003 0.003
 3 0.035 0.032 0.014 0.012 0.011 0.009 0.009 0.009 0.009 0.009 0.009 0.009 0.009 0.009 0.009 0.009 0.009 0.009 0.009
 4 0.037 0.037 0.037 0.037 0.037 0.037 0.037 0.037 0.037 0.037 0.037 0.037 0.037 0.037 0.037 0.037 0.037 0.037 0.037
 5 0.037 0.037 0.037 0.037 0.037 0.037 0.037 0.037 0.037 0.037 0.037 0.037 0.037 0.037 0.037 0.037 0.037 0.037 0.037

DATA SET 1 IDT IDA IDC IDR IDL Y12 Y12 PD PDP R2 IDC12 IDC45 PHIN PHAX
 *OUTBOARD 0.0937 0.0647 0.0315 0.0388 0.4966 0.0076 1.0003 1.2618 0.9756 0.8116 0.0315 0.9125 1.0011
 INBOARD 0.1100 0.0831 0.0419 0.0422 0.5691 0.0024 3.0002 1.2599 0.9747 0.8031 0.0419 0.8936 1.0009

DATA SET 2
 *OUTBOARD 0.0937 0.0647 0.0663 0.0398 0.7770 1.0106 1.2444 0.9756 0.8963 0.0395 0.9125 1.0011
 INBOARD 0.1103 0.0831 0.0887 0.0422 0.9385 1.0110 1.2370 0.9747 0.8087 0.0537 0.8936 1.0009

PSTR1 PSTR2 PSTR3 PSTR4 PSTR5 PSTR6 PSTR7 PSTR8 PSTR9 PSTR10 PSTR11 PSTR12 PSTR13
 7.59 7.58 6.95 0.00 0.00 0.00 0.00 0.00 0.00 0.00 0.00 144.35 7.85 7.00 74.90 7.50 6.60

*** STEADY STATE ***

PART PRINT PROJECT TEST DATE DAY HR MIN SEC ENCODE MODE SETIDATE WIND-OFF AEDC PROPULSION WIND TUNNEL
521 1.441.502A 27519 9/28/76 2721 71 301 28 0 3110/2776 5721 -1 TRANSCNIC 46T

M PI P C REX10-6 TT PTA-3 PTR-2 PCA-1 PCB-2 ITA-1 ITB-0 PTI NCM WAE MAW IPR WA/WT MB SCHED
0.701 1470.3 1059.0 364.3 2.492 569 1470.3 1471.2 1058.6 1069.0 109 110 1173.4 0-0.00 0.00 1.253 0.0063 0.700 1

ALPHA BETA VANFO VANEI SHOCK TUBE SELECT 145 S19 L7 J27 E10 U1 M6 G34-2 M8-1 M16-1 M30-1 B5-1 C3
3.0 -0.004 24.67 20.68 5015 RB-1E7ARC0-1s21.1AB10-1s.5AB20-1s0.HLs2.733.HL1s2.724.CsD.JMS

R2 WFR2 WFR100 M2R J2R-FS T12 10T IDR IDC IDL PD PDP JDA
0.965 0.6524 0.6613 3.034 303.42 0.0761 0.0701 0.0266 0.0268 0.3601 0.9946 1.2709 0.0541

M25 M2 MA MSP IAVG M2 CP155 CP255 CP355
OUTBOARD 0.437 0.418 0.579 0.8595 0.8747 1.986 0.1734 0.769 0.735
INBOARD 2.435 0.412 0.000 0.8626 0.8790 1.981

*** RAMP PRESSURES ***
PL435 PL450 PL470 PL480 PL490 PL620 PL630 PL635 PL645 PL543 PL573
0.549 0.8571 0.8437 0.8847 0.8860 0.8534 0.8505 0.8708 0.9028 0.8129 0.8592

*** FLOWMETER PRESSURE ***
PL640 PL661 PL682 PL683 PL690 PL691 PL692 PL693 PL702 PL703 PL704 PL705 PL706
0.3199 0.5232 0.5201 0.5205 0.4189 0.4180 0.4146 0.4165 0.9986 0.8583 0.8467 0.9992 0.7963

*** OUTBOARD PT2/PTC ***
RING 27.0DEG 67.5 112.5 157.5 202.5 247.5 292.5 337.5 382.5 427.5 472.5 517.5 562.5 607.5 652.5 697.5
1 1.001 1.001 1.001 1.001 1.001 1.001 1.001 1.001 1.001 1.001 1.001 1.001 1.001 1.001 1.001

*** INBOARD RMS2 ***
RING 27.0DEG 67.5 112.5 157.5 202.5 247.5 292.5 337.5 382.5 427.5 472.5 517.5 562.5 607.5 652.5 697.5
1 1.003 0.003 0.003 0.003 0.003 0.003 0.003 0.001 0.001 0.001 0.001 0.001 0.001 0.001 0.001

DATA SET 1 IDY JDA IDC JDR IDL T12 PD PDP R2 ITC12 IDC45 PMIN PMAK
1.0349 0.0516 0.0234 0.0294 0.0375 0.0266 0.3801 0.0061 0.9946 1.2709 0.9865 0.0022 0.0268 0.9332 1.0024

DATA SET 2
1.3748 0.0449 0.0516 0.0642 0.0294 0.5888 1.0029 1.2567 0.9865 0.0681 0.0370 0.9332 1.0024

PSTCE1 PSTCE2 PSTCE3 PSTCD1 PSTCD2 PSTCD3 PSTC11 PSTC12 PSTC13 PSTR01 PSTR02 PSTR03 PSTR11 PSTR12 PSTR13
2.508 7.59 6.94 0.00 0.00 0.00 0.00 0.00 0.00 14.15 112.25 12.30 14.15 59.15 14.15

THIS PAGE IS BEST QUALITY PRACTICABLE FROM COPY FURNISHED TO DDC

THIS PAGE IS BEST QUALITY PRACTICABLE
 FROM COPY FURNISHED TO DDC

*** STEADY STATE ***																			
PART	POINT	PROJECT	TEST	DATE	DAY	HR	MIN	SEC	ERCODE	MODE	SET	DATE	WIND-OFF	AEDC	PROPULSION	WIND	TUNNEL		
57A	3	4411-22A	7F419	9/28/76	2721	71	281	38	0	0	311027/76	5727	-1	IRANSONIC	16Y				
*** RAMP PRESSURES ***																			
W	BY	P	PC	REX10-6	TT	PTA-1	PTB-2	PCA-1	PCB-2	TTA-1	ITB-0	PTI	NCN	WAE	WAW	TPR	WAYUT	MB	SCHED
0.731	1467.6	1.572	303.5	2.487	569	1467.6	1468.2	1066.8	1067.0	109	110	1171.7	0-0.00	0.00	1.253	0.0063	0.700	1	
ALPHA SETA VANEI SHOCK TUBE SELECT																			
1.0	2.022	24.75	21.09	3317	140	S19	L7	J27	E10	U1	M6	G34-2	M8-1	H10-1	N30-1	B5-1	C3		
*** FLOWMETER PRESSURE ***																			
W2	W1	W2	W3	W4	W5	W6	W7	W8	W9	W10	W11	W12	W13	W14	W15	W16	W17	W18	W19
0.400	0.409	0.400	0.400	0.400	0.400	0.400	0.400	0.400	0.400	0.400	0.400	0.400	0.400	0.400	0.400	0.400	0.400	0.400	0.400
*** COML INTERNAL PRESSURES ***																			
PL435	PL450	PL470	PL480	PL490	PL500	PL510	PL520	PL530	PL540	PL550	PL560	PL570	PL580	PL590	PL600	PL610	PL620	PL630	PL640
0.6455	0.6515	0.6604	0.6694	0.6784	0.6874	0.6964	0.7054	0.7144	0.7234	0.7324	0.7414	0.7504	0.7594	0.7684	0.7774	0.7864	0.7954	0.8044	0.8134
*** OUTBOARD P2/P10 ***																			
OUTWARD	PL682	PL681	PL682	PL683	PL690	PL691	PL692	PL693	PL700	PL701	PL702	PL703	PL704	PL710	PL711	PL712	PL713	PL714	PL715
0.5234	0.5236	0.5234	0.5234	0.5234	0.5234	0.5234	0.5234	0.5234	0.5234	0.5234	0.5234	0.5234	0.5234	0.5234	0.5234	0.5234	0.5234	0.5234	0.5234
*** INBOARD RMS2 ***																			
INBOARD	PL722	PL722	PL722	PL722	PL722	PL722	PL722	PL722	PL722	PL722	PL722	PL722	PL722	PL722	PL722	PL722	PL722	PL722	PL722
0.15222	0.15224	0.15222	0.15222	0.15222	0.15222	0.15222	0.15222	0.15222	0.15222	0.15222	0.15222	0.15222	0.15222	0.15222	0.15222	0.15222	0.15222	0.15222	0.15222
*** CONTROL PARAMETERS ***																			
INBOARD	PL722	PL722	PL722	PL722	PL722	PL722	PL722	PL722	PL722	PL722	PL722	PL722	PL722	PL722	PL722	PL722	PL722	PL722	PL722
0.9993	0.9993	0.9993	0.9993	0.9993	0.9993	0.9993	0.9993	0.9993	0.9993	0.9993	0.9993	0.9993	0.9993	0.9993	0.9993	0.9993	0.9993	0.9993	0.9993
*** OUTBOARD RMS2 ***																			
OUTWARD	PL722	PL722	PL722	PL722	PL722	PL722	PL722	PL722	PL722	PL722	PL722	PL722	PL722	PL722	PL722	PL722	PL722	PL722	PL722
0.15222	0.15222	0.15222	0.15222	0.15222	0.15222	0.15222	0.15222	0.15222	0.15222	0.15222	0.15222	0.15222	0.15222	0.15222	0.15222	0.15222	0.15222	0.15222	0.15222
*** INBOARD RMS2 ***																			
INBOARD	PL722	PL722	PL722	PL722	PL722	PL722	PL722	PL722	PL722	PL722	PL722	PL722	PL722	PL722	PL722	PL722	PL722	PL722	PL722
0.15222	0.15222	0.15222	0.15222	0.15222	0.15222	0.15222	0.15222	0.15222	0.15222	0.15222	0.15222	0.15222	0.15222	0.15222	0.15222	0.15222	0.15222	0.15222	0.15222
*** CONTROL PARAMETERS ***																			
INBOARD	PL722	PL722	PL722	PL722	PL722	PL722	PL722	PL722	PL722	PL722	PL722	PL722	PL722	PL722	PL722	PL722	PL722	PL722	PL722
0.9993	0.9993	0.9993	0.9993	0.9993	0.9993	0.9993	0.9993	0.9993	0.9993	0.9993	0.9993	0.9993	0.9993	0.9993	0.9993	0.9993	0.9993	0.9993	0.9993
*** CONTROL PARAMETERS ***																			
INBOARD	PL722	PL722	PL722	PL722	PL722	PL722	PL722	PL722	PL722	PL722	PL722	PL722	PL722	PL722	PL722	PL722	PL722	PL722	PL722
0.9993	0.9993	0.9993	0.9993	0.9993	0.9993	0.9993	0.9993	0.9993	0.9993	0.9993	0.9993	0.9993	0.9993	0.9993	0.9993	0.9993	0.9993	0.9993	0.9993

*** STEADY STATE ***

PART PROJECT TEST DATE DAY HR MIN SEC ERCODE MODE SFT:DATE WIND-OFF AERC PRODUCTION WIND TUNNEL
 429 5-24-75 12430 0724776 2721201-431-24 0 -2110/24776.586/ -1 2044501R-141
 P.047 1405.5 1007.6 532.4 3.169 570 1095.5 1426.5 1073.9 110 110 1343.8 0-0-00 0.00 1.242 0.0770 0.850 1

ALPHA BETA VANE0 VANE1 SMOCK TIME SELECT 140 519 L7 J77 E10 U1 M6 G34-2 X8-1 W14-1 X30-1 05-1 C3
 140 -4-023- 25-10 24-24 5043 R00=127.RC0=142.1.AM10=127.5-1450-127.733-141.2-724776.586/0.850

CUTBACK 0.9051 0.5049 0.6140 3.014 301.57 0.0066 0.0704 0.0282 0.0280 0.3820 0.9057 1.2803 0.0544
 1426455 0.02002 0.4008 0.6021 0.822 208.18 0.0028 0.0444 0.0274 0.0247 0.3615 0.9057 0.0500

INTERAD 0.404 0.415 0.669 0.8587 0.8749 2.271 0.648 0.701 0.647
 1426453 0.304 0.405 0.669 0.8584 0.8733 2.255

*** FAN PRESSURES ***

PL435 PL450 PL470 PL480 PL490 PL020 FL030 PL035 PL045 PL543 PL578
 CUTBACK 0.8111 0.8764 0.0700 0.8840 0.8902 0.9507 0.8524 0.8720 0.9064 0.7906 0.9550
 1426450 0.8435 0.8775 0.8441 0.8041 0.8335 0.8624 0.8554 0.8913 0.9126 0.7309 0.9500

*** FLOWMETER PRESSURE ***

PL600 PL620 PL630 PL640 PL650 PL660 PL670 PL680 PL690 PL700 PL710 PL720 PL730 PL740 PL750 PL760
 CUTBACK 0.8724 0.4710 0.4718 0.4716 0.3487 0.3489 0.3465 0.3474 0.9907 0.8585 0.8471 0.9098 0.7407
 1426452 0.4315 0.4322 0.4320 0.4320 0.3480 0.3474 0.3484 0.3481 0.0000 0.8655 0.8540

*** OUTBOARD RMS2 ***

PL770 PL780 PL790 PL800 PL810 PL820 PL830 PL840 PL850 PL860 PL870 PL880 PL890 PL900 PL910 PL920
 CUTBACK 0.8724 0.4710 0.4718 0.4716 0.3487 0.3489 0.3465 0.3474 0.9907 0.8585 0.8471 0.9098 0.7407
 1426452 0.4315 0.4322 0.4320 0.4320 0.3480 0.3474 0.3484 0.3481 0.0000 0.8655 0.8540

*** OUTBOARD RMS2 ***

PL930 PL940 PL950 PL960 PL970 PL980 PL990 PL000 PL010 PL020 PL030 PL040 PL050 PL060 PL070 PL080
 CUTBACK 0.8724 0.4710 0.4718 0.4716 0.3487 0.3489 0.3465 0.3474 0.9907 0.8585 0.8471 0.9098 0.7407
 1426452 0.4315 0.4322 0.4320 0.4320 0.3480 0.3474 0.3484 0.3481 0.0000 0.8655 0.8540

*** OUTBOARD RMS2 ***

PL1000 PL1010 PL1020 PL1030 PL1040 PL1050 PL1060 PL1070 PL1080 PL1090 PL1100 PL1110 PL1120 PL1130 PL1140
 CUTBACK 0.8724 0.4710 0.4718 0.4716 0.3487 0.3489 0.3465 0.3474 0.9907 0.8585 0.8471 0.9098 0.7407
 1426452 0.4315 0.4322 0.4320 0.4320 0.3480 0.3474 0.3484 0.3481 0.0000 0.8655 0.8540

*** OUTBOARD RMS2 ***

PL1150 PL1160 PL1170 PL1180 PL1190 PL1200 PL1210 PL1220 PL1230 PL1240 PL1250 PL1260 PL1270 PL1280 PL1290
 CUTBACK 0.8724 0.4710 0.4718 0.4716 0.3487 0.3489 0.3465 0.3474 0.9907 0.8585 0.8471 0.9098 0.7407
 1426452 0.4315 0.4322 0.4320 0.4320 0.3480 0.3474 0.3484 0.3481 0.0000 0.8655 0.8540

*** OUTBOARD RMS2 ***

PL1300 PL1310 PL1320 PL1330 PL1340 PL1350 PL1360 PL1370 PL1380 PL1390 PL1400 PL1410 PL1420 PL1430 PL1440
 CUTBACK 0.8724 0.4710 0.4718 0.4716 0.3487 0.3489 0.3465 0.3474 0.9907 0.8585 0.8471 0.9098 0.7407
 1426452 0.4315 0.4322 0.4320 0.4320 0.3480 0.3474 0.3484 0.3481 0.0000 0.8655 0.8540

THIS PAGE IS BEST QUALITY PRACTICABLE FROM COPY FURNISHED TO DDC

*** STEADY STATE ***														
FACT PROJECT TEST DATE DAY HP MIN SEC				ERCODE M/JUE				SET: DATE WIND-OFF				AERC PROPULSION WIND TUNNEL		
1471450 144.0 145.5 530.0				3.177 560 1696.9 1697.5 1074.7 1074.8 109				111 1143.9 0-0.00 0.00 1.243 0.0245 0.450 1				1471450 1471450 1471450		
ALPHA BETA VANEI SNOCK TUBF SELECT 140 S19 L7 J07 E10 L1 M6 G14-2 M0-1 M4= A30=1 R5=1 C3														
3.0 0.000 0.000 2.742 5000														
OR 0.000 0.000 1.000 1.000 1.000 1.000 1.000 1.000 1.000 1.000 1.000 1.000 1.000 1.000 1.000														
CUTBACKD 0.0000 0.5773 0.5961 2.879 287.07 0.0001 0.0282 0.0780 0.3430 0.9955 1.2408 0.0545														
149C450 0.0000 0.5753 0.5815 2.854 285.64 0.0023 0.0634 0.0276 0.0240 0.3430 0.9955 1.2408 0.0545														
CUTBACKD 0.415 0.415 0.648 0.8586 0.8750 2.171 0.848 0.701 0.647														
149C450 0.415 0.415 0.648 0.8586 0.8750 2.171 0.848 0.701 0.647														
*** RAMP PRESSURES ***														
2.455 2.450 2.470 2.460 2.460 2.460 2.460 2.460 2.460 2.460 2.460 2.460 2.460 2.460 2.460														
CUTBACKD 0.4705 0.4705 0.4705 0.4705 0.4705 0.4705 0.4705 0.4705 0.4705 0.4705 0.4705 0.4705 0.4705 0.4705 0.4705														
149C450 0.4705 0.4705 0.4705 0.4705 0.4705 0.4705 0.4705 0.4705 0.4705 0.4705 0.4705 0.4705 0.4705 0.4705														
*** FLOWMETER PRESSURE ***														
CUTBACKD 0.4570 0.4568 0.4579 0.4571 0.3469 0.3387 0.3385 0.9996 0.9583 0.9471 0.9994 0.7411														
149C450 0.4568 0.4566 0.4566 0.4566 0.3421 0.3410 0.3442 0.9992 0.9583 0.9471 0.9994 0.7411														
*** OUTBOARD PT2/P10 ***														
2.455 2.450 2.470 2.460 2.460 2.460 2.460 2.460 2.460 2.460 2.460 2.460 2.460 2.460 2.460														
CUTBACKD 0.4705 0.4705 0.4705 0.4705 0.4705 0.4705 0.4705 0.4705 0.4705 0.4705 0.4705 0.4705 0.4705 0.4705 0.4705														
149C450 0.4705 0.4705 0.4705 0.4705 0.4705 0.4705 0.4705 0.4705 0.4705 0.4705 0.4705 0.4705 0.4705 0.4705														
*** OUTBOARD RMS2 ***														
2.455 2.450 2.470 2.460 2.460 2.460 2.460 2.460 2.460 2.460 2.460 2.460 2.460 2.460 2.460														
CUTBACKD 0.4705 0.4705 0.4705 0.4705 0.4705 0.4705 0.4705 0.4705 0.4705 0.4705 0.4705 0.4705 0.4705 0.4705 0.4705														
149C450 0.4705 0.4705 0.4705 0.4705 0.4705 0.4705 0.4705 0.4705 0.4705 0.4705 0.4705 0.4705 0.4705 0.4705														
*** CONTROL PARAMETERS ***														
CUTBACKD 0.4705 0.4705 0.4705 0.4705 0.4705 0.4705 0.4705 0.4705 0.4705 0.4705 0.4705 0.4705 0.4705 0.4705 0.4705														
149C450 0.4705 0.4705 0.4705 0.4705 0.4705 0.4705 0.4705 0.4705 0.4705 0.4705 0.4705 0.4705 0.4705 0.4705														

THIS PAGE IS BEST QUALITY PRACTICABLE FROM COPY FURNISHED TO DDC

*** STEADY STATE ***

PART PROJECT TEST DATE DAY HR MIN SEC ERCODE MODE SET:DATE WIND-OFF AEFC PRODUCTION WIND TUNNEL
 0.546 173.7 1444.8 305.2 2.546 569 1773.7 1774.1 1453.4 109 110 1661.0 0-0-0 0.00 1.136 0.0105 0.550 3
 ALPHA RFTA VANEO VANE1 SHOCK TUBE SELECT 140 S19 L7 J27 E10 L1 M6 G14-2 K4-1 M14-1 L30-1 P5-1 C3

CUTBACKED 0.9488 0.8522 0.9797 1.514 351.45 0.0085 0.0999 0.0704 0.0293 0.5007 1.0000 1.2412 0.0667
 14364ED 0.0241 0.0244 0.0214 1.481 348.13 0.0080 0.1068 0.0435 0.0100 0.5376 1.0001 1.2400 0.0743
 CUTBACKED 0.511 0.487 0.511 0.298 0.4104 2.724 0.425 0.841 0.825
 14364ED 0.481 0.508 0.490 0.4584 0.4125 2.700

*** EXP PRESSURES ***
 0.5023 0.5023 0.5023 0.5023 0.5023 0.5023 0.5023 0.5023 0.5023 0.5023 0.5023 0.5023 0.5023 0.5023 0.5023
 0.5023 0.5023 0.5023 0.5023 0.5023 0.5023 0.5023 0.5023 0.5023 0.5023 0.5023 0.5023 0.5023 0.5023 0.5023
 0.5023 0.5023 0.5023 0.5023 0.5023 0.5023 0.5023 0.5023 0.5023 0.5023 0.5023 0.5023 0.5023 0.5023 0.5023
 0.5023 0.5023 0.5023 0.5023 0.5023 0.5023 0.5023 0.5023 0.5023 0.5023 0.5023 0.5023 0.5023 0.5023 0.5023

*** FLOWMETER PRESSURE ***
 0.5023 0.5023 0.5023 0.5023 0.5023 0.5023 0.5023 0.5023 0.5023 0.5023 0.5023 0.5023 0.5023 0.5023 0.5023
 0.5023 0.5023 0.5023 0.5023 0.5023 0.5023 0.5023 0.5023 0.5023 0.5023 0.5023 0.5023 0.5023 0.5023 0.5023
 0.5023 0.5023 0.5023 0.5023 0.5023 0.5023 0.5023 0.5023 0.5023 0.5023 0.5023 0.5023 0.5023 0.5023 0.5023
 0.5023 0.5023 0.5023 0.5023 0.5023 0.5023 0.5023 0.5023 0.5023 0.5023 0.5023 0.5023 0.5023 0.5023 0.5023

THIS PAGE IS BEST QUALITY PRACTICABLE FROM COPY FURNISHED TO DDC

*** OUTBOARD P12/P10 ***
 0.5023 0.5023 0.5023 0.5023 0.5023 0.5023 0.5023 0.5023 0.5023 0.5023 0.5023 0.5023 0.5023 0.5023 0.5023
 0.5023 0.5023 0.5023 0.5023 0.5023 0.5023 0.5023 0.5023 0.5023 0.5023 0.5023 0.5023 0.5023 0.5023 0.5023
 0.5023 0.5023 0.5023 0.5023 0.5023 0.5023 0.5023 0.5023 0.5023 0.5023 0.5023 0.5023 0.5023 0.5023 0.5023
 0.5023 0.5023 0.5023 0.5023 0.5023 0.5023 0.5023 0.5023 0.5023 0.5023 0.5023 0.5023 0.5023 0.5023 0.5023

*** INBOARD RV52 ***
 0.5023 0.5023 0.5023 0.5023 0.5023 0.5023 0.5023 0.5023 0.5023 0.5023 0.5023 0.5023 0.5023 0.5023 0.5023
 0.5023 0.5023 0.5023 0.5023 0.5023 0.5023 0.5023 0.5023 0.5023 0.5023 0.5023 0.5023 0.5023 0.5023 0.5023
 0.5023 0.5023 0.5023 0.5023 0.5023 0.5023 0.5023 0.5023 0.5023 0.5023 0.5023 0.5023 0.5023 0.5023 0.5023
 0.5023 0.5023 0.5023 0.5023 0.5023 0.5023 0.5023 0.5023 0.5023 0.5023 0.5023 0.5023 0.5023 0.5023 0.5023

DATA SET 1
 CUTBACKED 0.0005 0.0467 0.0743 0.0998 0.0435 0.8441
 14364ED 0.1068 0.0743 0.0998 0.0435 0.8441
 DATA SET 2
 CUTBACKED 0.1068 0.0743 0.0998 0.0435 0.8441
 14364ED 0.1068 0.0743 0.0998 0.0435 0.8441

*** STEADY STATE ***

PART PC1AT PROJECT TEST DATE DAY MO MIN SEC ENCODE MODE SETTDATE WIN-OFF AFPC POPULATION WIND TUNNEL
 53 0.645 0.2 1640 1779.6 1780.1 1456.9 1457.0 109 110 1565.0 0-0.00 0.00 1.137 0.0093 0.550 1
 0.55F 1770.4 1448.2 307.2

ALPHA RETA VANED VANE1 SHOCK TUBE SELECT 140 S19 L7 J27 E10 U1 M6 G34-2 HA-1 WA-1 X30-1 P5-1 C3
 300 A-055 10-33 1A-41 5020

GA	NR22	MR400	WPR	WPR-SFS	T12	INT	INC	INC	INC	INC
0.9485	0.8442	0.8714	3.484	348.63	0.0086	0.0997	0.0401	0.0294	0.4983	1.0008
0.9408	0.8365	0.8632	3.453	345.34	0.0038	0.1064	0.0434	0.0307	0.5350	1.0000
4CS	MS	MA	NSR	LAUG	W2	CRSS	CRSS	CRSS	CRSS	CRSS
0.482	0.511	0.488	0.201	0.8106	2.713	0.824	0.841	0.824		
0.477	0.509	0.490	0.252	0.8122	2.688					

*** FAN PRESSURES ***

PL01	PL02	PL03	PL04	PL05	PL06	PL07	PL08	PL09	PL10
0.8090	0.8427	0.0000	0.8282	0.8335	0.7800	0.7727	0.8030	0.6507	0.5447
0.8084	0.8236	0.7320	0.8309	0.8304	0.7575	0.7689	0.8135	0.6547	0.7959

*** CO-2 INTERNAL PRESSURES ***

PL11	PL12	PL13	PL14	PL15	PL16	PL17	PL18	PL19	PL20
0.7727	0.7727	0.8030	0.6507	0.7727	0.8030	0.6507	0.7727	0.8030	0.6507
0.7575	0.7689	0.8135	0.6547	0.7575	0.7689	0.8135	0.7575	0.7689	0.8135

*** FLOWMETER PRESSURE ***

PL21	PL22	PL23	PL24	PL25	PL26	PL27	PL28	PL29	PL30
0.4572	0.4572	0.4598	0.4568	0.3224	0.3183	0.3224	0.3183	0.3141	0.3185
0.4572	0.4572	0.4598	0.4568	0.3224	0.3183	0.3224	0.3183	0.3141	0.3185

*** OUTBOARD PMS2 ***

PL31	PL32	PL33	PL34	PL35	PL36	PL37	PL38	PL39	PL40
0.500	0.080	0.090	1.000	1.000	1.000	1.000	1.000	1.000	1.000
0.585	0.060	0.067	0.999	1.001	0.998	0.998	0.998	0.998	0.998

*** OUTBOARD PMS1 ***

PL41	PL42	PL43	PL44	PL45	PL46	PL47	PL48	PL49	PL50
0.500	0.080	0.090	1.000	1.000	1.000	1.000	1.000	1.000	1.000
0.585	0.060	0.067	0.999	1.001	0.998	0.998	0.998	0.998	0.998

PL51	PL52	PL53	PL54	PL55	PL56	PL57	PL58	PL59	PL60
0.500	0.080	0.090	1.000	1.000	1.000	1.000	1.000	1.000	1.000
0.585	0.060	0.067	0.999	1.001	0.998	0.998	0.998	0.998	0.998

PL61	PL62	PL63	PL64	PL65	PL66	PL67	PL68	PL69	PL70
0.500	0.080	0.090	1.000	1.000	1.000	1.000	1.000	1.000	1.000
0.585	0.060	0.067	0.999	1.001	0.998	0.998	0.998	0.998	0.998

PL71	PL72	PL73	PL74	PL75	PL76	PL77	PL78	PL79	PL80
0.500	0.080	0.090	1.000	1.000	1.000	1.000	1.000	1.000	1.000
0.585	0.060	0.067	0.999	1.001	0.998	0.998	0.998	0.998	0.998

PL81	PL82	PL83	PL84	PL85	PL86	PL87	PL88	PL89	PL90
0.500	0.080	0.090	1.000	1.000	1.000	1.000	1.000	1.000	1.000
0.585	0.060	0.067	0.999	1.001	0.998	0.998	0.998	0.998	0.998

THIS PAGE IS BEST QUALITY PRACTICABLE FROM COPY FURNISHED TO DDC

THIS PAGE IS BEST QUALITY PRACTICABLE
FROM COPY FURNISHED TO DDC

*** STEADY STATE ***

TEST	DATE	DAY	HR	MIN	SEC	ENCODE	MODE	SET/DATE	WIND-OFF	AFC	PRODUCTION	WIND	TUNNEL
22.5DEG	67.5	157.5	202.5	247.5	292.5	337.5	377.5	427.5	477.5	527.5	577.5	627.5	677.5
1	1.000	1.001	1.001	1.001	1.001	1.001	1.001	1.001	1.001	1.001	1.001	1.001	1.001
2	1.000	1.001	1.001	1.000	0.994	1.000	1.001	1.001	1.001	1.001	1.001	1.001	1.001
3	1.000	1.001	1.001	1.001	0.975	0.960	0.943	0.926	0.909	0.892	0.875	0.858	0.841
4	0.978	0.924	0.890	0.875	0.861	0.849	0.833	0.817	0.801	0.785	0.769	0.753	0.737
5	0.647	0.674	0.670	0.673	0.655	0.638	0.621	0.605	0.589	0.573	0.557	0.541	0.525
22.5DEG	67.5	157.5	202.5	247.5	292.5	337.5	377.5	427.5	477.5	527.5	577.5	627.5	677.5
1	1.000	1.001	1.001	1.001	1.001	1.001	1.001	1.001	1.001	1.001	1.001	1.001	1.001
2	1.000	1.001	1.001	1.000	0.994	1.000	1.001	1.001	1.001	1.001	1.001	1.001	1.001
3	1.000	1.001	1.001	1.001	0.975	0.960	0.943	0.926	0.909	0.892	0.875	0.858	0.841
4	0.978	0.924	0.890	0.875	0.861	0.849	0.833	0.817	0.801	0.785	0.769	0.753	0.737
5	0.647	0.674	0.670	0.673	0.655	0.638	0.621	0.605	0.589	0.573	0.557	0.541	0.525
22.5DEG	67.5	157.5	202.5	247.5	292.5	337.5	377.5	427.5	477.5	527.5	577.5	627.5	677.5
1	1.000	1.001	1.001	1.001	1.001	1.001	1.001	1.001	1.001	1.001	1.001	1.001	1.001
2	1.000	1.001	1.001	1.000	0.994	1.000	1.001	1.001	1.001	1.001	1.001	1.001	1.001
3	1.000	1.001	1.001	1.001	0.975	0.960	0.943	0.926	0.909	0.892	0.875	0.858	0.841
4	0.978	0.924	0.890	0.875	0.861	0.849	0.833	0.817	0.801	0.785	0.769	0.753	0.737
5	0.647	0.674	0.670	0.673	0.655	0.638	0.621	0.605	0.589	0.573	0.557	0.541	0.525

*** FLOWMETER PRESSURE ***

*** COHL-INTERNAL-PRESSURES ***

*** CONTROL-PARAMETERS ***

*** OUTBOARD-P1/P10 ***

*** INBOARD RMS2 ***

*** INBOARD RMS2 ***

DATA SET 4 INT IDL IDC IDR IDL IDL PD POP P2 INC45 DMIX PMAX

INSCARD 0.704 0.530 0.0274 0.0274 0.360 0.0059 0.995 1.2697 0.9851 0.0028 0.0274 0.9320 1.0014

DATA SET 7

INSCARD 0.704 0.530 0.0274 0.0274 0.360 0.0059 0.995 1.2697 0.9851 0.0028 0.0274 0.9320 1.0014

INSCARD 0.704 0.530 0.0274 0.0274 0.360 0.0059 0.995 1.2697 0.9851 0.0028 0.0274 0.9320 1.0014

PSTC1 PSTC2 PSTC3 PST-D1 PSTC-D2 PSTC-D3 PSTC1 PSTC12 PSTC13 PSTD1 PSTD1 PSTD1 PSTD1 PSTD1 PSTD1 PSTD1

7.64 7.27 7.43 7.43 7.43 7.43 7.43 7.43 7.43 7.43 7.43 7.43 7.43 7.43

THIS PAGE IS BEST QUALITY PRACTICABLE
FROM COPY FURNISHED TO DDC

*** STEADY STATE ***			AIRC PROPULSION WIND TUNNEL		
PART POINT PROJECT TEST DATE DAY HR MIN SEC	ERCODE MODE	SFTIDATE	WIND-OFF	AIRC PROPULSION WIND TUNNEL	
563 2-24-1-22 0 0 0 0	0	210/24/74	5047		
P. 409 1455.4 1456.2 533.7 3.174 560 1695.4 1696.4 1072.4 1072.6 110 111 1335.1 0-0.00 0.00 1.270 0.0265 0.850 1					
ALPHA BETA VANED VANET SHOCK TUBE SELECT 140 S19 L7 J27 E10 L1 M6 G14-2 H8-1 W14-1 N10-1 05-1 C1					
M3 M4 M5 M6 M7 M8 M9 M10 M11 M12 M13 M14 M15 M16 M17 M18 M19 M20 M21 M22 M23 M24 M25 M26 M27 M28 M29 M30 M31 M32 M33 M34 M35 M36 M37 M38 M39 M40 M41 M42 M43 M44 M45 M46 M47 M48 M49 M50 M51 M52 M53 M54 M55 M56 M57 M58 M59 M60 M61 M62 M63 M64 M65 M66 M67 M68 M69 M70 M71 M72 M73 M74 M75 M76 M77 M78 M79 M80 M81 M82 M83 M84 M85 M86 M87 M88 M89 M90 M91 M92 M93 M94 M95 M96 M97 M98 M99 M100 M101 M102 M103 M104 M105 M106 M107 M108 M109 M110 M111 M112 M113 M114 M115 M116 M117 M118 M119 M120 M121 M122 M123 M124 M125 M126 M127 M128 M129 M130 M131 M132 M133 M134 M135 M136 M137 M138 M139 M140 M141 M142 M143 M144 M145 M146 M147 M148 M149 M150 M151 M152 M153 M154 M155 M156 M157 M158 M159 M160 M161 M162 M163 M164 M165 M166 M167 M168 M169 M170 M171 M172 M173 M174 M175 M176 M177 M178 M179 M180 M181 M182 M183 M184 M185 M186 M187 M188 M189 M190 M191 M192 M193 M194 M195 M196 M197 M198 M199 M200 M201 M202 M203 M204 M205 M206 M207 M208 M209 M210 M211 M212 M213 M214 M215 M216 M217 M218 M219 M220 M221 M222 M223 M224 M225 M226 M227 M228 M229 M230 M231 M232 M233 M234 M235 M236 M237 M238 M239 M240 M241 M242 M243 M244 M245 M246 M247 M248 M249 M250 M251 M252 M253 M254 M255 M256 M257 M258 M259 M260 M261 M262 M263 M264 M265 M266 M267 M268 M269 M270 M271 M272 M273 M274 M275 M276 M277 M278 M279 M280 M281 M282 M283 M284 M285 M286 M287 M288 M289 M290 M291 M292 M293 M294 M295 M296 M297 M298 M299 M300 M301 M302 M303 M304 M305 M306 M307 M308 M309 M310 M311 M312 M313 M314 M315 M316 M317 M318 M319 M320 M321 M322 M323 M324 M325 M326 M327 M328 M329 M330 M331 M332 M333 M334 M335 M336 M337 M338 M339 M340 M341 M342 M343 M344 M345 M346 M347 M348 M349 M350 M351 M352 M353 M354 M355 M356 M357 M358 M359 M360 M361 M362 M363 M364 M365 M366 M367 M368 M369 M370 M371 M372 M373 M374 M375 M376 M377 M378 M379 M380 M381 M382 M383 M384 M385 M386 M387 M388 M389 M390 M391 M392 M393 M394 M395 M396 M397 M398 M399 M400 M401 M402 M403 M404 M405 M406 M407 M408 M409 M410 M411 M412 M413 M414 M415 M416 M417 M418 M419 M420 M421 M422 M423 M424 M425 M426 M427 M428 M429 M430 M431 M432 M433 M434 M435 M436 M437 M438 M439 M440 M441 M442 M443 M444 M445 M446 M447 M448 M449 M450 M451 M452 M453 M454 M455 M456 M457 M458 M459 M460 M461 M462 M463 M464 M465 M466 M467 M468 M469 M470 M471 M472 M473 M474 M475 M476 M477 M478 M479 M480 M481 M482 M483 M484 M485 M486 M487 M488 M489 M490 M491 M492 M493 M494 M495 M496 M497 M498 M499 M500 M501 M502 M503 M504 M505 M506 M507 M508 M509 M510 M511 M512 M513 M514 M515 M516 M517 M518 M519 M520 M521 M522 M523 M524 M525 M526 M527 M528 M529 M530 M531 M532 M533 M534 M535 M536 M537 M538 M539 M540 M541 M542 M543 M544 M545 M546 M547 M548 M549 M550 M551 M552 M553 M554 M555 M556 M557 M558 M559 M560 M561 M562 M563 M564 M565 M566 M567 M568 M569 M570 M571 M572 M573 M574 M575 M576 M577 M578 M579 M580 M581 M582 M583 M584 M585 M586 M587 M588 M589 M590 M591 M592 M593 M594 M595 M596 M597 M598 M599 M600 M601 M602 M603 M604 M605 M606 M607 M608 M609 M610 M611 M612 M613 M614 M615 M616 M617 M618 M619 M620 M621 M622 M623 M624 M625 M626 M627 M628 M629 M630 M631 M632 M633 M634 M635 M636 M637 M638 M639 M640 M641 M642 M643 M644 M645 M646 M647 M648 M649 M650 M651 M652 M653 M654 M655 M656 M657 M658 M659 M660 M661 M662 M663 M664 M665 M666 M667 M668 M669 M670 M671 M672 M673 M674 M675 M676 M677 M678 M679 M680 M681 M682 M683 M684 M685 M686 M687 M688 M689 M690 M691 M692 M693 M694 M695 M696 M697 M698 M699 M700 M701 M702 M703 M704 M705 M706 M707 M708 M709 M710 M711 M712 M713 M714 M715 M716 M717 M718 M719 M720 M721 M722 M723 M724 M725 M726 M727 M728 M729 M730 M731 M732 M733 M734 M735 M736 M737 M738 M739 M740 M741 M742 M743 M744 M745 M746 M747 M748 M749 M750 M751 M752 M753 M754 M755 M756 M757 M758 M759 M760 M761 M762 M763 M764 M765 M766 M767 M768 M769 M770 M771 M772 M773 M774 M775 M776 M777 M778 M779 M780 M781 M782 M783 M784 M785 M786 M787 M788 M789 M790 M791 M792 M793 M794 M795 M796 M797 M798 M799 M800 M801 M802 M803 M804 M805 M806 M807 M808 M809 M810 M811 M812 M813 M814 M815 M816 M817 M818 M819 M820 M821 M822 M823 M824 M825 M826 M827 M828 M829 M830 M831 M832 M833 M834 M835 M836 M837 M838 M839 M840 M841 M842 M843 M844 M845 M846 M847 M848 M849 M850 M851 M852 M853 M854 M855 M856 M857 M858 M859 M860 M861 M862 M863 M864 M865 M866 M867 M868 M869 M870 M871 M872 M873 M874 M875 M876 M877 M878 M879 M880 M881 M882 M883 M884 M885 M886 M887 M888 M889 M890 M891 M892 M893 M894 M895 M896 M897 M898 M899 M900 M901 M902 M903 M904 M905 M906 M907 M908 M909 M910 M911 M912 M913 M914 M915 M916 M917 M918 M919 M920 M921 M922 M923 M924 M925 M926 M927 M928 M929 M930 M931 M932 M933 M934 M935 M936 M937 M938 M939 M940 M941 M942 M943 M944 M945 M946 M947 M948 M949 M950 M951 M952 M953 M954 M955 M956 M957 M958 M959 M960 M961 M962 M963 M964 M965 M966 M967 M968 M969 M970 M971 M972 M973 M974 M975 M976 M977 M978 M979 M980 M981 M982 M983 M984 M985 M986 M987 M988 M989 M990 M991 M992 M993 M994 M995 M996 M997 M998 M999 M1000					

THIS PAGE IS BEST QUALITY PRACTICABLE
FROM COPY FURNISHED TO DDC

PAST PCIT PROJECT TEST		DATE	DAY	HR	MIN	SEC	ERCODE	MODE	SETIDATE	WIND-OFF	AETC	PROPULSION	WIND	TUNNEL
483	1-24-67	0-20-67	23	1	12	0	0	0	2110	0-30	500	2	18-2-70	167
484	1-24-67	0-20-67	23	1	12	0	0	0	2110	0-30	500	2	18-2-70	167
*** STEADY STATE ***														
ALPHA BETA VANEF VANFI SHOCK TUBE SELECT														
1AN S10 L7 J77 E10 U1 M6 G14-2 HA-1 W1A-1 N30-1 P5-1 C3														
485	1-24-67	0-20-67	23	1	12	0	0	0	2110	0-30	500	2	18-2-70	167
486	1-24-67	0-20-67	23	1	12	0	0	0	2110	0-30	500	2	18-2-70	167
*** COL-INTERNAL-PRESSES ***														
487	1-24-67	0-20-67	23	1	12	0	0	0	2110	0-30	500	2	18-2-70	167
488	1-24-67	0-20-67	23	1	12	0	0	0	2110	0-30	500	2	18-2-70	167
*** FLOWMETER PRESSURE ***														
489	1-24-67	0-20-67	23	1	12	0	0	0	2110	0-30	500	2	18-2-70	167
490	1-24-67	0-20-67	23	1	12	0	0	0	2110	0-30	500	2	18-2-70	167
*** OUTBOARD RMS2 ***														
491	1-24-67	0-20-67	23	1	12	0	0	0	2110	0-30	500	2	18-2-70	167
492	1-24-67	0-20-67	23	1	12	0	0	0	2110	0-30	500	2	18-2-70	167
*** INBOARD RMS2 ***														
493	1-24-67	0-20-67	23	1	12	0	0	0	2110	0-30	500	2	18-2-70	167
494	1-24-67	0-20-67	23	1	12	0	0	0	2110	0-30	500	2	18-2-70	167
*** CONTROL PARAMETERS ***														
495	1-24-67	0-20-67	23	1	12	0	0	0	2110	0-30	500	2	18-2-70	167
496	1-24-67	0-20-67	23	1	12	0	0	0	2110	0-30	500	2	18-2-70	167
*** PLG-PLENUM ***														
497	1-24-67	0-20-67	23	1	12	0	0	0	2110	0-30	500	2	18-2-70	167
498	1-24-67	0-20-67	23	1	12	0	0	0	2110	0-30	500	2	18-2-70	167
*** DATA SET 1 ***														
499	1-24-67	0-20-67	23	1	12	0	0	0	2110	0-30	500	2	18-2-70	167
500	1-24-67	0-20-67	23	1	12	0	0	0	2110	0-30	500	2	18-2-70	167
*** DATA SET 2 ***														
501	1-24-67	0-20-67	23	1	12	0	0	0	2110	0-30	500	2	18-2-70	167
502	1-24-67	0-20-67	23	1	12	0	0	0	2110	0-30	500	2	18-2-70	167
*** DATA SET 3 ***														
503	1-24-67	0-20-67	23	1	12	0	0	0	2110	0-30	500	2	18-2-70	167
504	1-24-67	0-20-67	23	1	12	0	0	0	2110	0-30	500	2	18-2-70	167

PART PROJ TEST			DATE	DAY HR MIN SEC	ERCODE	MODE	SET: DATE	WIND-OFF	AERC	POPULATION	WIND TUNNEL
A1-074			02/20/76	07:44	47	0	2/10/76	0057	1	1	1
*** STEADY STATE ***											
ALPHA BETA VANED VANEI SHOCK TUBE SELECT 140 S19 L7 J27 E10 U1 M6 G14-2 HP1 M1A-1 M30-i P5-1 C3											
CUTBACK 0.984R 0.6724 0.6117 3.607 300.71 0.0060 0.0708 0.0277 0.8224 0.9554 1.2604 0.0542											
CUTBACK 0.984R 0.6724 0.6117 3.607 300.71 0.0060 0.0708 0.0277 0.8224 0.9554 1.2604 0.0542											
CUTBACK 0.402 0.413 0.473 0.4587 0.4757 2.268 0.647 0.700 0.646											
CUTBACK 0.402 0.413 0.473 0.4587 0.4757 2.268 0.647 0.700 0.646											
*** COIL INTERNAL PRESSURES ***											
CUTBACK 0.8149 0.768 0.700 0.6857 0.8528 0.8720 0.8719 0.8047											
CUTBACK 0.8149 0.768 0.700 0.6857 0.8528 0.8720 0.8719 0.8047											
*** FLOWMETER PRESSURE ***											
CUTBACK 0.4713 0.4714 0.4710 0.4713 0.3498 0.3503 0.3464 0.3475											
CUTBACK 0.4713 0.4714 0.4710 0.4713 0.3498 0.3503 0.3464 0.3475											
*** OUTBOARD P12/P10 ***											
P12 0.4255 0.4255 0.4255 0.4255 0.4255 0.4255 0.4255 0.4255 0.4255 0.4255 0.4255 0.4255											
P10 0.4255 0.4255 0.4255 0.4255 0.4255 0.4255 0.4255 0.4255 0.4255 0.4255 0.4255 0.4255											
*** OUTBOARD RMS2 ***											
P12 0.4255 0.4255 0.4255 0.4255 0.4255 0.4255 0.4255 0.4255 0.4255 0.4255 0.4255 0.4255											
P10 0.4255 0.4255 0.4255 0.4255 0.4255 0.4255 0.4255 0.4255 0.4255 0.4255 0.4255 0.4255											
*** INBOARD RMS2 ***											
P12 0.4255 0.4255 0.4255 0.4255 0.4255 0.4255 0.4255 0.4255 0.4255 0.4255 0.4255 0.4255											
P10 0.4255 0.4255 0.4255 0.4255 0.4255 0.4255 0.4255 0.4255 0.4255 0.4255 0.4255 0.4255											

THIS PAGE IS BEST QUALITY PRACTICABLE FROM COPY FURNISHED TO DDC

THIS PAGE IS BEST QUALITY PRACTICALLY
FROM COPY FURNISHED TO DDC

PART		PROJECT	TEST	DATE	DAY	HR	MIN	SEC	ERCODE		MODE	SFT:DATE	WIND-OFF	AERC PRODUCTION WIND TUNNEL		
*** STEADY STATE ***																
					PCA=1			PCA=2			PCA=3		PCA=4		PCA=5	
ALPHA					BETA					GAMMA			DELTA		EPSILON	
VANFO					VANFI					VANF2			VANF3		VANF4	
SHOCK TUBE SELECT 140 S10 L7 J27 E10 L1 M6 G14=2 M8=1 M1A=1 M30=1 P5=1 C3																
*** RAW PRESSURES ***																
CUTBACK				M2				M4				M8				
CUTBACK				M2				M4				M8				
*** FLOWMETER PRESSURE ***																
*** CONTROL PARAMETERS ***																
*** INBOARD RMS2 ***																
*** INBOARD RMS7 ***																
*** OUTBOARD RMS2 ***																
*** OUTBOARD RMS7 ***																
*** INTERNAL PRESSURES ***																
*** PLENUM ***																

THIS PAGE IS BEST QUALITY PRACTICABLE
FROM COPY FURNISHED TO DDC

*** STEADY STATE ***

FAST POINT PROJECT TEST	DATE	DAY	HR	MIN	SEC	ERCODE	MODE	SFTID	DATE	WIND-OFF	AERC	POPULATION	WIND TUNNEL
1050	1059.5	11	07A-1	11A-2	PCA-1	PCA-2	TTA-1	TTA-2	TTA-3	TTA-4	TTA-5	TTA-6	TTA-7
<p>ALPHA BETA VANEO VANEI SHOCK TUBE SELECT</p> <p>140 S19 L7 J27 E10 L1 M6 G74-2 M0-1 M16-1 M30-1 M5-1 C3</p> <p>500-15746-1-2-3-4-5-6-7-8-9-10-11-12-13-14-15-16-17-18-19-20-21-22-23-24-25-26-27-28-29-30</p>													
M02	0.9702	0.7090	0.7157	3.519	351.6A	0.0047	0.0102	0.0351	0.0172	0.5237	1.0018	1.2597	0.0779
M03	0.9009	0.6097	0.713A	3.510	350.95	0.0050	0.0071	0.0449	0.0315	0.5547	1.0112	1.2504	0.0754
M04	0.888	0.519	0.689	0.7091	0.8251	2.641	0.650	0.697	0.649				
M05	0.486	0.51	0.000	0.0007	0.8282	2.637							
*** RAW PRESSURES ***													
M06	PL440	PL470	PL480	PL480	PL480	PL480	PL480	PL480	PL480	PL480	PL480	PL480	PL480
M07	0.7791	0.836A	0.0000	0.8312	0.8365	0.7800	0.7752	0.8110	0.8604	0.7410	0.7943	0.7334	0.7069
M08	0.7244	0.826A	0.7420	0.6357	0.0467	0.748A	0.733A	0.820A	0.666A				
*** FLOWMETER PRESSURE ***													
M09	PL600	PL651	PL652	PL6A3	PL600	PL601	PL602	PL603	PL604	PL700	PL701	PL702	PL703
M10	0.5085	0.5072	0.5079	0.5077	0.3243	0.3239	0.3183	0.3199	0.9907	0.7919	0.7685	0.9998	0.7277
M11	0.5080	0.507A	0.5071	0.5070	0.3224	0.3194	0.3220	0.324A	0.9886	0.7826	0.7771		
*** OUTWARD PT2/PT0 ***													
M12	0.5050	0.475	0.475	0.475	0.475	0.475	0.475	0.475	0.475	0.475	0.475	0.475	0.475
M13	1.001	1.001	1.001	1.001	1.001	1.001	1.001	1.001	1.001	1.001	1.001	1.001	1.001
M14	1.001	1.001	1.001	1.001	1.001	1.001	1.001	1.001	1.001	1.001	1.001	1.001	1.001
M15	1.001	1.001	1.001	1.001	1.001	1.001	1.001	1.001	1.001	1.001	1.001	1.001	1.001
M16	1.001	1.001	1.001	1.001	1.001	1.001	1.001	1.001	1.001	1.001	1.001	1.001	1.001
M17	1.001	1.001	1.001	1.001	1.001	1.001	1.001	1.001	1.001	1.001	1.001	1.001	1.001
M18	1.001	1.001	1.001	1.001	1.001	1.001	1.001	1.001	1.001	1.001	1.001	1.001	1.001
*** OUTWARD RMS2 ***													
M19	20.5050	7.5	127.5	157.5	202.5	247.5	337.5	337.5	337.5	337.5	337.5	337.5	337.5
M20	1.001	1.001	1.001	1.001	1.001	1.001	1.001	1.001	1.001	1.001	1.001	1.001	1.001
M21	1.001	1.001	1.001	1.001	1.001	1.001	1.001	1.001	1.001	1.001	1.001	1.001	1.001
M22	1.001	1.001	1.001	1.001	1.001	1.001	1.001	1.001	1.001	1.001	1.001	1.001	1.001
M23	1.001	1.001	1.001	1.001	1.001	1.001	1.001	1.001	1.001	1.001	1.001	1.001	1.001
M24	1.001	1.001	1.001	1.001	1.001	1.001	1.001	1.001	1.001	1.001	1.001	1.001	1.001
M25	1.001	1.001	1.001	1.001	1.001	1.001	1.001	1.001	1.001	1.001	1.001	1.001	1.001
M26	1.001	1.001	1.001	1.001	1.001	1.001	1.001	1.001	1.001	1.001	1.001	1.001	1.001
M27	1.001	1.001	1.001	1.001	1.001	1.001	1.001	1.001	1.001	1.001	1.001	1.001	1.001
M28	1.001	1.001	1.001	1.001	1.001	1.001	1.001	1.001	1.001	1.001	1.001	1.001	1.001
M29	1.001	1.001	1.001	1.001	1.001	1.001	1.001	1.001	1.001	1.001	1.001	1.001	1.001
M30	1.001	1.001	1.001	1.001	1.001	1.001	1.001	1.001	1.001	1.001	1.001	1.001	1.001
M31	1.001	1.001	1.001	1.001	1.001	1.001	1.001	1.001	1.001	1.001	1.001	1.001	1.001
M32	1.001	1.001	1.001	1.001	1.001	1.001	1.001	1.001	1.001	1.001	1.001	1.001	1.001
M33	1.001	1.001	1.001	1.001	1.001	1.001	1.001	1.001	1.001	1.001	1.001	1.001	1.001
M34	1.001	1.001	1.001	1.001	1.001	1.001	1.001	1.001	1.001	1.001	1.001	1.001	1.001
M35	1.001	1.001	1.001	1.001	1.001	1.001	1.001	1.001	1.001	1.001	1.001	1.001	1.001
M36	1.001	1.001	1.001	1.001	1.001	1.001	1.001	1.001	1.001	1.001	1.001	1.001	1.001
M37	1.001	1.001	1.001	1.001	1.001	1.001	1.001	1.001	1.001	1.001	1.001	1.001	1.001
M38	1.001	1.001	1.001	1.001	1.001	1.001	1.001	1.001	1.001	1.001	1.001	1.001	1.001
M39	1.001	1.001	1.001	1.001	1.001	1.001	1.001	1.001	1.001	1.001	1.001	1.001	1.001
M40	1.001	1.001	1.001	1.001	1.001	1.001	1.001	1.001	1.001	1.001	1.001	1.001	1.001
M41	1.001	1.001	1.001	1.001	1.001	1.001	1.001	1.001	1.001	1.001	1.001	1.001	1.001
M42	1.001	1.001	1.001	1.001	1.001	1.001	1.001	1.001	1.001	1.001	1.001	1.001	1.001
M43	1.001	1.001	1.001	1.001	1.001	1.001	1.001	1.001	1.001	1.001	1.001	1.001	1.001
M44	1.001	1.001	1.001	1.001	1.001	1.001	1.001	1.001	1.001	1.001	1.001	1.001	1.001
M45	1.001	1.001	1.001	1.001	1.001	1.001	1.001	1.001	1.001	1.001	1.001	1.001	1.001
M46	1.001	1.001	1.001	1.001	1.001	1.001	1.001	1.001	1.001	1.001	1.001	1.001	1.001
M47	1.001	1.001	1.001	1.001	1.001	1.001	1.001	1.001	1.001	1.001	1.001	1.001	1.001
M48	1.001	1.001	1.001	1.001	1.001	1.001	1.001	1.001	1.001	1.001	1.001	1.001	1.001
M49	1.001	1.001	1.001	1.001	1.001	1.001	1.001	1.001	1.001	1.001	1.001	1.001	1.001
M50	1.001	1.001	1.001	1.001	1.001	1.001	1.001	1.001	1.001	1.001	1.001	1.001	1.001

436762

THIS PAGE IS BEST QUALITY PRACTICABLE FROM COPY FURNISHED TO DDC

... BREADY DATE ...

... PROJECT ... DATE ... TIME ...

... FRT ... C ... REX ...

... ALPHA ...

... CONT ...

... CONTOR ...

... CONTOR ...

... CONTOR ...

... CONTOR ...

... CONTOR ...

... CONTOR ...

... CONTOR ...

... CONTOR ...

... CONTOR ...

... CONTOR ...

... CONTOR ...

... CONTOR ...

... CONTOR ...

THIS PAGE IS BEST QUALITY PRACTICABLE
FROM COPY FURNISHED TO DDC

*** STEADY STATE ***																		
PROJECT	TEST	DATE	DAY	HR	MIN	SEC	ERRCODE	MODE	SETI	DATE	WIND-OFF	AERC	PROBATION	WIND	TUNNEL			
P25	2	541	02A	Tf410	9/20/76	273: 7: 36: 46	0	0	2:10/2A/76	623/ -1			FRANCONIC	167				
*** CONTROL PARAMETERS ***																		
BT	PC	REM10-6	TT	PTA-1	PTR-2	PCA-1	PCR-2	ITA-1	ITD-0	PTI	NCN	WAF	TAW	IPD	WAF/UT	MB	SCHED	
0.70	0.40	0.30	0.30	0.30	0.30	0.30	0.30	0.30	0.30	0.30	0.30	0.30	0.30	0.30	0.30	0.30	0.30	
*** FLOWMETER PRESSURE ***																		
ALPHA	BETA	VANE1	SHOCK	TUBE	SELECT	140	S10	L7-J27	E10	L1-M6-G74-2	W0-1	W1-1	K30-1	05-1	C3			
3.0	0.00	0.77	14.53	3917	PB0-1	7.PCO-1	42.1	AE10-1	5.5	4B20-1	0.0	MLC2	2.733	MLI2	2.726	C=0	UsS	
*** FAN PRESSURES ***																		
M2S	W2	MA	NSP	TAVG	W2	CP1SS	CP2SS	CP3SS										
0.844	0.511	0.593	0.6043	0.8197	2.274	0.737	0.767	0.737										
*** COHL INTERNAL PRESSURES ***																		
PL445	PL450	PL470	PL480	PL490	PL020	PL035	PL045											
0.7997	0.5463	0.0000	0.5364	0.8357	0.7494	0.7617	0.8450	0.8404										
*** FLOWMETER PRESSURE ***																		
PL690	PL691	PL692	PL693	PL694	PL695	PL696	PL697	PL698	PL699	PL700	PL701	PL702	PL703	PL704	PL705	PL706	PL707	PL708
0.5465	0.5464	0.5463	0.5462	0.5461	0.5460	0.5459	0.5458	0.5457	0.5456	0.5455	0.5454	0.5453	0.5452	0.5451	0.5450	0.5449	0.5448	0.5447
*** FAN PRESSURES ***																		
PL709	PL710	PL711	PL712	PL713	PL714	PL715	PL716	PL717	PL718	PL719	PL720	PL721	PL722	PL723	PL724	PL725	PL726	PL727
0.7690	0.8017	0.7749	0.7749	0.7749	0.7749	0.7749	0.7749	0.7749	0.7749	0.7749	0.7749	0.7749	0.7749	0.7749	0.7749	0.7749	0.7749	0.7749
*** OUTWARD PT2/PT0 ***																		
RING	22	03EG	47.5	112.5	157.5	202.5	247.5	292.5	337.5	382.5	427.5	472.5	517.5	562.5	607.5	652.5	697.5	742.5
1	1.001	1.001	1.001	1.001	1.001	1.001	1.001	1.001	1.001	1.001	1.001	1.001	1.001	1.001	1.001	1.001	1.001	1.001
2	1.001	1.001	1.001	1.001	1.001	1.001	1.001	1.001	1.001	1.001	1.001	1.001	1.001	1.001	1.001	1.001	1.001	1.001
3	1.001	1.001	1.001	1.001	1.001	1.001	1.001	1.001	1.001	1.001	1.001	1.001	1.001	1.001	1.001	1.001	1.001	1.001
4	1.001	1.001	1.001	1.001	1.001	1.001	1.001	1.001	1.001	1.001	1.001	1.001	1.001	1.001	1.001	1.001	1.001	1.001
5	1.001	1.001	1.001	1.001	1.001	1.001	1.001	1.001	1.001	1.001	1.001	1.001	1.001	1.001	1.001	1.001	1.001	1.001
*** OUTWARD PMS2 ***																		
DATA SET 1	IDA	IDC	IDR	IDL	T12	PD	PP	P2	INC12	INC45	PMIN	PMAX						
0.0664	0.0734	0.0734	0.0734	0.0734	0.0734	0.0734	0.0734	0.0734	0.0734	0.0734	0.0734	0.0734	0.0734	0.0734	0.0734	0.0734	0.0734	0.0734
*** CONTROL PARAMETERS ***																		
INRCARD	0.0672	0.0700	0.0253	0.0463	0.5590	0.0038	1.0009	1.2556	0.975A	0.0253	0.064A	1.0021						
DATA SET 2	0.0664	0.0734	0.0734	0.0734	0.0734	0.0734	0.0734	0.0734	0.0734	0.0734	0.0734	0.0734	0.0734	0.0734	0.0734	0.0734	0.0734	0.0734
*** CONTROL PARAMETERS ***																		
INRCARD	0.0664	0.0734	0.0734	0.0734	0.0734	0.0734	0.0734	0.0734	0.0734	0.0734	0.0734	0.0734	0.0734	0.0734	0.0734	0.0734	0.0734	0.0734
*** CONTROL PARAMETERS ***																		
INRCARD	0.0664	0.0734	0.0734	0.0734	0.0734	0.0734	0.0734	0.0734	0.0734	0.0734	0.0734	0.0734	0.0734	0.0734	0.0734	0.0734	0.0734	0.0734
*** CONTROL PARAMETERS ***																		
INRCARD	0.0664	0.0734	0.0734	0.0734	0.0734	0.0734	0.0734	0.0734	0.0734	0.0734	0.0734	0.0734	0.0734	0.0734	0.0734	0.0734	0.0734	0.0734

*** STEADY STATE ***

PUMP POINT PROJECT TEST DATE DAY HR MIN SEC FREQRE MODE SFTIDATE WIND-OFF SERPC POPULATION-WIND-TUNNEL
 426 1 24T-024 7F410 9/20/76 273: 7: 38: 54 0 0 211022/76 633/ -1
 P D C REY10-6 TT PTA-1 PIR-2 PCA-1 PCR-2 TTA-1 TTR-0 PTI NCV WAF HAW JPP WAMT MB SCHED
 (70) 14719 14719 2064 2.403 560 14719 14719 10701 10701 109 110 11775 0.000 0.000 1.200 0.000 0.700
 ALPHA BETA VANE0 VAME1 SMOCK TUBF SELECT 140 519 U7 U27 E10 U1 M6 G14 2 H14 T N30 J 09 J 03
 3.0 -0.001 18.74 14.53 RBC-1=7,RCC-1=211,AB10-1=7,AB20-1=0,MUC=2.733,H1=2.726,C=0,U=5
 P2 WFR MFR100 WTR W2-RFS T12 IDR JPC IOL PR PPP IDA
 CUTBACKED 0.7506 0.7471 1.515 354.66 0.0064 0.0311 0.6001 1.0007 1.0440 0.0730
 INCREASED 0.9754 0.7494 1.523 352.35 0.0038 0.1099 0.0462 0.0260 0.5608 1.0009 1.2594 0.0718
 W2S W7 MA NSP TAVG W2 CP1SS CP2SS CP3SS
 CUTBACKED 0.488 0.500 0.503 0.4044 0.6108 2.266 0.737 0.767 0.737
 INCREASED 0.485 0.502 0.000 0.8281 0.6212 2.283

*** FWP PRESSURES ***
 PL435 PL450 PL470 PL480 PL490 PL020 FL030 PL035 PL045
 CUTBACKED 0.7602 0.4466 0.0000 0.8358 0.8401
 INCREASED 0.7602 0.8308 0.7449 0.8407 0.8463
 *** COAL INTERNAL PRESSURES ***
 PL020 FL030 PL035 PL045
 CUTBACKED 0.5484 0.5484 0.5480 0.4063 0.4071 0.4034 0.4042
 INCREASED 0.5477 0.5481 0.5478 0.5483 0.4050 0.4037 0.4052 0.4078
 *** FLOWMETER PRESSURE ***
 PL691 PL692 PL693 PL690 PL691 PL692 PL693
 CUTBACKED 0.5484 0.5484 0.5480 0.4063 0.4071 0.4034 0.4042
 INCREASED 0.5477 0.5481 0.5478 0.5483 0.4050 0.4037 0.4052 0.4078

*** CONTROL PARAMETERS ***
 PL691 PL692 PL693 PL690 PL691 PL692 PL693 PL702 PL703 PL704 P1700 P1701
 CUTBACKED 0.5484 0.5484 0.5480 0.4063 0.4071 0.4034 0.4042 0.0646 0.7919 0.7740 0.9998 0.7883
 INCREASED 0.5477 0.5481 0.5478 0.5483 0.4050 0.4037 0.4052 0.0646 0.7919 0.7740 0.9998 0.7883
 *** INBOARD PT2/PT0 ***
 P1NE 22.825G 47.5 112.5 157.5 202.5 247.5 292.5 337.5 47.5 112.5 157.5 202.5 247.5 292.5 337.5
 1 1.000 1.000 1.000 1.000 1.000 1.000 1.000 1.000 1.000 1.000 1.000 1.000 1.000 1.000 1.000
 2 1.000 0.928 0.890 1.000 1.000 1.000 0.902 1.000 1.000 1.000 1.000 1.000 1.000 1.000 1.000
 3 0.203 0.378 0.049 1.000 1.000 1.000 0.954 1.000 1.000 1.000 1.000 1.000 1.000 1.000 1.000
 4 0.581 0.054 0.072 0.902 0.988 0.945 0.938 0.954 0.959 0.935 0.991 0.982 0.975 0.939 0.957
 5 0.581 0.031 0.047 0.975 0.944 0.936 0.907 0.922 0.910 0.906 0.944 0.943 0.950 0.921 0.916
 *** OUTBOARD PT2/PT0 ***
 P1NE 22.825G 47.5 112.5 157.5 202.5 247.5 292.5 337.5 47.5 112.5 157.5 202.5 247.5 292.5 337.5
 1 0.003 0.003 0.002 0.002 0.003 0.003 0.003 0.003 0.003 0.003 0.003 0.003 0.003 0.003 0.003
 2 0.000 0.000 0.002 0.004 0.015 0.009 0.010 0.006 0.004 0.004 0.004 0.004 0.004 0.004 0.004
 3 0.006 0.012 0.013 0.011 0.011 0.009 0.011 0.013 0.004 0.003 0.003 0.004 0.004 0.004 0.004
 DATA SET 1 IDT IDA IDC IDR IDL T12 T12 PDP P2 INC12 INC45 PW1V PWAY
 CUTBACKED 0.0044 0.0030 0.0044 0.0044 0.4061 0.0064 1.0003 1.2556 0.0084 0.0084 0.0084 0.0084 1.0011
 INCREASED 0.0000 0.0071 0.0071 0.0071 0.4062 0.5608 1.0003 1.2556 0.0084 0.0084 0.0084 0.0084 1.0022
 DATA SET 2
 CUTBACKED 0.0044 0.0030 0.0044 0.0044 0.4061 0.0064 1.0003 1.2556 0.0084 0.0084 0.0084 0.0084 1.0011
 INCREASED 0.0000 0.0071 0.0071 0.0071 0.4062 0.5608 1.0003 1.2556 0.0084 0.0084 0.0084 0.0084 1.0022

*** GUTBOARD PMS2 ***
 P1NE 22.825G 47.5 112.5 157.5 202.5 247.5 292.5 337.5 47.5 112.5 157.5 202.5 247.5 292.5 337.5
 1 0.003 0.003 0.002 0.002 0.003 0.003 0.003 0.003 0.003 0.003 0.003 0.003 0.003 0.003 0.003
 2 0.000 0.000 0.002 0.004 0.015 0.009 0.010 0.006 0.004 0.004 0.004 0.004 0.004 0.004 0.004
 3 0.006 0.012 0.013 0.011 0.011 0.009 0.011 0.013 0.004 0.003 0.003 0.004 0.004 0.004 0.004
 DATA SET 1 IDT IDA IDC IDR IDL T12 T12 PDP P2 INC12 INC45 PW1V PWAY
 CUTBACKED 0.0044 0.0030 0.0044 0.0044 0.4061 0.0064 1.0003 1.2556 0.0084 0.0084 0.0084 0.0084 1.0011
 INCREASED 0.0000 0.0071 0.0071 0.0071 0.4062 0.5608 1.0003 1.2556 0.0084 0.0084 0.0084 0.0084 1.0022
 DATA SET 2
 CUTBACKED 0.0044 0.0030 0.0044 0.0044 0.4061 0.0064 1.0003 1.2556 0.0084 0.0084 0.0084 0.0084 1.0011
 INCREASED 0.0000 0.0071 0.0071 0.0071 0.4062 0.5608 1.0003 1.2556 0.0084 0.0084 0.0084 0.0084 1.0022

THIS PAGE IS BEST QUALITY PRACTICABLE FROM COPY FURNISHED TO DDC

APPENDIX C

LIST OF COMMON SYMBOLS AND CONVENTIONS

d	shock tube diameter	
IDA	average distortion index	
IDC	total circumferential distortion index	} see Table 5.1
IDL	stall margin allocation ratio	
IDR	total radial distortion index	
IDT	total distortion index	
M	Mach number	
PSi	overpressure at i'th claw probe (i=1,2,3)	
Δp	shock overpressure at blast arrival (scaled to 1 atm. ambient pressure conditions)	
p	pressure	
p_o	pre-blast tunnel ambient pressure	
p_t	total pressure	
p_{t_o}	pre-blast tunnel total pressure	
p_{t_2}	average engine face total pressure (psf)	
R2I	average engine face total pressure for inboard inlet (nondimensional)	
R2O	average engine face total pressure for outboard inlet (nondimensional)	
r	distance from end of shock tube	
SM	fan stall margin (Sec. 8.3)	
TT	pre-blast tunnel total temperature ($^{\circ}R$)	
W2	engine-face weight flow	
W2R	engine-face weight flow corrected to standard conditions (for full scale inlet (lb/sec)	
W2R	$= W2 \times (TT/519)^{1/2} / (P_{t_2} / 2116)$	
β	side-slip angle t_2	
θ	polar angle from shock tube axis	
ϕ	angle between shock tube axis and wind tunnel axis	
ϕ	blast intercept angle (between a normal to the blast front and the inlet longitudinal axis)	

Notes:

In most pressure plots in this report the ordinate label designates the variable measured and the vertical scale is either pressure/ p_{t_o} or pressure/ p_o , the latter being designated by an asterisk after the label.

All blast pressure values in this report designated as Δp are scaled to a tunnel ambient pressure of one atmosphere. The actual test values can be obtained by dividing Δp by the ambient pressure in atmospheres (obtained from P in Appendix B).

Inlet mass flow rates in this report are always expressed in terms of full scale inlet conditions. To obtain model values divide by 100.

A separate table of symbols is provided for Appendix B in that appendix.

DISTRIBUTION LIST

DEPARTMENT OF DEFENSE

Assistant to the Secretary of Defense
Atomic Energy
ATTN: Executive Assistant

Defense Documentation Center
12 cy ATTN: DD

Defense Nuclear Agency
ATTN: SPAS
ATTN: DDST
ATTN: STSP
4 cy ATTN: TITL

Field Command
Defense Nuclear Agency
ATTN: FCPR

Livermore Division, Fld. Command, DNA
Lawrence Livermore Laboratory
ATTN: FCPRL

Commandant
NATO School (SHAPE)
ATTN: U.S. Documents Officer

Under Secy. of Def. for Rsch. & Engrg.
ATTN: Strategic & Space Systems (OS)
ATTN: Strategic & Space Systems, M. Atkins

DEPARTMENT OF ARMY

Harry Diamond Laboratories
Department of the Army
ATTN: DELHD-N-NP
ATTN: DELHD-N-P, J. Gwaltney

U.S. Army Ballistic Research Labs.
ATTN: DRXBR-BLE, W. Taylor
ATTN: DRDAR-BLV, J. Meszaros

U.S. Army Materiel Dev. & Readiness Cmd.
ATTN: DRCDE-D, L. Flynn

U.S. Army Nuclear & Chemical Agency
ATTN: Library

DEPARTMENT OF THE NAVY

Naval Material Command
ATTN: MAT 08T-22

Naval Research Laboratory
ATTN: Code 2627, Tech. Lib.

Naval Surface Weapons Center
ATTN: K. Caudle

Naval Weapons Evaluation Facility
ATTN: L. Oliver

Office of Naval Research
ATTN: Code 464

Strategic Systems Project Office
ATTN: NSP-272

DEPARTMENT OF THE AIR FORCE

Aeronautical Systems Division, AFSC
ATTN: ENFT, R. Bachman
4 cy ATTN: ENFTV, D. Ward

Air Force Aero-Propulsion Laboratory
ATTN: M. Stibich

Air Force Materials Laboratory
ATTN: MBE, G. Schmitt

Air Force Weapons Laboratory
ATTN: DYV, A. Sharp
ATTN: SUL
ATTN: DYV, G. Campbell

Foreign Technology Division, AFSC
ATTN: PDBF, Mr. Spring

Strategic Air Command/XPFS
Department of the Air Force
ATTN: XPFS, B. Stephan

DEPARTMENT OF DEFENSE CONTRACTORS

Aerospace Corp.
ATTN: W. Barry

Avco Research & Systems Group
ATTN: J. Patrick
ATTN: P. Grady

Boeing Co.
ATTN: R. Dyrdaht
ATTN: S. Strack
ATTN: E. York

Boeing Wichita Co.
ATTN: R. Syring

Calspan Corp.
ATTN: M. Dunn

Effects Technology, Inc.
ATTN: E. Bick
ATTN: R. Parisse
ATTN: R. Wengler

General Dynamics Corp.
ATTN: R. Shemensky

General Electric Co.-TEMPO
Center for Advanced Studies
ATTN: DASIAc

General Research Corp.
ATTN: T. Stathacopoulos

Kaman Avidyne
Division of Kaman Sciences Corp.
ATTN: N. Hobbs
ATTN: R. Ruetenik
ATTN: E. Criscione
ATTN: R. Smiley

Kaman Sciences Corp.
ATTN: D. Sachs

DEPARTMENT OF DEFENSE CONTRACTORS (Continued)

Los Alamos Technical Assoc., Inc.
ATTN: P. Hughes

McDonnell Douglas Corp.
ATTN: J. McGrew

Prototype Development Associates, Inc.
ATTN: C. Thacker
ATTN: J. McDonald

R & D Associates
ATTN: C. MacDonald
ATTN: J. Carpenter
ATTN: F. Field
ATTN: A. Kuhl

Rockwell International Corp.
ATTN: R. Sparling
ATTN: R. Moonan

DEPARTMENT OF DEFENSE CONTRACTORS (Continued)

Sandia Laboratories
ATTN: Doc. Con. for A. Lieber

Science Applications, Inc.
ATTN: D. Hove

Science Applications, Inc.
ATTN: J. Dishon

SRI International
ATTN: G. Abrahamson